USAARL Contract Report No. CR-96-1

Development of a Standard for the Health Hazard Assessment of Mechanical Shock and Repeated Impact in Army Vehicles

Phase 4--Experimental Phase

By

Barbara Cameron
James Morrison
Dan Robinson
Alen Vukusic
Steven Martin
George Roddan

B.C. Research Inc.
Vancouver, B.C., Canada

19971217 051

and

John P. Albano

Aircrew Protection Division

January 1996

DTIC QUALITY INSPECTED 3

Approved for public release; distribution unlimited.

U.S. Army Aeromedical Research Laboratory
Fort Rucker, Alabama 36362-0577

Notice

Qualified requesters

Qualified requesters may obtain copies from the Defense Technical Information Center (DTIC), Cameron Station, Alexandria, Virginia 22314. Orders will be expedited if placed through the librarian or other person designated to request documents from DTIC.

Change of address

Organizations receiving reports from the U.S. Army Aeromedical Research Laboratory on automatic mailing lists should confirm correct address when corresponding about laboratory reports.

Disposition

Destroy this document when it is no longer needed. Do not return it to the originator.

Disclaimer

The views, opinions, and/or findings contained in this report are those of the author(s) and should not be construed as an official Department of the Army position, policy, or decision, unless so designated by other official documentation. Citation of trade names in this report does not constitute an official Department of the Army endorsement or approval of the use of such commercial items.

Human use

Human subjects participated in these studies after giving their free and informed voluntary consent. Investigators adhered to AR 70-25 and USAMRMC Reg 70-25 on Use of Volunteers in Research.

Reviewed:

KEVIN T. MASON
LTC(P), MC, MFS
Director, Aircrew Protection Division

Released for publication:

DENNIS F. SHANAHAN
Colonel, MC, MFS
Commanding

Unclassified
SECURITY CLASSIFICATION OF THIS PAGE

REPORT DOCUMENTATION PAGE

Form Approved
OMB No. 0704-0188

1a. REPORT SECURITY CLASSIFICATION
Unclassified

1b. RESTRICTIVE MARKINGS

2a. SECURITY CLASSIFICATION AUTHORITY

2b. DECLASSIFICATION / DOWNGRADING SCHEDULE

3. DISTRIBUTION / AVAILABILITY OF REPORT
Approved for public release, distribution unlimited

4. PERFORMING ORGANIZATION REPORT NUMBER(S)
USAARL Report No. CR-96-1

5. MONITORING ORGANIZATION REPORT NUMBER(S)

6a. NAME OF PERFORMING ORGANIZATION
U.S. Army Aeromedical Research Laboratory

6b. OFFICE SYMBOL (If applicable)
MCMR-UAD

7a. NAME OF MONITORING ORGANIZATION
U.S. Army Medical Research and Materiel Command

6c. ADDRESS (City, State, and ZIP Code)
P.O. Box 620577
Fort Rucker, AL 36362-0577

7b. ADDRESS (City, State, and ZIP Code)
Fort Detrick
Frederick, MD 21702-5012

8a. NAME OF FUNDING / SPONSORING ORGANIZATION

8b. OFFICE SYMBOL (If applicable)

9. PROCUREMENT INSTRUMENT IDENTIFICATION NUMBER
DAMD17-91-C-1115

8c. ADDRESS (City, State, and ZIP Code)

10. SOURCE OF FUNDING NUMBERS

PROGRAM ELEMENT NO.	PROJECT NO.	TASK NO.	WORK UNIT ACCESSION NO.
62787A	30162787A878	FA	145

11. TITLE (Include Security Classification)
Development of a standard for the health hazard assessment of mechanical shock and repeated impact in Army vehicles, Phase 4--Experimental Phase

12. PERSONAL AUTHOR(S)
B. Cameron, J. Morrison, D. Robinson, A. Vukusic, S. Martin, G. Roddan, and J. Albano

13a. TYPE OF REPORT
Final

13b. TIME COVERED
FROM TO

14. DATE OF REPORT (Year, Month, Day)

15. PAGE COUNT

16. SUPPLEMENTAL NOTATION

17. COSATI CODES

FIELD	GROUP	SUB-GROUP

18. SUBJECT TERMS (Continue on reverse if necessary and identify by block number)
mechanical shock, repeated impact, vibration exposure, jolt, jolt standards, biomechanic modeling

19. ABSTRACT (Continue on reverse if necessary and identify by block number)

Military Significance: New tactical ground vehicles developed by the U.S. Army are lower in weight and capable of higher speeds than their predecessors. This combination produces repetitive mechanical shocks that are transmitted to the soldier primarily through the seating system. Under certain operating conditions, this exposure poses health and safety threats to the crew as well as performance degradation due to fatigue. The Army Surgeon General urgently required the Medical Research and Materiel Command to develop exposure standards for repetitive impacts that are relevant to the environment of soldiers operating modern tactical vehicles.

Methods: A five-phase research study was designed to develop a standard for the health hazard assessment of mechanical shock and repeated impact in army vehicles. Phase 1 reviewed the relevant scientific, medical and military literature. Phase 2 analyzed and characterized the shock and vibration environment of Army tactical ground vehicles (TGVs). Phase 3, a pilot study, determined the most sensitive human response measures to mechanical shock and repeated impact for use in the development of the experimental phase and in

20. DISTRIBUTION / AVAILABILITY OF ABSTRACT
☒ UNCLASSIFIED/UNLIMITED ☐ SAME AS RPT. ☐ DTIC USERS

21. ABSTRACT SECURITY CLASSIFICATION
Unclassified

22a. NAME OF RESPONSIBLE INDIVIDUAL
Chief, Science Support Center

22b. TELEPHONE (Include Area Code)
(334) 255-6907

22c. OFFICE SYMBOL
MCMR-UAX-SS

DD Form 1473, JUN 86 Previous editions are obsolete.

SECURITY CLASSIFICATION OF THIS PAGE
Unclassified

19. Abstract (Continued):

a dose-effect model. Phase 4, the experimental phase, identified important factors (based on the biomechanical, physiological, biochemical and subjective responses to motion exposure) to include in the development of health hazard assessment model. Fifty four healthy subjects, ages 19-40, participated in a series of short-duration (ST1) and long-duration (LT1-LT5) motion exposures using the multiaxis ride simulator (MARS) at Fort Rucker. Experiment ST1 assessed relative severity of shock characteristics. Experiments LT1-LT5 assessed fatigue and recovery to repeated shocks (up to 7 hours per day, or 4 hours per day for 5 days).

Results: Biomechanical responses at the spine were dependent on shock axis, amplitude and direction. The largest response resulted from z-axis inputs. Internal pressure responses were similar to spinal transmission. Subjective severity ratings to individual shocks were highly correlated with spinal acceleration. Electromyography (EMG) data from back muscles showed increased activity indicative of fatigue with as little as 2.5 hours motion exposure. No evidence of cumulative fatigue or trauma in EMG, biochemistry or subjective data. Rest breaks, including overnight recovery, temporarily improved the subjective comfort rating, but did not change the predicted tolerance to motion exposures. Subjects tolerated daily exposure in excess of the recommended daily dose of 15, based on the British Standard Vibration Daily Value (VDV). Some subjects were able to tolerate a VDV of 66 over a 7-hour period, or a VDV of 60 per day over a 5-day period.

Conclusion: Existing standards and models either over- or underestimate the observed response to motion exposure. Recommendations were made to incorporate nonlinear weighting factors to account for the most severe characteristics of motion exposure into a new model to assess the health hazards of exposure to mechanical shocks.

Executive Summary

This document is the fourth report on the development of a standard for the health hazard assessment of mechanical shock and repeated impact in army vehicles. The overall objective of the project is to develop a dose-effect model that will predict, and ultimately minimize, the risk of injury to a soldier when exposed to the repeated impact environment of tactical ground vehicles. The project supports the Army's health hazard assessment initiative to evaluate and control health hazards to enhance the Army's military capabilities and performance.

The specific objectives of Phase 4 are:

- To characterize the human response to individual shocks with a range of motion characteristics, including shock frequency, amplitude, and shock direction.
- To compare the biomechanical and subjective response to shocks to existing biodynamic models.
- To identify the biomechanical, physiological, biochemical and subjective responses that will predict injury risk to tactical ground vehicle (TGV) motion.
- To identify factors which should be included in the development of a new guideline for human exposure to mechanical shocks.

These objectives were met by a series of short duration (ST1) and long duration (LT1 to LT5) motion exposures conducted at the multiaxis ride simulator (MARS) facility at Fort Rucker, Alabama. The motion signatures which were used to simulate the TGV motion were computed from Army vehicle motion data characterized in Phase 2. Information which assessed the relative severity of shock characteristics was obtained from the short term experiments. Individual shocks ranged from 0.5 to 4 g in amplitude with a frequency range of 2 to 20 Hz, in the positive and negative x, y, and z axes. Longer duration exposures were designed to assess the potential fatigue and recovery in reponse to repeated shocks for up to 7 hours in one day, or 4 hours per day for 5 consecutive days. Experiments LT1 and LT2 provided a conservative, walk up design to monitor the response to increased exposure intensity and duration. Experiments LT3 to LT5 were designed to more closely resemble the prolonged motion exposure of sustained operations.

Biomechanical responses at the spine, measured by transmission of acceleration from the shocks input at the seat, were dependent on shock axis, amplitude and direction. The largest effect of shock amplitude on the human response was observed in the z axis. Internal pressure response to shock input was frequency-dependent, similar to the spinal transmission response. Subjective severity

ratings to individual shocks were highly correlated with spinal acceleration. These data provided the most comprehensive evaluation of the effect of shock exposures in humans.

Electromyography (EMG) data from muscles of the back showed increased activity indicative of fatigue with as little as 2.5 hours motion exposure. However, no persistent muscle fatigue was measurable within 5 minutes after motion had ceased. The EMG data were consistent with the biochemistry and subjective data, in which no evidence of cumulative fatigue or trauma resulting from these exposures were found. Rest breaks, including overnight recovery, temporarily improved the subjective rating of comfort, but did not change the predicted tolerance to motion exposures.

In relation to prolonged exposure to mechanical shocks, it was clear that subjects who volunteered for these experiments could tolerate a daily exposure in excess of the recommended daily exposure dose of 15 of the British Standard Vibration dose Value (VDV). Some subjects were able to tolerate a VDV of 66 over a 7-hour period, or a VDV of 60 per day over a 5-day period.

The Phase 4 experiments have made a significant contribution to the understanding of the human response to repeated shocks. Existing biodynamic models and guidelines were not developed to predict the effect of repeated shock exposures. As a result, they either overestimate or underestimate the observed human response over the range of shock inputs tested. Linear characteristics of the existing biodynamic models and guidelines limit their ability to model the nonlinear amplitude and frequency response to shock inputs observed in this study. These factors are critical to the development of a realistic health hazard assessment model. Recommendations were made to incorporate nonlinear weighting factors into a new model to assess the health hazard of exposure to mechanical shocks to account for the most severe characteristics of motion exposure.

Table Of Contents

EXECUTIVE SUMMARY i
TABLE OF CONTENTS iii
LIST OF TABLES vii
LIST OF FIGURES xii

INTRODUCTION 1
PHASE 4 PROJECT OBJECTIVES 2
Short Term Exposures 2
Long Term Exposures 3
BACKGROUND 4
MILITARY SIGNIFICANCE 10
HUMAN SUBJECT USE JUSTIFICATION 12
EXPERIMENTAL DESIGN 13
Experimental Design Overview 13
Motion Exposures 16
Experimental Objectives and Hypotheses 18
Experiment ST1 18
Objectives: 18
Null Hypotheses: 18
Experiment LT1 19
Objectives: 19
Null Hypotheses: 19
Experiment LT2 19
Objectives: 19
Null Hypotheses: 19
Experiment LT3 20
Objectives: 20
Null Hypotheses: 20
Experiment LT4 20
Objectives: 20
Null Hypothesis: 21
Experiment LT5 21
Objectives: 21
Null Hypothesis: 21
Experiment ST1 21
Long Term Experiments LT1 to LT5 23
Experiment LT1 24
Experiment LT2 26
Experiment LT3 27
Experiment LT4 28
Experiment LT5 29
Risk Assessment and Safety Procedures 30
Risk Assessment 30
Safety Procedures 32
Safety in Experimental Design 33
Subject Briefing and Orientation 33
Subject Monitoring 33
Biochemical Measurements 34
MARS Safety Features 34
Medical Monitoring 35

MATERIALS AND METHODS 36
Multi-Axis Ride Simulator 36
Development of Motion Signatures 36
Generation of Background Vibration 37
Generation of Shock Waveforms 37
Development of Control Signal 38
Equipment List 39
Equipment Calibration 40
Internal Pressure Probe 40
Accelerometers 40
Force Transducer 41
Selection of Subjects 41
Subject Prescreening/Orientation 42
Electrocardiography 43
Electromyography 44
Acceleration 45
Waveform Analysis 46
z Axis Response 46
y Axis Response 47
x Axis Response 48
Spectral Analysis of Shock Waveforms 48
Treatment of Acceleration Data 49
Skin Transfer Function 50
Linear Modeling Approaches for Identifying the Transfer Function of the Skin. 50
y Axis Spinal Accelerations 51
z Axis Spinal Accelerations 52
Parametric Modeling 52
Two Degrees of Freedom Linear Approximation 53
Transmission Ratios 55
Comparison of Filtering Effects on the z Axis Transmission Ratio 55
Shock Peak Detection and Transmission Ratio 56
Processing Transmission Data 58
Optotrak 58
Internal Pressure 59
Subjective Response 60
Measurement Scale for Responses 60
Training Procedures 61
Experimental Procedures for Subjective Responses 61
Short Term Experiments (ST1) 61
Effect of Motion Characteristics on Severity Ratings 61
Linearity of Subjective Response to Shock Amplitude 62
Comparison of Subjective Responses with Biodynamic Model Outputs and Transmitted Acceleration 62
Long Term Experiments (LT1 to LT5) 63
The Effect of Shock Axis, Direction, Amplitude and Rate 63
Effect of Exposure Duration on Subjective Response . 63
Effect of Rest Breaks on Subjective Response 64
Comparison of the VDV and Subjective Response 64
Physical Status 65

Blood and Urine Collection 65
Synthetic Work Task 68
Activity Monitor 69

RESULTS 70
Electromyography 70
Mean Frequency 70
RMS EMG 70
Acceleration Transmission 71
Spinal Acceleration 71
Spinal (L2 and T1) x Axis Acceleration Response to Positive and Negative x Axis Shocks at the Seat 71
Spinal (L3 and T2) y Axis Acceleration Response to Positive y Axis Shocks at the Seat 72
Spinal (L4 and T3) z Axis Acceleration Response to Positive and Negative z Axis Shocks at the Seat 73
Second Component of Spinal (L4 and T3) z Axis Acceleration Response to Positive and Negative z Axis Shocks at the Seat 74
Comparison of the Spinal Transmission Curves to Existing Standards and Models 75
Delay Between Shock Input and Peak Response 77
Internal Pressure Response 77
Internal Pressure Response to x Axis Shocks 77
Internal Pressure Response to Positive y Axis Shocks 78
Internal Pressure Response to z Axis Shocks 78
Second Internal Pressure Response to z Axis Shocks 79
Subjective Response 79
Short Term Experiments (ST1) 79
Effect of Motion Characteristics 79
Linearity of Subjective Severity to Shock Amplitude 80
Comparison of Subjective Severity with Biodynamic Model Outputs 80
z Axis Shocks 80
x and y Axis Shocks 81
Comparison of Subjective Responses with Spinal Transmission 81
Long Term Experiments (LT1 to LT5) 82
Effect of Shock Axis, Direction, Amplitude and Rate 82
Effect of Exposure Duration on Subjective Response . 82
Effect of Rest Breaks on Subjective Response 83
Comparison of the VDV and Subjective Response 84
Physical Status 86
Blood and Urine 86
Muscle Damage 87
Fluid Shift 88
Blood Clotting 89
Glucose in Blood and Urine 89
Fatigue 89
Inflammation 89
Bone Stress and Remodeling 89
Kidney, Bladder, or Urinary Tract Dysfunction 89
Synthetic Work Task 90

DISCUSSION 92
Spinal Acceleration 92
Transmission of Spinal Acceleration 93
Shock And Impact 94
High Frequency Spikes (Impacts) 94
Internal Pressure 95
EMG and Fatigue 96
Biochemistry 98
Subjective Response 100
Short Term Experiments (ST1) 100
The Effect of Motion Characteristics 101
Linearity of Subjective Response with Shock Amplitude 102
Relationship Between Subjective Severity and the Biodynamic Models 102
Relationship Between Subjective Severity and Spinal Transmission 102
Long Term Experiments (LT1 to LT5) 103
Effect of Shock Axis, Direction, Amplitude and Rate 103
Effect of Exposure Duration on Subjective Response 103
Effect of Rest Breaks on Subjective Response 104
Comparison of the VDV and Subjective Response 105
Existing Biodynamic Models 105
Relationship to Project Goals 106
Requirements for the Development of a Health Hazard Assessment Model 107
Key Features of a Model for Health Hazard Assessment 108

CONCLUSIONS 111
Short Duration Experiments (ST1) 111
Long Duration Experiments (LT1 to LT5) 112
Overall 112

RECOMMENDATIONS 113
ACKNOWLEDGMENTS 114
REFERENCES 115
APPENDIX A: THE PROJECT TEAM A-1
APPENDIX B: SUBJECTIVE ASSESSMENT SCALES B-1
APPENDIX C: BIOCHEMISTRY C-1
APPENDIX D: MULTIAXIS RIDE SIMULATOR (MARS) D-1
APPENDIX E: TABLES E-1
APPENDIX F: FIGURES F-1
APPENDIX G: GLOSSARY G-1

List of Tables

Table 1 Summary of short term and long term experiments. ... 14
Table 2 Shock Characteristics in Experiment ST1. 22
Table 3 Summary of motion signatures for experiment ST1. ... 23
Table 4 Motion signatures for Experiment LT1. Each signature was repeated in +x, -x, +y, +z, -z, and combined x, y, z directions.* 25
Table 5 Motion signatures for Experiment LT2.* 26
Table 6 Motion signature for Experiment LT3.* 27
Table 7 Motion signature for Experiment LT4.* 29
Table 8 Motion signatures for Experiment LT5.* 30
Table 9 Summary table of daily exposures, including a comparative comfort rating based on existing models. 32
Table 10 Existing biodynamic models which were compared to subjective severity ratings. 62
Table 11 Exposure and rest break combinations examined for experiments LT3, LT4 and LT5. 64
Table 12 Metabolites measured in blood samples. 65
Table 13 Metabolites and characteristics measured in urine samples.....66
Table 14 Summary of collection times for blood and urine samples. 67
Table 15 Correlation coefficients for subjective severity responses with biodynamic model outputs in response to single shocks in the z axes. 80
Table 16 Correlation coefficients for subjective severity responses with biodynamic model outputs in response to single shocks in the x and y axes. 81
Table 17 Correlation coefficients for subjective severity ratings with spinal transmission to the lumbar and thoracic vertebrae in response to single shocks. ... 82
Table 18 Linear regression equations of comfort and tiredness ratings with exposure time, for each successive day of exposure. 83
Table 19 Regression equations for subjective ratings with exposure time for both continuous and intermittent exposure conditions. 84
Table 20 The ratio of subjective ratings in Experiment LT1 between two motion exposures (VDV=14.5 and 29.1) where VDV was doubled by a two-fold increase in amplitude for a given shock rate, for Comfort (A), Severity (B) and Tolerance (C). 85
Table 21 List of data tables (located in the Appendix E) for blood and urine metabolites measured in experiment LT2, LT3, and LT4. 87
Table 22 Means and standard deviations of synthetic work task composite scores by trial in experiment LT2. .. 91

Appendix C

Table C-1 Metabolite Assays of Blood and Urine C-1
Table C-2 Dietary Recall Questionnaire C-11
Table C-3 Quality Control C-12

Appendix E

Table E-1 Physical characteristics of subjects in experiment ST1. ..... E-1
Table E-2 Physical characteristics of subjects in experiment LT1. ..... E-1
Table E-3 Physical characteristics of subjects in experiment LT2. ..... E-2
Table E-4 Physical characteristics of subjects in experiment LT3. ..... E-2
Table E-5 Physical characteristics of subjects in experiment LT4. ..... E-3
Table E-6 Physical characteristics of subjects in experiment LT5. ..... E-3
Table E-7 Low-pass filter level and correction effects on ratios of peak lumbar (L4) positive z acceleration to peak seat positive 4g z acceleration. E-4
Table E-8 Low-pass filter level and correction effects on ratios of peak thoracic (T3) positive z acceleration to peak seat positive 4g z acceleration. E-4
Table E-9 Low-pass filter level and correction effects on ratios of peak lumbar (L4) positive z acceleration to peak seat negative 4g z acceleration. E-4
Table E-10 Low-pass filter level and correction effects on ratios of peak thoracic (T3) positive z acceleration to peak seat negative 4g z acceleration E-4
Table E-11 Statistical summary of the mean frequency (MF) EMG response for pre- and post-exposure test contractions in experiment LT3 for the right and left lumbar (RL and LL) and right and left thoracic (RT and LT) EMG muscles. (n=10, T = 2.26). E-5
Table E-12 Statistical summary of the mean frequency (MF) EMG response for pre- and post-exposure test contractions in experiment LT4 on days 1, 3 and 5 for the right and left lumbar (RL and LL) and right and left thoracic (RT and LT) EMG muscles. (n=8, T=2.36). E-5
Table E-13 Ratio of peak lumbar (L2) positive x acceleration to peak seat positive x acceleration. E-6
Table E-14 Ratio of peak thoracic (T1) positive x acceleration to peak seat positive x acceleration. E-6
Table E-15 Ratio of peak lumbar (L2) negative x acceleration to peak seat negative x acceleration. E-7

Table E-16 Ratio of peak thoracic (T1) negative x acceleration to peak seat negative x acceleration. E-7
Table E-17 Ratio of peak lumbar (L3) positive y acceleration to peak seat positive y acceleration. E-8
Table E-18 Ratio of peak thoracic (T2) positive y acceleration to peak seat positive y acceleration. E-8
Table E-19 Ratio of peak lumbar (L4) positive z acceleration to peak seat positive z acceleration. E-9
Table E-20 Ratio of peak thoracic (T3) positive z acceleration to peak seat positive z acceleration. E-9
Table E-21 Ratio of peak lumbar (L4) positive z acceleration to peak seat negative z acceleration. E-10
Table E-22 Ratio of peak thoracic (T3) positive z acceleration to peak seat negative z acceleration. E-10
Table E-23 Ratio of second peak of the lumbar (L4) positive z acceleration to a single peak seat positive z acceleration. E-11
Table E-24 Ratio of second peak of the thoracic (T3) positive z acceleration to a single peak seat positive z acceleration. E-11
Table E-25 Ratio of second peak of the lumbar (L4) positive z acceleration to a single peak seat negative z acceleration. E-12
Table E-26 Ratio of second peak of the thoracic (T3) positive z acceleration to a single peak seat negative z acceleration. E-12
Table E-27 Time delay (sec) between peak seat positive x acceleration and peak lumbar (L2) positive x acceleration. E-13
Table E-28 Time delay (sec) between peak seat negative x acceleration and peak lumbar (L2) negative x acceleration. E-13
Table E-29 Time delay (sec) between peak seat positive x acceleration and peak thoracic (T1) positive x acceleration. E-14
Table E-30 Time delay (sec) between peak seat negative x acceleration and peak thoracic (T1) negative x acceleration. E-14
Table E-31 Time delay (sec) between peak seat positive x acceleration and peak internal pressure (IP) response. E-15
Table E-32 Time delay (sec) between peak seat negative x acceleration and peak internal pressure (IP) response. E-15
Table E-33 Time delay (sec) between peak seat positive y acceleration and peak lumbar (L3) positive y acceleration. E-16
Table E-34 Time delay (sec) between peak seat positive y acceleration and peak thoracic (T2) positive y acceleration. E-16

Table E-35 Time delay (sec) between peak seat positive y acceleration and peak internal pressure (IP) response. E-17
Table E-36 Time delay (sec) between peak seat positive z acceleration and peak lumbar (L4) positive z acceleration. E-17
Table E-37 Time delay (sec) between peak seat negative z acceleration and peak lumbar (L4) negative x acceleration. E-18
Table E-38 Time delay (sec) between peak seat positive z acceleration and peak thoracic (T3) positive z acceleration. E-18
Table E-39 Time delay (sec) between peak seat negative z acceleration and peak thoracic (T3) negative z acceleration. E-19
Table E-40 Time delay (sec) between peak seat positive z acceleration and peak internal pressure (IP) response. E-19
Table E-41 Time delay (sec) between peak seat negative z acceleration and peak internal pressure (IP) response. E-20
Table E-42 Ratio of peak internal pressure (IP) response to peak seat positive x acceleration (mm $Hg.m^{-1}.s^2$) ... E-20
Table E-43 Ratio of peak internal pressure (IP) response to peak seat negative x acceleration (mm $Hg.m^{-1}.s^2$) ... E-21
Table E-44 Ratio of peak internal pressure (IP) response to peak seat positive y acceleration (mm $Hg.m^{-1}.s^2$) ... E-21
Table E-45 Ratio of peak internal pressure (IP) response to peak seat positive z acceleration (mm $Hg.m^{-1}.s^2$) ... E-22
Table E-46 Ratio of peak internal pressure (IP) response to peak seat negative z acceleration (mm $Hg.m^{-1}.s^2$) ... E-22
Table E-47 Ratio of second peak internal pressure (IP) response to single peak seat positive z acceleration (mm $Hg.m^{-1}.s^2$) E-23
Table E-48 Ratio of second peak internal pressure (IP) response to single peak seat negative z acceleration (mm $Hg.m^{-1}.s^2$) E-23
Table E-49 Subjective comfort ratings to LT1 motion exposures. E-24
Table E-50 Subjective predicted tolerance ratings to LT1 motion exposures. E-24
Table E-51 Subjective severity ratings to LT1 motion exposures. E-24
Table E-52 The response of blood biochemical data in Experiment LT2 to motion exposures including 4 g shocks in the negative x axis. E-25
Table E-53 The response of blood biochemical data in Experiment LT2 to motion exposures including 4 g shocks in the positive z axis. E-29

Table E-54 The response of blood biochemical in Experiment LT3 in motion exposures (7 hours per day). E-33
Table E-55 The response of blood biochemical data in Experiment LT4 (5 days of 4 hours per day). E-37
Table E-56 The response of urinary biochemical measurements in Experiment LT2 to motion exposures including 4 g shocks in the negative x axis. E-44
Table E-57 The response of urinary biochemical measurements in Experiment LT2 to motion exposures including 4 g shocks in the positive z axis. E-50
Table E-58 The response of urinary biochemical measurements in Experiment LT3 (7 hours per day). E-56
Table E-59 The response of urinary biochemical measurements in Experiment LT4 (5 days of 4 hours per day). ... E-62

List of Figures

Figure 1. Relationship of the Phase 4 experiments to the development of a health hazard assessment model. ... 15
Figure 2. The idealized damped sinusoidal waveform used to design shocks for Phase 4 experiments. 17

Appendix F

Figure F-1. Acceleration measured at the seat and lumbar spine for a +4 g, 4 Hz z axis shock. F-1
Figure F-2. Acceleration measured at the seat and thoracic spine for a +4 g, 4 Hz z axis shock.. F-1
Figure F-3. Acceleration measured at the seat and lumbar spine for a +4 g, 4 Hz y axis shock..... F-2
Figure F-4. Acceleration measured at the seat and thoracic spine for a +4 g, 4 Hz y axis shock.. F-2
Figure F-5. Acceleration measured at the seat and lumbar spine for a +4 g, 4 Hz x axis shock..... F-3
Figure F-6. Acceleration measured at the seat and thoracic spine for a +4 g, 4 Hz x axis shock.. F-3
Figure F-7. Spectral density of acceleration measured at seat, lumbar and thoracic spine for a +4 g, 20 Hz z axis shock..... F-4
Figure F-8. Spectral density of acceleration measured at seat, lumbar and thoracic spine for a +4 g, 4 Hz z axis shock..... F-4
Figure F-9. Spectral density of acceleration measured at seat, lumbar and thoracic spine for a +4 g, 20 Hz y axis shock..... F-5
Figure F-10. Spectral density of acceleration measured at seat, lumbar and thoracic spine for a +4 g, 20 Hz x axis shock. F-5
Figure F-11. Example of a free damped oscillation of the L3 accelerometer (y axis) in response to perturbation of the skin..... F-6
Figure F-12. Example of a free damped oscillation of the LT4 accelerometer (z axis) in response to perturbation of the skin..... F-6
Figure F-13. Spectral density of a free damped oscillation of the skin-accelerometer system at L4 (z axis)..... F-7
Figure F-14. The high pass acceleration component of a skin perturbation..... F-7
Figure F-15. The low pass acceleration component of a skin perturbation..... F-8

Figure F-16. The amplitude components of low frequency (dotted line) and high frequency (solid line) bone-skin transfer functions derived from a free damped oscillation. The cross-over frequency (f_i) was used to establish the cut-off frequency for low pass and high pass filtering of the measured acceleration signal. F-8
Figure F-17. Recorded L4 accelerometer response to a -4 g, z axis shock at the seat and the predicted acceleration at the spinous process after correction by the skin transfer function..... F-9
Figure F-18. Spine (L4) z acceleration to seat z acceleration for 4 g shocks using 40 Hz, 150 Hz, and Skin Transfer Function (STF) analysis..... F-9
Figure F-19. Spine (T3) z acceleration to seat z acceleration for 4 g shocks using 40 Hz, 150 Hz, and Skin Transfer Function (STF) analysis..... F-10
Figure F-20. Spine (L4) z acceleration to seat z acceleration for -4 g shocks using 40 Hz, 150 Hz, and Skin Transfer Function (STF) analysis..... F-10
Figure F-21. Spine (T3) z acceleration to seat z acceleration for -4 g shocks using 40 Hz, 150 Hz (Raw), and Skin Transfer Function (STF) analysis..... F-11
Figure F-22. Change in mean frequency (delta MF) at right lumbar muscle site (L3) after exposure to motion during experiment LT3..... F-11
Figure F-23. Change in mean frequency (delta MF) at left lumbar muscle site (L3) after exposure to motion during experiment LT3..... F-12
Figure F-24. Change in mean frequency (delta MF) at right thoracic muscle site (T9) after exposure to motion during experiment LT3. ..... F-12
Figure F-25. Change in mean frequency (delta MF) at left thoracic muscle site (T9) after exposure to motion during experiment LT3..... F-13
Figure F-26. Change in mean frequency (delta MF) at right lumbar muscle site (L3) after exposure to motion on day 1 of experiment LT4..... F-13
Figure F-27. Change in mean frequency (delta MF) at left lumbar muscle site (L3) after exposure to motion on day 1 of experiment LT4..... F-14
Figure F-28. Change in mean frequency (delta MF) at right lumbar muscle site (L3) after exposure to motion on day 3 of experiment LT4. ..... F-14
Figure F-29. Change in mean frequency (delta MF) at left lumbar muscle site (L3) after exposure to motion on day 3 of experiment LT4. ..... F-15

Figure F-30. Change in mean frequency (delta MF) at right lumbar muscle site (L3) after exposure to motion on day 5 of experiment LT4.....F-15
Figure F-31. Change in mean frequency (delta MF) at left lumbar muscle site (L3) after exposure to motion on day 5 of experiment LT4. .....F-16
Figure F-32. Change in mean frequency (delta MF) at right thoracic muscle site (T9) after exposure to motion on day 1 of experiment LT4. .....F-16
Figure F-33. Change in mean frequency (delta MF) at left thoracic muscle site (T9) after exposure to motion on day 1 of experiment LT4. .....F-17
Figure F-34. Change in mean frequency (delta MF) at right thoracic muscle site (T9) after exposure to motion on day 3 of experiment LT4.....F-17
Figure F-35. Change in mean frequency (delta MF) at left thoracic muscle site (T9) after exposure to motion on day 3 of experiment LT4. .....F-18
Figure F-36. Change in mean frequency (delta MF) at right thoracic muscle site (T9) after exposure to motion on day 5 of experiment LT4. .....F-18
Figure F-37. Change in mean frequency (delta MF) at left thoracic muscle site (T9) after exposure to motion on day 5 of experiment LT4. .....F-19
Figure F-38. Spine (L2) x acceleration to seat x acceleration for 0.5, 1, 2, 3, 4 g shocks....F-19
Figure F-39. Spine (T1) x acceleration to seat x acceleration for 0.5, 1, 2, 3, 4 g shocks....F-20
Figure F-40. Spine (L2) x acceleration to seat x acceleration for -0.5, -1, -2, -3, -4 g shocks. F-20
Figure F-41. Spine (T1) x acceleration to seat x acceleration for -0.5, -1, -2, -3, -4 g shocks. F-21
Figure F-42. Comparison of the mean transmission ratios of all shock amplitudes measured at the lumbar (L2) and thoracic (T1) spine in response to positive x axis shocks.....F-21
Figure F-43. Comparison of the mean transmission ratios of all shock amplitudes measured at the lumbar (L2) and thoracic (T1) spine in response to negative x axis shocks.....F-22
Figure F-44. Comparison of the mean transmission ratios of all shock amplitudes measured at the lumbar (L2) spine in response to positive and negative x axis shocks.....F-22
Figure F-45. Comparison of the mean transmission ratios of all shock amplitudes measured at the lumbar (T1) spine in response to positive and negative x axis shocks.....F-23

Figure F-46. Spine (L3) y acceleration to seat y acceleration for 0.5, 1, 2, 3, 4 g shocks.... F-23
Figure F-47. Spine (T2) negative y acceleration to seat y acceleration for -0.5, -1, -2, -3, -4 g shocks. F-24
Figure F-48. Comparison of the mean transmission ratios of all shock amplitudes measured at the lumbar (L3) and thoracic (T2) spine in response to positive y axis shocks..... F-24
Figure F-49. Spine (L4) z acceleration to seat z acceleration for 0.5, 1, 2, 3, 4 g shocks.... F-25
Figure F-50. Spine (T3) z acceleration to seat z acceleration for 0.5, 1, 2, 3, 4 g shocks.... F-25
Figure F-51. Spine (L4) positive z acceleration to seat z acceleration for -0.5, -1, -2, -3, -4 g shocks. F-26
Figure F-52. Spine (T3) positive z acceleration to seat z acceleration for -0.5, -1, -2, -3, -4 g shocks F-26
Figure F-53. Percent difference of spine (L4) z acceleration to seat z acceleration..... F-27
Figure F-54. Percent difference of spine (T3) z acceleration to seat z acceleration..... F-27
Figure F-55. Spine (L4) z acceleration to 4g, seat z acceleration for 4, 8 and 20 Hz shocks..... F-28
Figure F-56. Spine (T3) positive z acceleration to 4g, seat z acceleration for 4, 8 and 20 Hz shocks. F-28
Figure F-57. Spine (L4) positive z acceleration to -4g, seat z acceleration for 4, 8 and 20 Hz shocks. F-29
Figure F-58. Spine (T3) positive z acceleration to -4g, seat x acceleration for 4, 8 and 20 Hz shocks. F-29
Figure F-59. Second peak of the spinal (L4) z acceleration to a single seat z acceleration for 2, 3, 4 g shocks. F-30
Figure F-60. Second peak of the spinal (T3) z acceleration to a single seat z acceleration for 2, 3, 4 g shocks. F-30
Figure F-61. Second peak of the spinal (L4) positive z acceleration to a single seat z acceleration for -2, -3, and -4 g shocks..... F-31
Figure F-62. Second peak of the spinal (T3) positive z acceleration to a single seat z acceleration for -2, -3, and -4 g shocks..... F-31
Figure F-63. Comparison of measured spine x transmission ratio (positive shocks) with predicted transmission ratios using BS 6841 filter and DRI models..... F-32

Figure F-64. Comparison of measured spine x transmission ratio (negative shocks) with predicted transmission ratios using BS 6841 filter and DRI model.....F-32
Figure F-65. Comparison of measured spine y transmission ratio (positive shocks) with predicted transmission ratios using BS 6841 filter and DRI model.....F-33
Figure F-66. Comparison of measured spine z transmission ratio (4g shocks) with predicted transmission ratios using BS 6841 filter, Fairley-Griffin model and DRI model.....F-33
Figure F-67. Comparison of measured spine z transmission ratio (1 g shocks) with predicted transmission ratios using BS 6841 filter, Fairley-Griffin model and DRI model.....F-34
Figure F-68. Delay time for peak acceleration measured at spine (L2) to seat x acceleration for 0.5, 1, 2, 3, and 4 g shocks.....F-34
Figure F-69. Delay time for peak acceleration measured at spine (L2) to seat x acceleration for -0.5, -1, -2, -3, and -4 g shocks.....F-35
Figure F-70. Delay time for peak acceleration measured at spine (T1) to seat x acceleration for 0.5, 1, 2, 3, and 4 g shocks.....F-35
Figure F-71. Delay time for peak acceleration measured at spine (T1) to seat x acceleration for -0.5, -1, -2, -3, and -4 g shocks.....F-36
Figure F-72. Delay time for peak internal pressure response to seat x acceleration for 0.5, 1, 2, 3, and 4 g shocks.....F-36
Figure F-73. Delay time for peak internal pressure response to seat x acceleration for -0.5, -1, -2, -3, and -4 g shocks.....F-37
Figure F-74. Delay time for peak acceleration measured at spine (L3) to seat y acceleration for 0.5, 1, 2, 3, and 4 g shocks.....F-37
Figure F-75. Delay time for peak acceleration measured at spine (T2) to seat y acceleration for 0.5, 1, 2, 3, and 4 g shocks.....F-38
Figure F-76. Delay time for peak internal pressure response to seat y acceleration for 0.5, 1, 2, 3, and 4 g shocks.....F-38
Figure F-77. Delay time for peak acceleration measured at spine (L4) to seat z acceleration for 0.5, 1, 2, 3, and 4 g shocks.....F-39
Figure F-78. Delay time for peak acceleration measured at spine (L4) to seat z acceleration for -0.5, -1, -2, -3, and -4 g shocks.....F-39
Figure F-79. Delay time for peak acceleration measured at spine (T3) to seat z acceleration for 0.5, 1, 2, 3, and 4 g shocks.....F-40

Figure F-80. Delay time for peak acceleration measured at spine (T3) to seat z acceleration for -0.5, -1, -2, -3, and -4 g shocks.....F-40
Figure F-81. Delay time for peak internal pressure response to seat z acceleration for 0.5, 1, 2, 3, and 4 g shocks.....F-41
Figure F-82. Delay time for peak internal pressure response to seat z acceleration for -0.5, -1, -2, -3, and -4 g shocks.....F-41
Figure F-83. Internal pressure response to seat x acceleration for 0.5, 1, 2, 3, and 4 g shocks. F-42
Figure F-84. Internal pressure response to seat x acceleration for -0.5, -1, -2, -3, and -4 g shocks. F-42
Figure F-85. Internal pressure response to seat y acceleration for 0.5, 1, 2, 3, and 4 g shocks. F-43
Figure F-86. Internal pressure response to seat z acceleration for 0.5, 1, 2, 3, and 4 g shocks. F-43
Figure F-87. Internal pressure response to seat z acceleration for -0.5, -1, -2, -3, and -4 g shocks. F-44
Figure F-88. Second internal pressure response to a single seat z acceleration for 2, 3, and 4 g shocks. F-44
Figure F-89. Second internal pressure response to a single seat z acceleration for -2, -3, and -4 g shocks. F-45
Figure F-90. Subjective severity ratings to single shocks in the positive x axis as a function shock frequency and amplitude.....F-45
Figure F-91. Subjective severity ratings to single shocks in the negative x axis as a function shock frequency and amplitude.....F-46
Figure F-92. Subjective severity ratings to single shocks in the y axis as a function shock frequency and amplitude.....F-46
Figure F-93. Subjective severity ratings to single shocks in the positive z axis as a function shock frequency and amplitude.....F-47
Figure F-94. Subjective severity ratings to single shocks in the negative z axis as a function shock frequency and amplitude.....F-47
Figure F-95. Comparison between subjective severity ratings to single shocks in the positive and negative x axis as a function shock frequency and amplitude.....F-48
Figure F-96. Comparison between subjective severity ratings to single shocks in the positive and negative z axis as a function shock frequency and amplitude.....F-48

Figure F-97. Comparison of normalized subjective severity ratings to single shocks in the positive x axis for different shock magnitudes..... F-49
Figure F-98. Comparison between severity ratings (SR) and expected output from the Fairley-Griffin (FG) model to positive z axis shocks..... F-49
Figure F-99. Comparison between severity ratings (SR) and expected output from the DRI model (8.4 Hz) to positive z axis shocks..... F-50
Figure F-100. Comparison between severity ratings (SR) and expected output from the DRI model (11.9 Hz) to positive z axis shocks..... F-50
Figure F-101. Comparison between severity ratings (SR) and expected output from the BS 6841 Wb filter to positive z axis shocks..... F-51
Figure F-102. Comparison between severity ratings (SR) and expected output from the Fairley-Griffin (FG) model to negative z axis shocks..... F-51
Figure F-103. Comparison between severity ratings (SR) and expected output from the DRI model (8.4 Hz) to negative z axis shocks..... F-52
Figure F-104. Comparison between severity ratings (SR) and expected output from the DRI model (11.9 Hz) to negative z axis shocks..... F-52
Figure F-105. Comparison between severity ratings (SR) and expected output from the BS 6841 Wb filter to negative z axis shocks..... F-53
Figure F-106. Comparison between severity ratings (SR) and expected output from the BS 6841 Wd filter to positive x axis shocks..... F-53
Figure F-107. Comparison between severity ratings (SR) and expected output from the DRI model (10 Hz) to positive x axis shocks..... F-54
Figure F-108. Comparison between severity ratings (SR) and expected output from the BS 6841 Wd filter to positive y axis shocks..... F-54
Figure F-109. Comparison between severity ratings (SR) and expected output from the DRI model (10 Hz) to positive y axis shocks..... F-55
Figure F-110. Comparison between severity ratings (SR) and expected output from the BS 6841 Wd filter to negative x axis shocks..... F-55
Figure F-111. Comparison between severity ratings (SR) and expected output from the DRI model (10 Hz) to negative x axis shocks..... F-56
Figure F-112. Comparison between severity ratings (SR) and acceleration measured at the thoracic spine (T1) in response to positive x axis shocks (T1 x). F-56

Figure F-113. Comparison between severity ratings (SR) and acceleration measured at the lumbar spine (L2) in response to positive x axis shocks (L2 x). F-57
Figure F-114. Comparison between severity ratings (SR) and acceleration measured at the thoracic spine (T1) in response to negative x axis shocks (T1 x). F-57
Figure F-115A. Comparison between severity ratings (SR) and acceleration measured at the lumbar spine (L2) in response to negative x axis shocks (L2 x). F-58
Figure F-115B. Comparison between severity ratings (SR) and acceleration measured at the thoracic spine (T2) in response to positive y axis shocks (T2 y). F-58
Figure F-115C. Comparison between severity ratings (SR) and acceleration measured at the lumbar spine (L3) in response to positive y axis shocks (L3 y). F-59
Figure F-116. Comparison between severity ratings (SR) and acceleration measured at the thoracic spine (T3) in response to positive z axis shocks (T3 z). F-59
Figure F-117. Comparison between severity ratings (SR) and acceleration measured at the lumbar spine (L4) in response to positive z axis shocks (L4 z). F-60
Figure F-118. Comparison between severity ratings (SR) and acceleration measured at the thoracic spine (T3) in response to negative z axis shocks (T3 z). F-60
Figure F-119. Comparison between severity ratings (SR) and acceleration measured at the lumbar spine (L4) in response to negative z axis shocks (L4 z). F-61
Figure F-120. Subjective comfort ratings as a function of exposure duration for 2-hour repeated shock exposures..... F-61
Figure F-121. Subjective predicted tolerance ratings as a function of exposure duration for 2-hour repeated shock exposures..... F-62
Figure F-122. Subjective tiredness ratings as a function of exposure duration for 2-hour repeated shock exposures..... F-62
Figure F-123. Subjective severity ratings as a function of exposure duration for 2-hour repeated shock exposures..... F-63

Figure F-124. Subjective comfort ratings as a function of exposure duration for a 7-hour repeated shock exposure.....F-63
Figure F-125. Subjective predicted tolerance ratings as a function of exposure duration for a 7-hour repeated shock exposure.....F-64
Figure F-126. Subjective tiredness ratings as a function of exposure duration for a 7-hour repeated shock exposure.....F-64
Figure F-127. Subjective severity ratings as a function of exposure duration for a 7-hour repeated shock exposure.....F-65
Figure F-128. Subjective comfort ratings as a function of cumulative exposure duration for 4-hour repeated shock exposures in five consecutive days. F-66
Figure F-129. Subjective tiredness ratings as a function of cumulative exposure duration for 4-hour repeated shock exposures in five consecutive days. F-66
Figure F-130. Subjective predicted tolerance ratings as a function of cumulative exposure duration for 4-hour repeated shock exposures in five consecutive days.....F-67
Figure F-131. Subjective severity ratings as a function of cumulative exposure duration for 4-hour repeated shock exposures in five consecutive days. F-67
Figure F-132. Comparison between subjective comfort ratings to continuous and intermittent shock exposures.....F-68
Figure F-133. Comparison between subjective predicted tolerance ratings to continuous and intermittent shock exposures.....F-68
Figure F-134. Comparison between subjective tiredness ratings to continuous and intermittent shock exposures F-69
Figure F-135. Comparison between subjective severity ratings to continuous and intermittent shock exposures.....F-69
Figure F-136. Comparison of tiredness ratings and the VDV as a function of time for a prolonged exposure to repeated shocks.....F-70
Figure F-137. Comparison between subjective tiredness ratings and the VDV as a function of cumulative exposure duration for 4-hour repeated shock exposures in five consecutive days. F-70

Figure F-138. The individual subject responses of blood lactate dehydrogenase (LDH) in Experiment LT2 with a motion exposure including 4 g shocks in the -x axis. F-71
Figure F-139. The individual subject responses of blood lactate dehydrogenase (LDH) in Experiment LT2 with a motion exposure including 4 g shocks in the +z axis. F-71
Figure F-140. The individual subject responses of blood lactate dehydrogenase (LDH) in Experiment LT3 with up to 7 hours of motion exposure including 2 and 4 g shocks in + x, y and z axes. F-72
Figure F-141. The individual subject responses of blood lactate dehydrogenase (LDH) in Experiment LT4 with up to 5 days of 4 hours per day of motion exposure including 2 and 4 g shocks in + x, y and z axes. F-72
Figure F-142 The individual subject responses of blood creatine phosphokinase (CPK) in Experiment LT2 with a motion exposure including 4 g shocks in the -x axis. F-73
Figure F-143. The individual subject responses of blood creatine phosphokinase (CPK) in Experiment LT2 with a motion exposure including 4 g shocks in the +z axis. F-74
Figure F-144. The individual subject responses of blood creatinine phosphokinase (CPK) in Experiment LT3 with up to 7 hours of motion exposure including 2 and 4 g shocks in + x, y and z axes. F-75
Figure F-145. The individual subject responses of blood creatine phosphokinase (CPK) in Experiment LT4 with up to 5 days of 4 hours per day of motion exposure including 2 and 4 g shocks in + x, y and z axes. F-76
Figure F-146. The individual subject responses of Creatinine Clearance (CC) in Experiment LT2 with a motion exposure including 4 g shocks in the -x axis. F-77
Figure F-147. The individual subject responses of Creatinine Clearance (CC) in Experiment LT2 with a motion exposure including 4 g shocks in the +z axis. F-77
Figure F-148. The individual subject responses of Creatinine Clearance (CC) in Experiment LT3 with up to 7 hours of motion exposure including 2 and 4 g shocks in + x, y and z axes. F-78

Figure F-149. The individual subject responses of Creatinine Clearance (CC) in Experiment LT4 with up to 5 days of 4 hours per day of motion exposure including 2 and 4 g shocks in + x, y and z axes. F-78
Figure F-150. The individual subject responses of Creatinine Clearance (CC) normalized to body surface area (BSA) in Experiment LT2 with a motion exposure including 4 g shocks in the - x axis. F-79
Figure F-151. The individual subject responses of Creatinine Clearance (CC) normalized to body surface area (BSA) in Experiment LT2 with a motion exposure including 4 g shocks in the +z axis. F-79
Figure F-152. The individual subject responses of Creatinine Clearance (CC) normalized to body surface area (BSA) in Experiment LT3 with up to 7 hours of motion exposure including 2 and 4 g shocks in + x, y and z axes. F-80
Figure F-153. The individual subject responses of Creatinine Clearance (CC) normalized to body surface area (BSA) in Experiment LT4 with up to 5 days of 4 hours per day of motion exposure including 2 and 4 g shocks in + x, y and z axes. F-80

Introduction

The overall objective of the project is to develop a dose-effect model that will predict, and ultimately minimize, the risk of injury to a soldier when exposed to the repeated impact environment of tactical ground vehicles. The project spans five years and five phases.

In the first phase a review of literature was conducted. This phase concluded with a list of potential measures or indices that might be sensitive to vibration and impact and could be measured in the pilot experiments in Phase 3 and the Phase 4 experiments. Phase 2, the vehicle characterization phase, ran concurrently with Phase 1. Phase 2 involved receiving and analyzing tapes of data from USAARL containing vibration measurements from tactical ground vehicles (TGVs). A variety of unique characterization methods were developed and programmed for data containing mechanical shocks and repeated impacts. These methods were meant to be more sensitive to shocks than previously available methods. This allowed "typical" vibration and impact environments to be defined based upon the TGV data tapes. The characterization methods were used to develop motion signatures to drive the multiaxis ride simulator (MARS) for Phase 3 and Phase 4 experiments. Phase 3 consisted of pilot tests conducted using the MARS in Fort Rucker, Alabama (AL). In this phase, a number of biomechanical, physiological and biochemical indices were measured in short duration (6 minute) and longer duration (1 and 2 hour) experiments. Details of the experimental methods, data analyses, and results of the pilot tests were provided in the Phase 3 report.

Phase 4 was the full experimentation phase. A series of six short and long term experiments were conducted at the MARS facility at Fort Rucker, AL between August 1994 and January 1995. Phase 5 is the analysis and model development phase. The final output of Phase 5 will be recommendations for a health hazard assessment index sensitive to the health effects of shocks and repeated impacts.

Phase 4 Project Objectives

The overall objective of the Phase 4 experiments was to evaluate the most promising biomechanical, physiological and biochemical indices of injury, identified during the Phase 1 literature review and Phase 3 experiments, in order to predict risk of injury and develop a health hazard assessment standard. Both short and long duration pilot tests conducted between January and March, 1993, provided valuable information for design of Phase 4 experiments. Shock signatures and health-related measures were selected from results of the pilot tests that could best be correlated with the motion environment.

In Phase 4, the short-duration experiments evaluated the human response to a range of impact situations, including varying shock frequencies, shock amplitudes, shock directions and the response to a single amplitude swept sine wave. These experiments were designed to provide information about the transmission characteristics of single shocks in the x, y and z axes. The longer duration experiments were designed to assess the potential fatigue and recovery effects of repeated shocks during exposure periods of up to 7 hours.

Global objectives of the Phase 4 study were defined relative to short term and long term experiments.

Short Term Exposures

- To establish a relationship between the human response to shock (spinal acceleration, spinal displacement, electromyography (EMG), internal pressure) and shock frequency in the +x, -x, ±y, +z and -z axes (where shock frequency is defined as the inverse of the time period of the biphasic shock waveform and where the shock waveform is presented as a damped sinusoid consisting of a single time period).

- To compare the biomechanical response to shock frequencies and subjective ratings of shock severtiy to International Standards Organization (ISO) 2631, British Standards (BS) 6841, and Dynamic Response Index (DRI) frequency weighting factors.

- To establish whether the relationship between shock amplitude and transmission is linear or non-linear.

Long Term Exposures

- To determine human tolerance of prolonged exposure to repetitive shocks in different directions (i.e., in the +x, -x, ±y, +z and -z axes).
- To estimate a daily and weekly exposure limit for repetitive shocks (of different magnitudes) in the +x, -x, ±y, +z and -z axes.
- To examine the effects of recovery on the human response to repetitive shocks.
- To compare subjective tolerance ratings of shock exposure severity with the British Standard Vibration Dose Value (VDV) and other predictors of fatigue or material failure.

Background

Many epidemiological studies have been conducted of heavy equipment operators from industries such as agriculture, construction, mining, forestry, and the military (Rosegger and Rosegger, 1960; Konda et al., 1985; Beevis and Forshaw, 1985; Boshuizen, Bongers, and Hulshof, 1990; and Milby and Spear, 1974). Some studies focused on subjective symptoms of health problems, such as backache. Other studies investigated objective findings of disease, such as back disorders (intervertebral disc herniation and spondylolisthesis), as diagnosed through clinical or radiological findings.

Most disorders associated with vibration are not specific to vibration, but occur generally in the population. They may be aggravated by other ergonomic or environmental problems. However, sufficient evidence is available to conclude that long-term exposure to vibration can be harmful to the spine and possibly other systems of the body (gastro-intestinal and cardio-respiratory). Several hypotheses have been developed to explain the etiology of back disorders. One hypothesis suggests vibration alters nutrition of the disc (Dupuis and Zerlett, 1986). A second suggests dynamic loading of the intervertebral joints causes fatigue damage to the annulus of the intervertebral discs (Sandover, 1981).

There is no single clinical disorder linked to whole body vibration or impact. Instead, there is some agreement that vibration accelerates the onset and progression of currently recognizable syndromes, rather than causing specific pathologies (Seidel and Heide, 1986; Dupuis and Zerlett, 1986; Hulshof and van Zanten, 1987). Although some studies include exposure to vibration and mechanical shock, there have been few studies where repeated shock is a variable under consideration.

Numerous reviews show that vibration and shocks have acute effects on a number of different systems in the body, including the cardiovascular, respiratory, and gastrointestinal (Guignard, 1972; Guignard, 1985; Guignard, 1974; Weaver, 1979; Barnes, 1987; Ramsay and Beshir, 1981). Physiological effects are related to two potential mechanisms: the movement of organs and tissues and a generalized stress response related to intensity and duration of vibration exposure. Many of the responses to vibration are attributed to stimulation or over-activation of the sympathetic nervous system. This can result in increased concentrations of catecholamines and vasoactive metabolites which in turn cause a generalized stress response. An increase in heart rate, cardiac output, respiration rate and oxygen uptake occurs in response to whole body vibration (WBV). In some cases, peripheral vasoconstriction has also been reported (Spaul, Spear, and Greenleaf, 1986; Abu-Lisan, 1979). Acute pathological effects of

vibration and shock have included injury to viscera, lung and myocardium (Guignard, 1972), bleeding in the gastro-intestinal system (Sturges et al.,1974), and occasionally, hemorrhage of kidney and brain (Guignard, 1972). The majority of this work has been conducted using animals.

Vibration and shocks have been shown to have a number of different effects on the ECG signal. Changes have been seen in the R-R interval (Ullsperger, Seidel, and Menzel, 1986; Harada, Kondo and Kinura, 1990), heart rate variability (Harstela and Pilirainen, 1985; Auffret, Demange, and Vettes, 1974), P-R interval (Abu-Lisan, 1979) and T-wave amplitudes (Roman et al.,1968). It is also possible that mechanical vibration of the intestines will increase motility, or movement of ingested material without appropriate breakdown or absorption taking place. A number of epidemiology papers have suggested that hearing loss due to noise is exacerbated by vibration (Rehm and Wieth, 1984; Chernyuk and Tashker, 1989).

The literature was reviewed to identify a biochemical marker for general stress, fatigue, and tissue or organ damage in response to vibration and shock. Animal studies have shown that exposure to vibration resulted in damage to heart, lung, brain, kidney, gastro-intestinal (GI) tract, liver, skeletal muscle, adrenal glands, and reproductive organs. Some damage was detectable in blood and urine, while others required histological examination of tissue. In humans, biochemical measures in blood and urine are routinely used to evaluate general stress and tissue damage. While inflammation is not specific to vibration, an inflammatory response has been linked to Raynaud's phenomenon both of occupational and non-occupational origin (Langauer-Lewowicka, 1976). A marker of fatigue is particularly important in this study, since increased fatigue may impair physical and psychological performance, and increase recovery time. Peripheral muscle fatigue has been related to changes in carbohydrate metabolism (lactate, glucose), protein and energy metabolism (ammonia), cortisol, and electrolyte balance (K^+, Mg^{2+}, Ca^{2+}) (Roberts and Smith, 1989). Maintenance of blood glucose is important in occupational settings to prevent hypoglycemia which interferes with task performance.

Electromyography (EMG) can be used to monitor various aspects of muscle function. The response of paraspinal muscles to whole-body vibration has been studied using EMG to assess localized muscle fatigue (Hansson, Magnusson, and Broman, 1991; Hosea et al., 1986; Magnusson, Hansson, and Broman, 1988; Robertson and Griffin, 1989; and Wilder, Frymoyer, and Pope, 1983), phase and timing relationships between muscle response and acceleration (Hagena et al.,1986; Robertson, 1987; Robertson and Griffin, 1989), and to estimate compressive loading and torque about the spine (Marras and Mirka, 1991; Seidel, Bluethner and Hinz, 1986; and Ortengren, Andersson, and Nachemson, 1981). These parameters are of interest because of their association with stabilization of the spine, and their subsequent association with back pain and injury to spinal

tissues. Muscle fatigue may diminish the ability of muscle to adequately compensate for perturbing forces, while out-of-phase or untimely muscle response can contribute to postural destabilization and increase both torque and compressive loading of the spine (Seroussi, Wilder, and Pope, 1989; Seroussi et al.,1987).

When the human body is subject to vibration or shocks, it demonstrates a dynamic response. The displacement of tissues and the forces transmitted by them alters as a function of time. A useful method to assess the potentially harmful effects is to measure the relative displacements and hence stresses of different regions of the body in response to vibration amplitude and frequency.

Transmission of acceleration can be expressed in terms of a transfer function that defines the relative magnitude and phase relationship of the output acceleration in a particular region (for example, the spine) compared with the input acceleration (for example, at the seat). Knowledge of acceleration transfer functions provide insight into behaviour of the body sub-systems, and enables assessment of input acceleration levels and frequencies where a particular tissue is more likely to be damaged. A substantial body of knowledge has been reported concerning the transmission of vibration. However, little is known about the repeated impact environment and the dynamic response of individual body segments to vibration and repeated shock. Attempts have been made to model the biodynamic characteristics of the human body, from simple mass spring models (Payne, 1991) to highly complex representations of the human body containing multiple degrees of freedom (Amirouche and Ider, 1988). A well developed model could prove to be an ideal tool for assessing the health effects of impacts and vibration.

All of the biomechanical, physiological and biochemical measures and analytical procedures that were proposed in Phase 4 experiments have been used previously in human research applications. Many of the measures, such as ECG and EMG, are common clinical tools and several people on the research team have used them in other research studies.

Phase 4 experiments are an extenstion of the Phase 3 pilot studies. Phase 3 evaluated the biomechanical, physiological and biochemical human responses to repeated impact, determined from the review of literature to be the most promising for the prediction of injury risk. Both short-term exposures (5.5 minutes) and long duration exposures (1 and 2 hour) were investigated in the pilot tests.

The following conclusions were made in the Phase 3 report:

1. Responses measured in spinal acceleration, internal pressure, chest and abdominal displacement, and EMG showed similar patterns of frequency response.

2. Response measured for shock frequencies of 2 to 11 Hz do not agree with transmission (weighting) curves in current standards (ISO 2631, 1982; BSI 6841, 1987; Air Standardization Coordinating Committee (ASCC), 1982).

3. There is evidence of non-linearity in response to shocks as reflected in :

   - Changes in frequency of peak (transmission) response in the x and z axis with different shock magnitudes.

   - Changes in transmission ratio with different magnitudes of shock.

   - Shape of the spinal acceleration response to individual shocks in the negative z axis.

4. The dominant spinal acceleration and internal pressure responses to negative z axis shocks are associated with the subject hitting the seat. This response contained very high frequency components (>20 Hz).

5. The pilot experiments did not show conclusive evidence of fatigue induced by 2 hour exposures to shock and vibration in either biochemical indicators, EMG response or ECG parameters.

6. There was biochemical evidence of muscle damage in some subjects following 2-hour exposures to shocks and vibration.

7. The magnitude of muscle response to shocks is typically less than 10 percent of maximal voluntary contraction.

8. The pattern of muscle response to shocks,involves two phases: stabilization of the upper torso and re-establishment of a neutral posture.

9. Performance measures induced changes in some ECG parameters.

These Phase 3 conclusions lead to five major recommendations for further research and formed the basis for development of the Phase 4 research protocol. The major recommendations, taken directly from the Phase 3 report were:

1. Standards developed for exposure to vibration and repeated shocks should account for:

   - non-linearity of response
   - differing responses to x, y, and z axis inputs
   - differing responses to positive and negative directions of shocks in the x and z axes

2. Further investigations of individual shock responses are required, including:

   - shocks in the negative x axis and positive z axis directions
   - shocks at low frequencies (for example, 1 to 4 Hz)
   - higher frequencies of shocks (for example, >20 Hz)
   - larger magnitudes of shocks

3. Further investigation is required of cumulative exposures that are of longer duration and increased severity to more accurately simulate a typical military mission.

4. More frequent recovery measures should be taken over a longer recovery period to observe possible fatigue.

5. The fourth phase of the project should include the following measures: acceleration at the spine; displacement of the spine (measured by Optotrak); internal pressure; EMG (including more muscles and sustained contractions at levels similar to those induced by shocks); ECG; biochemical markers (including hydroxyproline, lactate, K^+, CPK and glomerular filtration rates); and performance measures.

All of the biomechanical, physiological and biochemical measures and analytical procedures proposed in the Phase 4 test protocols have been conducted previously in Phase 3 and in other research applications. Many of the measures, such as ECG and EMG, are common clinical tools and have been used by members of the research team in other studies (Morrison, Conn and Hayes, 1982; Mekjavic and Morrison, 1985, 1986; Taylor and Morrison, 1989; 1991; Robinson, 1991, and Cameron, 1992). Most of the measures have been used by others in vibration environments (Zagorski et al., 1976; Hansson, Magnusson, and Broman 1991; Harada, Kondo and Kinura, 1990; Kjellberg and Wikstrom, 1987; Robertson and Griffin 1989; Seidel, Bluethner and Hinz 1986; Spaul, Spear and Greenleaf, 1986; Ullsperger, Seidel and Menzel 1986). The research has not indicated an unusual risk of harm to subjects from the experimental measures proposed, provided experienced personnel administer the protocol.

A thorough review of the literature emphasized that few studies have exposed humans to vibration with repeated shocks in a controlled laboratory environment. This type of control is essential to study the physiological, biochemical and biomechanical responses of the body to motion environment, and to accurately use these data to develop exposure guidelines. Most of the measures have been reported by others in vibrating environments (Zagorski et al., 1976; Hansson, Magnusson, and Broman 1991; Harada, Kondo and Kinura, 1990; Kjellberg and Wikstrom, 1987; Robertson and Griffin 1989; Seidel, Bluethner and Hinz, 1986; Spaul, Spear and Greenleaf, 1986; Ullsperger, Seidel and Menzel, 1986). This study, whose primary objective is to develop a dose-effect model that will predict, and ultimately minimize, the risk of injury to a soldier when exposed to the repeated impact environment of tactical ground vehicles, fills an important gap in the literature.

Military Significance

The U.S. Army has established a Health Hazard Assessment (HHA) Program to evaluate and control health hazards in support of the Army's military capabilities and performance. Overall, the HHA Program is an integrated effort that supports all areas and mission needs. Its specific objectives which are relative to this contract are to: preserve and protect the health of individual soldiers; enhance soldier performance; reduce readiness deficiencies related to health hazards; and reduce personnel compensations claims by eliminating or reducing injury or illness caused by health hazards associated with the use of Army systems (Liebrecht, 1990).

Health hazard assessment refers to the process of identifying, evaluating, and controlling risks to the health and effectiveness of personnel who test, use, service, or support Army systems. Many of the effects of health hazards are not immediate and may appear only after months or years of exposure. Such delayed effects may limit long-term contributions to the Army and may develop into serious health problems in the future, although the short-term impact the soldier's performance may be minimal (Liebrecht, 1990).

The HHA program utilizes resources to apply biomedical knowledge and principles to support the development of military material systems (Liebrecht, 1990). A variety of health hazards can directly affect the soldier operating military systems. In relation to this project, soldiers who operate or are transported in tactical ground vehicles (TGV) are exposed to mechanical forces which are considered health hazards, including vibration and shocks.

With the continuing emphasis on increased mobility and firepower, new TGVs developed by the U.S. Army are generally lighter in weight and capable of considerably higher speeds than their predecessors. This combination of lower weight and higher speed over rough terrain produces repetitive mechanical shocks that are transmitted to the soldier primarily through the seating system. Anecdotal evidence indicated that 50 percent of a company reported blood in the urine following operation of fast attack vehicles (USAARL, unpublished). Under certain motion environments, exposure to shock and vibration poses health and safety threats to the crew and performance degradation due to fatigue (Larson et al., 1973; Heslegrave et al., 1990).

Currently the Army relies on standard guidelines to assess the effects of repeated shock and vibration on performance, fatigue and health and safety of the soldier while he operates or is transported by TGVs. Most standards cited in MIL-STD 1472D are predicated on ISO 2631 "Guide for the Evaluation of Human Exposure to Whole-Body Mechanical Vibration" (ISO 2631, 1982). The ISO

standard is largely based on subjective measurements of fatigue and comfort, rather than health, and does not adequately account for the health effects of repeated shock (Village and Morrison, 1989). It is essential that cause-effect relationships between the mechanical environment and injury (acute and chronic) be determined for quantification of a health hazard assessment. There is an urgent requirement to develop exposure standards for repetitive whole-body shocks which are relevant to the environment of soldiers operating modern tactical vehicles and weapon systems.

Human Subject Use Justification

The primary objective of this 5 year project is to evaluate the human response to whole body vibration and mechanical impacts with the intention of developing a health hazard index. Since this is a study of the human response to vibration and impacts, the use of human subjects was an absolute requirement in this endeavour. Other species do not have the same transmission, biomechanical structure, physiological or biochemical response to vibration and repeated impacts.

Only male subjects were studied in this protocol. A male subject pool was selected because these experiments represented the Phase 4 effort of a five phase study. Earlier phases of this study were focused exclusively on male subjects as applied to crew members of tactical combat vehicles. Males were initially selected for this project based on the restricted number of subjects in the experimental design and because at the outset of this study females did not participate in combat maneuvers in tactical ground vehicles. Change in the design of the project to include females would have adversely affected the experimental design of this multi-phased program. Female subjects are likely to have a different response to shock and impact than males, based on differences in body morphology and hormonal environment. Hence, to maintain consistency with other phases of the project and reduce variability in the subject pool, the subjects who were recruited were male volunteers ranging from 20 to 40 years of age, within one standard deviation of the mean for height and weight, and having height proportional to weight (to eliminate subjects who were very light or very heavy for their height).

The selection of male subjects in this study does not preclude follow-up experiments addressing female response to repeated impact exposures. B.C. Research Inc. (BCRI) is prepared to respond to programmatic changes which support follow-up studies investigating the effect of repeated impact exposures on female soldiers.

Experimental Design

Experimental Design Overview

The Phase 4 protocol represents one part of a five phase project. The objectives and hypotheses, which are presented below, were developed from a through review of the literature as well as data collected in a pilot study in Phase 3. A series of six experiments were designed to test these hypotheses. The first experiment was designed to examine the human response to individual shocks (short term experiment ST1). The remaining five experiments were designed to examine human tolerance of repeated impacts (long term experiments LT1, LT2, LT3, LT4, and LT5). The results of Phase 4 will be used to develop a health hazard assessment model in the final phase of this project.

Fifty four male subjects participated in the experiments after medical screening. Prior to collection of experimental data, each subject undertook a 15 minute ride on the MARS at USAARL to become familiar with the motion environment. Including orientation and screening sessions, a total of 262 simulated vehicle rides were completed on the MARS. During the experiments, subjects were exposed to a series of mechanical shocks in three biodynamic axes (x, y, z) superimposed on a background of random vibration. Exposure duration ranged from 3.75 minutes to 7 hours.

Table 1 outlines the six series of experiments which were carried out in Phase 4. The protocol was designed so that subjects participating in more than one experiment did not exceed the cumulative weekly and monthly exposure limits specified in the section entitled "Risk Assessment and Safety Procedures".

Table 1
Summary of short term and long term experiments.

Exp.#	Experiment Duration (minutes)	# Sessions per Subject	# Subjects	# Experimental Sessions
ST1	35	3	10	30
LT1	18.75	5	10	50
LT2	120	5	6	30
LT3	420	1	10	10
LT4	240	5	8	40
LT5	60/180	2	10	20
Total			54	180

Figure 1 summarizes the way in which results of the Phase 4 experiments will be used in the development of the Health Hazard Assessment (HHA) standard. Experiments ST1, LT3 and LT4 are the main experiments relative to the primary objectives of this study. The specific details of each experiment are described below under the individual experiment heading.

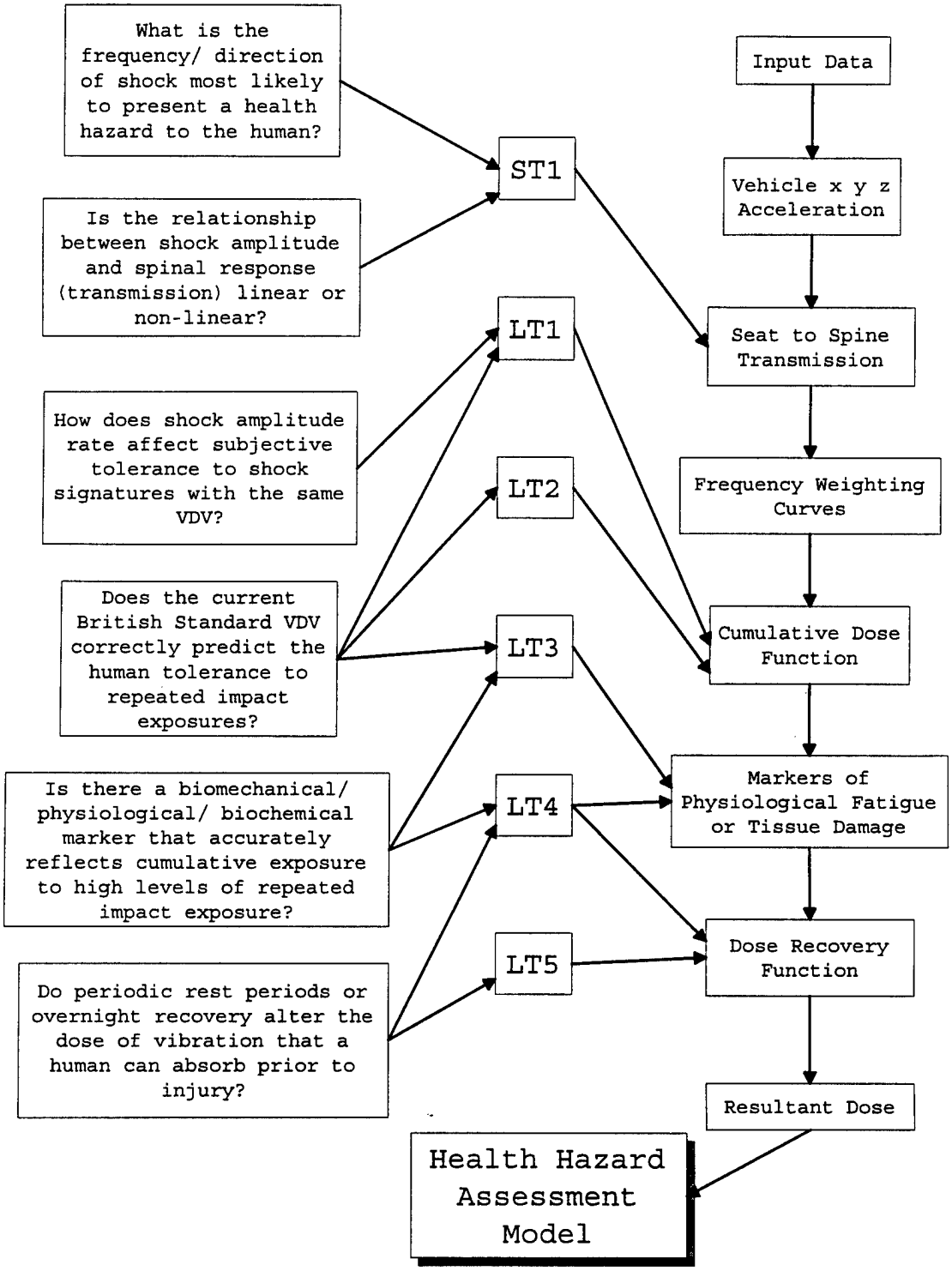

Figure 1. Relationship of the Phase 4 experiments to the development of a health hazard assessment model.

Motion Exposures

Unique motion signatures were developed by BCRI to control the MARS during Phase 4 experiments. Guidelines which were used to develop the motion signatures included data from TGVs, the British Standard 6841 VDV, and risk assessment derived from the Air Standard Coordinating Committee (ASCC) Standard for human tolerance to repeated shock. Similar motion signatures developed for the Phase 3 pilot experiments provided an indication of subject tolerance.

Data recorded from U.S. Army TGVs were used to gauge the magnitude of vibration and shocks included in the motion signatures. These data were analysed by BCRI during Phase 2 of the project. The range of shock amplitudes (acceleration amplitude, $m.s^{-2}$), shock frequencies (expressed as the fundamental frequency of the shock waveform, Hz) and shock rates ($shocks.min^{-1}$) reflected military exposures expected to be encountered when driving on a variety of surfaces including paved, tracked and cross-country. Figure 2 illustrates a basic shock waveform and its characteristic components. The terminology expressed in this diagram will be used throughout the report to describe the motion signatures.

The shock waveform in Figure 2 is a single oscillation of a damped sinusoidal waveform. The shock amplitude is the amplitude of the first shock peak, while the shock duration is the length of time from where the shock begins to where it first crosses zero acceleration. The shock period, T, is the time for a single complete oscillation, which is twice the shock duration. The shock frequency, f, is defined as the reciprocal of the period, i.e., $f=1/T$.

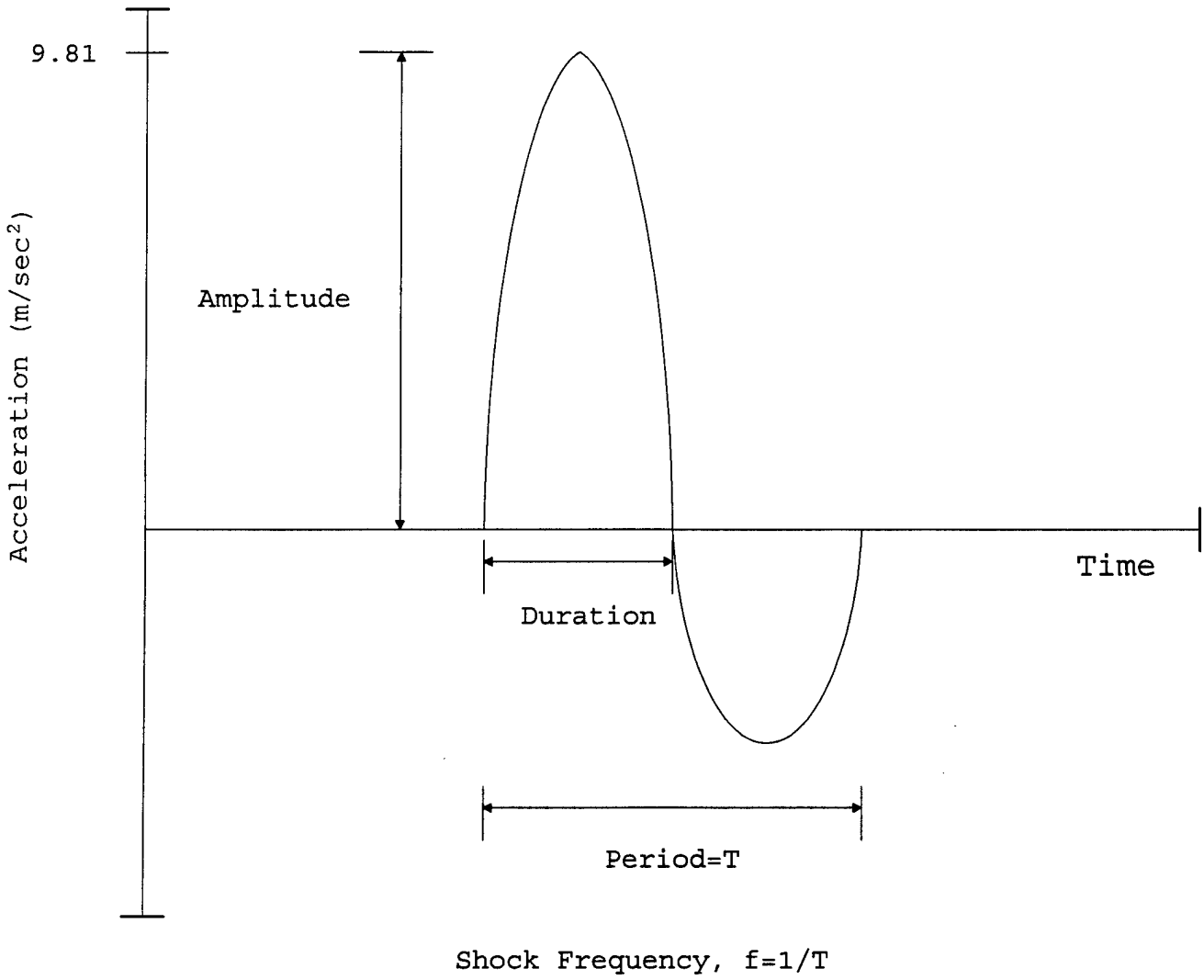

Figure 2. The idealized damped sinusoidal waveform used to design shocks for Phase 4 experiments.

In designing the individual shock signatures for these experiments, the VDV value of BS 6841 was used to develop comparative exposures containing different shock amplitudes and rates. Hence by using motion signatures with the equivalent VDVs, the human response to individual shocks and prolonged motion exposures could be compared according to shock frequency, amplitude, direction and rate.

The VDV of any shock signature is proportional to the amplitude of the shocks and to the fourth root of the shock duration and number of shocks. It is defined by the function:

$$VDV = (\int_0 a_w(t)^4 dt)^{1/4} \qquad m.s^{-1.75}$$

where $a_w(t)$ is the frequency weighted acceleration. Based on the above equation, if shock amplitude is doubled, when shock rate is constant, the VDV is doubled. However, to double the VDV when both shock rate and amplitude are constant, the exposure duration must be increased by a factor of 16.

In BS 6841, the z axis has a higher frequency weighting factor than the x and y axes. As the purpose of experiments LT1 and LT2 was to compare the relative severity and tolerance of similar shocks in the three axes, comparative VDV values were calculated using the BS 6841 z axis weighting for all shock signatures and directions.

Experimental Objectives and Hypotheses

The specific objectives and hypotheses for the six Phase 4 experiments, which are outlined below, were developed to support the overall objective of the project. The overall objective of the Phase 4 experiments was to evaluate human biomechanical, physiological and biochemical responses for the prediction of injury risk and development of a health hazard assessment standard.

Experiment ST1

Objectives:

- To identify the frequency and direction of shocks most likely to present a health hazard to the human.
- To determine whether the relationship between shock amplitude and spinal response (transmission ratio) is linear or non-linear.
- To establish response curves that will assist in the design of frequency weighted filters in Phase 5.

Null Hypotheses:

- The spinal response (transmission ratio) is not dependent on shock frequency or shock direction.

- The spinal response to shocks is not dependent upon shock amplitude.

Experiment LT1

Objectives:

- To use short duration shock signatures (3.75 min.) to predict the subjective tolerance of continuous exposure to shocks (Predictions will be validated in experiments LT2, LT3 and LT4).

- To compare the subjective tolerance to shock signatures having a similar VDV but different shock amplitudes, shock rates and shock directions.

- To determine whether the current British Standard, VDV, correctly predicts the subjective tolerance to shock signatures.

Null Hypotheses:

- Shock signatures of the same amplitude and rate delivered in different axes and directions will not result in different subjective tolerance times.

- Subjective tolerance is not dependent upon shock amplitude or shock direction.

- The current British Standard VDV does not accurately reflect subjective tolerance to shock signatures.

Experiment LT2

Objectives:

- To test the time dependence of a constant shock signature delivered over two time intervals (3.75 minutes and 120 minutes).

- To compare the subjective predicted tolerance to similar shock signatures with the same VDV in different axes and at different shock rates.

Null Hypotheses:

- There will be no change in predicted tolerance time with exposure duration, when subjective tolerance is rated at regular intervals throughout a 120 minute exposure.

- There will be no difference in the subjective tolerance to similar shock signatures with the same VDV delivered in different axes or at different shock rates.

Experiment LT3

Objectives:

- To evaluate the physiological, biomechanical and biochemical responses to a 7 hour acute exposure to shock and vibration.

- To test the subjective predicted tolerance a 7 hour exposure. (This will provide validation of the predictions obtained in LT1 and LT2).

- To determine the acceptable VDV level for a daily (7 hour) exposure and to provide a guideline for the maximum tolerable exposure level for a single day.

- To establish whether a biochemical marker can be used to establish dose limits within a tolerable range of VDV.

Null Hypotheses:

- There will be no change in the measures of physiological, biomechanical and biochemical response to high levels of repetitive shocks over an exposure of 7 hours.

- Short term predictions of subjective tolerance (i.e., prediction of tolerance from LT1) do not provide a realistic estimate of daily tolerance limits.

Experiment LT4

Objectives:

- To expose subjects to a prolonged vibration and shock environment on repeated days, simulating a sustained operational field environment where soldiers would be exposed to repeated shocks on several consecutive days.

- To determine the acceptable (daily) VDV level for a one week exposure (five consecutive days).

- To estimate a one-week threshold of subjective tolerance to cumulative exposures to high levels of repetitive shocks.

- To test for change in the biochemical, physiological, and biomechanical responses to cumulative exposures to high levels of repetitive shocks over a period of five days.

- To examine the effect of overnight recovery on the biochemical, physiological, and biomechanical measures and to cumulative high level repetitive shock exposures over a period of five days.

Null Hypothesis:

- There will be no progressive change in the biochemical, physiological, biomechanical or subjective tolerance measures as a result of cumulative exposures to high levels of repetitive shocks representative of field conditions, over a period of five days.

Experiment LT5

Objectives:

- To examine the effect of recovery on human tolerance to repetitive shocks.

- To compare the subjective response to the same accumulated VDV in two different motion environments (an intermittent compared to a continuous exposure).

- To test whether it is appropriate to include a short term recovery function in a dose measure of repetitive shock.

Null Hypothesis:

- There will be no difference in the human response to equal doses of impacts (VDV), with or without rest intervals.

Experiment ST1

Experiment ST1 was designed to evaluate the human response (biomechanical, physiological, and subjective) to individual shocks of different amplitude, duration and direction. This information is fundamental to identify the shock characteristics most likely to present a health hazard to the human. The response curves obtained from this experiment will be used to determine frequency weighting curves for seat input accelerations to be applied in the health hazard model of Phase 5.

The human response to mechanical shocks depends on shock magnitude, direction and frequency. For example, the spinal response (transmission ratio) is different for each shock direction and frequency. However, the limited data collected in Phase 3 were insufficient to fully characterize the human response to individual shocks. Hence it was necessary to examine the response to shocks

having different durations, amplitudes and directions to assess the relative severity of their insult to the human body.

To fully characterize the human response to shocks, a full range of shock frequencies and amplitudes is desirable. In this study the experimental conditions were constrained by the mechanical limitations of the MARS and safety concerns for the subject. That is, the MARS facility was not capable of producing 4 g shocks at frequencies lower than 5 Hz or greater than 20 Hz and there was concern for the safety of the subjects if exposed to repeated shocks greater than 4g. These factors placed constraints on the range of shock frequencies chosen for the short-term experiment.

Motion signatures were prepared with individual shocks having a range of amplitudes from 0.5 to 4 g and frequencies from 2 to 20 Hz in the +x, -x, +y, +z and -z directions. The maximum length of each signature was 327 sec, with 2 warn-up shocks followed by 2 shocks of each type listed in Table 2 presented in random order (maximum of 34 shocks per signature).

Table 2
Shock Characteristics in Experiment ST1.

Amplitude (g)	Frequency (Hz)							
0.5	2	4	5	6	8	11	15	20
1	2	4	5	6	8	11	15	20
2		4	5	6	8	11	15	20
3		4	5	6	8	11	15	20
4		4	5	6	8	11	15	20
0.4 g Swept Sinusoid	40 Hz to 2 Hz							

The responses to positive and negative shocks were expected to differ in the x and z axes, due to the asymmetrical nature of the musculoskeletal system in those directions. Hence shock signatures were presented separately in both positive and negative directions for the x and z axes. As the body is symmetrical about the sagittal plane (lateral movement), y axis shocks were presented in a single direction.

Separate signatures were also prepared to generate sinusoidal motion in each axis in the form of a swept sinusoid. The swept sinusoid was a continuous motion signature with an amplitude of 0.4 g in which the sinusoid decreased in frequency from 40 Hz to 2 Hz over a time interval of 90 seconds.

Each of the shocks shown in Table 2 were presented twice for each shock direction. To present this number of shocks, 3 separate

shock signatures of approximately 5.5 minutes were designed to complete the shock pattern in one axis and in one direction. The 3 signatures were presented to the subjects in each of the five directions, resulting in a total of fifteen shock signatures (plus the swept sinusoid). The shock amplitudes contained in each signature were organized according to Table 3. The order of presentation of shock frequencies was random within each signature. The interval between shocks ranged from 7 to 13 seconds.

Table 3
Summary of motion signatures for experiment ST1.

Shock Amplitudes	Axes	Duration of each Signature (minutes)	Number of Signatures*
0.5 and 1 g shocks	+x,-x, +y,+z,-z	5.5	5
2 g and 3 g shocks	+x,-x, +y,+z,-z	5.5	5
4 g shocks	+x,-x, +y,+z,-z	5.5	5
swept sine (40 to 2 Hz)	±x, ±y, ±z	1.5	3

* A motion signature is a continuous signal containing a series of acceleration waveforms (shocks) at discrete time intervals delivered by the MARS controller to the motion platform.

A 20 second warm-up period containing 2 shocks was included in each signature. These data were not included in the analysis. Each subject experienced a maximum of 7 signatures per day (1 axis, positive and negative directions, plus the swept sinusoid). Signatures were separated by a 2.5 minute rest period. Including rest periods, the total time a subject was seated on the MARS was approximately 60 minutes, with a motion exposure of 35 minutes per day. Each subject completed 3 sessions (one for each axis) on separate days, with a minimum of 48 hours between each session.

Eleven subjects participated in this protocol of whom ten completed the experiment. The subject who did not complete the experiment did not want to be exposed to all of the shock amplitudes and therefore was excused from the protocol. Each subject was instrumented with 3-lead ECG, EMG electrodes, accelerometers, infrared emitting diodes, and an internal pressure transducer. Specific instrumentation procedures are described in detail under "Data Collection and Analysis".

Long Term Experiments LT1 to LT5

Long-term experiments were conducted in five different experimental series, designated as LT1, LT2, LT3, LT4, and LT5.

Experiments LT3 and LT4 were designed to assess the biomechanical, physiological and biochemical effects of repeated mechanical shocks. These experiments were intended to reflect the prolonged exposures encountered in a sustained operational field environment. The purpose of experiments LT1 and LT2 was to provide a conservative walk-up design leading to the extended exposures of LT3 and LT4.

Experiment LT5 was designed to examine whether short term recovery occurs during intermittent exposure to repetitive shock. This information was supplemented by additional recovery data obtained from scheduled rest breaks or between daily ride exposures in LT3 and LT4. A short term recovery process could have a significant impact on the acceptable exposure level during combat maneuvers.

The first experiment (LT1) consisted of a series of 3.75 minute shock signatures, in which subjects were asked to predict their maximum tolerance time for continuous exposure to each motion signature which contained one type of shock. In the second experiment (LT2) the subjective fatigue and predicted tolerance times were examined over a 120 minute period for time dependence. Experiment LT3 evaluated the physiological, biomechanical and biochemical responses to a one day (7 hours) exposure to shock and vibration. In experiment LT4, subjects were exposed to prolonged vibration and shock environments (4 hours) on five consecutive days. Finally, experiment LT5 investigated the effect of rest breaks on the subjective fatigue and predicted tolerance times for exposure to repetitive shocks.

In these experiments, a single shock frequency was selected to limit the number of variables in the experiment. The frequency of 6 Hz was selected as an intermediate value between the peak response observed in the Phase 3 pilot study (4 Hz), and the natural frequencies of the Fairley-Griffin model (5 Hz) and the DRI model (8.4 Hz) (Fairley and Griffin, 1989; ASCC, 1982).

Experiment LT1

In the development of a health hazard assessment index for shock and vibration, it is necessary to develop a model to predict the cumulative dose of repeated shocks that may result in injury or chronic health effects. However, it is not ethical to expose subjects to a high enough dose to cause physical damage. In this experiment each subject was exposed to a short duration shock signature and asked to predict the amount of time that this type of motion could be tolerated in an operational environment. Comparisons were made between signatures having equivalent vibration dose values (VDVs), but containing shocks of different amplitudes, and delivered in different directions.

Five shock signatures were prepared to provide a VDV of approximately 15 or 30 $m.s^{-1.75}$, in the z axis. Identical shock signatures were then presented in each axis and direction. For each signature, the amplitude, shock rate and VDV are listed in Table 4.

Table 4
Motion signatures for Experiment LT1. Each signature was repeated in +x, -x, +y, +z, -z, and combined x, y, z directions.*

Amplitude (g)	Direction	Rate (shocks min^{-1})	Time (min)	VDV ($m.s^{-1.75}$)
1	+x, -x, +y, +z, -z	128	3.75	14.5
2	+x, -x, +y, +z, -z	8	3.75	14.4
2	+x, -x, +y, +z, -z	128	3.75	29.1
2	combined x,y,z	128	3.75	29.1
4	+x, -x, +y, +z, -z	8	3.75	28.9
Daily Total			18.75	38.6

* A shock frequency of 6 Hz was used in all signatures.

Each subject participated in experiment LT1 on five separate days with a minimum of 48 hours rest between experimental days. On each experimental day, the subject was exposed to five shock signatures separated by a ten minute rest. Of these five signatures, four presented shocks in a single direction (+x, -x, +y, +z, or -z), with a different direction being presented on individual days. The fifth signature was a combined x, y, z signature which was presented on each day to provide a consistent frame of reference.

Ten subjects participated in this experiment. To allow a rest period between signatures, two or more subjects rotated through the protocol simultaneously. During the final minute of each exposure, subjects were asked to estimate the maximum time the specific motion signature could be tolerated, and to rate their subjective comfort and the severity of the shocks. Details of the subjective measures are provided in the "Materials and Methods" section. The subjective questionnaire and rating scales are provided in Appendix B. A subset of the predictions of tolerance time obtained in LT1 were compared to predicted tolerance time in experiments LT2 and LT3.

Experiment LT2

Experiment LT2 was designed as an extension of LT1, and as part of the walk-up design for LT3 and LT4. In this experiment, the predictions of subjective tolerance were validated over an exposure duration of 120 minutes to compare to those obtained in LT1 from a 3.75 minutes exposure.

The shocks were delivered at a lower shock rate in LT2 than in LT1. The amplitude, axis and shock rate of each shock signature used in LT2 are listed in Table 5. The signatures were designed to test subjective predictions of tolerance at 3.75 minutes and 15 minutes of LT1 and LT2 respectively.

Subjects received a VDV of 29 after 15 minutes of exposure. This corresponded to the same VDV received after 3.75 minutes in LT1. Hence, it was expected that there should be a corresponding 1:4 relationship between the predicted exposure tolerance times. A lack of correspondence between the predicted tolerance times of the two experiments would indicate that subjective tolerance does not depend on VDV alone.

Experiment LT2 was also designed to evaluate the effect that direction of shock has on the subjective tolerance to shock signatures. It was expected that predictions of tolerance for the same signature would differ depending on the dominant axis and direction of the shocks.

Subjects performed the synthetic work task at 30 minutes and 90 minutes of exposure time. Each subject was also asked to report his subjective responses to the motion at regular time intervals throughout the 120 minute exposure. Subjective responses evaluated the severity of the shocks, the level of discomfort, the predicted tolerance time to the level of shock exposure, and how the motion environment affected their performance of the synthetic work task. Details of the subjective questionnaire are included in Appendix B. Predictions were obtained at 3.75, 7.5, 15, 30, 60, 90 and 120 minutes.

Table 5
Motion signatures for Experiment LT2.*

Amplitude (g)	Direction	Rate (shocks·min^{-1})	Duration (min)	VDV (m.s$^{-1.75}$)
2 g	+y	32	120	48.3
2 g	-z	32	120	48.3
2 g	combined x,y,z	32	120	48.3
4 g	-x	2	120	48.3

4 g	+z	2	120	49.5

* A shock frequency of 6 Hz was used in all signatures.

In conjunction with the two exposures to 4 g motion signatures, blood and urine samples were collected. Blood and urine samples were collected in accordance with procedure outlined in "Methods: Blood and Urine Collection". Subjects wore an activity monitor (Actigraph) during the period in which blood and urine samples were collected.

Six subjects participated in experiment LT2. The total daily exposure time for each subject was 120 minutes. To complete all motion signatures, each subject completed a 120 minute session on five different occasions, separated by a minimum recovery period of 48 hours.

Experiment LT3

Sustained operations in tactical ground vehicles may require soldiers to be exposed to a motion environment for prolonged periods of time. In order to simulate a vehicle ride representative of operational field conditions, a motion signature was created containing shocks in the positive and negative directions of all three axes (Table 6). The motion signature consisted of 2 g shocks delivered in the ±x,±y, and ±z directions and 4 g shocks delivered in the +z direction. All shocks had a fundamental frequency of 6 Hz. During each five minute period, subjects were exposed to 128 shocks of 2 g amplitude (randomly distributed as 32 ±x, 32 ±y and 64 ±z) and 2 shocks of 4 g in the +z direction.

A total of 10 subjects participated in this protocol. Each subject was exposed to seven hours of motion in a single eight hour session which included three rest intervals.

The exposure consisted of 4 motion periods of 105 minutes. The motion periods were separated by a 15 minute rest period at mid-morning, a 30 minute rest period at approximately noon and a 15 minute rest period at mid-afternoon. The rest periods allowed the subject a reasonable opportunity for washroom, food and beverage breaks. The VDV to which the subject was exposed was calculated to be: 29 at 15 minutes; 41 at 60 minutes; 48 at 120 minutes; 57 at 240 minutes; and 66 at 420 minutes of exposure.

Table 6
Motion signature for Experiment LT3.*

Amplitude (g)	Direction	Time (min)	VDV ($m.s^{-1.75}$)

2 g	±x,±y,±z	420	66.1
4 g	+z		

* All shocks were 6 Hz.

Each subject was fully instrumented for 3-lead ECG, EMG, spinal accelerometers, internal pressure, and Optotrak. During the experiment, data were collected for 5 minutes every 30 minutes, resulting in 15 collections over 7 hours. During each 5 minute period of data collection, a measurement of the effect of posture on biomechanical measures was made. Subjects normally adopted a slightly relaxed (i.e., curved back) posture while exposed to the shock signature. During the third minute of data collection, subjects were instructed to move to an erect posture for one minute, and then return to their preferred posture.

Blood and urine samples were collected in accordance with procedures outlined in "Methods: Blood and Urine Collection" Subjects wore an activity monitor (Actigraph) during the five day period in which biochemical measures were taken.

Subjects performed four trials of the synthetic work task at 35, 155, 245 and 365 minutes of motion exposure. Subjects were asked to report their subjective responses to the effect of the motion exposure at 3.75, 15, 30, 60, 90, 120, 150, 180, 210, 240, 270, 300, 330, 360, 390 and 410 minutes. Each subject rated the severity of the shocks, their level of discomfort, their predicted tolerance time, and how the motion environment affected their task performance.

Experiment LT4

These exposures were designed to establish subjective tolerance and physiological responses during sustained operations over a period of 5 days. Experiment LT4 was also designed to investigate markers related to physical damage following prolonged exposure. This allowed investigators to relate subjective tolerance to possible biochemical or physiological markers of tissue damage or fatigue. Evidence of changes in the biochemical, physiological, biomechanical and subjective tolerance may be used as a weighting factor or recovery factor in the development of a health hazard index in Phase 5.

Subjects were exposed to four hours of motion each day on five consecutive days. In order to simulate operational field conditions, subjects were exposed to the same shock signature as in LT3, consisting of 2 g and 4 g shocks at 6 Hz in a combined x,y,z signature (Table 7). This resulted in a VDV of: 29 at 15 minutes; 41 at 60 minutes; 48 at 120 minutes; and 57 at 240 minutes On each day, the motion exposure consisted of 2 motion periods of 120 minutes. The motion periods were separated by a 15 minute

rest period to allow the subject a washroom and beverage break. A total of 8 subjects participated in this protocol.

Table 7
Motion signature for Experiment LT4.*

Amplitude (g)*	Direction	Time (min)	VDV ($m.s^{-1.75}$)
2 g	±x,±y,±z	240	57.4
4 g	+z		

* All shocks were 6 Hz.

Each subject was fully instrumented for 3-lead ECG, EMG, spinal accelerometers, internal pressure, and Optotrak. Data were collected for 5 minutes every 15 minutes, allowing 17 collections over 4 hours. During periods of data collection, a measurement of the effect of posture on biomechanical measures were made as described above in "Experiment LT3". On each day, subjects performed trials of the synthetic work task starting at 35, 95, 155, and 215 minutes of motion exposure.

Blood and urine samples were collected in accordance with procedures outlined in "Methods: Blood and Urine Collection". Subjects wore an activity monitor during the nine day period in which biochemical measures were taken.

Subjective responses to the effects of the motion exposure were obtained at 3.75, 15, 30, 60, 90, 120, 150, 180, 210, and 240 minutes. Each subject rated the severity of the shocks, their level of discomfort, their predicted tolerance time to the level of shock exposure, and how the motion environment affected their task performance.

Experiment LT5

Operations in a TGV expose soldiers to an intermittent motion environment. A rest interval may allow soldiers to recover from the previous motion exposure. In this event, then rest breaks could be an important component of operational procedures, whether they are naturally occurring or deliberately imposed. To investigate this type of exposure pattern, subjects were exposed to a series of 3.75 minute shock signatures, totaling one hour per day, with or without a rest interval between each 3.75 minute signature. A total of 10 subjects participated in this protocol.

Each subject was exposed to two motion conditions having the same maximum VDV (Table 8). The motion signature contained the same shock pattern as experiments LT1 and LT2 with 2 g shocks combined in x, y, z directions at a rate of 128 shocks min^{-1}. In one condition, a 3.75 minute shock signature with a VDV of 29 was followed by 7.5 minutes of rest. This was repeated over 16 cycles for a total exposure time of 60 minutes distributed over a three hour period. The other motion condition consisted of the same 3.75 minute shock signature repeated 16 times without recovery periods.

This resulted in a continuous motion exposure of 60 minutes. In both conditions the subject was asked to rate the severity of the shocks, level of discomfort, and their tolerance time after each 3.75 minutes exposure The VDV of each condition was 58. Subjects completed each exposure on separate days, with a minimum of 48 hours between exposures.

Table 8
Motion signatures for Experiment LT5.*

Amplitude (g)	Axis	Rate (shocks·min^{-1})	Time (min)	VDV ($m.s^{-1.75}$)
2 g	combined x,y,z	128	60	58.2
2 g	combined x,y,z	128	16 cycles of: 3.75 motion 7.5 rest	58.2

* A shock frequency of 6 Hz was used in all conditions.

Risk Assessment and Safety Procedures

Risk Assessment

The levels of vibration and shock in the motion signatures of each experiment were compared with appropriate standards: British Standard "Measurement and evaluation of human exposure to whole-body mechanical vibration and repeated shock" BS 6841 (1987); and Air Standardization Coordinating Committee "Human tolerance to repeated shock" ASCC Advisory Publication 61/25 (1982). The International Organization for Standardization "Guide for Exposure of Human Response to Whole Body Vibration" ISO 2631 (1982);, although widely used, is not applicable to exposures containing non stationary events such as repeated shocks. It was therefore rejected for this purpose.

Appendix A of the British Standard 6841 is designed to account for the effects of repeated shocks, and as such is a more appropriate basis for assessment of the exposures contained in this study. Hence, the various motion signatures utilized in these

experiments were designed to produce equivalent, or proportional VDVs as defined in the BS 6841. However, the BS 6841 does not specify limits of comfort or safe exposure, as it is considered that there is insufficient data on which to base these limits. For reference, the ISO Exposure Limit for health effects due to random vibration (not including shocks) has a VDV of approximately 15 $m.s^{-1.75}$. This is considered the maximum safe daily exposure to avoid cumulative damage over a number of years. The BS 6841 states that "vibration dose values in the region of 15 $m.s^{-1.75}$ will usually cause severe discomfort. It is reasonable to assume that increased exposure to vibration will be accompanied by increased risk of injury".

A primary concern in this study was the safe level of acute exposure measured over seven hours or five days. For this reason we also referred to ASCC 61/25 (1982) for guidance. The ASCC guidelines indicate the magnitudes and numbers of shocks (in the +z direction) that can safely be sustained during a 24 hour period. The guidelines include levels of moderate discomfort, severe discomfort and 5% injury risk. The ASCC curves are based on the DRI Model of Payne (MIL-SPEC-9478A). This model was originally designed for a single high amplitude shock. It was subsequently revised to estimate the cumulative effects of multiple shocks using Miner's Hypothesis for material fatigue characteristics (Sandover, 1986), and adopted in the ASCC Advisory Publication 61/25 (1982).

The Payne-DRI model contains a higher natural frequency (8.4 Hz) and lower damping ratio (0.22) than the comparable model of Fairley-Griffin (1989). The Fairley-Griffin model, based on a large subject number exposed to random vibration, contains a natural frequency of 5 Hz and a critical damping ratio of 0.48. The results obtained in Phase 3 suggest that the Fairley-Griffin model may be more accurate for lower amplitude, repetitive signals. Hence, the level of exposure for each experiment was calculated and compared with the ASCC curve for severe discomfort using both the Payne-DRI model and the Fairley-Griffin model.

The cumulative VDV according to BS 6841, together with the level of exposure relative to the severe discomfort curve of the ASCC standard, are shown in Table 9 which includes:

1) VDV according to BS 6841
2) ASCC comfort rating based on Fairley-Griffin model
3) ASCC comfort rating based on Payne-DRI model

Table 9
Summary table of daily exposures, including a comparative comfort rating based on existing models.

Experiment	VDV	ASCC severe discomfort rating*	
	BS 6841 (z axis)	Fairley-Griffin model	Payne-DRI model
ST1	31.6	0.003	1.11
LT1	38.6	0.007	0.42
LT2 (2 g)	48.3	0.01	0.26
LT2 (4 g)	49.5	0.03	2.82
LT3	66.1	0.05	2.69
LT4	57.4	0.03	1.54
LT5	58.2	0.02	0.51

* Discomfort rating is expressed as a ratio of the number of shocks in the daily exposure/number of shocks (of the same type) required to cause severe discomfort

Comfort rating is reported as a "fractional dose" (i.e., the ratio of the number of shocks experienced to the number required to cause severe discomfort). Hence a value of less than 1.0 falls below the severe discomfort limit of the ASCC contours. These values indicate the worst case value for each experiment.

The large differences in predicted severity of exposure between the Fairley-Griffin and Payne-DRI models results from the different natural frequencies of the two models. The long-term experiments proposed in this study will contain shocks having a frequency of 6 Hz. The results of the Phase 3 pilot study show that for these shocks, the spinal transmission ratio is intermediate between the Fairley-Griffin and Payne-DRI models. Hence, it is reasonable to assume that the level of discomfort predicted in the table is underestimated by the Fairley-Griffin model and overestimated by the Payne-DRI model.

In this study, experimental daily exposures to shock are designed to be well below the limits of 5% injury. All experiments fall well below the severe discomfort level when using the Fairley-Griffin model in the ASCC standard. The highest exposure is 0.05 of the severe discomfort boundary. Four experimental exposures are above the severe discomfort boundary according to the Payne-DRI model.

Safety Procedures

A number of operating procedures were incorporated into the experimental protocol to ensure the safety of the subject and research team. These included subject screening, limiting shock exposure dose, controls in the experimental design, and safety features built into the MARS facility.

Safety in Experimental Design

The experimental design controlled shock exposure dose based on guidelines of BS 6841, (1987) ASCC Advisory Publication 61/25 (1982) and ISO 2631. The cumulative exposure to motion signatures of any one subject did not exceed 20 hours per week, or 30 hours per month. The maximum daily exposure took place in experiment LT3 in which each subject was exposed to motion for a maximum of 7 hours in one day. The maximum weekly exposure took place in experiment LT4, when each subject was exposed to the motion for a maximum of 4 hours per day for 5 consecutive days. Subjects did not participate in any further experiments for a minimum of one month after participation in either LT3 or LT4.

Subject Briefing and Orientation

Each subject completed the Volunteer Registry Data Sheet (USAMRDC Form 60-R) which documented participation in research conducted or sponsored by U.S. Army Medical Research and Development Command. These forms were copied and filed with the appropriate governing bodies to allow any delayed effect from these experimental protocols to be traced through USAMRDC.

A verbal explanation of the experimental protocol was given to each subject prior to motion exposure. Each subject completed a medical questionnaire to draw special attention to specific disorders and conditions as specified in the British Standards Institute 7085: 1989, "Safety aspects of experiments in which people are exposed to mechanical vibration and shock" and in the "Guide to experimentation involving human subjects", Human Experimentation Safety and Ethics Committee, Institute of Sound and Vibration Research, Southampton University, U.K. Prior to participation in experiments, subjects underwent a medical examination conducted at USAARL, Fort Rucker by the medical monitor of this project (a USAARL physician). This examination included health record review, history, focused physical exam, lumbo-sacral spine series, and blood and urine analysis.

Prior to collection of experimental data, each subject underwent a 15 minute motion exposure to familiarize him with the motion environment. This exposure consisted of three five minute epochs of 2 g shocks delivered at a rate of 32 per minute in each direction of the x, y, and z axes.

Subject Monitoring

Experimenters performed an ongoing assessment of pain, discomfort and fatigue reported by the subject. Subjects had the opportunity to report any adverse reaction or subjective evaluation of the vibration exposure both during and after motion exposure. Subjective tolerance times were assessed at regular intervals to prevent exposing subjects to the point where they would be harmed. The experiment was terminated if the subject

predicted a tolerance time which indicated that he had already sustained 75% of his tolerance level. All vibration experiments were carefully recorded in a log book including: date; subject identification code; duration; characteristics of the vibration exposure; results of start-up and pre-trial checks; researchers operating the equipment and conducting the experiments; and any unusual reactions or after-effects noticed either by the subject or the experimental team. A medical technician from USAARL was present at the MARS during all experimental procedures to assist in the event of an emergency.

Biochemical Monitoring

Prior to participation in experiments, a blood and urine sample was obtained from each subject for baseline biochemical measurements. When these data exceeded the normal values indicated in Appendix C, the medical monitor was informed. Medical treatment was ordered if appropriate. When this occurred, additional baseline blood and urine samples were obtained prior to the subject's participation in the experiment, until biochemical values were within the normal range. One subject was excluded from participation in the experiments due to a biochemical measurement that was outside the normal range after repeated measurements.

In the event that there was biochemical evidence of injury or tissue damage caused or aggravated by the experiments, a plan was developed to immediately refer the subject to the medical monitor. The medical monitor would then monitor the subject, and request additional tests or treatment as required. The subject would not be released from the study until the biochemical measure(s) returned to the range of normal values. This action was not required in the current study.

Biochemical measurements in blood and urine samples from subjects involved in LT2, LT3 and LT4 monitored acute and delayed (up to 4 days post-exposure) effects of motion exposure that might indicate tissue damage or stress. Results from biochemical tests were received between 36 to 72 hours from when the samples were submitted to the laboratory.

MARS Safety Features

The motion simulator was operated only by trained MARS technicians. The MARS controls included touch sensitive switches placed in the area of the MARS controller and within easy reach of the experimenters. Experimenters were in visual and voice contact with the subject at all times, and monitored the well being of the subject. Additionally, the MARS operator continuously monitored the vibration and shock exposure from the control booth. He was also in clear view of the subject, and in voice communication with other experimenters via headsets. If the subject wished to discontinue the exposure for any reason he spoke to the

experimenter or signaled the operator in the MARS control booth to stop the motion. Subjects were instructed to mount and dismount the simulator only when it was at rest.

Several safety and shut-down features were built into the MARS facility to ensure that vibration and shock levels did not exceed pre-determined levels. The computer control system included an automatic shutdown in case of control system failure. Automatic shutdown could be triggered by excessive table velocity, position, feedback failure, or power failure. The end stops of the MARS were also buffered mechanically to limit any overshoot deceleration to a maximum of 6 g.

Medical Monitoring

The medical monitor of the study was in radio contact with the MARS operator at all times, but was not present during testing procedures due to the relatively low risk of injury. An emergency response team was located at Lyster Hospital, Fort Rucker, AL, within 1 km of the MARS facility and could be on-site within five minutes. The MARS operator started the MARS only after making radio contact with the medical monitor and informing Lyster Hospital, on a daily basis, that motion exposure experiments were being conducted.

Materials and Methods

Multi-Axis Ride Simulator

The mechanical shake table (Multiaxis ride simulator, MARS, Schenk Pegassus, Detroit) was used to produce the vibration and shock signatures. Full specifications are provided in Appendix D. The MARS has a frequency range from 2 to 40 Hz. and a displacement range of ±3.5 inches. It consists of hydraulically driven actuators in each axis to control the amplitude and frequency output during operation. The frequency and acceleration amplitude are determined from a pre-recorded synthesized input signal. The output acceleration signal at the shake table is corrected for the table transfer function by means of a correction matrix and an iterative process in which the input signal and output signals are compared for quality of fit. Motion signatures were developed and the signals were input to the MARS in the form of a displacement command signal and the output motion was iterated to produce an acceptable fit. Control signals were then stored in the DEC-PDP11 computer system at the MARS facility.

A solid metal seat was securely mounted on the shake table and a bean-bag cushion taped on top of the seatpan. The seat did not have a backrest, since it was determined from communication with USAARL personnel that most drivers and occupants of TGVs do not utilize a backrest. The seat could be adjusted such that the subject's feet could rest comfortably on the MARS table with the knees and hips at approximately 90°. The cushion was designed to distribute the subject's weight without altering the input acceleration signal. The cushion was taped firmly to the metal seatpan in order to minimize lateral shear effects between the seatpan and cushion.

Development of Motion Signatures

Higher shock amplitudes, frequencies and VDVs were used during Phase 4 experiments than in the Phase 3 pilot tests. To accomplish this, some of the software safety stops had to be temporarily removed from the MARS system during signal development. Extensive testing of shock waveforms with target amplitudes up to 16 g and shock frequencies up to 40 Hz revealed that the actual attained acceleration profiles were significantly lower amplitude than desired. It was concluded that the dynamic response of the shaker table was limited to accurately reproducing shocks with frequencies less than or equal to 20 Hz and with amplitudes less than or equal to 4 g. In addition, the lower frequency shocks (i.e., shocks with frequencies in the 4 or 5 Hz range and in the 4 g amplitude range),

caused the shaker table to strike the shock absorber limit stops, causing unwanted distortion of the shock profiles. Additional processing of the control signal was necessary to prevent this from happening, as described below.

The shock waveforms were based on data from tactical ground vehicles (TGVs) analyzed by BCRI personnel in the Phase 2 report. Control of motion in each axis was performed by a digitized time series, corresponding to the target, or desired, acceleration waveform. The characteristics of the digital control sequence followed the stringent requirements of the software. The system software required the target acceleration time series to be digitized at a rate of 100 samples per second using a bipolar 13-bit data conversion, with an input range of 10.0 volts (i.e., + 10.0 V is represented by the digital values + 8192). The system calibration was set so that 1.0 V corresponded to 1.0 g acceleration.

Control records of up to 330 seconds were generated and reproduced on the MARS system. The digital control sequence for each axis was prepared using a number of programs developed on the GEDAP software system. Generation of the desired motion signatures required development of control signals for the MARS that incorporated background vibration with superimposed shock waveforms. For longer duration experiments, short motion signatures (300 seconds) were sequentially repeated to provide a relatively continuous motion exposure. This required a smooth transition between sequential motion signatures.

Generation of Background Vibration

Background vibration was synthesized using a Gaussian random number generator to produce an appropriate distribution of acceleration amplitudes. The Gaussian random number time series was synthesized with a 1.0 m sec^{-2} rms amplitude (frequency unweighted), and with an 82.0 second duration. This basic building block was used to construct all subsequent vibration signatures. Gaussian waveforms of any duration could be constructed using the GEDAP programs EXTRACT and APPEND. Although this particular waveform had zero mean amplitude and was band-limited to frequencies from 0 to 80 Hz, it was further band limited to frequencies between 2 and 40 Hz, to satisfy the performance requirements of the MARS vibration exciter. The acceleration amplitude could be adjusted using the GEDAP program TRANSFORM1. In all Phase 4 test signals, the Gaussian background vibration was adjusted to an ISO weighted amplitude of 0.5 $m.sec^{-2}$.

Generation of Shock Waveforms

Two GEDAP programs, RANDOM and S_RANDOM2, were developed to generate the shock waveforms. This was necessary to automate the

process of preparing a record containing a large number of shocks (with different amplitudes and frequencies) along with the requirement that the exact location of each shock be randomized. The program generated a series of user specified damped sinusoid waveforms, each defined by its fundamental frequency, initial peak amplitude (either negative or positive), and nominal location in the time series. The program randomized the actual location of each shock about its nominal location according to a user defined random interval. RANDOM enforced the rule that no two adjacent shocks could be of the same frequency. Another program, S_RANDOM2, allowed adjacent shocks to be of the same frequency. Two shocks were appended to the beginning of each motion signature to allow subjects to become accustomed to the motion prior to the start of data collection.

The resulting shock time series was then superposed on the appropriate Gaussian random background time series. To ensure that the shock amplitude was not altered by background vibration, the Gaussian signal had its amplitude reduced to zero in the immediate vicinity of where the shocks were to be inserted. This process was automated by using two new GEDAP programs SHOCK_ENDPOINTS and SNIP_NOISE2. The program SHOCK_ENDPOINTS determined the left and right flanking indices of each shock in a shock time series and output these values to another user-defined endpoint file. SNIP_NOISE2 took the background Gaussian file and utilized the times in the endpoints file to zero the background amplitude at shock locations. The combined record (Gaussian waveform plus shocks) was then produced by adding the shock record and the modified Gaussian record, using GEDAP program ADDXY.

Development of Control Signal

Once a specific acceleration time series (Gaussian waveform plus shocks) was generated, it was further manipulated to eliminate abrupt transitions on start up, or when the control sequence was repeated (to construct a long-term exposure). This was achieved by introducing one or more transitional blocks of data into the time series, each of which contained 256 elements and lasted for 2.56 seconds. A one or two block ramp was constructed at the beginning and end of each exposure. This allowed the MARS to reach its full acceleration without unwanted discontinuities in the motion. The ramp was linear, and was implemented by running the GEDAP program RAMP. One or two blocks of zero acceleration data were placed at the beginning and end of each signature using GEDAP program APPEND. This allowed a brief quiescent period on start-up, or between sequence repetitions, as required by the MARS control software.

Some signals, as constructed above, caused the MARS to exceed its travel limits, hit the shock absorbers, and distort the output waveform. This occurred for the low frequency, high amplitude

signals, (i.e., 3 and 4 g, 5 Hz shocks). By applying an appropriate high pass filter to the control signal, the limit problem was alleviated. The short term 4 g signals were high pass filtered with a cut-off of 2.5 Hz, while all other signals were high pass filtered at 2.0 Hz. After applying a high pass filter to a control signal, some of the shock peaks were attenuated, most notably at lower frequencies. To correct this effect, the amplitudes of the un-filtered shock files were increased using a transfer ratio. Transfer ratios were determined by calculating the ratio of the amplitudes of each shock before and after high pass filtering. Because each shock amplitude and frequency was affected differently, the transfer ratio had to be applied to each shock separately. After constructing the control signal, the result was a suitably high pass filtered signal which had the correct acceleration amplitudes, and which did not cause the MARS to hit the stops.

The complete signature was then scaled to the appropriate data format using the GEDAP program TRANSFORM1, and converted to ASCII format using the GEDAP program EXPORT. Once control signatures were generated for each of the three axes, the output file was formatted for use at the MARS facility, using the program TOUSA.

Equipment List

The following equipment were used during the phase 4 experiments:

1. MARS Multiaxis ride simulator (Schenck/Pegasus 5900)
2. VAX 4000 computer system
3. Two PC computers
4. Electromyograph: Telemg, Bioengineering Technology Systems, Milan, Italy
5. Force transducer (Maywood Instruments Ltd., Basingstoke, U.K., Model U4000 Load Cell)
6. Voltmeter
7. Electrocardiograph: 3 lead Hewlett Packard (Model 78304)
8. Electrocardiograph: 12 lead Marquette Electronics Inc. (Model MAC15)
9. Miniature accelerometers (9) range of ±10g and ±25g (EGAX-25, Entran Devices, N.J.)

10. Seatpad to house triaxial accelerometer cluster

11. Channel amplifiers and signal conditioning unit (Terrascience, Canada)

12. Optotrak Motion Analysis System (Northern Digital, Canada)

13. Entran miniature pressure transducer (model EPB-140-5s)

14. Piezo-electric accelerometers (P.C.B. 301A03)

15. Power supply (PCB 482A05)

16. Tape recorder (14 Channel analog recorder, Hewlett Packard)

17. Other general laboratory equipment and supplies.

Equipment Calibration

Internal Pressure Probe

Calibration of the internal pressure probes required determining a conversion factor for the voltage output in response to known pressure increments for each probe. The transducer output (volts) was initially calibrated at BCRI. with a mercury column manometer using air pressure and a sealed pressure-ported vessel (Erlenmeyer flask). The pressure transducer was installed into the Erlenmeyer flask through a hole in a rubber stopper, using waxed paper (parafilm) as a seal. To provide a simple field calibration, the pump valve and pressure gauge of a blood pressure cuff (sphygmomanometer) were calibrated using the mercury manometer within ± 2 mmHg and found to be accurate. At USAARL, the transducer was then calibrated using the pump valve and pressure gauge connected to the Erlenmeyer flask using rubber tygon tubing and a plastic t-junction. The pressure inside the flask was increased to approximately 300 mmHg and then reduced in 10 mmHg increments. At each increment, the pressure was stabilized and a voltage output from the pressure probe was recorded with a voltmeter. As the response of the pressure transducer was linear, a conversion factor was calculated in units of $mmHg \cdot volt^{-1}$ using a linear regression. The calibration factors did not change significantly from day to day. Hence, pressure transducers were calibrated on a weekly basis and again after termination of the last experiment to confirm that calibration values had not drifted.

Accelerometers

Spinal and seat accelerometers were calibrated by exposing the accelerometers to a 20 second duration, 1.0 g, 20 Hz sinusoidal

acceleration signal, using a portable mechanical shaker. The miniature accelerometers were taped directly onto the vibration platform of the portable shaker using double sided carpet tape. The seat accelerometers remained in the triaxial accelerometer block, which was oriented in the proper direction, taped to the platform, and tested individually for the x, y and z axis accelerometers. The voltage output from the 20 second signal was collected on the VAX 4000 computer system. Using the MATCHUP peak detection program, the voltage outputs for the 1 g acceleration waveforms were determined and averaged to produce a conversion factor in units of $m.s^{-2}.volt^{-1}$. Calibration values were found to be very stable from day to day. Therefore, calibration of the accelerometers was performed approximately every two weeks during Phase 4. In addition, calibration was performed each time an accelerometer was repaired or replaced.

Force Transducer

A calibration factor was determined for the load cell by recording output voltage in response to known forces, applied by suspending known masses (0 to 30 kg), and calculating the force of gravity on the mass. The output voltage was plotted as a function of force applied, and determined to be a linear relationship. An average calibration factor was determined in the units of $kg.m.s^{-2}.volt^{-1}$, or $N.volt^{-1}$. The load cell was calibrated once before Phase 4 experiments had been initiated, at the mid-point and at the end of the experiments to confirm the stability of calibration.

Selection of Subjects

A total of 76 volunteers were recruited from U.S. Army personnel assigned to Fort Rucker, AL. 22 of these volunteers were excluded from participation due to medical screening criteria or lack of availability for experiments. All 54 subjects that participated in experiments were healthy, fully informed, male volunteers between the ages of 19 and 40 years. All subjects had experience with motion from military or civilian exposure, (e.g., TGVs, air transport, heavy equipment, participation in operation Desert Shield/Storm). Some subjects participated in more than one experiment, with a minimum of one month for recovery between experiments.

Prior to participation in experiments, anthropometric data was collected from each subject. The data provided information on body composition and body proportions. Anthropometric measurements included height, weight, girths (biceps, forearm, wrist, chest, waist, gluteal, thigh, calf, ankle) and skin folds

(biceps, triceps, sub-scapular, chest, abdominal, supra-spinale, supra-iliac, mid-thigh, calf).

Overall, the mean age of subjects was 25.5 (±4.5) years, with mean height and weight of 70.5 (±2.4) inches and 182 (±23) pounds. Subject data for each experiment are summarized in Tables E-1 to E-6.

Subject Prescreening/Orientation

The experimental protocol, procedures and associated risks were explained verbally to each subject. Subjects read and signed the Volunteer Agreement Affidavit, Information for Subjects, and Instructions to Subjects forms. The Instructions form details procedures to be followed by the subjects prior to the experiments, such as exclusion of physical exercise. Subjects were not paid for their involvement as subjects in the motion experiments, but were renumerated for blood draws in accordance with the guidelines of the US Army Medical Research, Development, Acquisition and Logistics Command (USAMRDALC). Subjects were informed that they may select not to participate in the study, or to terminate participation at any point in the study, without concern for retribution. Each subject was instructed to notify an investigator if any back pain was experienced.

Prior to participation in experiments, subjects underwent a focused medical examination conducted at USAARL, Fort Rucker by a physician. The medical examination included x-ray examination of the anterior/posterior and lateral lumbar spine. It also included such measures as heart rate, blood pressure, range of motion and identification of special disorders or contraindications to vibration exposure. A medical questionnaire was used to draw special attention to specific disorders and conditions as specified in the British Standards Institute 7085: 1989, "Safety aspects of experiments in which people are exposed to mechanical vibration and shock" and in the "Guide to experimentation involving human subjects", Human Experimentation Safety and Ethics Committee, Institute of Sound and Vibration Research, Southampton University, U.K. Exclusionary criteria include: mental disorders, recent trauma or surgical procedures, presence of internal or external prosthesis (internal prostheses include pins, artificial hip joints and pacemakers; external prostheses include artificial limbs and eyes, false teeth and bridgework), history of back pain or strain (regardless of whether medical attention was sought) and disorders of the respiratory system, gastro intestinal tract, genito-urinary system, cardiovascular system, musculo-skeletal system, or nervous system. Thirteen subjects were excluded due specifically to the presence of spina bifida occulta.

After providing informed consent and obtaining medical clearance to participate, each subject was given an orientation session at the MARS. Safety precautions and procedures at the MARS facility were carefully explained to each subject. A seat height was established for each subject such that their feet could rest flat on the platform, and their knee formed a ninety degree angle. All subjects were instrumented for single lead ECG as a safety precaution to monitor heart rate during motion exposure.

In orientations for experiments ST1, LT3 and LT4, subjects were also instrumented for EMG. Baseline EMG calibration procedures were performed to establish maximal voluntary contraction levels, to train subjects on correct technique for calibration contractions, and to obtain data for dynamic EMG-calibration protocols. Subjects were then exposed to fifteen minutes of motion, representative of the motion expected in the respective experiments. During motion, the subjective response questions were asked to familiarize subjects with the questions and the response scales.

Subjects were encouraged to ask questions about procedures, protocols, and the experiments as often as they wished.

In experiments LT2, LT3 and LT4, biochemical measurements were taken before, during and after exposure. As a pre-screening device during the pre-exposure measure, any biochemical marker which was deemed to be outside the range of normal variance (including the effects of exercise stress), identified the subject for exclusion from exposure.

Electrocardiography

Electrocardiography (ECG) involved single lead (3 electrodes) and 12-lead ECG measurements with rhythm strip. Single lead ECG was monitored at rest prior to vibration exposure, throughout the vibration exposure, and during recovery for a minimum of 5 minutes or until heart rate returned to less than 100 bpm. ECG was monitored and recorded during exposures by connecting a Hewlett Packard (HP) single-lead electrocardiograph (Monitor model no. 7830A with patient lead HP14056B and HP14358-A) to an oscilloscope. An experiment was stopped if the heart rate was elevated greater than 150 bpm, or a sudden, unexplained increase in heart rate of greater than 30 bpm was observed. During long term exposure, single-lead ECG data was recorded and collected to disk. A pre- and post-experiment 12-lead ECG was performed by a laboratory technician using a Marquette Electronics Inc. (MAC15) device. Any abnormality indicated in the automated printout analysis was referred to the medical monitor. Two irregularities were observed, but medical follow-up showed normal variance.

Electromyography

Electromyography (EMG) was measured using surface electrodes placed bilaterally over muscles of the lumbar (L3) and thoracic (T9) spine (erectors spinae, spinalis thoracis, longissimus thoracis, trapezius, and latissimus dorsi), and over the right rectus abdominus and external obliques. An electromyographic amplifier with fiber optic coupling was employed for all EMG measures (BTS Telemg, Milan). The fiber-optic converter (patient box) was powered using a 12 volt drycell battery. Electrode leads with 100x preamplification at the electrodes were employed to reduce the influence of electromagnetic noise on signal integrity. The gain was set to 2, 5 or 10 at the EMG amplifier, as required to provide optimum signal magnitude. The high pass filter of the EMG amplifier was set at 10 Hz and the low pass filter was set at 200 Hz to minimize motion artifact and prevent signal aliasing.

EMG activity was calibrated against force generated during a series of test contractions. Force generated was measured using a force transducer (Maywood Instruments Ltd., Model U4000, range ± 100 kg) attached to a climbing harness worn by the subject at chest level. Feedback of target force levels was provided to subjects using a voltmeter which displayed the force transducer output. Calibration contractions of the back muscles were performed while subjects were seated. Subjects were required to attempt extending the trunk at the waist against the resistance of the chest harness. The pelvis was stabilized during contractions using 2 canvas cargo straps and a seat belt. Calibration of abdominal muscles required the subject to attempt to flex the trunk against the resistance of the chest harness, while the lower body was stabilized as above.

During the orientation session for experiments ST1, LT3, and LT4, three brief maximum voluntary contractions (MVCs) were completed to determine a 100% MVC level. The equivalent force transducer voltages were calculated for 5%, 10%, 20%, 30%, and 40% MVC. Subjects then performed a series of five submaximal (5 to 40% MVC) contractions of ten seconds in duration. To assess the influence of non-static contractions on force-EMG calibrations, three ramp contractions and three pulse contractions were performed. During ramp contractions, subjects progressively increased the force exerted from rest to 50% MVC within 10 seconds. During pulse contractions, subjects attempted to produce a very brief 50% MVC contraction using a rapid exertion against the harness.

For experiments ST1, LT3, and LT4, subjects performed the series of five submaximal (5 to 40% MVC) contractions, and one ramp contraction. This series of contractions was performed immediately prior to exposure in ST1 and both pre- and post-exposure for LT3 and LT4. To avoid the potential of damage to

accelerometers or IREDs by the harness, all calibration contractions were performed prior to attachment of this equipment for pre-exposure tests, and after removal of this equipment for post-exposure tests.

Muscle fatigue due to long duration motion exposure in experiments LT3 and LT4 was assessed using a series of ten consecutive test contractions, each lasting ten seconds at 20% MVC. This series of contractions was performed following the EMG-force test contractions, both prior to and after the exposure condition. Subjects were allowed a brief rest of approximately five to ten seconds between contractions.

Localized muscle fatigue was investigated using two methods of analysis with EMG data. The shift in mean frequency (MF) of the EMG spectrum between pre- and post-exposure test contractions was evaluated for experiments LT3 and LT4. The experimental method and analysis was based upon the methods of Voss and Krogh-Lund (1989) and Hagg (1991). In addition, the rms magnitude of EMG activity was quantified for the first and last measurement intervals in experiment LT3 to establish whether there was an overall increase in motor unit recruitment for similar motion exposure.

Frequency spectra were averaged for the ten submaximal contractions to provide a mean spectrum. The mean frequency was computed as the ratio of the first and zeroth spectral moments of the mean spectrum, for each of the four muscle sites. The delta mean frequency was computed as the difference between pre- and post-exposure mean frequency, and compared with the standard deviation of the group data for each muscle site. A two-tailed paired t-test was then computed for each set of pre-exposure and post-exposure mean frequencies, with a null hypothesis that the difference between the means was zero.

The root mean square of rectified EMG was computed across the entire 370 seconds of the first and last measurement interval of experiment LT3. A two tailed paired t-test was computed to test the hypothesis that there was no difference between means in the first and last data sampling trials.

Acceleration

Acceleration was measured at the seatpad, and at the skin surface over the lumbar and thoracic spine. Acceleration at the seat was measured using three single axis Entran accelerometers (± 25 g), positioned in a triaxial accelerometer block, and housed within a molded flexible epoxy seatpad constructed according to the SAE specifications (1974). The seatpad accelerometer system was securely taped to the seat cushion between the subject and the cushion. Acceleration at the spine was measured using Entran

miniature accelerometers (weight 0.3 gm; range of ± 10 g or ± 25 g) attached to the skin by a small square (< 1 cm^2) of two-sided adhesive tape. Acceleration signals were amplified (500x or 200x) and lowpass filtered (220 Hz) by a Terrascience signal conditioning amplifier. Acceleration signals were recorded, in parallel, to the VAX computer system and to a TEAC VHS recorder.

In order to characterize the vertebra-skin properties, the response of each tissue-accelerometer sub-system was measured prior to the start of the motion protocol. Data were obtained for each subject for the y and z accelerometers. While the subject was sitting on the MARS table, the y axis accelerometer was perturbed by placing a finger on the skin beside the accelerometer, pulling the skin sideways, and then releasing. The z axis accelerometer was similarly perturbed by pulling the skin downwards and releasing. During a 20 second data collection, several perturbations of both the thoracic and the lumbar accelerometers were performed. In this document, this process is referred to as a skin pluck.

Waveform Analysis

Prior to analysis, the unprocessed acceleration data and shock spectra were inspected to gain a detailed understanding of the waveform shape and frequency content. This was required to establish optimal signal processing methods. Characteristics of the acceleration waveforms were utilized in the selection of bandpass filters, development of a method to correct for motion of the skin-accelerometer system, and development of peak detection algorithms. Several distinct features were evident in the spinal acceleration response to shocks applied at the seat.

z Axis Response

The lumbar z axis acceleration response to a positive z axis 4 g, 4 Hz seat shock in the z axis is illustrated in Figure F-1. Two distinct features were observed in the acceleration response to z axis shocks:

1. A high frequency component (>20 Hz) in the acceleration response, and

2. Two acceleration events in the response to a single shock input.

High frequency components were evident in the response to large amplitude shocks (2 to 4 g) at frequencies less than 11 Hz. These high frequency components had a sufficient amplitude to significantly influence acceleration transmission ratios. It was believed that a high frequency response of the skin-accelerometer system may have produced these components superimposed on the

underlying spinal acceleration. A method of correcting the acceleration signals recorded from the spine was therefore developed. This method is described in the "Skin Transfer Function" section. All skin accelerometer data in the z and y axes were processed to correct for the response of the skin-accelerometer system.

The acceleration response to a single z axis shock contained two distinct events. The initial response to the input shock caused the subject to briefly leave the seat. This was then followed by a second response as the subject impacted the seat. The impact of the subject on the seat was also recorded in the seat acceleration signal as a high frequency pulse approximately 0.3 seconds after the initial shock peak. Because there were two distinct acceleration events in response to a single shock input, a method of selectively analyzing either the first or second acceleration response needed to be developed. The initial acceleration event was analyzed to provide transmission ratios for all shock amplitudes and frequencies, since this represented the primary response to a shock input at the seat. Transmission ratios were also calculated for the second acceleration event in response to 2, 3 and 4 g input shocks, since the secondary response at these shock amplitudes had a similar magnitude to the initial response. The specific analysis methods used to determine transmission ratios are described below.

Figure F-2 shows the input positive z axis 4 g, 4 Hz seat shock and the unprocessed z axis thoracic accelerometer response. The thoracic response showed similar characteristics as the lumbar response, with dual acceleration events in response to a single shock input. The impact as the subject returns to the seat is again observed in the seat signal as a high frequency pulse approximately 0.3 seconds after the initial shock peak.

y Axis Response

The unprocessed y axis lumbar skin accelerometer response is shown in response to positive 4 g, 4 Hz shock input at the seat in the y axis (Figure F-3). The spinal response was attenuated to approximately 60% of the peak input shock at the seat. The peak response at the lumbar spine lagged behind the input peak by about 50 milliseconds.

Figure F-4 shows the comparable unprocessed y axis thoracic accelerometer response to a positive 4 g, 4 Hz y axis shock input at the seat. Again, attenuation of the response relative to the input shock was observed. The thoracic response peak was typically reduced to about 20% of the peak input seat acceleration. The thoracic response was also inverted relative to the seat and lumbar acceleration profile. For example, the maximum positive acceleration response measured at the thoracic spine corresponded

to the maximum negative peak in the seat input shock and in the lumbar response. Hence, the thoracic data had to be inverted prior to implementation of the peak detection program which was used to compute thoracic transmission ratios. The peak response also lagged the input peak by approximately 50 milliseconds.

x Axis Response

Figure F-5 is an example of the unprocessed x axis lumbar accelerometer response to a positive x axis shock of 4 g, 4 Hz input at the seat. As in the y axis, the x axis response was attenuated and lagged the input peak.

The thoracic accelerometer response is illustrated in Figure F-6. This plot also illustrates attenuation of the spinal response to an x axis shock and a delay between peak shock input and peak response. The thoracic acceleration waveform was inverted relative to both the seat and lumbar spine shock waveforms. Therefore, the thoracic acceleration signal also needed to be inverted prior to peak detection.

Spectral Analysis of Shock Waveforms

Spectral density functions were computed for input shocks and corresponding lumbar and thoracic acceleration responses in each of the x, y, and z axes. This provided some insight into the nature of shock transmission that was useful in understanding the details of transmission ratios calculated later.

Figure F-7 shows the spectral density functions of a positive 4 g, 20 Hz z axis shock, with the lumbar and thoracic z axis response. The energy (defined by the area under the spectral density plot) was significantly reduced for the response spectra compared to the energy of the input shock spectrum. The peak frequency of the response was shifted toward a lower frequency, with the lumbar response showing a clear peak frequency at 4 to 5 Hz.

The spectral density functions of a positive 4 g, 4 Hz z axis shock, with the lumbar and thoracic z axis response are illustrated in Figure F-8. Unlike the response spectra to a 20 Hz input shock, the spectra of the spinal responses to a 4 Hz shock demonstrated greatly increased energy and maintained the same peak frequency as the input spectrum. There was slightly greater energy in the lumbar response than in the thoracic response.

Figure F-9 illustrates the spectral density of a positive 4 g, 20 Hz y axis shock and the responses at both lumbar and thoracic levels. The corresponding data for a positive 4 g, 20 Hz shock in the x axis is illustrated in Figure F-10. The spectral density functions in both x and y axes showed similar trends. The energy

in the response spectra was considerably reduced from that in the spectrum of the input shock, and the peak frequency of the response was shifted to 4 or 5 Hz from the input peak of 20 Hz. The y axis showed the greatest reduction of energy, followed by the x axis. The response spectra for both x and y axes demonstrated a greater reduction in energy than the response spectra for the z axis.

Treatment of Acceleration Data

Seat and spinal acceleration records were visually inspected on the VAX 4000 using GEDAP software. The seat acceleration waveforms contained higher frequency components superimposed on the original shock signal computed for input to the MARS controller. A number of software filters were evaluated to improve the signal quality.

A low pass filter with a cut-off frequency of 60 Hz was used for the x and y axes spinal acceleration data, whereas a 150 Hz cut-off frequency was used for the z axis spinal acceleration records. Different cut-off frequencies were used between axes because of the existence of valid, high frequency (up to 100 Hz) accelerometer responses in the z axis, which were absent from the x and y axes responses. The cut-off frequencies were selected so that most of the invalid high frequency components were removed with minimal attenuation of the signal peaks for the underlying shock waveform. To maintain consistency in the treatment of acceleration data, and avoid distortion of transmission ratios, the seat acceleration records were also low pass filtered. Seat acceleration data for the x and y axes were filtered at 60 Hz, whereas the z axis seat data was filtered at 110 Hz. The 110 Hz cut-off frequency for the seat accelerometer was selected due to high frequency waveform components (response peaks up to 250 Hz) caused by the subject leaving the seat and then impacting the seat on the MARS in response to both positive and negative 2, 3, and 4 g shocks.

Low pass filtering caused a frequency-dependent attenuation of the seat acceleration peaks. When acceleration data filtered at 110 Hz were compared to data filtered at 150 Hz, only the positive 4 g, z axis data had significant (greater than 2.5 per cent) attenuation of the accelerometer signals. Therefore only these data sets were corrected. Several multiplication factors were calculated based on the difference in amplitude between data filtered at 110 Hz or at 150 Hz. A multiplication factor was derived for each of the impact frequencies present in the signal profile (i.e., 4, 5, 6, 8, 11, 15 and 20 Hz). The positive 4 g transmission ratios were corrected using these multiplication factors. The acceleration data were also high pass filtered at 0.5 Hz to remove any baseline bias or zero drift from the data.

Skin Transfer Function

Prior to analysis of acceleration data, it was necessary to determine, and correct for, any movement of the skin surface relative to the underlying bone (spinous process). This correction required a knowledge of the "bone-skin transfer function" for the y and z spinal accelerometers for each subject. Measured acceleration signals were then multiplied by their respective inverse transfer functions. This correction eliminates any contribution of bone-skin movement and provides the true acceleration at the spinous process. In this document, this procedure is referred to as the skin transfer function (STF) method.

As x axis accelerometers measured motion perpendicular to the skin surface, they were not sensitive to shearing motion between the spinous process and the skin. Hence a skin transfer function was not computed for these accelerometers.

The influence of the STF on calculated transmission ratios, relative to low pass filtering at 150 Hz or at 40 Hz, is described below in the section "Comparison of Filtering Effects on the z axis Transmission Ratio".

Linear Modeling Approaches for Identifying the Transfer Function of the Skin.

Hinz et al. (1988) developed a method of calculating bone accelerations from miniature accelerometers attached to the skin. The soft tissues between the spinous process and the accelerometer were modeled as a simple Kelvin element, whose parameters described an approximate transfer function between the bone (input) and skin surface-accelerometer (output). System parameters were determined from free damped oscillations of the accelerometer-tissue complex in response to an initial displacement, using the "logarithmic decrement" method (Korn & Korn, 1961). This approach was based on the assumption of Franke (1951) that the skin can be described in the first approximation as a Kelvin element for a single excitation and small amplitudes. A similar technique was reported by Smeathers (1989) for measuring accelerations of the spine during walking and running, and by Kitazaki and Griffin (1995) to measure accelerations of the spine and abdomen during low level (2.0 $m.sec^{-2}$) sinusoidal vibration. Both Hinz et al. (1988) and Smeathers (1989) applied this method to measurement of accelerations that were less than 20 Hz. Kitazaki and Griffin (1995) applied the method to accelerations below 35 Hz.

Skin perturbation data showed that the free response of the vertebra - skin subsystem contained both high and low frequency components. Hence the system could not be truly represented as a simple Kelvin element (i.e., a single degree of freedom, second order system). Frequency components of the y and z axis

accelerations measured in response to shocks at the seat were inspected using power spectral analysis. Only low frequency accelerations (<20 Hz) were recorded at the y axis spinal accelerometers in response to shocks at the seat. Skin perturbation data collected in the y axis were therefore low pass filtered, and the tissue-accelerometer subsystem was then modeled as a simple Kelvin element.

y Axis Spinal Accelerations

Skin perturbation data were band pass filtered at 0.5 to 40 Hz. The free response of the tissue-accelerometer system to each perturbation was viewed on the computer monitor using MATLAB® software (The Mathworks Inc., Natick, MA). A typical free damped oscillation of the L3 accelerometer is shown in Figure F-11. The magnitude and timing of adjacent acceleration peaks were digitized on the display monitor. The damping ratio (ζ) and natural frequency (ϖ_n) of the tissue-accelerometer system were then calculated from the logarithmic decrement in amplitude (δ) and the period of the waveform (τ) using the relationships:

$$\zeta = \frac{\delta}{(4\pi^2 + \delta^2)^{1/2}} ;$$

and,

$$\varpi_n = \frac{2\pi}{\tau(1-\zeta^2)^{1/2}}$$

where,

δ = logarithmic decrement
τ = period (s)
ζ = fraction of critical damping
ϖ_n = undamped angular natural frequency (rads/s)

The transfer function, $H(\varpi)$, between the spinous process and accelerometer was characterized by the amplitude ratio

$$H(\varpi) = \sqrt{\frac{1+(2\zeta\varpi/\varpi_n)^2}{(1-(\varpi/\varpi_n)^2)^2 + (2\zeta\varpi/\varpi_n)^2}}$$

and the phase angle, $\phi(\varpi)$

$$\phi(\varpi) = TAN^{-1}\frac{2\zeta(\varpi/\varpi_n)^3}{(1-(\varpi/\varpi_n)^2)^2 + (2\zeta\varpi/\varpi_n)^2}$$

where

ϖ = angular frequency.

The bone-skin transfer function of each accelerometer for each subject was based on the average values of ζ and ϖ_n obtained from four separate perturbations.

To estimate the acceleration response of the vertebra underlying the accelerometer, spinal acceleration data of each experimental exposure were converted from the time domain to the frequency domain using a forward FFT. The frequency spectrum was multiplied by the inverse of the bone-skin transfer function, and the data then reconstructed in the time domain using an inverse FFT. This mathematical treatment of the data provided an estimate of the input acceleration signal at the spinous process necessary to produce the output acceleration signal measured at the skin surface.

z Axis Spinal Accelerations

Analysis of spinal accelerations in the z axis revealed substantial acceleration "spikes" in response to shocks input at the seat. These acceleration spikes occurred in response to 2, 3 and 4 g shocks and contained frequency components well above 20 Hz. The higher frequency responses (in the range 20 to 150 Hz) were most noticeable as a result of the 4 to 8 Hz shock inputs, and were present in response to both positive and negative shock directions. Acceleration spikes tended to coincide with the subject hitting the seat. Therefore, they could not be considered to be artifacts in the data which could be removed by low pass filtering. Hence, the assumption of a simple Kelvin element in determining the z axis skin transfer function was inadequate. When this model was applied (using the method described above), the inverse transfer function resulted in an artificial magnification of the high frequency components of the accelerometer signal. Theoretically, these high frequencies would not have been transmitted if the second order linear model was correct. To circumvent this problem, new approaches to modeling of the bone-skin transfer function were investigated. These method included parametric modeling using Least Squares Estimation, Prony's algorithm (Parks and Burrus, 1987) and Steiglitz-McBride (STMCB) iteration (Steiglitz and McBride, 1965); and a linear approximation of a two degrees of freedom model.

Parametric Modeling

A parametric model was developed based on measured input and output data. Assuming a linear system, there were various approaches which could be used for developing such a model. Several of these approaches were investigated and are discussed below.

The general parametric model for the skin transfer function was expressed as a linear, constant coefficient, differential equation which predicted the output acceleration given the input acceleration, and vice versa. Because data were sampled, the discrete-time version of this model was used, namely a recursive difference equation, in which the output of the system at a given time was a linear function of the previous inputs and previous outputs:

$$y(k) + a_{n-1}y(k-1) + \ldots + a_0 y(k-n) = b_m u(k) + b_{m-1}u(k-1) + \ldots + b_0 u(k-m),$$

where u(k) and y(k) were the input and output values, respectively, sampled at instant k, with coefficients a_i and b_i .

Three modeling methods were investigated, all of which involved optimizing the coefficients a_i and b_i given the measured input and output data from the system. The first method was the Least Squares Estimation (LSE) technique, which fits the data to a polynomial corresponding to the difference equation. As anticipated, this approach was not appropriate for the skin transfer function problem since there is, in fact, no input data, only an initial excitation (the skin pluck). It was hoped that the initial acceleration at time t=0 could be modeled as an input signal $u(k) = A_0$ for k=0 and $u(k) = 0$ for $k \neq 0$. This approach did not yield a functional result.

Two other approaches were tried: Prony's algorithm (Parks and Burrus, 1987) and the Steiglitz-McBride (STMCB) iteration (Steiglitz and McBride, 1965). Both approaches seemed to overcome the limitation of having no true input signal available. Both methods utilize the fact that a linear system can be completely characterized by its impulse response. (Intuitively, this can be seen from the fact that an impulse, by definition, consists of all frequencies and, therefore, excites all modes of a system). The Prony and STMCB algorithms determine the difference equation coefficients from the assumed impulse response of the system. It was assumed that plucking the skin resulted in an acceleration impulse and that the signal measured by the accelerometer was the approximate impulse response. Both algorithms produced a 4th order model with two resonant frequencies, the lower of which was similar to that obtained using the "logarithmic decrement" method. The main disadvantage was that a true impulse is assumed to have a weight of 1, which was not the case for the skin pluck impulse. As a result, the true magnitude of the transfer function's frequency response was subject to a scaling factor error.

Two Degrees of Freedom Linear Approximation

From the above analyses it appeared that the soft tissues between the vertebra and skin contained two resonant frequencies,

or possibly represented a non-linear system. To overcome this problem and obtain a linear approximation of the system the following method was utilized.

A series of perturbations were applied to the skin immediately below the z axis accelerometer, and the resultant acceleration data recorded. The skin perturbation data were band pass filtered at 0.5 to 150 Hz. The free damped response of the tissue-accelerometer system to each perturbation was viewed on the display monitor using MATLAB® software. An example of free damped oscillation of the LT4 accelerometer is shown in Figure F-12. The frequency spectrum of the free damped oscillations of the vertebra-skin subsystem was computed and plotted, and the (two) dominant frequency components of the acceleration data were identified as shown in Figure F-13. The skin perturbation data were then low pass (0.5 to 50 Hz) and high pass filtered (50 to 150 Hz) to isolate the two main frequency components. The high and low pass time domain components of the same perturbation are shown in Figure F-14 and F-15).

It was assumed that the data within each frequency band could be modeled independently as the outputs of separate Kelvin elements. The magnitudes and timing of adjacent acceleration peaks within each frequency band were digitized on the display monitor. The system parameters (ϖ_n and ζ) of the two frequency bands were then determined separately using the "logarithmic decrement" method. These parameters defined two independent models for the low and the high frequency components of the tissue-accelerometer subsystem. The bone-skin transfer function of each model was then determined from the system parameters as described above (ϖ_n and ζ).

A compensation filter was developed with frequency response characteristics derived from the low pass and high pass models. The transfer function of each 'model' was obtained using a MATLAB® subroutine. The magnitude of the frequency response curves were plotted and the frequency (f_i)at which the two curves intersected was determined. This frequency was used to delineate the low and high frequency ranges of the compensation filter. An example of this procedure is shown in Figure F-16.

In order to correct the spinal acceleration response, the following procedure was used. The measured spinal acceleration in the z axis was low pass, and then high pass filtered to create two separate data records. The common cut-off frequency (f_i) was determined as described above. The filter characteristics of the appropriate model were then applied to the low pass and high pass frequency components of the spinal acceleration data. The corrected acceleration data within the two frequency bands were then added to obtain the predicted acceleration at the spinous

process. This procedure provided a piecewise inverse transfer function over the complete frequency range (0.5 to 150 Hz).

In summary, the spinal acceleration data were separated into low frequency and high frequency components; each component was treated separately with a linear correction; and then the two components were summed to obtain the corrected acceleration at the vertebra. The spinal acceleration data recorded by the L4 accelerometer in response to a negative 4 g, z axis shock at the seat is shown in Figure F-17. For comparison, the predicted acceleration at the spinous process after correction by the compensation filter is superimposed on the acceleration data.

Transmission Ratios

Spinal acceleration was reported as a transmission ratio of the acceleration output at specific spinal vertebral levels to the seat acceleration input. The transmission ratios were averaged from the response to 2 shocks at each frequency applied to each of 10 subjects in experiment ST1. The mean transmission value reported at each frequency was calculated from these 20 transmission ratios. The mean transmission ratio of all five shock amplitudes input at the seat (based on 100 measures of transmission) was also reported at each frequency. The lumbar acceleration data from 2 subjects were excluded from analysis of z axis transmission ratios because of technical problems with the accelerometers. The transmission values reported for spinal acceleration at L4 in response to z axis shocks were therefore derived from 16 transmission ratios. Hence the mean transmission ratios for z axis data were computed from 180 measures of transmission.

The spinal acceleration response to a single z axis 2 g, 3 g, or 4 g shock contained two distinct acceleration responses, as discussed in the section "Waveform Analysis" above. Transmission ratios in the z axis were computed for the first acceleration response at all shock magnitudes and for the second acceleration response to shocks of 2 g or greater.

Comparison of Filtering Effects on the z Axis Transmission Ratio

The mean lumbar transmission ratios for positive and negative 4 g shocks measured at L4 and T3 were calculated using three different analysis methods. This included data that were low pass filtered at 150 Hz (raw data), data that were low pass filtered at 40 Hz, and data corrected for skin-accelerometer response using the skin transfer method (STF). These data are listed in Tables E-7 and E-8 and shown graphically in Figures F-18 to F-21. The three methods were examined to establish the relative effect of applying the STF method compared with no elimination of high frequency signal components (raw data) and compared with the

simpler approach of eliminating all high frequency signal components (40 Hz low pass filter).

There were distinct differences in the transmission curves derived by each method of analysis. For positive and negative 4 g shocks, the raw data transmission ratios were higher than those computed using the STF method or 40 Hz low pass filtering (Tables E-9 and E-10). The only exception to this was the seat to T3 transmission for negative 4 g impacts at 20 Hz, as seen in Table E-10. Figure F-17 demonstrates that the STF method removes some of the high frequency components from the spinal acceleration response. In the positive direction, the STF method produced lower transmission ratios than those computed for the raw data, while maintaining the frequency dependent shape of the response curves. Low pass filtering at 40 Hz produced transmission ratios lower than those for the STF and raw data, except for positive impacts above 8 Hz and negative impacts above 12 Hz. In the negative direction, the pattern of response computed with STF follows the pattern of raw data. However, the 40 Hz response curve shows much lower transmission ratios at low frequencies (< 11 Hz).

Because the use of a 40 Hz low pass filter significantly altered the pattern of transmission ratios at low frequencies, this method was not used to compute transmission ratios. The STF method reduced the magnitude of transmission, but maintained the frequency dependent pattern of the response. Data were therefore processed using the STF method, as described in the section above, "Skin Transfer Function".

Shock Peak Detection and Transmission Ratio

To determine the transmission of acceleration from the seat to the spine for this phase of experiments, a previously developed program (MatchUp) was used to identify the discrete shock events within the ST1 acceleration data in response to positive and negative 2 g, 3 g, and 4 g shocks. The program allowed the user to input the number of shocks to be identified at the seat, the spinal acceleration (input data file) to be compared to the accelerations at the seat, and the time period (window) to be analyzed around each shock event. The program first identified the highest peak acceleration values occurring within the seat acceleration data file. To prevent two maxima being identified within a single shock (due to higher frequencies superimposed on the shock waveform), an exclusion window was set around the shock peak once the (highest) maxima had been identified. The timing of each shock peak detected at the seat was provided as output from the program to allow confirmation that the correct peaks had been identified. Comparison of identified shock peak location with the known location of shock peaks in the MARS control signal allowed for verification of peak detection.

Once the positive peak value of seat acceleration was identified, the program identified the acceleration minima (negative peak) within the shock window. The program next analyzed the spinal response data to identify the corresponding positive and negative acceleration peaks occurring within the shock window. The time delay between the seat and spinal peaks acceleration was then quantified.

The analysis of both positive and negative 0.5 g and 1 g acceleration data sets proved difficult because the background vibration was equal to or greater than the expected shocks. Thus, the original analysis program could not find the correct signal peaks. A new program (MatchUp_Time) was developed (based on the original MatchUp program) which allowed the user to enter the expected (dependent) signal shock timing profile, and thus find the shocks from within a shock signal of equal or greater amplitude surrounding noise. Identification of each shock within the signals was achieved by entering the expected number of shocks, maximum response time (window), exclusion window, shock timing profile, offset to first shock, tolerance for each shock (window to find the input shock's peak amplitude), drift between the dependent and independent signals, 2 input data filenames, ASCII output file, and the output style. Using the entered information this program performed the same signal analyses as the original program and also generated the same output information for 0.5 g and 1 g shocks.

For the positive and negative 2, 3, and 4 g data sets, in the z axis, there was a second peak in the spinal acceleration data that was associated with the subject landing on the seat, after having left the seat in response to the initial shock input. Analysis for the second spinal acceleration peak was performed for the lumbar, thoracic and internal pressure data sets. This was achieved through the development of a third program (MatchUp_Skip) based on the original analysis tool (MatchUp). The difference between the original and the new tool was that the user could input a "skip" time which allowed the signal analysis of the dependent data set to begin after the skip time, while still using a maximum response time (window) exactly like the method for the first peak analysis. Thus the skip time could be set to exclude detection of the first spinal acceleration peak.

Analysis and visual inspection of a number of data files established that a shock window of 300 msec (for the x and y axes) and 225 msec (for the z axis) was adequate to provide identification of the positive and negative acceleration peaks in response to the shock input at the seat. The output from the program provided the time of each shock event, initial peak and peak-to-peak acceleration at the seat, initial peak and peak-to-peak acceleration at the spine, seat to spine transmission ratio for the initial and peak-to-peak accelerations, and time delay between the initial seat and spinal acceleration peaks. Data

output was presented in an ASCII file that could readily be exported to a PC and analyzed by Microsoft Excel.

The same peak detection program was used to analyze shock transmission for internal pressure. In this case, transmission was expressed as the ratio of the peak internal pressure response to acceleration input (units of $mm.Hg.m^{-1}.sec^2$). A window of 300 msec (for the x and y axes) and 225 msec (for the z axis) was also used to analyze internal pressure data.

Processing Transmission Data

Several batch programs were written to process the transmission data of all ten subjects for the short-term exposures to 0.5 g, 1.0 g, 2.0 g, 3.0 g and 4.0 g shocks for each of the anatomical locations measured (lumbar, thoracic, and internal pressure). The batch program first demultiplexed the data files of one subject at a given exposure condition. The acceleration and internal pressure data files were then treated by GEDAP software to remove the mean amplitude, which eliminated any offset error. The data files were filtered as described in the previous section. For both the y and z axis spinal accelerations, the signals were treated with the appropriate inverse STF. The appropriate peak detection program for the desired analysis was then used to compare the spinal accelerations and internal pressures to the input seat accelerations. Shock transmission ratios were calculated for each shock event, and transferred from the VAX to a PC for further analysis using the Excel. This process was repeated for all five shock amplitudes, in all three directions of acceleration and for all ten subjects.

In Excel, tables were created to combine transmission data and delays (between peak shock input and peak response) for all 10 subjects for 0.5 g, 1.0 g, 2.0 g, 3.0 g and 4.0 g shocks for each axis. Transmission data included: lumbar to seat (L2(x)/Sx, L3(y)/Sy, L4(z)/Sz); thoracic to seat (T1(x)/Sx, T2(y)/Sy, T3(z)/Sz); internal pressure to seat (IP/Sx, IP/Sy, IP/Sz). These tables and plots were developed to show each of the 10 subjects' individual response to the average of 2 shocks at each frequency and amplitude. For each variable, the mean value for the 10 subjects was calculated and superimposed on the plots as points at the appropriate frequencies.

Optotrak

Positional data from the spine was measured by Optotrak (Optotrak/3200, Northern Digital). The Optotrak system included the Optotrak/3020, a system unit, the Optotrak Data Acquisition Unit (ODAU), computer adapter interface card, and data acquisition

and analysis software. The sensors consisted of infra-red emitting diodes (IREDS) imbedded in a black plastic casing. These were attached to the skin of the subject using two-sided adhesive tape over the vertebral processes between C1 and L5. One IRED was also attached to the rear of the seat to give a reference location. The IRED sensors were connected by a thin cable to a strobe unit that could accommodate twelve IREDS. The IREDS were sensed by three cameras mounted on a 1.1 m long bar positioned approximately 2 m behind the subject. Error of measurement for calibrated displacements were of the order of 0.5 mm for objects placed 3 m from the camera position. Data were collected at a rate of 200 Hz from a 10 IRED's (9 on the spine and 1 on the seat). These data were synchronized with data collected on the VAX.

Data for both spinal acceleration and displacement were collected for two reasons. Displacement data are required to examine posture and will be used in Phase 5 biomechanical modeling; acceleration data are required for the calculation of shock transmission. Although Optotrak data may provide information at several spinal levels, the use of Optotrak to measure spinal acceleration is a relatively new technique. Accelerometer data are required to validate Optotrak displacement data and to ensure acceptance of the methodology by the scientific community. Also, Optotrack data are collected at too low a sampling rate to capture all of the motion required to assess spinal transmission.

Internal Pressure

Internal pressure was monitored before, during and after vibration exposure by a specially constructed rectal pressure probe. Internal pressure was measured in the short-term experiment (ST1) only. The probe was 50 cm in length and terminated in an Entran (model EPB-140W-5S) miniature pressure transducer (range ± 5 psi). The transducer and wiring were encapsulated in heat shrink tubing, 20 cm in length, to provide a suitable degree of strength and flexibility. Latex rubber was injected around the transducer walls and wiring junction to seal and protect the pressure transducer. Tygon plastic tubing was placed over the distal end of the connection wires and sealed at the heat shrink interface. An amphenol electrical connector was attached at the distal end. Wires within the tubing were kept slack to provide strain relief.

After proper instruction, the subject inserted the probe to a depth of 15 centimeters beyond the anal sphincter. This was performed by the subject in private, as the 15 cm mark was clearly labeled on the probe. After the experiment, the probe was removed, washed with detergent and rinsed in clean water by the subject. The probe was then disinfected by immersion in a 2% solution of

glutaraldehyde (e.g., Cidex) for a minimum of 4 hours. The probe was then rinsed thoroughly in clean water.

Response ratios of the internal pressure output to the seat acceleration input were analyzed for each shock magnitude at each frequency in experiment LT1. The response ratio reported at each frequency was derived from 20 response ratios, obtained from 2 shocks applied to each of 10 subjects. A mean response ratio of all five shock amplitudes input at the seat (based on 100 measures of internal pressure response) was also computed at each frequency. One subject's x axis data were excluded from analysis of the response ratios, due to poor signal quality. Therefore, x axis response ratios were calculated for 9 subjects rather than 10. Hence, the response ratios reported at each frequency in the x axis were derived from 18 response ratios, and the mean response was based on 90 measures of internal pressure.

The internal pressure response to a single z axis shock of 2 g, 3 g, or 4 g amplitude contained two distinct peak pressure responses. These two events are associated with the initial response to an input shock and then the subsequent impact of the subject against the seat which was also observed and discussed for the acceleration response. Internal pressure response ratios were computed in the z axis for the first internal pressure response at all shock amplitude and for the second internal pressure response to shocks of 2 g or greater.

Visual inspection of the internal pressure data also showed a characteristic pressure response to shock inputs at the seat, superimposed on slower fluctuations of internal pressure with time. Thus, to analyze the internal pressure response to shocks, the pressure data were high pass filtered at 0.5 Hz to remove basal fluctuations, then low pass filtered at either 60 Hz (x, y axes) or 150 Hz (z axis). Inspection of typical shock responses showed that the low pass filter generally did not affect the waveform, since frequency components of the internal pressure signal were well below this value.

Subjective Response

Measurement Scale for Responses

Subjective response to motion exposure was rated through as series of questions asked at specific measurement intervals in each experiment. A seven point scale was used for determining the subjective response ratings of comfort, tiredness and severity to shock exposures. Subjects rated the exposures from 1 to 7 (e.g., 1=barely perceptible; 7=extremely severe). To expand the limits of accuracy for ratings to single shocks in ST1, a scale

with gradations of 0.1 of a unit was presented visually to the subjects. For LT1 to LT5, a sample scale with gradations of 1.0 units was presented. Predicted tolerance ratings were obtained using an unrestrained time scale, and ratings were measured in hours of exposure. Appendix B includes subjective data forms which contain the subjective response semantic scales, the format of the questions and the measurement interval times for short term and long term experiments.

Training Procedures

Subjects were given a 15 minute orientation exposure several days before their experimental trials to train them with subjective questions. The subjective response scales and questions were explained to each subject. During the orientation exposure, the subjects responded to each question on several occasions. This enabled the subjects to practice the subjective response questions, to provide a frame of reference for the response scale in reference to motion exposure, and to bring forth any questions or concerns.

Experimental Procedures for Subjective Responses

During short term experiments, subjects rated each shock during the motion exposures, for severity between 1 and 7. Subjects were also asked to indicate whether the shock was less or more severe than the previous shock. For long term experiments, subjects provided ratings for comfort, predicted tolerance, tiredness and severity to repeated shock exposures (rather than for single shocks as in ST1) at scheduled measurement intervals. In LT1, subjects provided subjective ratings at the 30 second and 3 minute duration points of each 3.75 minute exposure. For the longer duration experiments (LT2, LT3 and LT4), ratings were obtained at scheduled intervals throughout the exposure. The time at which questions were asked in each experiment are included in Appendix B. Subjective ratings during LT5 experiments were obtained at the 3 minute point of each of the 16 shock exposure signatures which were 3.75 minutes in duration.

Subjective response ratings were analyzed by calculating the means and standard deviations for comfort, predicted tolerance, tiredness, and severity, in each of the short term and long term experiments. In each experiment, data were further analyzed to address the specific objectives of the experiment.

Short Term Experiments (ST1)

Effect of Motion Characteristics on Severity Ratings

The mean and standard deviation of subjective severity ratings were generated for each shock frequency and amplitude, axis and direction (i.e., ±x, +y, and ±z). The data were then graphed as

a function of shock frequency for each acceleration amplitude and direction. Data were then compared to determine the axis and direction in which shocks would most likely present a health hazard.

Linearity of Subjective Response to Shock Amplitude

The linearity of subjective severity ratings to shock amplitude was assessed by examining the effect of increasing amplitude over the range of tested shock frequencies. Severity ratings were normalized and graphed as a function of frequency to compare amplitude effects. The data were normalized by calculating the ratio of severity to mean severity for each amplitude at frequencies between 4 and 20 Hz. A non-linear regression was applied to the data to obtain a mean curve for all amplitudes.

Comparison of Subjective Responses with Biodynamic Model Outputs and Transmitted Acceleration

Subjective severity ratings and expected outputs were compared for the existing biodynamic models listed in Table 10. The scale for biodynamic output was normalized to correspond with the subjective severity rating scale to directly compare subjective severity and model output. The correlation between the subjective severity ratings and the models for all amplitudes was determined by linear regression analysis.

Table 10
Existing biodynamic models which were compared to subjective severity ratings.

Model	Axis	Undamped f_n (Hz)	Critical damping ratio	Reference
Fairley-Griffin	z	5	0.475	Fairley and Griffin, 1989
DRI (8.4 Hz)	z	8.4	0.224	ASCC, 1982
DRI (11.9 Hz)	z	11.9	0.35	Payne, 1991
BS 6841 W_b filter	z	NA	NA	BS 6841, 1987
BS 6841 W_d filter	x	NA	NA	BS 6841, 1987
DRI (10 Hz)	x	10	0.15	Payne, 1984
BS 6841 W_d filter	y	NA	NA	BS 6841, 1987
DRI (7.2 Hz)	y	7.2	0.15	Payne, 1984

The same method of normalizing data was used to compare the relationship between subjective severity rating and acceleration transmitted to the lumbar (L2, L3, L4) and thoracic (T1, T2, T3) vertebral levels.

Long Term Experiments (LT1 to LT5)

The Effect of Shock Axis, Direction, Amplitude and Rate

In relatively short duration repeated shock experiments (LT1: 3.75 minutes), subjective response ratings were compared between exposure conditions to determine the relative effect of amplitude, rate, axis and direction of input shocks. Subjective rating data were compared at 30 seconds and 3 minutes within each exposure.

Paired t-tests were used to compare the subjective response ratings between:

- two different shock amplitude/rate combinations within a dose level (e.g., 1 g shocks at 128 shocks per minute were compared to exposures of 2 g shocks at 8 shocks per minute).
- positive and negative direction shocks (e.g., +z axis 4 g shocks at 8 per minute to -z axis 4 g shocks at 8 per minute).
- shocks in different axes with similar shock directions and amplitude and rate conditions (e.g., positive z axis 2 g shocks at 128 per minute and positive x axis 2 g shocks at 128 per minute).

The experimental protocol for LT3 was designed to limit the permitted exposure time of an individual to 75% of his predicted tolerance rating. Thus, the subjects experienced exposures of varying duration. To examine general trends in the data, the mean subjective ratings were calculated from three subject subsets (n=10, n=6 and n=2), based on the maximum exposure duration a subset of subjects completed. Using these subject groups, mean values were determined for 2.5 hours of exposure for n=10, 4.5 hours for n=6, and the full 7 hours of exposure for n=2. The subset n=10 was chosen to represent the full sample population; the n=6 subset was chosen to represent the maximum number of subjects remaining past the second break; and n=2 to represent the subjects which completed the experiment.

Effect of Exposure Duration on Subjective Response

To examine the effect of exposure duration on subjective ratings of comfort, predicted tolerance, tiredness and severity, mean values for subjective response for each measurement interval were graphed as a function of exposure time for experiments LT2, LT3 and LT4. The differences between mean subjective ratings for first and last measurement intervals were assessed by paired t-tests. These methods also examined whether short term predictions

of tolerance provided realistic estimates of tolerance at later measurement intervals.

Effect of Rest Breaks on Subjective Response

Rest breaks of varying duration were assessed for their effect on subjective response. Rest breaks were included in experiments LT3, LT4 and LT5. The combination of exposure and rest break duration for the experiments are listed in Table 11. Paired t-tests were used to determine the differences between the means of pre- and post-break subjective response ratings in LT3 and LT4. In LT5, the effect of intermittent breaks was examined by comparing mean subjective ratings of comfort, tolerance, tiredness and severity between continuous and intermittent motion exposure conditions. These ratings were graphed as a function of exposure duration for both conditions.

Table 11
Exposure and rest break combinations examined for experiments LT3, LT4 and LT5.

Experiment	Exposure	Rest Break Type
LT3	7 hours	two 15 minute and one 30 minute breaks per exposure
LT4	4 hours, 5 days	one 15 minute break per exposure and overnight between consecutive days
LT5 (Intermittent condition)	1 hour total (3.75 minute signatures)	sixteen 7.5 minute breaks for 1 hour of exposure

Comparison of the VDV and Subjective Response

In LT1 subjective response ratings were compared between high and low dose (VDV) exposures, to examine the relationship between subjective response and the VDV in the evaluation of shock exposure. For example, the mean subjective severity or tiredness response to a shock exposure with a VDV of 29.1 was expected to be twice as great as an exposure with a VDV of 14.5. The time dependence of subjective tiredness ratings was compared to the VDV by superimposing the response curves as a function of exposure duration for LT3 and LT4. The VDV values were normalized to correspond with the subjective tiredness scale by calculating a ratio between the mean value for all subjective tiredness ratings and the mean for all VDV values at specific exposure duration intervals.

For all paired t-tests, significance for difference testing was set at $p<0.05$. In the case of multiple t-tests within a set of subjects, the Dunn's test was used to determine the statistical

confidence level (p) for individual tests, to yield an overall alpha level of $p<0.05$ for the comparisons.

Physical Status

In addition to subjective response ratings, comments regarding physical status during exposure and recovery periods were recorded. During exposure, subjects were asked to describe any pain, soreness or stiffness experienced. During recovery periods, and post-exposure intervals when blood and urine samples were collected (i.e., at 24, 48, 72 and 96 hours), subjects provided estimates of predicted tolerance of a similar motion exposure. Time estimates were given in context of being with or without breaks, and as military or non-military missions. Subjects were also asked to describe any sensation of pain, discomfort or soreness, the body part affected, and to compare the soreness to any previous experience (e.g., delayed soreness following exercise).

Blood and Urine Collection

Blood and urine samples were analyzed to study changes in selected metabolites which could indicate fatigue, excessive stress, or tissue damage. Samples were collected and analyzed in three of the long duration experiments (LT3, LT4, and the two exposures in LT2 which included 4 g shocks).

Table 12 and Table 13 summarize the variables analyzed in blood and urine samples. A more detailed description of the relevance of each metabolite to the study, and the normal range of each metabolite, is provided in Appendix C, Table C-1. Blood samples were obtained by a laboratory technician using single draw vacutainers and standard venipuncture techniques. Blood samples (15 ml) for baseline measurement of all metabolites listed in Table 12 were obtained for each subject at least 2 days before the start of long term experiments to familiarize the subject with the procedure and to screen subjects for biochemical values outside of the normal range.

Table 12
Metabolites measured in blood samples.

Metabolite Name	Relevance to Study
Alkaline Phosphatase	Bone remodeling
Blood Urea Nitrogen	Kidney/liver function
Creatine Phosphokinase (CPK)	Skeletal muscle damage
Creatinine	Renal function

Glucose	Hypoglycemia
Hematocrit	Fluid shift
Hemoglobin	Fluid shift
Lactate	Fatigue
Lactate Dehydrogenase (LDH)	Skeletal muscle damage
Platelets	Initiation of blood clotting
Total Protein	Fluid/protein shift
Uric Acid	1° or 2° Hyperuricemia
White blood cell profile	Inflammation/infection

Table 13
Metabolites and characteristics measured in urine samples.

Metabolite or Characteristic	Relevance to Study
Appearance (Turbidity)	Particulate matter
Bilirubin	Hemoglobin breakdown
Blood Cells	Renal or urinary tract bleeding
Color	Particulate matter
Creatinine	Renal function
Glucose	Renal function or carbohydrate metabolism
Ketones	Fat metabolism
Leukocyte Esterase	Renal or urinary tract inflammation
Nitrite	Urinary tract infection
pH	Renal function
Protein	Renal function or plasma proteins
Specific Gravity	Urinary concentration
Urine Volume	Hydration
Urobilinogen	Hemoglobin/bilirubin breakdown

In all three experiments (LT2, LT3, and LT4) 15 ml blood samples were collected at the following experimental time points: pre-exposure; post-exposure; and 24 hours post-exposure. A smaller blood sample (5 ml) for measurement of CPK, LDH, and creatinine were obtained at 48 hours, 72 hours, and 96 hours post-exposure. In experiment LT4 (which included a four hour motion exposure for five consecutive days), the 24 hour sample for day 1 to 4 was used as the pre-exposure sample for days 2 to 5. This reduced the number of samples, and thus the volume of blood, required from each subject. Blood and urine collection was continued for 4 days post-exposure to monitor delayed effects of exposure to the motion environment. The schedule for collection of blood and urine is summarized in Table 14.

Table 14
Summary of collection times for blood and urine samples.

Experiment	Sample Time						
LT2	Baseline						
		Pre-	Post-	24h	48h	72h	96h
LT3	Baseline						
		Pre-	Post-	24h	48h	72h	96h
LT4	Baseline						
	Day 1:	Pre-	Post-				
	Day 2:	Pre-	Post-				
	Day 3:	Pre-	Post-				
	Day 4:	Pre-	Post-				
	Day 5:	Pre-	Post-	24h	48h	72h	96h

In experiments LT2 and LT3, a total of 60 ml of blood was taken in the period of the experiment (15 ml at 3 time points and 5 ml at 3 time points). In experiment LT4, the maximum blood draw in a 24 hour period was 45 ml (15 ml at 3 time points). The maximum volume drawn from a single subject over the five days of exposure and 4 days of follow-up was 180 ml (15 ml at 11 time points and 5 ml at 3 time points). For comparison, 450 ml of blood is taken at a blood donor clinic. Each subject also completed a 24 hour daily dietary recall (Appendix C, Table C-2) to provide information useful in the explanation of potential irregularities in biochemical results.

Urine specimens for measurement of kidney function were collected at the times described in Table 14. A 100 ml urine sample and a 24 hour urine collection were obtained from each subject. A baseline urine sample was obtained also from each subject at least 2 days before participating in the experiments. Each 24 hour urine sample was collected from approximately 0800 h on day one to 0800 h of the following day.

Blood and urine samples were processed at the MARS facility by a team of laboratory technicians. Blood samples were allowed to clot for 30 minutes in serum separator tubes (SST), centrifuged for 10 minutes, then the serum was pipetted into a storage container. Hematology tubes containing 7.5% EDTA were inverted gently then stored until analysis. Blood samples collected with 3 ml glycolytic inhibitor tubes containing 6.0 mg potassium oxalate and 7.5 mg sodium fluoride for lactate analysis were inverted gently, then centrifuged for 15 minutes. Blood and urine samples were stored at 4°C until transport to Lyster Hospital at Fort Rucker, AL. Analyses were completed on a daily basis. Data from Lyster Hospital were returned to the medical monitor and to researchers on a regular basis.

A summary of the method used in each biochemical analysis, and the coefficient of variation of the method reported by Lyster Hospital is shown in Appendix C, Table C3. In addition to the subject's samples, duplicate blood and urine samples were sent to Lyster Hospital on eight occasions to verify the quality control of their methods. The coefficient of variation, determined without the knowledge of Lyster Hospital, is also shown in Appendix C, Table C3. A coefficient of variation could not be calculated for qualitative measures.

All of the biochemical measures were time dependent. Some metabolites were not measured at all time points, either because blood or urine samples were missing (some subjects did not report for all post-samples), or because of obvious clotting or hemolysis of the blood sample which affected the reliability of the measure.

Numeric data for both blood and urine are reported as the group mean, standard deviation of the mean, minimum and maximum values, and the number of samples included in the analysis. The minimum and maximum values of each variable provided a measure of the inter-individual range of each metabolic variable. Each dependent variable was analyzed by a one way repeated measures analysis of variance (ANOVA) with time as the within subjects factor. Significance was set at an alpha value of less than 0.05. Some individual data were plotted for variables when a pattern was noted in the individual's data. These plots were examined for trends which may have been obscured by the group analysis.

Urinary metabolites recorded as categorical data were analyzed by group according to frequency and percent of valid responses. Visual inspection indicated clearly that the group data did not show any changes that warranted further statistical analysis.

In experiments LT2 and LT3, the CPK profile of at least one subject was extremely high in relation to normal values and the values of other subjects. Intense muscular exercise was suspected. The group data for these experiments were re-analyzed for CPK, excluding this subject.

Synthetic Work Task

During experiments exceeding one hour (LT2, LT3, LT4), subjects completed a cognitive performance test battery called the "Synthetic Work Environment" (SynWork). The test battery consisted of four tasks performed simultaneously on a single large screen monitor. The tasks evaluated each subject's ability to divide attention and complete multi-tasks. Subjects used a trackball device which was attached to a splint-like structure loosely attached to the dominant forearm. The 4 tasks include: Sternberg

Memory Task; Stability Tracking Task; 4-column Addition Task; and Auditory Monitoring Task.

Each subject was required to perform the SynWork 10 to 15 times prior to the experiment to become familiar with the tasks and reach a plateau in their performance curve. The SynWork was conducted for 20 minute periods during the long duration experiments, separated by a minimum of 20 minute periods of other tasks. The data were updated as the mean composite score.

Activity Monitor

In experiments LT2, LT3 and LT4, in which serial biochemical measures were taken, subjects were asked to wear an activity monitor (Actigraph) on their wrist for the duration of collection of biochemical measures. This was intended to provide information on their work/sleep pattern. The use of these monitors has been validated in other studies to provide a record of the intensity of daily activity and of the quality of an individual's sleep (Brooks et al., 1988). These data were not analyzed as part of the Phase 4 report.

Results

Electromyography

Mean Frequency

Table E-11 and E-12 show summary statistics for group EMG data in LT3 and LT4. Several subjects in both LT3 and LT4 demonstrated a decrease in mean frequency (MF) after exposure to motion, as expected with the spectral compression which has been shown to accompany localized muscle fatigue. However, an increase in MF was equally likely and group means demonstrated no evidence of a consistent decline in MF. The average MF for all muscle sites and all subjects was 64.0 Hz in the pre-exposure trials, and 63.9 Hz in the post-exposure trials. Only the left thoracic muscle site on day 3 of LT4 showed a consistent trend in group data, with a very small increase in MF ($p=0.03$).

Figure F-22 to F-25 illustrate the delta mean frequency at each muscle site and standard deviation of group data after exposure to motion for 7 hours in experiment LT3. A decline in MF greater than one standard deviation was found for subject 6 (left thoracic), subject 9 (lumbar bilaterally and right thoracic), subject 10 (right lumbar and left thoracic), and subject 11 (right lumbar and right thoracic). An increase in MF greater than one standard deviation was evident for subject 2 (left thoracic), subject 4 (right thoracic), subject 8 (left lumbar), and subject 12 (lumbar bilaterally and left thoracic).

Figure F-26 to F-37 illustrate the delta mean frequency at each muscle site and standard deviation of group data after exposure to motion for 4 hours on each of five consecutive days in experiment LT4. Decline in MF greater than one standard deviation was found for subject 1 (left thoracic - day 5), subject 3 (lumbar bilaterally and right thoracic - day 1), subject 4 (left thoracic - day 1; lumbar bilaterally - day 3), and subject 6 (left thoracic - day 1; right thoracic - day 3; all sites - day 5). Increases in MF greater than one standard deviation were found for subject 1 (right thoracic - day 3), subject 3 (thoracic bilaterally - day 3; left thoracic - day 5), subject 4 (left thoracic - day 3), subject 6 (left thoracic - day 3), subject 9 (lumbar bilaterally - days 1, 3 and 5; right thoracic - day 5), and subject 10 (left thoracic - day 5).

RMS EMG

In experiment LT3 there was an increase in rms EMG activity in the last measurement interval compared with the first measurement interval at all muscle sites recorded on the back ($p \leq 0.01$ for all

comparisons, p=0.00001 overall). There was an increase in rms EMG of forty percent, on average, with a group mean rms EMG of 0.20 volts (variance = 0.01) in the first sampling trial and 0.28 volts (variance = 0.02) in the last sampling trial.

Acceleration Transmission

Spinal Acceleration

Spinal (L2 and T1) x Axis Acceleration Response to Positive and Negative x Axis Shocks at the Seat

Tables E-13 to E-16 list the mean lumbar and thoracic transmission ratios measured at L2 and T1, in both the positive and negative x axis for each shock amplitude and shock frequency applied to the seat. These data are illustrated in Figures F-38 to F-41. The response curves for each shock direction and amplitude showed a similar curvilinear relationship with shock frequency. The transmission ratios are highest at 2 to 4 Hz and typically decline in a curvilinear manner with increasing frequency to 20 Hz. Although similar in nature, the transmission curves at each shock amplitude are not identical.

The response curves for high amplitude shocks (2, 3, and 4 g) had a higher peak transmission ratio and showed a more rapid rate of decline than the response curves for low amplitude shocks (0.5 and 1 g). There was some evidence of an amplitude effect in the transmission ratios of both positive and negative x axis shocks. However, as the differences between amplitudes were small, it was considered reasonable to collapse the data of each amplitude in order to obtain a mean transmission response as a function of frequency. These data are expressed in the final row of Tables E-13 and E-14. The mean transmission ratios of all amplitudes of positive x axis shocks were generally higher at L2 than at T1. This effect is shown in Figure F-42. A similar tendency was present in the negative shock transmission data at the higher shock frequencies, as shown in Figure F-43.

Transmission ratios for positive and negative shocks measured at L2 showed a different dependence on shock amplitude than those measured at T1. Low frequency, negative 0.5 and 1 g shocks produced higher transmission ratios at L2 than produced by negative 2, 3 or 4 g shocks. For a 4 Hz shock input at the seat, the L2 transmission ratio was 0.44 for a negative 0.5 g shock, whereas the transmission ratio declined to 0.32 for a negative 4 g shock. These data differ from the results seen at the thoracic level, where a 4 Hz shock input at the seat produced a T1 transmission ratio of 0.33 for a negative 0.5 g shock and 0.41 for a negative 4 g shock. In the positive direction, 3 and 4 g shocks produced the

highest transmission ratios at L2 (0.53 and 0.54 respectively). Transmission ratios at T1 were consistent for shocks in both directions, with the highest ratios produced by 3 and 4 g shocks.

Some differences were observed in the frequency at which peak transmission ratios occurred. Transmission ratios measured at T1 for both positive and negative 0.5 and 1 g shocks was greatest at 2 Hz. However, the L2 response to positive 0.5 g shocks peaked at 4 Hz. The T1 transmission ratios in response to positive 0.5 and 1.0 g shocks did not decline between frequencies of 11 to 20 Hz, unlike other amplitudes. The L2 transmission ratios in response to negative 0.5 and 1 g shocks did not continue to attenuate at frequencies above 8 Hz, and the transmission ratios to negative 0.5 g shocks showed an increased response above 11 Hz.

Mean transmission ratios at L2 were generally greater in the positive x axis than in the negative x axis. This effect is shown in Figure F-44. A similar effect was also evident in the thoracic transmission ratios in response to shocks at low frequencies (4 to 6 Hz), but was not evident at higher frequencies up to 20 Hz. Comparative results are shown in Figure F-45.

Spinal (L3 and T2) y Axis Acceleration Response to Positive y Axis Shocks at the Seat

As the body is symmetrical in the sagittal plane, data were collected only in the positive y axis. Table E-17 lists the mean lumbar transmission ratios, measured at L3 for each shock amplitude and shock frequency applied to the seat. These data are shown graphically in Figure F-46. The transmission curves in response to each shock amplitude showed a similar relationship with shock frequency. Transmission ratios were highest at the lower frequencies (2 to 5 Hz) and declined in a curvilinear manner with increasing frequency. The transmission ratios of 4 g and 3 g shocks attenuated more rapidly with frequency to yield the lowest transmission ratios at 20 Hz. The 4 g shocks showed a peak transmission ratio at 5 Hz, but this effect was not evident at the other shock amplitudes.

Comparable thoracic transmission data measured at T2 are shown in Table E-18 and Figure F-47. The individual curves of the response to each shock amplitude showed the same comparative trends as at the lumbar level. The 4 g shocks produced the highest transmission ratios at low frequencies and again showed the greatest attenuation at the higher shock frequencies (11 to 20 Hz). Although the transmission curves of 0.5 g and 1 g shocks decreased rapidly from 2 Hz to 8 Hz, the 3 g and 4 g shocks showed a flatter transmission curve between 4 and 6 Hz.

As seen in the x axis, there was some evidence of an amplitude effect in the curves of transmission ratios, particularly in the 4 g data at 4 to 6 Hz, and in the 0.5 g and 1 g data at 11 to 20

Hz. However, as differences between amplitude were small, the data of each amplitude were collapsed to obtain a mean transmission response as a function of frequency. These data are expressed in the final row of Tables E-17 and E-18.

Examination of the mean transmission ratios of all shock amplitudes indicated that the transmission ratios were consistently higher at the lumbar (L3) level than at the thoracic (T2) level, particularly at the higher shock frequencies. This effect, shown in Figure F-48, was more pronounced in the y axis than shown in the x axis data (Figure F-42).

Spinal (L4 and T3) z Axis Acceleration Response to Positive and Negative z Axis Shocks at the Seat

Tables E-19 to E-22 list the mean lumbar and thoracic transmission ratios measured at L4 and T3, for each shock amplitude and shock frequency applied to the seat in the positive and negative z axis. These data are shown graphically in Figures F-49 to F-52. Although there were distinct differences in the L4 and T3 transmission curves in response to shock amplitude, some similarities are apparent at both locations and in both the positive and negative directions. Transmission ratios were highest at the low shock frequencies (2 to 4 Hz) and declined in a curvilinear manner with increasing frequency to 20 Hz. High amplitude shocks (2, 3, and 4 g) shocks produced higher transmissions ratios than the low amplitude shocks (0.5 and 1 g) for both positive and negative inputs. The amplitude effect on transmission ratio was most evident at low frequencies (2 to 8 Hz) but diminished as the shock frequency increased towards 20 Hz.

Examination of the mean transmission ratios of all amplitudes of positive shocks indicated that the transmission ratios were similar at both the lumbar (L4) and thoracic (T3) levels. The only exception to this pattern was the transmission of 4 g shocks at frequencies of 2 to 6 Hz, where the thoracic transmission ratio exceeded the lumbar transmission ratio. The transmission ratios of negative z axis shocks were similar at the lumbar and thoracic levels. At 2, 3, and 4 g shock amplitudes, the thoracic transmission was greater than lumbar transmission at input frequencies below 8 Hz. The L4 and T3 transmission ratios of 3 g and 4 g shocks were much higher than those of 0.5 g and 1 g shocks, particularly in the range of 4 to 8 Hz. For a shock input of 4 Hz at the seat, a T3 transmission ratio of 0.9 was obtained for a 1 g shock, whereas, the transmission ratio increased to 2.6 in response to a 4 g shock.

In response to z axis shocks, transmission ratios tended to increase with input amplitude, except for the transmission curve in response to negative 2 g shocks, which demonstrated the highest transmission ratios at L4 of all shock amplitudes between 4 and 6 Hz. The transmission ratio of negative 2 g shocks at T3 increased

rapidly at lower frequencies, and produced the greatest response to 4 Hz shocks at the seat.

The reversal of the T3 transmission ratio amplitude effect was only evident in shocks of negative 2 g to 4 g at low frequencies. For these shocks, comparison of mean transmission ratios for all shock amplitudes indicated a cross-over in the relationship in the positive and negative directions between transmission ratio and shock frequency. The lumbar transmission ratios were generally greater in the negative z axis than in the positive z axis at low frequencies (2 to 6 Hz). This tendency became reversed at the high frequencies (11 to 20 Hz) where the lumbar transmission in the positive direction was greater than in the negative direction. This effect is demonstrated in Figure F-53 in which the percent difference (where percent difference = (positive Lz - negative Lz)/positive Lz) between the transmission ratios was plotted as a function of frequency. In response to positive and negative shocks, the same pattern was evident in the transmission ratios at the thoracic spine, as illustrated in Figure F-59.

There was a clear amplitude effect in the transmission ratios of both positive and negative z axis shocks. Figures F-55 to F-58 illustrate the relationship of transmission ratio to shock amplitude for z axis shocks of 4, 8, and 20 Hz. This effect was much greater than noted in either the x axis or y axis data.

Second Component of Spinal (L4 and T3) z Axis Acceleration Response to Positive and Negative z Axis Shocks at the Seat

Figure F-1 illustrates the two-component response of a positive 4 g, 4 Hz seat shock measured at the lumbar spine. This effect is seen in both the positive and negative z axis. The initial response to the input shock causes the subject to briefly leave the seat. This is followed by a second response as the subject impacts the seat. The impact of the subject on the seat is also recorded in the seat acceleration signal as a high frequency pulse approximately 0.3 seconds after the initial shock peak.

The mean transmission ratios of the second identified response to 2, 3, and 4 g shock amplitudes applied to the seat are listed in Tables E-23 to E-26. These data are illustrated in Figures F-59 to F-62. The second acceleration response to positive z axis shocks had transmission ratios similar to the initial acceleration response for shocks at 4 Hz (transmission ratios of 1.5 to 3 in both the first and second response), in contrast, the negative z axis shocks produced a second acceleration response that was less than the first response for both lumbar and thoracic acceleration (transmission ratios of 2.5 to 5 for the first response and 0.3 to 0.8 for the second response). For both positive and negative z axis inputs, the shock frequencies above 4 Hz produced transmission ratios for the second response that were progressively less than the transmission ratios computed for the first response. The

lumbar and thoracic transmission ratios of the second response declined rapidly as frequency increased, reaching nearly zero transmission by 11 Hz. The transmission ratios increased with shock amplitude (amplitude effect) for frequencies of 5 to 11 Hz for positive z axis shocks at both L4 and T2, and for all frequencies for negative z axis shocks when measured at T3. However there was no shock amplitude effect observed for lumbar transmission ratios for negative z axis shocks.

The thoracic transmission ratios were slightly larger than lumbar responses for all frequencies and amplitudes of positive z axis shocks. The response to low frequency (4 to 8 Hz), negative 2 and 3 g shocks produced transmission ratios that were marginally lower at T3 than those measured at L4, whereas the negative 4 g, 4 and 5 Hz shocks produced T3 transmission ratios slightly higher than those measured at L4.

Comparison of the Spinal Transmission Curves to Existing Standards and Models

The mean transmission curves of both positive x axis and negative x axis shocks were compared to the frequency response curves of the BS 6841 x axis filter and the DRI (10 Hz) model (Payne, 1984) for the x axis (Figures F-63 and F-64). The DRI (10 Hz) response curve consistently overestimates the magnitude of accelerations transmitted to the spine by 2 to 3 fold. The natural frequency of the DRI (10 Hz) model is also much higher than suggested by the spinal response data in the study. A better approximation of the current data was achieved by the output of the BS 6841 filter. However this filter consistently produced a slight overestimation of shock transmission in both positive and negative directions at the lumbar and thoracic levels.

Frequency response curves of the BS 6841 y axis filter and the DRI (7.2 Hz) model (Payne, 1984) for the y axis were compared to the measured mean transmission curves in response to y axis shocks (Figure F-65). The DRI (7.2 Hz) model response curve overestimated the amplitude of accelerations transmitted to the spine several fold. The natural frequency of the DRI model (7.2 Hz) is also much higher than suggested by the spinal transmission data. A possible exception was the transmission of 4 g shocks at L3 (Figure F-46), where there was evidence of a peak transmission at 5 Hz. This would suggest that the natural frequency of the DRI (7.2 Hz) model may be more applicable to large amplitude shocks in excess of 4 g. A much better approximation of the transmission curves was achieved by the output of the BS 6841 filter. However, this filter considerably underestimated shock transmission at the lumbar level for low frequency shocks (2 to 6 Hz), and had a slower decay rate with increasing shock frequency than the y axis spinal transmission data.

The current standards and models for estimating transmission of vibration and shock effects are based on linear models. Hence, in existing models, the transmission curves of all shock amplitudes are identical. The amplitude dependence illustrated in Figures F-55 to F-58 clearly demonstrates that the spinal response in the z axis is non-linear and therefore cannot be accurately predicted by existing linear models.

Due to the amplitude effect in the z axis response to shock input, it was not considered meaningful to compare the mean response curves of all shock frequencies with existing standards. Thus, the individual transmission curves in response to 1 g and 4 g shocks were compared to the output of biodynamic models and filters contained in current standards. Figure F-66 compares the transmission ratios in response to 4 g shocks measured at L4 and T3, with the frequency response curves of the BS 6841 (1987) z axis filter, the Fairley-Griffin model (Fairley and Griffin, 1989), the DRI (8.4 Hz) model contained in the ASCC (1982) and the revised DRI (11.9 Hz) model of Payne (1991). All four models clearly underestimate transmission effects at the spine. For example, the output of the Fairley-Griffin model predicted a peak transmission of 0.9 at 5 Hz, compared with a measured transmission of 1.8 at L4 and 2.6 at T3 for 5 Hz shocks. The maximum transmission ratio of any standard was obtained from the DRI (8.4 Hz) model, which predicted a peak transmission of 1.3 in response to the 4 g, 5 Hz shock input at the seat. All four standards similarly underestimated the transmission ratios measured in response to negative z axis shocks.

Due to the amplitude dependence of transmission ratios measured for the z axis, existing standards were compared with the transmission ratios measured in response to 1 g shocks input at the seat. Figure F-67 shows the comparison of 1 g transmission ratios at L4 with the frequency response curves of the BS 6841 z axis filter, the Fairley-Griffin model, and the DRI (8.4 Hz) model contained in the ASCC. Both the BS 6841 filter and the Fairley-Griffin model underestimated the transmission of 1 g shocks. Although the DRI (8.4 Hz) model approximated the amplitude of shock transmission over part of the frequency range, the DRI (8.4 Hz) response showed a distinctly different relationship with shock frequency than the response measured at L4. The measured L4 response to a 1 g shock is curvilinear, with the peak amplitude at the lowest shock frequency tested (2 Hz), whereas the DRI (8.4 Hz) response curve shows a peak amplitude at 5 Hz, which diminishes as frequency decreases to 2 Hz or increases to 20 Hz. The spinal transmission ratios at T3 and the revised DRI (11.9 Hz) model have been omitted from Figure F-67 in order to improve clarity.

Delay Between Shock Input and Peak Response

The time delay between peak input acceleration in each axis and peak response was calculated for spinal acceleration and internal pressure. These data are summarized in Tables E-27 to E-32 for x axis shocks, Tables E-33 to E-35 for y axis shocks, and Tables E-36 to E-41 for z axis shocks.

A consistent frequency dependent pattern was observed for both the acceleration response and the internal pressure response to shocks in all directions, except for positive z axis shocks (Figures F-68 to F-82). Acceleration and internal pressure responses to positive z axis shocks had a greater delay as frequency increased. The delay decreased in response to shocks in all other directions as shock frequency increased. An exception to this was shown for the delay after a 0.5 g positive x, negative x, or positive y shock, which increased with frequency from 11 to 20 Hz.

The delay for the positive z axis responses was shorter than those in other directions. Delays in the positive z axis ranged from 14 to 26 ms for lumbar and thoracic acceleration response, and 5 to 55 ms for internal pressure response. The acceleration delays in other directions and axes ranged from 50 to 200 ms.

Internal Pressure Response

Internal Pressure Response to x Axis Shocks

Tables E-42 and E-43 list the mean internal pressure response ratios for each shock amplitude and shock frequency applied to the seat in the positive and negative x axis. These data are shown graphically in Figures F-83 and F-84. The response curves of each input shock amplitude showed a similar pattern with shock frequency. Response ratios were highest at 2 to 4 Hz and declined in a curvilinear manner with increasing frequency to 20 Hz. One exception to this trend was observed for the response to negative 3 g shocks, which was greatest at 6 Hz. The internal pressure data showed an increased response at 6 Hz for all negative x axis shocks except 1 g, which showed an increased response at 11 Hz.

The x axis response ratio was non-linear with shock amplitude, particularly at frequencies less than 8 Hz. Negative 0.5 g and 1 g shocks showed consistently greater response ratios than the higher shock amplitudes for 2 to 20 Hz shocks, and declined much more rapidly from 2 to 5 Hz than the 2, 3, and 4 g shocks. The internal pressure response ratio to 4 g shocks was lower than that measured for other shock amplitudes at 8 to 20 Hz. At 4 to 6 Hz, the response ratio for 0.5 and 4 g shocks were lower than the ratios for 1, 2, or 3 g shocks.

The response ratio to negative shocks in the negative x axis was greater than that to positive shocks for 0.5 g shocks at all shock frequencies and for 1 g shocks at 2 to 8 Hz. Higher frequency 1 g, 2g and 3 g shocks had larger response ratios for positive shocks than for negative shocks. The response ratios for 4 g shocks were similar for both shock directions.

Internal Pressure Response to Positive y Axis Shocks

Table E-44 lists the mean internal pressure response ratios to y axis shocks for each shock amplitude and shock frequency applied to the seat in the positive direction. These data are shown graphically in Figure F-85. The response curves of each input shock amplitude showed some variation in the pattern with respect to shock frequency. The peak response ratio for each amplitude was observed at the lowest frequency measured. Response ratios for 2 g, 3 g, and 4 g shocks were highest at 4 Hz and declined in a curvilinear manner with increasing frequency to 20 Hz. The response curve for 1 g shocks declined similarly from a maximum at 2 Hz; however, there was very little change from 6 to 20 Hz. The response ratio for 0.5 g shocks followed a pattern similar to that for the 1 g ratios, with the exception that the response ratio increased between 11 and 20 Hz. The response ratio for 0.5 g shocks was greater than that calculated for all other shock magnitudes. The ratio for 1 g shocks was greater than that for larger shock magnitudes.

Internal Pressure Response to z Axis Shocks

The mean internal pressure response ratios to z axis shocks for each shock amplitude and shock frequency applied to the seat in the positive and negative directions are listed in Tables E-45 and E-46. Figures F-86 and F-87 illustrate these data. As observed for x and y axis shocks, response ratios were greatest at the lowest frequency measured and declined in a curvilinear manner with increasing frequency. There was very little change in response as frequency increased from 11 Hz to 20 Hz. There was a clear shock amplitude effect on internal pressure response ratios for frequencies of 8 Hz and below. At these frequencies, response ratio increased with shock amplitude.

A cross-over was observed for positive and negative z axis shocks in the relationship of the internal pressure response ratio to shock frequency. For each shock amplitude plus the overall frequency mean, the response ratio for negative z axis shocks was greater than positive z axis shocks in the range of 2 to 6 Hz. This pattern was reversed for input shocks of 8 to 20 Hz. An exception to this pattern was the mean response ratio curve for 0.5 g shocks, which was greater for positive shocks than for negative shocks at all frequencies.

Second Internal Pressure Response to z Axis Shocks

The mean internal pressure response ratios of the second response event for 2, 3 and 4 g shock amplitude are listed for positive and negative z axis shocks in Table E-47 and E-48. These data are illustrated in Figures F-88 and F-89. The response ratios followed a pattern similar to the acceleration transmission response at L4, with a maxima at 4 Hz and approaching zero response at 11 Hz. The second response ratio was greater for positive than negative shocks. The initial response to shocks was greater than the second response for both positive and negative shocks. For example, a negative z axis 4 Hz, 4 g shock produced an initial response ratio of 6.3 and a second response of 1.0.

Subjective Response

Short Term Experiments (ST1)

Effect of Motion Characteristics

Subjective severity ratings demonstrated trends in response to different motion characteristics including shock frequency, axis and direction. Each of these characteristics is directly relevant to health hazard concerns. The mean values for subjective severity for all axes, directions, frequency and amplitude are presented in Figures F-90 to F-94. For all shock conditions, the lowest tested shock frequency resulted in the highest mean severity rating, which decreased in a curvilinear manner with increasing shock frequency. Curves for each amplitude decreased as a function of shock frequency, with a high negative slope at low frequencies which rapidly became flatter at 11 Hz. However, the slope of the curves for positive z axis shocks did not decrease as rapidly as the other conditions.

Paired t-tests for differences between mean values of ratings in different axes demonstrated that z axis shocks were rated as significantly more severe than x or y axis shocks. The mean severity ratings for x and y axis shocks were not significantly different.

Paired t-tests between means of subjective severity at each amplitude demonstrated no significant difference between severity ratings to positive and negative shocks in the x and z axes. (Figures F-95 and F-96). Regression analysis between ratings for positive and negative shocks showed high correlation coefficients for x and z responses (r^2=0.986 and r2=0.933). Both regression lines were extremely close to the lines of identity (y=1.004x + 0.064 and y=0.968 x+ 0.0997, for x and z axes respectively).

Linearity of Subjective Severity to Shock Amplitude

A non-linear amplitude effect was present for all axes and shock directions. This was demonstrated by comparing normalized severity ratings in response to each shock amplitude. Common trends existed for amplitude, showing that at low frequencies (below 8 Hz), high amplitude shocks were rated relatively more severe than low amplitude shocks; at high frequencies (above 11 Hz), low amplitude shocks were rated relatively more severe than high amplitude shocks. An example of this is demonstrated for positive x axis shocks in Figure F-97. Comparing the mean non-linear regression line to the individual curves for each amplitude also demonstrated this interaction between shock amplitude and frequency.

Comparison of Subjective Severity with Biodynamic Model Outputs

z Axis Shocks

Comparison of subjective severity ratings and normalized output acceleration of existing biodynamic models in response to positive z axis shocks demonstrated both frequency and amplitude dependent effects. Each of these models underestimated subjective severity at low frequencies and overestimated severity at high frequencies. The cross-over point from underestimating to overestimating severity was dependent on shock amplitude for all models, ranging from 4 to 15 Hz. The closeness of the relationship between severity ratings and the existing biodynamic models decreased progressively in the following order: Fairley-Griffin model, DRI model (8.4 Hz version), DRI model (11.9 Hz version) and BS 6841 filter (Figures F-98 to F-101). The trends described for positive z axis shocks were also shown for negative z axis shocks. However, the relationship between severity ratings and the existing biodynamic models was not as good for negative z axis shocks as it was for positive z axis shocks (Figures F-102 to F-105). Correlation coefficients obtained from linear regression analysis for severity ratings and biodynamic model outputs are listed in Table 15.

Table 15
Correlation coefficients for subjective severity responses with biodynamic model outputs in response to single shocks in the z axes.

Shock axis	Model or Filter	Positive Direction (r^2, α=0.05)	Negative Direction (r^2, α=0.05)
z	Fairley-Griffin	0.985	0.896
z	DRI (8.4 Hz)	0.959	0.828
z	DRI (11.9 Hz)	0.897	0.712

z	BS 6841 filter	0.760	0.550

x and y Axis Shocks

Comparison of subjective severity ratings and normalized output acceleration of biodynamic models in response to x and y axis shocks demonstrated similar trends to those shown above for the z axis. The closeness of the relationship between severity ratings and the models was higher for the BS 6841 filter than for the DRI model, for both x and y axes. (Figures F-106 to F-111). Linear regression analysis for severity ratings and biodynamic model outputs are listed in Table 16.

Table 16
Correlation coefficients for subjective severity responses with biodynamic model outputs in response to single shocks in the x and y axes.

Shock axi	Model or Filter	Positive Direction (r^2, α=0.05)	Negative Direction (r^2, α=0.05)
x	DRI (10 Hz)	0.669	0.637
x	BS 6841 filter	0.878	0.856
y	DRI (7.2)	0.819	NA
y	BS 6841 filter	0.876	NA

Comparison of Subjective Responses with Spinal Transmission

Comparisons of subjective severity ratings and normalized spinal transmission measured at the T1 and L2 vertebral levels demonstrated that subjective severity had a close relationship with spinal transmission in response to both positive and negative x axis shocks. However, a better relationship was observed for positive shocks (Figures F-112 to F-115). Comparisons of subjective severity ratings and normalized spinal transmission also demonstrated close relationships for y axis shocks. (Figures F-112 to F-115). Similarly for z axis shocks, there was a close relationship between subjective severity and spinal transmission measured at T3 and L4. However, in the z axis, severity ratings appeared to underestimate spinal transmission to T3 in response to 2, 3 and 4 g shocks at very low frequencies (4 to 6 Hz) (Figures F-116 to F-119). The consistent frequency and amplitude effects which were observed in comparisons between subjective severity and the existing biodynamic models were not observed in spinal transmission data. Correlation coefficients obtained from linear regression analysis demonstrated the closeness of these relationships (Table 17).

Table 17
Correlation coefficients for subjective severity ratings with spinal transmission to the lumbar and thoracic vertebrae in response to single shocks.

Shock Axis and Direction	Vertebral Level	Correlation Coefficient (r^2, α=0.05)
+x	T1	0.954
+x	L2	0.909
-x	T1	0.858
-x	L2	0.872
+y	T2	0.958
+y	L3	0.940
+z	T3	0.918
+z	L4	0.936
-z	T3	0.935
-z	L4	0.954

Long Term Experiments (LT1 to LT5)

Effect of Shock Axis, Direction, Amplitude and Rate

The data for subjective response ratings for Comfort, predicted tolerance and severity to repeated shock exposures in LT1 are summarized in Tables E-49 to E-51. For both the x and z axes, there were no significant differences demonstrated between positive and negative shock exposures. Comparison of ratings for exposures in different axes showed that the x and y axis exposures were not significantly different, whereas motion exposure in the z axis was significantly less comfortable, less tolerable and more severe than in the x and y axes. Shock exposures of equal VDV, but with different shock rate and amplitude combinations, were not significantly different.

Effect of Exposure Duration on Subjective Response

Subjective ratings demonstrated duration-dependent trends with varying shock exposure conditions (i.e., shock axis, amplitude and shock rate) during the LT2 experiments which lasted for 2 hours. Duration-dependent trends included: decreased comfort; decreased predicted tolerance; increased tiredness; and increased severity (Figures F-120 to F-123). Paired t-tests demonstrated no significant differences between mean data for first and last measurement intervals, except for comfort ratings to the 2 g, 32 per minute condition in the combined x, y, z axis, and for tiredness ratings to 2 g, 32 per minute y axis shocks.

In experiment LT3, subjective comfort for both of the subject subsets (n=6 and n=10) demonstrated a rapid, significant decrease within the first 1.5 hours of exposure. Subjective comfort remained relatively constant beyond 1.5 hours, except for immediately following rest breaks when comfort ratings showed significant improvements (Figure F-124). Tolerance predictions

tended to decrease with increasing exposure duration for subject subsets n=6 and n=10. However, the decrease in predicted tolerance from first to last measurement interval was not significant for either subject subset (Figure F-125). Subjective tiredness for subsets n=6 and n=10 rapidly increased within the first 0.5 hours of exposure. From 0.5 to 1.5 hours tiredness ratings increased significantly, but at a slower, yet significant rate. However, there was no further increase in tiredness beyond 1.5 hours of exposure (Figure F-126). Severity ratings demonstrated a significant increase within the first 15 minutes of exposure, after which there was no significant increase present (Figure F-127).

A significant duration effect in subjective ratings of comfort and tiredness was also observed in LT4 experiments over the course of a daily (four-hour) exposure. However, predicted tolerance and severity were relatively constant over a single day of exposure, and showed no consistent differences between first and last measurement intervals (Figures F-128 to F-131).

Comparison of subjective ratings in LT4 at the 2 hour measurement interval between day 1 and the successive days showed no significant change for successive exposure days in the assessment of comfort, tolerance, tiredness or severity. Although the absolute subjective ratings did not varying from day to day, the change in ratings from first to last measurement interval within each daily exposure varied across the 5 days of exposure. The slope of the linear regression equation for comfort rating with daily exposure time was highest on the first day and decreased on the consecutive days. For tiredness, the slope of the regression function was highest on the first day of exposure, remained lower for the three following days, and then increased on the final day of exposure (Table 18).

Table 18
Linear regression equations of comfort and tiredness ratings with exposure time, for each successive day of exposure.

Exposure Day	Comfort	Tiredness
1	y=-0.36x+4.9	y=0.44x+1.7
2	y=-0.14x+4.4	y=0.20x+2.2
3	y=-0.21x+4.6	y=0.16x+2.2
4	y=-0.19x+4.5	y=0.16x+2.3
5	y=-0.19x+4.5	y=0.34x+1.7

Effect of Rest Breaks on Subjective Response

In LT3 experiments, short term rest breaks (i.e. 15 and 30 minute) had no significant effect on ratings of predicted tolerance, tiredness, or severity. However, a significant effect

was shown for comfort following the first (15 minute) and second (30 minute) break (Figure F-126). Similarly, comfort and tiredness tended to improve in LT4 experiments with daily, mid-exposure 15 minute breaks (Figures F-128 and F-129). Comparisons of the slopes of regression equations of continuous and intermittent exposures in LT5, indicated that intermittent rest breaks had a slight recovery effects on subjective comfort, predicted tolerance, tiredness and severity (Figures F-132 to F-135 and Table 19. The largest effect of rest breaks was demonstrated with subjective comfort ratings.

Table 19
Regression equations for subjective ratings with exposure time for both continuous and intermittent exposure conditions.

Subjective Rating	Continuous Exposure	Intermittent Exposure
Comfort	y=-1.40x+4.85	y=-0.765x+5.11
Predicted tolerance	y=-1.64x+5.56	y=-0.890x+5.26
Tiredness	y=2.04x+1.37	y=1.59x+1.26
Severity	y=1.24x+3.26	y=0.735x+3.18

The effect of overnight recovery breaks were had a consistent, significant improvement on comfort and tiredness ratings in LT4. This was shown by paired t-test comparison of the last measurement interval of one day and the first interval of the consecutive day of exposure (Figures F-128 and F-129). In addition, severity ratings decreased significantly between day 1 and 2, and day 3 and 4 (Figure F-131). Predicted tolerance did not change significantly with overnight rest breaks (Figure F-130).

Comparison of the VDV and Subjective Response

In experiment LT1, subjective ratings of comfort, predicted tolerance, and severity to equal VDV exposures were not significantly different. This was demonstrated for all shock input axes and directions, and at both dose levels tested (VDV=14.5 and VDV=29.1).

Ratios between subjective response to low and high VDV motion exposures showed that comfort ratings for low dose exposures were approximately 2 times higher than for high dose exposures. Table 20A shows that when VDV was halved, the ratio of comfort ratings changed approximately 2-fold. A comparison of severity ratings showed that low dose exposures were approximately half as severe as high dose exposures, ranging from a factor of 0.41 to 0.67 (Table 20B). These approximate 2-fold changes in comfort and severity ratings represent the expected 2-fold change in the VDV when shock amplitude was doubled in this experiment.

Predicted tolerance ratings for low dose exposures were approximately 2 to 5 times higher than high dose exposures (Table 20C). These results did not follow the anticipated 16-fold change expected from the amplitude and time dependence of the VDV. (For further explanation of the relationship between shock rate, shock amplitude, duration of exposure and the VDV, see section "Experimental Design: Motion Exposures".)

The change in subjective ratings with a 2-fold increase in the VDV appeared to be dependent on input shock axis. The change in ratings were more pronounced in the z axis than in either the x or y axis.

Table 20
The ratio of subjective ratings in Experiment LT1 between two motion exposures (VDV=14.5 and 29.1) where VDV was doubled by a two-fold increase in amplitude for a given shock rate, for Comfort (A), Severity (B) and Tolerance (C).

A. Comfort

Shock Amplitude for low and high VDV	Shock Rate (min^{-1})	+x	-x	+y	+z	-z
1 g vs 2 g	128	1.32	1.46	1.40	1.92	2.56
2 g vs 4 g	8	1.40	1.88	1.45	2.65	2.82

B Severity

Shock Amplitude for low and high VDV	Shock Rate (min^{-1})	+x	-x	+y	+z	-z
1 g vs 2 g	128	0.64	0.55	0.52	0.67	0.56
2 g vs 4 g	8	0.44	0.41	0.41	0.46	0.47

C. Tolerance

Shock Amplitude for low and high VDV	Shock Rate (min^{-1})	+x	-x	+y	+z	-z
1 g vs 2 g	128	1.70	1.75	1.81	3.48	3.46
2 g vs 4 g	8	1.48	2.17	1.98	4.08	5.47

For LT3 experiments, normalized cumulative VDV was similar to subjective tiredness ratings (r^2=0.860) (Figure F-136). Although tiredness generally followed increasing VDV with exposure caused tiredness ratings to fluctuate above and below the VDV values. In LT4 experiments, the similarity between the time dependence of the VDV and subjective tiredness ratings was demonstrated for exposure days 1, 2 and 5 (r^2=0.909, 0.806 and 0.934, respectively) (Figure F-137). In LT5 experiments, continuous and intermittent shock exposures, having equal VDV, did not have significantly different subjective ratings.

Physical Status

Body part discomfort reported by subjects during motion exposure, at rest breaks, and in conjunction with blood and urine sampling, was most often associated with the neck (C7-T3), between the scapulae (T6-T9), at the lumbar spine (L1-L3) and buttocks. Subjects reported discomfort as "tightness", "numbness", "throbbing", or "pain" in the muscles and occasionally in the spine. A few subjects reported headaches, which disappeared shortly after exposure (within 1 hour). Generally, the type of physical discomfort experienced post-exposure, was comparable to that experienced from strenuous physical activity, for example lifting weights. However, the onset of soreness was more rapid with repeated shock exposure than usually associated with such activity. For example muscular soreness, which is typically greatest two days after a weight lifting session, developed within 24 hours after a 4 hour exposure on the MARS.

During LT4 experiments the highest level of discomfort was reported during the second and third day. Generally by the fourth and fifth day, subjects were reporting lower discomfort than on previous days. LT3 subjects generally reported that discomfort had diminished to negligible levels after 48 hour to 72 hours of recovery.

Short term rest breaks relieved discomfort temporarily by allowing the subject to stretch, improve blood circulation, relieve postural discomfort from the seat and provide a mental break from the constant motion. However, subjects reported the same level of pre-rest discomfort within five to ten minutes of resuming motion exposure. Predicted tolerance estimates when question at the 24 hours post-exposure, were approximately 25% longer if the motion was to include breaks.

Blood and Urine

Biochemical data which were measured in experiments LT2, LT3 and LT4 are presented in Tables E-52 to E-59 for blood and urine data. Each table includes all of the measured metabolites for one experiment. Two additional variables (creatinine clearance and creatinine clearance normalized for body surface) included in the urinary data are calculated variables indicative of glomerular filtrate rate. Table 21 summarizes the biochemistry data tables which are located in Appendix E in relation to the motion signatures.

Table 21
List of data tables (located in the Appendix E) for blood and urine metabolites measured in experiment LT2, LT3, and LT4.

Table Number	Experiment Number	Blood or Urine	Motion Signature
Table E-52	LT2	Blood	4 g, -x axis
Table E-53	LT2	Blood	4 g, +z axis
Table E-54	LT3	Blood	2 & 4 g, ± x, y and z
Table E-55	LT4	Blood	2 & 4 g, ± x, y and z
Table E-56	LT2	Urine	4 g, -x axis
Table E-57	LT2	Urine	4 g, +z axis
Table E-58	LT3	Urine	2 & 4 g, ± x, y and z
Table E-59	LT4	Urine	2 & 4 g, ± x, y and z

The coefficient of variation (CV) of each analysis reported by Lyster Hospital and verified by BCRI is reported in Appendix C. With the exception of two variables (LDH and lactic acid), the CV determined by BCRI was similar to that reported by Lyster Hospital. Duplicate samples of LDH and lactic acid were poorly correlated, based on Pearson correlation coefficients. High variation was also noted on at least one occasion in the duplicate measurement of each the following variables: CPK, LDH, and blood urea nitrogen. On two other occasions, one of the two samples submitted for duplicate analysis was not reported for CPK or lactic acid. In other instances, the hospital laboratory reported that blood samples were clotted or hemolyzed, which likely affected certain analyses.

The data were reviewed under categories to look for trends that would suggest the type and location of any biochemical stress, fatigue, or damage. The categories were: muscle damage; fluid shift; blood clotting; glucose in blood and urine; fatigue; inflammation; bone stress or remodeling; and kidney, bladder or urinary tract dysfunction. Although trends were apparent in some of the blood and urine variables, significant differences were not found in any biochemical measurement. Graphs of CPK, LDH, and creatinine clearance (Figures F-138 to F-153) include plots of individual measurement to provide an example of the inter-individual differences which contributed to the large standard deviations recorded in Tables E-52 to E-59.

Muscle Damage

Several measures were taken to monitor muscle damage, including blood urea nitrogen, LDH, uric acid, and CPK. Although the pattern of CPK followed the expected pattern of delayed CPK

release following muscular trauma in some individuals, no consistent or significant trend was observed.

The upper range for normal is 190 U/L for CPK and 220 U/L for LDH. In each experiment in which blood was measured, CPK and LDH concentration was elevated above normal in one or more subjects (Figure F-138 to F-145). Elevated values were also present in some baseline or pre-exposure measurements. Figures F-142 to F-145 illustrate that the CPK concentration for at least one subject was markedly different from the group mean data in each experiment.

Although the motion exposure did not result in a significant change in CPK, Figures F-142A and F-142B show the effect on the mean CPK response when one subject (who had a delayed elevation in CPK) was removed from the group data. Similarly in Figure F-143, one subject had a peak CPK value of 2,962 at 48 hours post exposure, which is more than 10 times the maximum normal value. At debriefing, the subject reported that he completed an intense weight training session one day before the experiment. Thus, the delayed CPK elevation likely resulted from pre-experiment exercise. The group mean data which were recalculated, excluding this individual, are plotted in Figure F-143B. The recalculated data did not demonstrate a significant trend.

Similarly, the data of one subject was outside the range of the group data at every time point in experiment LT3 (Figure F-144A). Data for this subject were only recorded up to 24 hours post exposure, when the subject was excused from the protocol for other reasons. The group mean data were recalculated excluding this subject, and plotted in Figure F-144B. Again, the data which excluded this subject did not show a significant trend.

In Figure F-145, which represents experiment LT4, two subjects had several CPK measurements which were above the normal range. The pattern of CPK concentration for both subjects suggests that physical exercise was performed either shortly before or during the this experiment. Closer evaluation of individual LDH data (Figures F-138 to F-141), where many values were also greater than normal in baseline or pre-exposure measurements, provided further evidence that subjects participated in physical activity outside of the protocol.

Other measures which could be indicative of muscle damage (blood urea nitrogen and uric acid) did not change significantly as a result of the experimental exposures.

Fluid Shift

Fluid shifts were monitored by changes in hemoglobin, hematocrit, and total protein. No significant changes were observed in these data.

Blood Clotting

Platelet count, included in the complete hematology profile, did not show a significant change in any of the experiments.

Glucose in Blood and Urine

Blood glucose tended to decrease between pre- and post exposure measurements in LT3, LT4, and one of the LT2 experiments. The changes in blood glucose were neither rapid nor significant, and did not fall below normal plasma glucose values. The blood glucose measurement was not a fasting value, so fluctuations were expected as a result of food consumption. Urinary glucose was also normal throughout the experimental procedures in all but one subject who provided urine samples with glucose present on two occasions.

Fatigue

The group mean data for blood lactate did not indicate cumulative fatigue from muscular activity as a result of experimental exposure. In some subjects, particularly in Experiment LT3, blood lactate was higher in the pre- than in the post-exposure sample. Some of the baseline and pre-values were high enough to suggest moderate exercise (3.5 to 4.0 $mg \cdot dL^{-1}$), but were more likely due to improper blood handling procedures or incomplete glycolytic inhibition in the collection tubes.

Inflammation

Systemic inflammation was monitored by white blood cell count. Baseline blood samples screened subjects for a WBC count indicative of a pre-existing infection which would exclude their participation in the experiments. No large change in white blood cell count was observed in response to any of the experimental conditions. Uric acid, which may change in response to inflammation in synovial joints, also did not change in response to prolonged exposure to repeated shocks.

Bone Stress and Remodeling

Alkaline phosphatase did not show a consistent change which might be linked to bone stress or remodeling.

Kidney, Bladder, or Urinary Tract Dysfunction

Urine samples were tested up to 4 days post-exposure for many variables which could suggest dysfunction of the kidney, bladder, or urinary tract (e.g., the presence of blood cells, protein, leukocyte esterase, nitrite, appearance, color, and pH). Frequency

analysis of these data did not show consistent change in any of these variables as a result of motion exposure.

Glomerular filtration was assessed through measurement of creatinine clearance. Creatinine clearance measurements provide a relationship between plasma creatinine concentration, urinary creatinine excretion and urinary volume. Because creatinine clearance depends on the muscle mass of an individual, it is more appropriate to compare creatinine clearance values normalized to the external body surface area (BSA) of an average individual (1.73 m^2)(Brunzel, 1994). Normalization allows the comparison of the data, independent of an individual's body surface area. However, neither of these variables showed consistent change up to 4 days post exposure in the prolonged duration experiments (Figures F-146 to F-153). The normal reference value for creatinine clearance normalized to BSA is 80 to 135 $ml \cdot min^{-1} \cdot 1.73\ m^2$ for 20 to 39 year old males (Brunzel, 1994). In Figures F-146 to F-153, many of the subjects had creatinine clearance values outside of this range, even in baseline and pre-exposure measurements.

Synthetic Work Task

The motion environment, coupled with fatigue resulting from prolonged exposure, was expected to influence performance on synthetic work tasks. The mean and standard deviation of the composite scores of six subjects during each of two SynWork trials in LT2 are summarized in Table 22. Composite scores were consistently lower for the motion signature with negative 2 g shocks at a rate of 32 shocks per minute in the z axis, than for other conditions. Composite scores were also lower for all conditions with 2 g shocks at 32 shock per minute than conditions with 4 g shocks at 2 shocks per minute, although these differences were not shown to be significant. Because these conditions were randomized for each subject, no effect of habituation to motion was observed.

Composite SynWork scores improved progressively throughout the duration of experiments LT3 and LT4. Figure F-154 which summarizes the composite scores of ten subjects in LT3 shows a steady increase in overall scoring throughout the 7 hour exposure. Figure F-155 illustrates similar trends for the scores of eight subjects in LT4 with cumulative exposure duration. These data are limited by the fact that only two subjects completed the full seven hour experiment due to predicted tolerance time. This limited the number of synwork trials during the protocol. A habituation to cumulative motion exposure is shown both in the seven hour protocol (LT3) as well as motion exposure for four hours per day over a five day period (LT4). Further analysis of these data are required.

Table 22
Means and standard deviations of synthetic work task composite scores by trial in experiment LT2.

Motion Signature	1st Trial		2nd Trial	
	Mean	S.D.	Mean	S.D.
2 g -x axis, 32 shock·min^{-1}	1351	405	1496	289
2 g -z axis, 32 shock·min^{-1}	1093	335	1085	329
2 g x, y, z axis, 32 shock·min^{-1}	1266	462	1551	394
4 g -x axis, 2 shock·min^{-1}	1474	415	1655	459
4 g +z axis, 2 shock·min^{-1}	1572	312	1656	424

Discussion

The discussion is organized in the following manner. Findings which are related to specific aspects of this study are compared to expected findings and to the existing literature. The results of this study are then compared to existing biodynamic models and to the project goals. This leads to the requirements for development of a health hazard assessment model relative to the outcomes of the Phase 4 study. Finally, the key features are described which should be incorporated into an operationally relevant model for health hazard assessment of vehicle motion.

Spinal Acceleration

A consistent feature of the spinal response to shocks in the x axis was that the direction of the acceleration output at the thoracic spine (T1) was the inverse of the acceleration input at the seat. This result suggests that the sudden forward acceleration of the seat (positive x axis shock) induces a backward rotation of the upper body in the sagittal (x - z) plane. Anatomically, this motion can be achieved by extension of the hip joint and/or extension of the spine. In the case of negative x axis shocks, the pattern was reversed. A backward acceleration of the seat resulted in a forward acceleration at the T1 spinal level. This would indicate that the x axis shocks produce rotation of the upper torso rather than, or in addition to, a linear acceleration.

Similarly, the direction of the y axis acceleration output at the thoracic spine (T1) was consistently the inverse of the y axis acceleration input at the seat. The sudden lateral acceleration of the seat appears to produce a contra-lateral rotation of the upper body in the coronal (y - z) plane. Anatomically, this motion can be achieved by lateral flexion of the spine, or a rocking motion pivoting on the seat. The latter effect was limited by the seat belt. It would indicate that y axis shocks also produce rotation of the upper torso rather than, or in addition to, a linear acceleration.

The combined horizontal and rotational motion of the upper body or pelvis in response to x or y axis shocks is likely to result in rotation, torsion and shear forces in the spine. The response to z axis shocks has also been shown to result in horizontal and rotational forces in the spine associated with motion of individual vertebral segments during spinal flexion and extension (Hagena et al., 1986; Sandover and Dupuis, 1987). Ewing et al. (1972) and Prasad et al. (1974) demonstrated that forward flexion of the torso in response to axial shocks leads to tension in posterior spinal structures and unloading of facet joints. This

results in a greater load at the vertebral body than the applied axial force, due to the bending moment, as well as eccentric compression. Dupuis (1994) argues that these stresses are directly related to the pathophysiology of back pain in response to acute whole body vibration exposure, and result in degenerative changes to the intervertebral discs and vertebral structures in response to chronic motion exposure.

The application of uni-directional shocks (x, y or z axis) at the seat results in complex spinal motion involving not only linear displacement, but also flexion, extension, lateral bending and rotation. Hence, modeling approaches for predicting stress in the spine should account for the dynamic motion of the spine in response to shock at the seat. Displacement data (Optotrak) collected during Phase 4 experiments will be analyzed during Phase 5. These data will provide detailed information about spinal motion for implementation in a biomechanical model to estimate stress in the spine.

Transmission of Spinal Acceleration

The results of transmission of spinal acceleration clearly illustrate the non-linear relationship between an input shock at the seat and the acceleration response at the spine. In general, the effect of shock frequency on transmission ratio is stronger as shock amplitude increases. Therefore, the existing biodynamic models and guidelines, which have linear characteristics (i.e., the BS 6841 (1987) and DRI from the ASCC standard) will be valid for only a limited range of shock amplitudes and shock frequencies. The identified non-linearities identified in the current experiments indicate that existing linear models and weighting filters will incorrectly estimate the transmission of large amplitude shocks, particularly at low frequencies. The linear filter, BS 6841 (1987), underestimates the transmission ratios for all axes, whereas the DRI linear model overestimates the transmission ratios for the x and y axes, but underestimates for the z axis.

Transmission ratios of input shocks of similar amplitude and frequency were not the same across shock axes or directions. Positive z axis shocks show the greatest transmission ratios, likely reflecting the fact that the spinal system is more tightly coupled (stiffer) in the axial direction than in either lateral direction. The human body is symmetric about the sagittal plane, hence the direction of shock in the y axis did not influence transmission. Transmission ratios also failed to demonstrate a symmetrical response in the z axis. Therefore, predictions of the human response to x and z axis shocks must be sensitive to shock direction. The transmission curves generated from Phase 4 experiments support the need for development of a predictive model

that is both non-linear with shock amplitude and sensitive to shock direction and axis.

Shock And Impact

There are two distinct effects of motion input at the seat.

1. The direct effect of shock (transmission), and

2. The indirect effect of secondary impact.

Griffin (1990) defines shock as a sudden change in force, position, velocity or acceleration that excites transient disturbances in a system. In this report, mechanical shocks are low frequency (2-20 Hz) events imparted by direct transmission of vehicle motion through the seat.

An impact is defined as a single collision between one mass and a second mass (Griffin, 1990). The high frequency event (20-150 Hz) resulting from the collision of the subject with the seat is an impact. The biomechanical events associated with these impacts are not clearly understood. Measurement techniques need further development and validation before a full understanding is achieved. It is conceivable that the dual response to a single shock input of greater than 2 g in the z axis should be incorporated into a health hazard assessment model.

High Frequency Spikes (Impacts)

The results clearly establish the presence of high frequency acceleration spikes at both the lumbar and thoracic level in response to larger amplitude shocks (2 to 4 g at a frequency of 4 to 8 Hz). The nature of these high frequency spikes has not been reported previously in the literature. These effects were unexpected (in terms of acceleration magnitude and frequency content). Analysis of these data, in particular with regard to skin movement effects, have to be regarded as tentative.

A comparison has been provided of the shock transmission ratios obtained from the raw acceleration data, the data corrected for bone-skin transfer effects, and data which have been low pass filtered at 40 Hz. Although the skin transfer function and 40 Hz filter result in a considerable attenuation of the spinal accelerations recorded, the transmission ratios remain well in excess of those predicted by existing models.

Based on the raw data and subsequent analyses of spinal transmission, the high frequency acceleration spikes found in this study are not considered to represent either skin artifact or accelerometer measurement error. For high amplitude shocks, there is evidence of transmission of high frequency acceleration

spikes within the vertebral column, which are not present in lower amplitude vibration. The correction technique for bone-skin transfer reported by Hinz et al. (1988), Smeathers (1989) and Kitazaki and Griffin (1995) are inadequate in these circumstances and will grossly amplify the high frequency components measured. Therefore, an alternate correction technique was developed for this study.

At low levels of vibration and shock, the body acts as a low pass filter. As the magnitude of shocks increase, the body transmits the higher frequency components of the impact. The effect of these acceleration waveforms on any health hazard index will be highly dependent on the theoretical form of the dose response model.

Internal Pressure

The measured internal pressure response to shocks at the seat is likely to be a composite result of a combination of internal events. Co-activation of abdominal and back muscles in response to a shock was observed in Phase 3. This co-activation, along with activity of the diaphragm, will increase intra-abdominal pressure. In addition, internal pressure was measured in the colon at the base of the abdomen. Hence, the motion of organs and tissues positioned superior to the pressure transducer will influence the locally measured pressure. Downward motion of abdominal organs will exert a force on the lower colon, which will be recorded as a transient increase in internal pressure. It is not known what the respective contribution of these events may be in the measured pressure.

Phase 3 experiments demonstrated that the internal pressure response to a 3 g, z axis shock could exceed the maximal voluntary pressure that subject's could produce (>200 mmHg). Such large and relatively long lasting pressure transients in the abdomen may provide a counter-force to the inertial moment of the upper torso and head. If this is true, the internal pressure response may reduce axial loading of spinal elements by providing an alternate pathway for load transmission and reduce bending moments.

Phase 4 experiments characterized the frequency and amplitude dependence of the internal pressure response to shocks applied at the seat. As with acceleration transmission in the spine, the internal pressure response demonstrated non-linearity with shock amplitude for shock frequencies below 11 Hz. Hence, a biomechanical model designed to estimate stress in the spine in response to low frequency shocks should include the influence of internal pressure. If internal pressure significantly affects estimates of spinal stress, the development of a non-linear

predictive model to estimate internal pressure in response to seat shocks would enhance utility in the development of a health hazard assessment model. If internal pressure transients indicate movement of abdominal organs, the response curves suggest that high amplitude, low frequency (<11 Hz) shocks present the greatest risk of injury to the organ systems.

EMG and Fatigue

Long duration experiments (LT3 and LT4) were expected to result in fatigue of back muscles. This was of interest for health hazard assessment because of possible association between back muscle fatigue and chronic low back pain, diminished functional capabilities of the individual, and increased stress on passive tissues of the back. Back muscles are partially responsible for the maintenance of posture during motion, especially in a seated position. This may be critical for prevention of injury caused by a soldier hitting instrumentation or walls inside a vehicle. Muscle fatigue may also reduce a soldier's capacity to perform physical tasks immediately after prolonged motion exposure, particularly if those tasks involve extensive recruitment of back muscles. Thus, a soldier might be at higher risk of injury due to operational activities if physical tasks are preceded by prolonged travel in TGVs. Muscle fatigue is believed to be a contributing factor in the etiology of chronic low back pain (Roy et al., 1989), although the mechanism of this association is not well understood. It has also been suggested that the progression of muscle insufficiency or fatigue leads to increased stress on the passive tissues of the spine (Bogduk, 1984; Gracovetsky, 1988). Muscle fatigue, therefore, may have multiple consequences that are relevant to the health of the soldier.

Although the Phase 3 study reported that back muscle activity was typically less than ten percent of a maximal voluntary contraction during simulated motion, there was evidence of back muscle fatigue in the LT3 experiments in all subjects, despite a range in experiment duration of two and one half hours to seven hours. Increased rms EMG activity across the duration of the LT3 experiments suggests that localized muscle fatigue resulted from this motion exposure. However, the lack of consistent evidence of prolonged localized muscle fatigue in pre-exposure and post-exposure test contractions suggests that recovery occurred rapidly after motion was terminated. The time required to remove accelerometers and instrument subjects with the test contraction apparatus (less than 5 minutes) was sufficient to allow back muscles to recover. The increase in rms EMG activity during the motion exposure may also be due to alterations in posture or temperature. However, it is unlikely that either of these parameters would result in such a consistent finding between subjects.

Approximately twenty-five percent of subjects demonstrated a change in mean frequency of EMG during test contractions after motion exposure in this study. However, this change was equally likely to be an increase or decrease in mean frequency. Although the classical literature argues that muscle fatigue results in a decreased mean frequency, recent research has also identified an increase in mean frequency of back muscle EMG associated with fatigue (Voss and Krogh-Lund, 1989).

Lindstrom (1977) introduced the concept that a decrease in the motor unit action potential (MUAP) conduction velocity, resulting from localized muscle fatigue, altered characteristics of the EMG spectrum. Lindstrom evaluated MUAP conduction velocity using the ratio of the first and zeroth spectral moments of the EMG signal during test contractions. By definition, this parameter is also the mean spectral frequency (MF). Hence, it was postulated that fatigue-induced reduction in MUAP conduction velocity could be assessed using the spectral characteristics of surface EMG, with a decline in MF indicating localized muscle fatigue. Although this method is regularly applied to assess localized muscle fatigue using surface EMG, it is also apparent that there are multiple factors contributing to the surface EMG spectrum.

Hagg (1991) suggested that an increase in spectral characteristic parameters, such as MF, is not likely caused by an increase in motor unit action potential velocity, but rather successive recruitment of new motor units. Voss and Krogh-Lund (1989) expressed a similar theory that fatigue induces re-coordination among minor muscles that constitute the erector spinae group. Hence, either a large increase or decrease in MF may indicate localized muscle fatigue, since successive recruitment or re-coordination are in response to functional fatigue of the previously active muscle fibers.

In the present experiments there was no relationship between the change in MF and subjective reporting of discomfort, estimated tolerance time, or the time of exposure termination. Individuals who reported a great degree of discomfort, or had experiments terminated early did not demonstrate a greater probability of showing a change in MF than subjects who completed the full experimental duration. Similarly, there was no relationship between the magnitude of change in rms EMG and any of these factors, including total experiment duration.

In summary, the development of measurable, enduring muscle fatigue has not been demonstrated as a consistent result of exposure to relatively severe motion for up to seven hours in one day and for up to five consecutive days of four hours per day. However, an increase in rms EMG activity was consistently measured during exposure to motion in all LT3 volunteers, despite a range in experiment duration of two and one half hours to seven hours. The increased rms EMG activity may indicate a reduced capacity

or increased effort to exert control over posture during motion. However, the magnitude of muscle response to a typical shock remains well below the level of a maximal voluntary contraction. Muscle fatigue was not related to discomfort, subjective reporting of back pain, or diminished functional capacity in the generation of a contraction at twenty percent of a maximal voluntary contraction.

Biochemistry

The consistent absence of detectable biochemical change in blood and urine variables was unexpected and disappointing. Based on the results of the Phase 3 study, coupled with the increased exposure intensity (i.e., higher VDV) and duration of prolonged motion exposures, an indication of fatigue, stress or injury was anticipated. Although the subject numbers were large enough to provide sufficient analytical power in relation to the expected changes in biochemical variables, strong trends in the data were not identified.

At the outset of Phase 4, the most promising biochemical markers were indicators of muscle damage (CPK and LDH) and renal dysfunction (blood in urine and GFR). CPK and LDH are muscle enzymes that leak from damaged muscles into the blood stream. The peak concentration of these enzymes is normally reported between 24 to 48 hours post-trauma.

The irregular fluctuation in CPK and LDH in some subjects following motion exposure, as well as clinically elevated CPK in many pre-exposure measurements, strongly suggests that subjects did not strictly follow the repeated instruction to eliminate physical exercise for the duration of the study in either Phase 3 or Phase 4. Data from the Phase 3 study suggested that 2 of 4 subjects experienced an elevation in CPK between 12 and 36 hours following 2 hours of motion exposure. However in the present study, no clear elevation in either CPK or LDH were noted after up to 7 hours exposure to repeated impacts, or after 5 days of 4 hours exposure per day. As noted in the results, at least one subject in each experiment had a delayed elevation of CPK which would be expected after severe exercise. The elevation of CPK observed one subject in LT3 is as great as that recorded after a marathon race. Apple and Rhodes (1988) reported a CPK of 2,250 U/L in one individual after completion of a marathon. However, CPK concentration in most individuals in this study were close to the normal values expected in resting subjects. Hence, it is reasonable to suggest that even if the motion exposure in the current experiments increased CPK concentration in some subjects, it represented only moderate stress compared to severe exercise. The muscle mass under stress in the

current experiment is much less than the muscle mass utilized in severe physical exercise.

Glomerular filtration, evaluated by creatinine clearance measurements, required a timed (24 hour) collection of urine. In this study, subjects were relied upon to perform the collection. Because some 24 hour urine volumes were smaller that the normal daily minimum (as low as 190 ml in 24 hours) it was strongly suspected that some urine volume was lost. Inaccurate urine volumes affected calculated creatinine clearance, hence the mean creatinine clearance data are suspect at best. As well, some subjects did not return their urine collection containers resulting in missing data.

Anderson et al. (1977) reported a small elevation in serum CPK immediately following nap-of-the-earth helicopter flights. Because CPK is not expected to be elevated until 24 to 48 hours post-exertion, it is difficult to compare their result to the present study. Other evidence from exercise physiology literature suggests that muscles may adapt to repeated exercise sessions and physical conditioning. Thus, the release of CPK into the blood stream is attenuated in repeated exposures. Since all of the subjects were healthy, fit males, their muscles may have been habituated to repeated stress which would reduce the muscle enzyme release.

Biochemical measures are subject to wide inter- and intra-individual variation at rest and in response to physiological stress. Thus, a subject identified as a "responder" may be masked by the group data. In a practical sense, a "responder" in a variable which suggests severe fatigue or damage to a muscle or organ system may be at greater risk of injury than a non-responder.

Lack of a clear biochemical marker of stress, acute or persistent fatigue, or tissue damage is consistent with other measures in the study. EMG also did not reveal obvious fatigue, and subjects did not report severe discomfort or injury in their subjective responses. There was no evidence of even hypoglycemia in these experiments. The LT2 experiments (i.e., 2 hour exposure duration) were too short to expect a large reduction in blood glucose. During 4 and 7 hour exposures, subjects were able to eat during scheduled rest breaks that were no more than 2 hours apart.

There were several factors which affected the interpretation of the biochemical data including: loss of samples due to hemolysis or clotting of blood; loss of urine volume in 24 hour urine collections; high resting concentrations in some pre-exposure measurements which were not elevated in baseline measurements; general stress associated with blood sampling; high variability in subject characteristics; and several subjects who, based on LDH and CPK data, appeared to have participated in intense physical

activity. Because of the safety precautions observed in the design of the experiments, and the physical limitations of the MARS facility, is also likely that the exposures were not long enough or severe enough to affect the subjects in a way that could be measured through blood and urine. Even if the higher intensity shocks resulted in local tissue or structural trauma, the resulting biochemical changes in blood or urine may have been too small to be detected by current analytical techniques.

In this study, a biochemical measure was not identified which would contribute to the development of a health hazard assessment model. To reduce the problems in the interpretation of biochemical data, Any future experiments which include biochemical measurements to identify the effect of exposure to repeated shocks should:

- strictly control the physical activity of the subject, even if it requires providing an escort for the subject for the period of the study.
- provide more incentive to enhance subject compliance to data collection and satisfactory completion of all aspects of the experimental protocol.
- store all blood and urine samples to complete quantitative biochemical measurements in a single batch to improve quality control. Because of the level of quality control required, analyses should be performed in an analytical laboratory instead of a hospital laboratory. The exception to this is hematology. Complete blood count needs to be performed on fresh blood samples.

The Army's accident and injury data related to tactical ground vehicles needs to be thoroughly reviewed to identify and quantify the incidence of field-related mishaps associated with motion exposure. Biochemical data obtained, for example, in prolonged field studies would provide further insight to the physiological stress associated with whole body vibration and repeated shock.

Subjective Response

Short Term Experiments (ST1)

The subjective response to single shocks was examined to determine the most severe characteristics of motion exposure, to provide a relationship between subjective response and spinal transmission of shocks, and to examine the relationship between existing biodynamic models and subjective response. In Phase 5, knowledge of these characteristics and relationships will

contribute to the development of a health hazard assessment model related to exposure to mechanical shocks .

The Effect of Motion Characteristics

The subjective response to motion exposure has been previously studied for vibration exposure (Magid, 1960; Miwa, 1968; Griffin and Whitham, 1980; and Griffin, 1990), but rarely for mechanical shocks. Studies incorporating mechanical shocks have been limited to low amplitude acceleration and positive z axis shocks (Kjellberg and Wikstrom, 1985; Howarth and Griffin, 1991). The present study expands the existing literature by providing an accurate profile of subjective response to shock exposures which have a more comprehensive range of motion characteristics (i.e., amplitude, axis, direction and frequency).

Based on subjective severity ratings, the most problematic motion characteristics were z axis shocks at the lowest shock frequency tested (2 or 4 Hz, depending on the amplitude), in both the positive and negative direction. Severity ratings for the x and y axes were not significantly different from each other. This pattern between axes is consistent with studies of equivalent comfort contours collated by Griffin (1990) for low amplitude (0.01 to 1 g) sinusoidal vibration. Although overall ratings for shocks in the x and y axes were significantly lower than in the z axis, most significant differences between axes in this study were observed only at the higher shock amplitude levels (2, 3 and 4 g).

Subjective severity ratings decreased with increasing shock frequency for all axes, directions and amplitudes. These results are supported by Howarth and Griffin (1991), who showed that discomfort caused by low amplitude (0.4 to 1.4 g) shocks was highest for the lowest tested frequency (1 Hz), and decreased significantly for each increasing test frequency (1, 4 and 16 Hz). Some studies have shown a resonant frequency between 4 to 8 Hz for subjective ratings to sinusoidal vibration in the z axis (Magid et al., 1960; and Griffin, 1990). However, this finding was not duplicated in the present study. This may be because the response to single shocks, rather than sinusoidal vibration, was tested in this study. A resonant frequency in subjective response to shocks could exist at a lower frequency than tested in the present experiments. However, due to the mechanical limitations of the MARS, lower frequency shocks could not be generated.

Positive and negative direction shocks elicited similar severity ratings in the x and z axes. Howarth and Griffin (1991) also found that direction of low amplitude shocks (i.e., 0.4 to 1.4 g) did not have a significant effect on subjective discomfort. This suggests that negative and positive shocks may be weighted equally in the evaluation of motion severity.

If subjective severity is incorporated into a health hazard standard, low frequency z axis shocks should be rated as the most hazardous motion condition. Both the x and y axes shocks should be weighted less than z axis shocks. Weighting factors for all axes should decrease as shock frequency increases.

Linearity of Subjective Response with Shock Amplitude

A non-linear amplitude effect was demonstrated with subjective severity across the tested shock frequencies (2 to 20 Hz) for all shock axes and directions. Similar non-linear amplitude effects were evident in the spinal transmission responses. To accurately model severity of shocks, the frequency weighting function would need to account for the effect of amplitude. Thus, the development of a non-linear model is required.

Relationship Between Subjective Severity and the Biodynamic Models

All existing biodynamic models which were tested underestimated subjective severity at low frequency shocks, and overestimated severity at high frequencies. Additionally, the inaccuracy of the models was dependent on input shock amplitude. In this study, both subjective severity and spinal transmission exhibited a non-linear amplitude effect. However, the existing biodynamic models and filters to which both subjective and spinal transmission data were compared are based on the assumption that the human response to motion input is linear with increasing amplitude. As demonstrated by the non-linear effects exhibited in this study, it is unlikely that existing biodynamic models can account for the non-linear effect of amplitude observed in both subjective severity and spinal transmission.

Relationship Between Subjective Severity and Spinal Transmission

Subjective severity accurately represented acceleration transmitted to the thoracic and lumbar vertebral levels in the x, y and z axes. For all axes, directions and vertebral levels, regression coefficients were found to be relatively high, ranging from $r^2=0.858$ to $r^2=0.954$. Subjective severity was more closely related to spinal transmission than to any of the existing biodynamic models and filters. This observation may be due to the common non-linear amplitude effect observed in both subjective severity and spinal transmission. In terms of evaluating health hazard effects, subjective severity may be a valid method of estimating the spinal acceleration transmitted to the thoracic and lumbar vertebral levels.

Long Term Experiments (LT1 to LT5)

Effect of Shock Axis, Direction, Amplitude and Rate

LT1 experiments demonstrated that the direction of shocks input had no significant effect on subjective response to shock exposures in either the x, y or z axis. However, the z axis shock exposures were rated significantly worse than exposure in the x and y axes. Different combinations of shock rate and amplitude, with exposures of equal VDV, had no significant effect on subjective response. In the context of subjective response, these results indicate that positive and negative shocks can be weighted equally, and that z axis shocks should have a higher weighting factor than shocks in either the x or y axes. These findings are supported by the frequency weighting, and repeated shock evaluation methods (VDV) presently outlined by the BS 6841 (BS 6841, 1987).

Effect of Exposure Duration on Subjective Response

Subjective ratings to repeated shock exposures for comfort, tiredness and severity were dependent upon exposure duration within a daily exposure. This was demonstrated in LT2 with time dependent trends, in LT3 with significant changes up to 1.5 hours of exposure, and in LT4 with significant differences from first to last measurement interval. Similarly, time dependency has been demonstrated for very short duration motion exposures (Miwa, 1968; Griffin and Whitham, 1980; Kjellberg and Wikstrom, 1985).

In terms of weekly exposures, LT4 demonstrated that overall subjective ratings for comfort, tiredness and severity remained constant. However, the slope of the functions for comfort and tiredness with daily exposure duration changed throughout the week, demonstrating less effect of exposure duration within each consecutive day. These results suggest that the effect of daily exposure was not cumulative over the course of five days. The change in slope could be due to habituation and adaptation to the effect of the daily motion exposure.

Predicted tolerance ratings were not dependent on exposure duration in LT2, LT3 and LT4 experiments. The lack of change in subjective predicted tolerance ratings from first to last measurement intervals indicates that the predicted tolerance times provided by subjects in the first 3.75 minutes of exposure are representative of their predicted tolerance at later times in the exposure. If the predicted tolerance ratings are a valid representation of the actual tolerance times of a subject, then predicted tolerance ratings provided in the first 3.75 minutes are valid for determining tolerable exposure times. This was observed in only one instance in the present study. In LT3, the predicted tolerance time of one subject (final rating: 3 hours) coincided with his actual tolerance time (experiment terminated: 3 hours), at

which time the subject was removed from the MARS (based on his earlier prediction time of 4 hours). However, this trend was not demonstrated for other subjects, either because their tolerance predictions were beyond the duration of the experiment, or because the motion exposure was discontinued at 75 % of the duration of their predicted tolerance times, to avoid potential of injury.

Effect of Rest Breaks on Subjective Response

Short term rest breaks (15 and 30 minute) in LT3 and LT4 experiments did not have a significant effect on subjective response ratings of predicted tolerance, tiredness or severity to repeated shock exposures. Although tiredness ratings improved after 15 minute breaks in LT4 and following intermittent exposure breaks in LT5, a significant overall effect was not present.

Comfort ratings to shock exposures LT3 were significantly affected by short term rest breaks. In LT4, improved trends following short term rest breaks were evident. In addition, comfort ratings in LT5 showed the greatest difference between continuous and intermittent exposures, compared to the other subjective ratings. Thus, short term breaks were able to temporarily relieve the discomfort experienced by exposure to mechanical shocks. These findings are supported by the subjective comments regarding physical status, which showed that short term rest breaks relieved discomfort by allowing the subject to stretch, improve blood circulation, relieve postural discomfort from the seat and provide a mental break from the constant motion.

Even though breaks were beneficial to the mental and physical state of the subject, these results do not support fully the inclusion of a short term recovery function in the development of health hazard assessment model. Although short term rest breaks did not affect all subjective response ratings at the tested shock exposure intensity they may be more effective when exposures are more severe. As well, the duration of the rest breaks may need to be longer to allow recovery processes to have a significant effect.

Overnight recovery was evident from the significant decreases between the ratings at the last measurement interval on one day and the initial ratings on the following day. There was also no increase in the absolute daily level of tiredness or severity ratings throughout the week. Overnight breaks appeared to return the subjects to the same subjective level before each daily exposure. If subjective responses accurately represent the physical well-being of the subject, then these findings suggest that overnight rest breaks are sufficient for recovery from daily four hour exposures to mechanical shocks at the VDV presented in this experiment. This concept is supported by findings in ST1 experiments which demonstrated that the subjective severity

response accurately represented the corresponding spinal transmission.

Comparison of the VDV and Subjective Response

The ability of the VDV to predict the subjective response to repeated shock exposures was supported in experiments LT1, LT3, LT4 and LT5. In LT1, subjective ratings were equal for repeated shock exposures with different shock amplitude and rate combinations at equal VDVs. Additionally, the change in subjective comfort and severity ratings which resulted from a 2-fold increase of shock amplitude (which doubled the VDV), showed that the subjective ratings reflected the corresponding increase in the VDV. This suggests that in terms of comfort and severity ratings, the VDV dose function is able to evaluate repeated shock exposures over a range of shock amplitudes (1.0 to 4.0g) and doses (VDV=14.5 to VDV=29.1).

In contrast, the relationship between shock amplitude and exposure duration described by the VDV was not supported by predicted tolerance ratings. According to the VDV, the predicted exposure time would have to be reduced by a factor of 16 for an equivalent exposure dose which had a two-fold increase in shock amplitude. Thus, it was expected that predicted tolerance times would decrease by a factor of 16, as shock amplitude was doubled in this experiment. However, when the VDV was doubled predicted tolerance times only increased by a factor of 2 to 5 for the different axes. Therefore, if predicted tolerance is a valid method for assessing the effects of exposure dose, the use of VDV is not supported. Conversely if the VDV is valid, predicted tolerance is not.

In experiments LT3 and LT4, the time dependence of the VDV matched subjective tiredness ratings for up to 4.5 hours. Also, the lack of a significant difference between subjective ratings to continuous and intermittent exposure conditions in LT5 experiments supports the concept that the VDV is able to evaluate motion exposure without concern for the acceleration-time history of the acceleration waveform (i.e., inclusion of rest breaks). The ability of the VDV to accurately evaluate motion exposure was previously reported with lower amplitude exposures of much shorter duration by Griffin and Whitham (1980), Hoddinott (1986), Hall (1987), Wikstrom et al. (1990), and Howarth and Griffin (1991).

Existing Biodynamic Models

In the ASCC model (1982) the cumulative acceleration dose is based on the peak amplitude of the waveform and the total number of shocks delivered during the exposure. In this model, the resultant

exposure dose is independent of the frequency of the spinal acceleration response. Thus, high frequency acceleration spikes, produced by shocks at the seat or by impacts caused by collision with the seat, will have a relatively large effect on the estimation of acceleration dose.

In contrast, the dose value in the BS 6841 (1987) VDV model is based on the integral of acceleration with respect to time. In dealing with a series of individual shock events, this translates to the area under the output acceleration waveform, and the total number of shocks. Thus the resultant dose value is highly dependent on the frequency of the shock profile as well as the peak amplitude. In this form of dose function, the high frequency accelerations measured in the present study will have much less effect on the predicted dose value, and hence predicted severity, than in the ASCC model.

With regard to biomechanical fatigue theory upon which both the ASCC and VDV models are based, it has been suggested that for most materials, fatigue life is independent of cycle rate (or shock duration) for frequencies less than 30 Hz (Lafferty, 1978). At frequencies above 30 Hz, material fatigue life becomes dependent on both the magnitude and frequency of the waveform. This effect should be considered in the development of a HHA model.

Relationship to Project Goals

The main goal of this project is to develop a Health Hazard Assessment (HHA) index for mechanical shocks and repeated impact. The first step in this process was to review and evaluate existing standards and biomechanical models. Results of Phase 4 have shown existing standards to be inadequate in describing the human response to shock. Specifically:

1. The magnitudes of shock transmission determined by the BS 6841 frequency weighting filters and the ASCC biodynamic model (DRI) do not accurately reflect spinal transmission of shocks.

2. In the z axis, there is a very distinct non-linear magnitude effect that cannot be simulated by current linear models such as the DRI.

3. The BS 6841 and ISO 2631 use the same frequency weighting function for x and y axes, yet measured transmission ratios differ in the x and y axis.

4. Subjective ratings of shock exposures do not correspond with exposure doses as measured by the VDV.

The above findings justify the development of a new and separate standard for exposure to mechanical shocks.

Requirements for the Development of a Health Hazard Assessment Model

The results of Phase 4 experiments indicate that a new HHA for mechanical shocks should incorporate a number of features not provided in existing assessment models. The present study provides extensive new information on the shock magnitudes and frequencies most likely to cause severe discomfort. The data also demonstrate the exposure durations necessary to cause post-exposure stiffness or pain, and to reach the limit of soldier tolerance. These data should provide a basis for development of a HHA model. This is the first comprehensive study of long duration exposure to high levels of mechanical shock and repeated impact. Given the different effects of axis and direction on shock tolerance, and the dependence on shock magnitude and frequency, limits developed from these data must be considered as a guideline. Further investigation will be required to validate these predictions.

In order to assess accelerations transmitted to the spine, separate frequency weighting functions should be developed for the x and y axes. In addition, the weighting function in the x and z axes should be sensitive to shock direction. The frequency weighting function for spinal accelerations in the z axis must include the effects of magnitude on shock transmission. To accomplish this, development of a non-linear model is necessary to predict shock transmission in the z axis.

The results of this study show a distinct magnitude effect on the transmission ratios of accelerations from the seat to the spine. In both the positive and negative z axis, there are significant secondary impacts following the initial shock, as the subject collides with the seat. Both of these effects are characteristic of a non-linear system and therefore cannot be represented by a simple linear model such as the DRI.

In order to be effective in tactical vehicle operations, any guideline for exposure to repeated shocks should contain information on levels of discomfort, predicted tolerance times, and potential risks of health effects or acute injury. The BS 6841 and the new draft ISO 2631 provide frequency weighting functions and a recommendation for assessing exposure in the form of a VDV. However, they do not contain clear recommendations or standards for daily tolerance of shock exposure. Hence, health effects due to either long term repeated exposure, or an acute single exposure are not predicted by these standards.

Only the ASCC standard provides a prediction of severe discomfort and percent injury level. However, these limits are based on the output of a model which has been shown to be a poor predictor of spinal transmission. In addition, the suggested dose level for severe discomfort contained in the BS 6841 (i.e., VDV less than or equal to 15) does not appear to be applicable to a military population. This study proved that most soldiers are capable of tolerating a daily VDV of approximately 60. It should be noted that at this level of exposure, some subjects experienced a high level of discomfort and residual stiffness post exposure. However, due to the non-linear nature of the VDV model, a VDV of 60 represents over 250 times the number of shocks required to attain a VDV of 15.

Although there is no evidence of biomechanical damage or serious muscular fatigue in the quantitative data, clear effects of discomfort, pain and stiffness lasting 24 to 72 hours beyond exposure were apparent in subjective data, subject debriefing and observation of the subjects. The EMG activity and biochemical responses were below those normally seen in strenuous exercise or related to metabolic fatigue. There was also an absence of post exposure fatigue in EMG spectral analysis.

The symptoms of soreness, pain and post exposure muscle stiffness may also be due to postural fatigue, caused either by increased muscle tone or sustained contraction in response to shocks. However, evidence strongly suggests that some localized pain and stiffness were derived from tissue stresses other than muscle. For example, irritation to ligamentous, connective tissues and possibly facet joint or discs may result in similar symptoms. Some subjects reported bilateral pain over the erector spinae muscles, whereas others reported pain more central to the spinal column and located directly over specific vertebrae. Several subjects noted severe soreness of the coccyx, which warranted treatment with analgesics and anti-inflammatory drugs. This specific case illustrates that the passive tissues (i.e., bone, ligament, tendon, cartilage) may be at greater risk of injury than muscle.

Key Features of a Model for Health Hazard Assessment

There are several key features identified in the Phase 4 experiments which must be included in the development of the HHA model. The HHA requires the ability to predict the human response to motion or motion dose measured on a vehicle. This must reflect the non-linearity of acceleration transmission through the body and of the subjective response to shocks. Exposure limits or guidelines must be related to a prediction of severe discomfort or probability of injury. Phase 4 experiments have provided data and insight with which to approach both of these modeling issues.

Although there was no objective evidence of injury to organ systems or tissues in the biochemical measures, and little evidence of muscle fatigue after exposure to severe motion, there was consistent subjective feedback regarding physical status and perception of motion severity, fatigue, and discomfort. It was clearly demonstrated that the motion conditions in these experiments could result in extreme soreness and pain. Given the lack of objective evidence of injury and the relatively low levels of muscle activity indicated by EMG, it is likely that this soreness was related to inflammation or damage to spinal structures (i.e., vertebrae, intervertebral discs, ligaments). Furthermore, long-term exposure to vehicle motion has been associated with degenerative changes and injury to these structures (e.g., Boshuizen et al., 1990; Wikstrom et. al., 1994). Hence, an estimate of stress in the spine, combined with known material properties of vertebrae and discs (e.g., Brinckmann, 1988) and existing models of mechanical fatigue of vertebrae (Lafferty, 1978; Sandover, 1983, 1985; Hansson et al., 1987) may provide a good estimation of the probability of acute injury. Incorporation of a recovery model with material fatigue principles will extend the model to the case of cumulative damage or degeneration over the longer term.

The phase 4 experiments have provided seat acceleration, spinal acceleration, displacement (Optotrak), internal pressure, and muscle activity data which could be incorporated into a biomechanical model to predict stress in spinal structures. Ultimately, stress prediction would be based solely on vehicle motion measurements and not on human response measures listed above. Therefore, it may be necessary to produce a number of sub-models that can predict these quantities from vehicle seat motion and provide the required inputs to a stress prediction model. For example, one sub-model will predict the spinal acceleration response to seat acceleration while another will predict the internal pressure response to seat acceleration. In this manner, a stress prediction model can be developed which does not rely upon human response measurements.

Development of the various sub-models will likely employ a modeling strategy known as system identification. This approach, often used when the system is difficult to characterize analytically or is overly complex, produces a "black box" model based on measured input and output data. Typically, a parametric model structure is assumed and a computer algorithm identifies the least-squares fit of the model parameters to the input-output data. Once the parameters are so determined, the resulting model can be used to predict the system output given any input.

System identification may assume a linear or nonlinear system. Linear identification techniques such as frequency response, deconvolution, maximum-likelihood estimation, correlation, and

least squares estimation are well-developed and understood, having been employed for decades in the areas of modeling and control system theory (Sinha and Kuszta, 1983). Nonlinear identification techniques include fuzzy logic (Tagaki and Sugeno, (1985), non-linear auto regressive moving average with exogenous inputs (NARMAX) (Leontardis and Billings, 1985), Volterra Series expansion (Hsia, 1977), and artificial neural networks (ANN) (Narendra and Parthasarathy, 1990). While some of these techniques are fairly new and fall outside the well-established realm of linear systems theory, they nevertheless can produce accurate models when linear approaches fail.

As previously discussed, the spinal response to large magnitude seat impacts is highly nonlinear. In addition, it is probable that other physiological responses (e.g., internal pressure, EMG, biochemical measurements) are nonlinear as well. Where this nonlinearity is weak, a linear model can adequately represent the response. When the nonlinearity is strong, as in the case of the transmission of acceleration to the spine, it is envisioned that an artificial neural network will be utilized. Once trained with the input and output data of the system, the resulting neural network model may be implemented as software in a personal computer or as a single integrated circuit. Ultimately, the HHA model could be developed into a portable device for assessment of vehicle motion in the field. This would provide a practical tool for the soldier or commanding officer to use during operations planning and deployment.

Conclusions

Conclusions related to the objectives of the Phase 4 study were based on the results of short and long duration experiments. These conclusions led to several recommendations for advancement of the study to Phase 5.

There are several limitations to the conclusions drawn from these experiments. Subjects in this study were males, aged 19 to 40, and represented a relatively fit, military population. The results of the study, therefore, pertain to similar populations. A major limitation of this study is the small sample size. Extreme data from one subject may have biased the group mean data. Inter-individual variation may have obscured a significant relation which would have been more obvious with a larger number of subjects. In the present study, subjects were exposed to a series of motion exposures with a fixed range of amplitude (0.5 g to 4 g) and frequency (2 Hz to 20 Hz) in positive and negative x, y, and z axes. Therefore the results and conclusions of this study pertain specifically to this range of motion exposures.

Short Duration Experiments (ST1)

1. Spinal response characteristics are dependent on the axis, direction and amplitude of shocks input at the seat.
2. There is a non-linear amplitude effect for the spinal response to shocks input at the seat. The non-linear amplitude effect is more pronounced in the z axis than in the x and y axes.
3. Low frequency shocks (2 to 8 Hz) are more severe than high frequency shocks.
4. Internal pressure showed a frequency-dependent response that was similar to that observed for spinal acceleration to shock inputs at the seat and was more pronounced in the z than in the x and y axes.
5. Spinal response to low frequency input at the seat (4-8 Hz) resulted in acceleration output at the spine containing high frequency (20-150 Hz) components associated with the subject hitting the seat.
6. Subjective severity of shocks input at the seat showed a high correlation with spinal acceleration for all axes.

Long Duration Experiments (LT1 to LT5)

1. Electromyography (EMG) data from muscles of the back showed consistent evidence of local muscle fatigue during motion exposure as brief as 2.5 hours in duration.

2. No evidence of cumulative fatigue or trauma resulting from motion exposures was found in EMG, biochemistry or subjective data, after either a single 7 hour exposure or 5 consecutive daily exposures of 4 hours each (Although there was no biochemical, EMG or subjective evidence of fatigue, subjects reported pain and discomfort during and up to 72 hours after ride exposure).

3. Rest breaks, including overnight recovery, temporarily improved the subjective rating of comfort, but did not change the predicted tolerance to motion exposures with the same VDV.

4. Subjects who volunteered for these experiments could tolerate a daily exposure in excess of the recommended daily dose of 15 (British Standard VDV). Some subjects were able to tolerate a VDV of 66 over a 7 hour period, or a VDV of 60 per day over a 5 day period.

5. Short term predictions of tolerance were consistent with those made at longer durations

Overall

1. Existing biodynamic models (BS 6841 and the DRI model) which are based on linear weighting factors for amplitude overestimated or underestimated spinal transmission and predicted subjective tolerance depending on the frequency for shocks in the range of 0.5 to 4.0 g.

2. The VDV is able to estimate the effect of shock exposures on the subjective rating of comfort, severity, and tiredness.

Recommendations

1. New hazard guidelines for human exposure to repeated mechanical shocks need to be developed.

2. These guidelines need to include:

   - biomechanical response curves for seat-vertebrae transmission
   - severe discomfort guidelines
   - hourly, daily, and weekly tolerance guidelines
   - health hazard guidelines

3. A new health hazard standard for the human response to shocks should include a nonlinear model for spinal transmission.

4. Further investigation of biomechanical effects of impacts is required.

5. Further investigation of dose-response relationships and dose-recovery relationships are required.

6. Two final recommendations which are based strictly on the results of this study, but are critical to the continuation of this program, are:

   a. To archive the data on a suitable nonvolatile media (i.e., CD-ROM) so that it will be preserved and accessible to future researchers.

   b. To develop a data access program on a PC platform to easily retrieve and display the data.

Acknowledgments

The authors would like to specifically thank a number of individuals who contributed to the successful completion of this phase of the project.

At USAARL: Major J. Albano for administrative support, medical monitoring and recruitment assistance; Major B. Butler for continued technical support; R. Dillard, and A. Lewis for programming and operation of the MARS facility; Dr. Jones for computer support services; B. Erickson, W. Reynolds, P. Tromblee and A. Whitted for on-site laboratory support; T. Terrill, F. Weatherbee and W. Adams for subject recruitment; M. Gramling for administrative support; the subject volunteers; laboratory support from Lyster Army Hospital and all members of the USAARL staff for including the BCRI team in their ongoing activities.

At BCRI: M. Garzone; L. Ritmiller; and G. Gibbs who assisted during data collection; A. Gomory for production support; the remaining members of the Ergonomics and Human Factors Group, as well as all staff at BCRI, for continued support and encouragement.

In addition, Dr. T. Brammer of the National Research Council of Canada assisted with programming of the MARS control signal; and Dr. J. Sandover for technical consultation in the development of the skin transfer function.

Their collaboration, advice, and encouragement facilitated the research team in conducting complex experiments while maintaining a very structured experimental timetable. Their contributions are sincerely appreciated.

References

A full list of references complied in the Phase 1 literature review is available in the Phase 1 Report, July 15, 1992.

Abu-Lisan, M.A. 1979. Environmental stress and coronary heart disease. Ph.D. Dissertation, Department of Human Sciences, University of Technology, Loughborough.

Air Standardization Coordinating Committee, 1982. Human tolerance to repeated shock. Air Standardization Coordinating Committee. ADV PUB 61/25: 1-6.

Amirouche, F.M.L. and Ider, S.K. 1988. Simulation and analysis of a biodynamic human model subjected to low accelerations - A correlation study. Journal of Sound and Vibration. 123: 281-292.

Anderson, D.B., McNeil, R.J., Pitts, M.L. and Perez-Poveda, D.A. 1977. The effect of nap-of-the-earth (NOE) helicopter flying on pilot blood and urine biochemicals. U.S.Army Aeromedical Research Laboratory. Report 77-20.

Apple, F. and Rhodes, M. 1988. Enzymatic estimation of skeletal muscle damage by analysis of changes in serum creatine kinase. Journal of Applied Physiology. 65: 2598-2600.

Auffret, R., Demange, J. and Vettes, B. 1974. Action des vibrations de basse frequence sur la frequence et la variabilite cardiaques (The effect of low frequency vibrations on the heart rate and variability). Revue de Medecine Aeronautique et Spatiale. 50: 122-126.

Barnes, G.R. 1987. Human Factors of helicopter vibration. 1: The physiological effects of vibration. In Helicopter vibration and its reduction symposium, 20-30. Nov. London,UK.

Beevis, D. and Forshaw, S.E. 1985. Back pain and discomfort resulting from exposure to vibration in tracked armoured vehicles. pp. 1-10. In AGARD Conference Proceedings No.378 on Backache and Back Discomfort. Pozzuoli, Italy, NATO.

Bogduk, N. 1984. The applied anatomy of the thoracolumbar fascia. Spine. 9: 164-170.

Boshuizen, H.C., Bongers, P.M. and Hulshof, C.T.J. 1990. Back disorders and occupational exposure to whole-body vibration. International Journal of Industrial Ergonomics. 6: 55-59.

Brinckmann, P. 1988. Stress and strain of human lumbar discs. Clinical Biomechanics. 3: 232-235.

British Standards Institution. 1987. British Standards guide to measurement and evaluation of human exposure to whole-body mechanical vibration and repeated shock. British Standards Institution. BS 6841.

British Standards Institution. 1989. British Standard guide to safety aspects of experiments in which people are exposed to mechanical vibration and shock. British Standards Institution. BS 7085.

Brunzel, N.A. 1994. Fundamentals of urine and body fluid analysis. Toronto: W.B. Saunders Co.

Cameron, B.J. 1992. The contribution of ammonia to exercise hyperpnea. Ph.D. Dissertation, Simon Fraser University, Burnaby.

Chernyuk, V.I. and Tashker, I.D. 1989. Combined effect on the human body of whole body and local vibration, noise and work stress characteristic of agricultural machinery. Noise and Vibration Bulletin. July: 160-161.

Dupuis, H. 1994. Medical and occupational preconditions for vibration-induced spinal disorders: occupational disease no. 2110 in Germany. International Archives of Occupational and Environmental Health. 66: 303-308.

Dupuis, H. and Zerlett, G. 1986. The Effects of Whole-Body Vibration. Berlin: Springer-Verlag.

Ewing, C.L., King, A.I., and Prasad, P. 1972. Structural considerations of the human vertebral column under +Gz impact acceleration. Journal of Aircraft. 9: 84-90.

Fairley, T.E. and Griffin, M.J. 1989. The apparent mass of the seated human body: vertical vibration. Journal of Biomechanics. 22: 81-94.

Franke, E.K. 1951. Mechanical impedance of the surface of the body. Journal of Applied Physiology. 3: 582-590.

Gracovetsky, S. 1988. The spinal engine. New York: Springer-Verlag.

Griffin, M.J. 1990. Handbook of Human Vibration. London: Academic Press Ltd.

Griffin, M.J. and Whitham, E.M. 1980. Discomfort produced by impulsive whole-body vibration. Journal of the Acoustical Society of America. 68(5): 1277-1284.

Guignard, J.C. 1972. Physiological effects of vibration. AGARD Conference Proceedings No. 151 Aeromedical aspects of vibration and noise. NATO, 36-45.

Guignard, J.C. 1974. Performance and physiological effects of combined stress including vibration. AGARD Conference Proceedings No. 145 on Vibration and Combined Stresses in Advanced Systems. Norway: NATO, B18-1-B18-6.

Guignard, J.C. 1985. Vibration. Patty's Industrial Hygiene and Toxicology Volume III Theory and rationale of industrial hygiene practice. 2nd Edition. Cralley, L.J. and Cralley, L.V., Editors. New York: John Wiley and Sons, 653-724.

Hagena, F.W., Piehler, J., Wirth, C.J., Hofmann, G.O. and Zwingers, T. 1986. The dynamic response of the human spine to sinuzoidal Gz-vibration. In-vivo experiments. Neuro-Orthopedics. 2: 29-33.

Hagg, G.M. 1991. Comparison of different estimators of electromyographic spectral shifts during work when applied on short test contractions. Medical & Biological Engineering & Computing. 29: 511-516.

Hall, L.C. 1987. Subjective response to combined random vibration and shock. UK Informal Group Meeting on Human Response to Vibration. Royal Military College of Science, Shrivenham.

Hansson, T., Magnusson, M. and Broman, H. 1991. Back muscle fatigue and seated whole body vibrations: an experimental study in man. Clinical Biomechanics. 6: 173-178.

Hansson, T.H., Keller, T.S., and Spengler, D.M. 1987. Mechanical behavior of the human lumbar spine. II. Fatigue strength during dynamic compressive loading. Journal of Orthopedic Research. 5: 479-487.

Harada, N., Kondo, H. and Kinura, K. 1990. Assessment of autonomic nervous function in patients with vibration syndrome using heart rate variation and plasma cyclic nucleotides. British Journal of Industrial Medicine. 47: 263-268.

Harstela, P. and Piirainen, K. 1985. Effects of whole-body vibration and driving a forest machine simulator on some physiological variables of the operator. Silva Fennica. 19(2): 197-202.

Heslegrave, R.J., Frim, J., Bossi, L.L. and Popplow, J.R. 1990. The psychological, physiological and performance impact of sustained NBC operations on fighter pilots. Defence and Civil Institute of Environmental Medicine Report 90-RR-08.

Hinz, B., Helmut, S., Brauer, D., Menzel, G., Bluthner, R. and Erdmann, U. 1988. Examination of spinal column vibrations: a non-invasive approach. European Journal of Applied Physiology. 57: 707-713.

Hoddinott, J.C. 1986. Investigation of the effect of duration on alternative methods of assessing human response to impulsive motion. UK Informal Group Meeting on Human Response to Vibration. University of Technology, Loughborough.

Hosea, T.M., Sheldon, R.S., Delatizky, J., Wong, M.A. and Chung-Cheng, H. 1986. Myoelectric analysis of the paraspinal musculature in relation to automobile driving. Spine. 11(8): 928-936.

Howarth, H.V.C. and Griffin, M.J. 1991. Subjective reaction to vertical mechanical shocks of various waveforms. Journal of Sound and Vibration. 147(3): 395-408.

Hsia, T.C. 1977. System Identification. D.C. Toronto: Heath and Company.

Hulshof, C. and van Zanten, B.V. 1987. Whole-body vibration and low-back pain. International Archives of Occupational and Environmental Health. 59: 205-220.

International Standards Organization. 1982. Guide for the evaluation of human exposure to whole-body vibration. ISO 2631.

Kitazaki, S. and Griffin, M.J. 1995. A data correction method for surface measurement of vibration on the human body. Journal of Biomechanics. 28(7): 885-890.

Kjellberg, A. and Wikstrom, B.O. 1985. Subjective reactions to whole-body vibration of short duration. Journal of Sound and Vibration. 99(3): 415-424.

Kjellberg, A. and Wikstrom, B.O. 1987. Acute effects of whole-body vibration. Scandinavian Journal of Work Environment & Health. 13: 243-246.

Konda, Y., Mito, H., Kadowaki, I., Yamashita, N. and Hosokawa, M. 1985. Low back pain among container tractor drivers in harbor cargo transportation. Proceedings of the Congress of the International Ergonomics Association. Bournemouth: Taylor and Francis, 802-804.

Korn, G.A. and Korn, T.M. 1961. Mathematical handbook for Scientists and Engineers. Sec 99.4-1. Toronto: McGraw-Hill Book Company Inc., 254.

Lafferty, J.L. 1978. Analytical Model of the Fatigue Characteristics of Bone. Aviation Space and Environmental Medicine. 49: 170-174.

Langauer-Lewowicka, H. 1976. Immunological studies on the pathogenesis of Raynaud's phenomenon in vibration disease. International Archives of Occupational and Environmental Health. 36: 209-216.

Larson, C., Wells G., and Kaplan, B. 1973. Study of flight environment effects on helicopter gunners. United States Army Aeromedical Research Laboratory Report 73-15.

Leontardis, I.J. and Billings, S.A. 1985. Input-output parametric model for nonlinear system part 1 and 2. Int. J. Control. 41: 303-344.

Liebrecht, B.C. 1990. Health Hazard Assessment Primer. Fort Rucker, AL: United States Army Aeromedical Research Laboratory. USAARL Report No. 90-5.

Lindstrom, L., Kadefors, R. and Petersen, I. 1977. An electromyographic index of localized muscle fatigue. Journal of Applied Physiology. 43(4): 750-754.

Magid, E.B., Coermann, R.R. and Ziegenruecker, G.H. 1960. Human tolerance to whole body sinusoidal vibration. Short-time, one-minute and three-minute studies. Journal of Aerospace Medicine. 31: 915-924.

Magnusson, M., Hansson, T. and Broman, H. 1988. Back muscle fatigue and whole body vibrations. International Society for the Study of the Lumbar Spine. 12:598.

Marras, W.S. and Mirka, G.A. 1991. Muscle activities during asymmetric trunk angular accelerations. Advances in Industrial Ergonomics and Safety III. Karwowski, W. and Yates, J.W., Editors. London: Taylor and Francis, 335-342.

Mekjavic, I.B. and Morrison, J.B. 1986. Evaluation of predictive formulae for determining metabolic rate during cold water immersion. Aviation, Space and Environmental Medicine. 57: 671-680.

Mekjavic, I.B., and Morrison, J.B. 1985. A model of shivering thermogenesis based on the neurophysiology of thermoreception. IEEE Transactions on Biomedical Engineering. 32(6): 407-417.

Milby, T.H. and Spear, R.C. 1974. Relationship between whole body vibration and morbidity patterns among heavy equipment operators. National Institute for Occupational Safety and Health. NIOSH 74-131: 1-71.

Miwa, T. 1968. Evaluation methods for vibration effect. Part 7. The vibration greatness of the pulses. Industrial Health. 6: 143-154.

Morrison, J.B., Conn, M.L. and Hayes, P.A. 1982. Influence of respiratory heat transfer on thermogenesis and heat storage after cold immersion. Clinical Science. 63: 127-135.

Narendra, K.S. and Parthasarathy, K. 1990. Identification and control of dynamical systems using neural networks. IEEE Transactions on Neural Networks. 1(3): 4-27.

Ortengren, R., Andersson, G.B. and Nachemson, A.L. 1981. Studies of relationships between lumbar disc pressure, myoelectric back muscle activity, and intra-abdominal (intragastric) pressure. Spine. 6(1): 98-103.

Parks, T.W. and Burrus, C.S. 1987. Digital Filter Design. New York: John Wiley and Sons Inc.

Payne, P.R. 1984. Linear and angular short duration acceleration allowables for the human body. Report Number, KTR 357-84, Ketron Inc., Arlington, VA.

Payne, P.R. 1991. A Unification of the ASCC and ISO Ride Comfort Methodologies. Unpublished report. Payne Associates.

Prasad, P., King, A.I., and Ewing, C.L. 1974. The role of articular facets during $+G_z$ acceleration. Journal of Applied Mechanics. 321-326.

Ramsay, J.D. and Beshir, M.Y. 1981. Vibration Diseases. In Clinical Medicine. Spittell, J.A., Editor. Philadelphia: Harper and Row.

Rehm, S. and Wieth, E. 1984. Combined effects of noise and vibration on employees in the Rhenish brown coal opencast working. Proceedings of 1st International Conference on Combined Effects of Environment Factors. Manninen, O., Editor., 291-315.

Roberts, D. and Smith, D.J. 1989. Biochemical Aspects of Peripheral Muscle Fatigue. Sports Medicine. 7: 125-138.

Robertson, C.D. 1987. The effect of frequency of whole-body vibration on the timing of the back muscle EMG. United Kingdom Informal Group Meeting on Human Response to Vibration. Hall, L.C., Editor. Shrivenham: Royal Military College of Science., 1-9.

Robertson, C.D. and Griffin, M.J. 1989. Laboratory studies of the electromyographic response to whole-body vibration. Institute of Sound and Vibration Research,University of Southampton. TR 184: 1-174.

Robinson, D.G. 1991. Pesticide exposure in tree planters. M.Sc. Thesis, Simon Fraser University, Burnaby.

Roman, E., Kakosy, T., Rozsahegyi, I. and Soos, G. 1968. EKG-changes of workers exposed to vibration. Munkavedelem. 14(4-6): 24-26.

Rosegger, R. and Rosegger, S. 1960. Health effects of tractor driving. Agricultural Engineering Research 5: 241-275.

Roy, S.H., De Luca, C.J., and Casavant, D.A. 1989. Lumbar muscle fatigue and chronic lower back pain. Spine 14(9): 992-1001.

Sandover, J. 1981. Vibration, posture and low-back disorders of professional drivers (part 1). Department of Health and Social Security. DHS 402: 1-141.

Sandover, J. 1983. Dynamic loading as a possible source of low-back disorders. Spine. 8: 652-658.

Sandover, J. 1985. Vehicle vibration and back pain. Advisory Group for Aerospace Research & Development Conference Proceedings No. 378 on Backache and Back Discomfort. 13-1-13-8. Pozzuoli, Italy: North Atlantic Treaty Organisation.

Sandover, J. 1986. Vibration and people. Clinical Biomechanics. 1: 150-159.

Sandover, J. and Dupuis, H. 1987. A reanalysis of spinal motion during vibration. Ergonomics. 30(6): 975-985.

Seidel, H. and Heide, R. 1986. Long-term effects of whole-body vibration: a critical survey of the literature. International Archives of Occupational and Environmental Health. 58: 1-26.

Seidel, H., Bluethner, R. and Hinz, B. 1986. Effects of sinusoidal whole-body vibration on the lumbar spine: the stress-strain relationship. International Archives of Occupational and Environmental Health. 57: 207-223.

Seroussi, R., Wilder, D.G., Pope, M.H. and Cunningham, L. 1987. The added torque on the lumbar spine during whole body vibration estimated using trunk muscle electromyography. Rehabilitation Engineering Society of North America 10th Annual Conference on Rehabilitation Technology. 811-813. San Jose, California: RESNA.

Seroussi, R.E., Wilder, D.G. and Pope, M.H. 1989. Trunk muscle electromyography and whole body vibration. Journal of Biomechanics. 22(3): 219-229.

Sinha, N.K. and Kuszta, B. 1983. Modeling and Identification of Dynamic Systems. New York, Van Nostrand Reinhold Company.

Smeathers, J.E. 1989. Measurement of transmissibility for the human spine during walking and running. Clinical Biomechanics. 4: 34-40.

Society of Automotive Engineers. 1974. Measurement of whole body vibration of the seated operator of agricultural equipment (The Society of Automotive Engineers recommended practice). The Society of Automotive Engineers SAE J1013. Handbook Part 11. 1404-1407. Society of Automotive Engineers, Detroit, Michigan.

Spaul, W.A., Spear, R.C. and Greenleaf, J.E. 1986. Thermoregulatory responses to heat and vibration in men. Aviation Space and Environmental Medicine. 57: 1082-1087.

Steiglitz, K. and McBride, L.E. 1965. A technique for the identification of linear systems. In IEEE Trans. Automatic Control AC-10: 461-464.

Sturges, D.V., Badger, D.W., Slarve, R.N. and Wasserman, D.E. 1974. Laboratory studies on chronic effects of vibration exposure. AGARD Conference Proceedings No.145 on Vibration and Combined Stresses in Advanced Systems. von Gierke, H.E., Editor. Oslo, Norway: NATO.

Takagi, T. and Sugeno, M. 1985. Fuzzy identification of systems and its applications to modeling and control. IEEE Transactions on Systems, Man, and Cybernetics. 1: 116-132.

Taylor, N.A.S. and Morrison, J.B. 1989. Lung centroid pressure in immersed man. Undersea Biomedical Research. 16(1): 3-19.

Taylor, N.A.S. and Morrison, J.B. 1991. Pulmonary flow-resistive work during hydrostatic loading. Acta Physiological Scandanavia. 142: 307-312.

Ullsperger, P., Seidel, H. and Menzel, G. 1986. Effect of whole-body vibration with different frequencies and intensities on auditory evoked potentials and heart rate in man. Applied Physiology. 54: 661-668.

Village, J.L. and Morrison, J.B. 1989. Exposure of Heavy Equipment Operators to Whole Body Vibration and Repeated Shock. Proc. Ann. Conf. Human Factors Assoc. of Canada. Toronto, Ontario.

Voss, P. & Krogh-Lund, C. 1989. Physiological effects of occupational exposures to whole-body vibration. Danish Acoustical Institute. Report No. 143: 1-222.

Weaver, L.A. 1979. Vibration: an overview of documented effects on humans. Professional Safety. April: 29-37.

Wikström, B-O, Kjellberg, A, and Landström, U. 1994 Health effects of long-term occupational exposure to whole-body vibration: A review. International Journal of Industrial Ergonomics. 14: 273-292.

Wikstrom, B., Kjellberg, A., Dallner, M. 1990. Whole-body vibration: A comparison of different methods for the evaluation of mechanical shocks. International Journal of Industrial Ergonomics. 7: 41-52.

Wilder, D.G., Frymoyer, J.W. and Pope, M.H. 1983. The effect of vibration on the spine of the seated individual. (UnPub)

Zagorski, J., Jakubowski, R., Solecki, L., Sadlo, A. and Kasperek, W. 1976. Studies on the transmission of vibrations in human organism exposed to low-frequency whole-body vibration. Acta Physiology Polonica. 27.4: 347-354.

Appendix A
The Project Team

Dr. Barbara Cameron Program Manager, BC Research	Principal Investigator 604 224-4331
Dr. James Morrison Consultant, Bio-medical Engineer Shearwater Human Engineering Ltd.	Principal Investigator 604 929-6589
Dan Robinson Ergonomist, BC Research	604 224-4331
Alan Vukusic Ergonomist, BC Research	604 224-4331
George Roddan Research Scientist, BC Research	604 224-4331
Steven Martin Research Scientist, BC Research	604 224-4331
Laurel Ritmiller Ergonomist, BC Research	604 224-4331
Mark Garzone Co-op Student, BC Research	604 224-4331
Gillian Gibbs Co-op Student, BC Research	604 224-4331

Appendix B

ST1 Subjective Response Data Sheet

Subject:	Date:	Time:	Axis:

Sample Response Scale

1	2	3	4	5	6	7

Barely Perceptible *Extremely severe*

Q1. **Compare:** Is this shock greater than, equal o, or less than the last shock?
Q2. Rate the severity of this shock. (Barely perceptible = 1 - Extremely severe = 7)
Q3. How do you rate the overall motion? (Very comfortable = 1 - Extremely uncomfortable = 7)

	Exposure Number: Shock Condition (g, axis)						
Shock #	**1:**	**2:**	**3:**	**4:**	**5:**	**6:**	**7:**
1							
2							
3							
4							
5							
6							
7							
8							
9							
10							
11							
12							
13							
14							
15							
16							
17							
18							
19							
20							
21							
22							
23							
24							
25							
26							
27							
28							
29							
30							
31							
32							
Q3 Rating:							

Comments:

LT1 Subjective Response Data Sheet

Subject:	**Date:**	**Time**
Experiment:	**Shock Axis:**	

Sample Response Scale

1	2	3	4	5	6	7
Not at all comfortable						*extremely comfortable*

Q1: Do you feel comfortable? (1 = Not at all comfortable - 7 = Extremely comfortable)

Q2: How long would you be able to tolerate this motion exposure if you were riding in a vehicle on a cross-country mission? (Unrestrained time scale)

Q3: Do you feel tired? (1 = Not at all tired - 7 = Extremely tired)

Q4: How severe do you rate the motion exposure right now? (1 = Extremely severe - 7 = Barely perceptible)

Q5: How well do you feel you could perform your tasks right now? (1 = Very well - 7 = Extremely poorly)

Q6: Rank the 5 exposures that you have had today in order of severity. (1 = least severe - 5 = most severe).

Procedure: (g, axis)	Time (min:sec)	Q1 comfort	Q2 tolerance	Q3 tired	Q4 severe	Q5 perform	Q6 Rank Order
#1:	**0:30**						
	3:00						
Rest							
#2:	**0:30**						
	3:00						
Rest							
#3:	**0:30**						
	3:00						
Rest							
#4:	**0:30**						
	3:00						
Rest							
#5:	**0:30**						
	3:00						
End							

LT2 Subjective Questionnaire Data Sheet

Question #:

1. **Do you feel comfortable?** ***(Not at all comfortable = 1 - Extremely comfortable = 7)***
2. **How long would you be able to tolerate this motion exposure if you were riding in a vehicle on a cross-country mission?** ***(Unrestrained time-scale response)***
3. **Do you feel tired?** ***(Not at all tired - Extremely tired)***
4. **How severe do you rate the motion exposures right now?** ***(Extremely severe = 1 - Barely perceptible = 7)***
5. **How well do you think you could perform your tasks right now?** ***(Very well = 1 - Extremely poorly = 7)***

Sample Response Scale

1	2	3	4	5	6	7
Not at all comfortable			*Extremely*			*comfortable*

Subject:	**Date:**	**Time:**	**Caffiene intake (type, time, amt.):**		/	/
Experiment:			**Caffiene intake (type, time, amt.):**		/	/

Exp. Time (min:sec)	Comfort	Tolerate	Tired	Severe	Perform	Comments
Start						
03:45						
07:30						
15:00						
30:00						
35:00						Synwork #1
1:00:00						
1:30:00						
1:35:00						Synwork #2
2:00:00						
END						

Experimental Notes: (Lunch, snacks, etc for subject - reattachment of sensors - distractions during exp't - etc.)

LT3 Subjective Questionnaire Data Sheet

Question #:

1. **Do you feel comfortable?** ***(Not at all comfortable = 1 - Extremely comfortable = 7)***
2. **How long would you be able to tolerate this motion exosure if you were riding in a vehicle on a cross-country mission?** ***(Unrestrained time-scale response)***
3. **Do you feel tired?** ***(Not at all tired - Extremely tired)***
4. **How severe do you rate the motion exposures right now?** ***(Extremely severe = 1 - Barely perceptible = 7)***
5. **How well do you think you could perfrom your tasks right now?** ***(Very well = 1 - Extremely poorly = 7)***

Sample Response Scale

1	2	3	4	5	6	7
Not at all comfortable			*Extremely*			*comfortable*

Subject:	Date:	Time:	Caffiene intake (type, time, amt.):	/	/
Experiment:			Caffiene intake (type, time, amt.):	/	/

Exp. Time (min:sec)	Comfort	Tolerate	Tired	Severe	Perform	Comments
Start			-			
03:45						
15:00						
30:00						
35:00						Synwork #1
60:00						
1:30:00						
1:45:00						15 minute rest - stop run time
2:00:00						
2:30:00						
2:35:00						Synwork #2
3:00:00						
3:30:00						30 minute rest - stop run time
3:35:00						
4:00:00						
4:05:00						Synwork #3
4:30:00						
5:00:00						
5:15:00						15 minute rest - stop run time
5:30:00						
6:00:00						
6:05:00						Synwork #4
6:30:00						
7:00:00						
END			-			

LT4 Subjective Questionnaire Data Sheet

Question #:

1. **Do you feel comfortable?** ***(Not at all comfortable = 1 - Extremely comfortable = 7)***
2. **How long would you be able to tolerate this motion exposure if you were riding in a vehicle on a cross-country mission?** ***(Unrestrained time-scale response)***
3. **Do you feel tired?** ***(Not at all tired - Extremely tired)***
4. **How severe do you rate the motion exposures right now?** ***(Extremely severe = 1 - Barely perceptible = 7)***
5. **How well do you think you could perform your tasks right now?** ***(Very well = 1 - Extremely poorly = 7)***

Sample Response Scale

1	2	3	4	5	6	7
Not at all comfortable			*Extremely*			*comfortable*

Subject:	Date:	Time:	Caffiene intake (type, time, amt.): / /
Experiment:			Caffiene intake (type, time, amt.): / /

Exp. Time (min:sec)	Comfort	Tolerate	Tired	Severe	Perform	Comments
Start						
03:45						
15:00						
30:00						
35:00						Synwork #1
1:00:00						
1:30:00						
1:35:00						Synwork #2
2:00:00						15 minute rest - stop run time
2:30:00						
2:35:00						Synwork #3
3:00:00						
3:30:00						
3:35:00						Synwork #4
4:00:00						
END						

Experimental Notes: (Lunch, snacks, etc for subject - reattachment of sensors - distractions during exp't - etc.)

LT5 Subjective Questionnaire Data Sheet
(Part A-60 Minute Exposure)

Question #:

1. **Do you feel comfortable?** ***(Not at all comfortable = 1 - Extremely comfortable = 7)***
2. **How long would you be able to tolerate this motion exposure if you were riding in a vehicle on a cross-country mission?** ***(Unrestrained time-scale response)***
3. **Do you feel tired?** ***(Not at all tired - Extremely tired)***
4. **How severe do you rate the motion exposures right now?** ***(Extremely severe = 1 - Barely perceptible = 7)***
5. **How well do you think you could perform your tasks right now?** ***(Very well = 1 - Extremely poorly = 7)***

Sample Response Scale

1	2	3	4	5	6	7
Not at all comfortable			*Extremely*			*comfortable*

Subject:	**Date:**	**Time:**	**Caffiene intake (type, time, amt.):**		/	/
Experiment:			**Caffiene intake (type, time, amt.):**		/	/

Exp. Time (min:sec)	Comfort	Tolerate	Tired	Severe	Perform	Comments
Start						
03:15						
07:00						
10:45						
14:30						
18:15						
22:00						
25:45						
29:30						
30:00						15 minute rest-stop run time
33:15						
37:00						
40:45						
44:30						
48:15						
52:00						
55:45						
59:30						
END						

Experimental Notes: (Lunch, snacks, etc for subject - reattachment of sensors - distractions during exp't - etc.)

LT5 Subjective Questionnaire Data Sheet
(Part B - Intermittent Exposure)

Question #:

1. **Do you feel comfortable?** ***(Not at all comfortable = 1 - Extremely comfortable = 7)***
2. **How long would you be able to tolerate this motion exposure if you were riding in a vehicle on a cross-country mission?** ***(Unrestrained time-scale response)***
3. **Do you feel tired?** ***(Not at all tired - Extremely tired)***
4. **How severe do you rate the motion exposures right now?** ***(Extremely severe = 1 - Barely perceptible = 7)***
5. **How well do you think you could perform your tasks right now?** ***(Very well = 1 - Extremely poorly = 7)***

Sample Response Scale

1	2	3	4	5	6	7
Not at all comfortable				*Extremely*		*comfortable*

Instructions:

1. Start data collection
2. Subjective Questions given at 3:15 of 3:45 exposure
3. 7:30 of rest
4. Repeat steps 1-4 to Signature 16

Subject:	**Date:**	**Time:**	**Caffiene intake (type, time, amt.):**	/	/
Experiment:			**Caffiene intake (type, time, amt.):**	/	/

Signature #	Comfort	Tolerate	Tired	Severe	Perform	Comments
1						
2						
3						
4						
5						
6						
7						
8						
9						
10						
11						
12						
13						
15						
16						

Experimental Notes: (Lunch, snacks, etc for subject - reattachment of sensors - distractions during exp't - etc.)

Appendix C

Table C1 - Metabolite Assays of Blood and Urine

	Blood Assays	Normal Values
Alkaline Phosphatase	Alkaline phosphatase is an enzyme produced mainly in the bone and liver. It is also secreted into the gastrointestinal tract at a constant rate, where it plays an important role in digestion and absorption. Serum concentration of alkaline phosphatase gives important information concerning osteoblastic activity (bone formation), and liver function. Increased serum levels indicate possible **bone destruction** and subsequent **remodeling** as a result of **fractures**, as well as an indication of **liver disease**.	19-74 IU/L (Treseler 1988)
Blood Urea Nitrogen (BUN)	BUN is the product of protein degradation within the liver. Serum BUN concentration is directly dependent on exogenous sources of protein and on the state of hydration, and indirectly dependent on the rate of tissue catabolism/ anabolism. BUN is increased in **renal failure**, **shock**, and **excessive muscle breakdown due to extraordinary physical activity**.	4-22 mg/dl (Treseler, 1992)
Creatine Phosphokinase (CPK)	CPK is an intracellular enzyme which metabolizes creatine phosphate in cardiac muscle, skeletal muscle and brain tissue. CPK is released upon cell injury. An increase in serum CPK is seen in cases of **skeletal muscle damage** and with **severe or prolonged exercise**.	10-190 U/L (Treseler, 1992)
	Blood Assays	Normal Values

Creatinine	Creatinine is the end product of muscle metabolism involving the breakdown of creatine phosphate in the liberation of energy. Serum creatinine concentration is constant in healthy persons and is produced in proportion to body muscle mass. As such it is an accurate index of glomerular filtration rate (GFR). Abnormally increased serum creatinine may be observed in cases of **impaired renal function**, **skeletal muscle damage**, or **strenuous exercise**.	0.7-1.5 mg/dl (Treseler, 1988)
Glucose	Glucose is the principal body fuel present in the blood and is obtained from the diet as well as being produced by metabolic processes in the liver and kidneys. Serum glucose concentration is increased during the stress response resulting from: **acute trauma, severe exercise, hemorrhage, severe pain, or emotional excitement**. Among the causes of decreased serum levels are: **impaired liver function** and **functional hypoglycemia**.	60-110 mg/dl (for adult <50 years) (Treseler 1988)

	Blood Assays	Normal Values
Hematocrit	Hematocrit is defined as the percentage of red blood cells (RBCs) in a volume of whole blood. The test allows for the measurement of size, capacity, and number of cells present in the blood. Hematocrit concentration can indicate extracellular **saline excess** and the consequent **fluid shift** involved. Causes of hematocrit changes: see Hemoglobin.	39-51 % (Treseler, 1988)
Hemoglobin (Hb)	Hb is the main component of red blood cells (RBCs) and can be used as an indication of the oxygen carrying capacity of blood. Abnormal serum levels arise from decreased production, hemorrhage, or interference with RBC production. Upon **hemorrhage** a fluid shift occurs to maintain blood volume (hemodilution), resulting in decreased Hb levels. Increased Hb levels are an indication of **severe dehydration**.	13.0-17.0 g/dl (Treseler, 1988)
Lactate	Lactate is a metabolic substrate in equilibrium with pyruvate in carbohydrate metabolism. In cases of tissue hypoxia, the equilibrium shifts toward lactate, as pyruvate is metabolized through anaerobic glycolysis. Tissue hypoxia results from **decreased perfusion** of the tissues, or **muscle fatigue**.	0.7 mmole/L (Berne & Levy, 1988)

	Blood Assays	Normal Values
Lactate Dehydrogenase (LDH)	LDH is a high concentration intracellular enzyme responsible for the metabolic conversion between pyruvic acid and lactic acid. It is present in substantial amounts in the following tissues, listed in order of decreasing concentration: skeletal muscle, liver, heart, pancreas, spleen, and brain. Serum LDH concentrations increase in response to injury in proportion to the extent of **tissue damage**, and the elapsed time from injury, e.g., **skeletal muscle injury**, and the period after **severe exercise**.	60-220 IU/L (Treseler, 1988)
Platelets	Platelet morphology is included in most standard hematology tests (e.g., complete blood count or CBC). Platelets are important in the initiation of blood clotting	250,000 - 400,000/mm^3
Total Protein (TP)	Serum Total Protein (TP) is a measure of albumin and globulin fractions present in the blood. Serum proteins maintain fluid equilibrium in the capillaries by exerting colloid osmotic pressure, and subsequently maintain blood/tissue fluid balance. Increased TP is observed in cases of severe fluid loss such as **severe vomiting**, **diarrhea**, and **dehydration**. TP is decreased in conditions associated with protein loss (**hemorrhage**) and body fluid dilution (**acute trauma**).	6.0-8.2 g/dl (Treseler, 1988)

	Blood Assays	Normal Values
Uric Acid	Uric acid is a nitrogenous waste product formed from the catabolism of purines from nucleic acids. Increased serum concentration (hyperuricemia) is associated with **inflammatory responses** in the synovial joints from uric acid crystal formation, and **renal damage** as a result of uric stones.	3.9-9.0 mg/dl (Treseler, 1988)
White Blood Cell (WBC) Profile	WBC count provides an indication of the level of activity of the immune system, and the presence and magnitude of **infection**.	Count: 4.0-10.0 x $10^3/mm^3$ (Treseler, 1988)

Urine Assays		
Name of Assay	Relevance to Study	Normal Values
Appearance (Turbidity)	Fresh urine usually has a clear appearance. When urine is cloudy or turbid, some visual particulate matter is present. Many substances may cause urine cloudiness, some of which indicate damage to the kidneys, disease, or a metabolic dysfunction.	Clear (Brunzel, 1994)
Blood Cells	The presence of RBCs in the urine, hematuria, indicates a pathological condition. Acute **inflammation of the urinary organs** as a result of disease is one cause. Another cause is **vascular trauma**, for example marathon runners damage blood vessels in the feet from repetitive impacts inherent to the exercise. Pyuria, the presence of WBCs in the urine indicates an **infection** of the kidneys and/or other urinary organs.	None
Color	Normal urine is usually a yellow or amber colored, transparent liquid. The color of urine may be affected by **diet** and by some **medications**, including multivitamin pills. A red, brown or black urine may indicate the presence of **red blood cells or hemoglobin** from bleeding in the urinary system, or **myoglobin** released from damaged muscles.	Light yellow/ yellow (Brunzel, 1994)

Urine Assays		
Name of Assay	Relevance to Study	Normal Values

pH	Because the kidneys play a major role in the regulation of the acid-base balance of the body, urinary pH provides valuable information to assess an individual. Urinary pH is affected by diet and sleep, as well as conditions which cause **metabolic or respiratory acidosis or alkalosis**. **Renal dysfunction** and medications also affect urinary pH.	4.5-8.0 (Brunzel, 1994)
Urine Volume	Daily urine output is directly dependent on **hydration, diet, and exercise** In normal healthy individuals. Normally, the kidneys produce a minimum urine volume of approximately 500 ml per day to eliminate the average daily load of solutes.	0.5-3.0 L/day (Brunzel, 1994)
Bilirubin	Bilirubin is a product of the breakdown of hemoglobin that is released in the normal turnover of red blood cells. Increased bilirubin in urine may indicate an **increased breakdown of red blood cells or liver dysfunction**.	Negative (Brunzel, 1994)

Urine Assays		
Name of Assay	Relevance to Study	Normal Values
Creatinine	Creatinine is derived from the constant turnover of creatine phosphate in muscle. Plasma creatinine is excreted through glomerular filtration, and may be measured as clearance (Clearance = urinary creatinine concentration times urine flow rate, divided by plasma creatinine concentration). Creatinine clearance gives an estimate of Glomerular Filtration Rate (GFR), which is an important indicator of **renal function**.	21-26 mg/kg/ 24 hours (Treseler, 1988)
Glucose	Normally, no glucose is present in the urine. Some causes of urinary glucose are **renal damage, diseases** such as diabetes mellitus, or **hormonal disorders**, including stress and anxiety which increase epinephrine and glucocorticoid concentration.	Negative (Brunzel, 1994)
Ketones	Ketones in urine indicate that fat is being mobilized as an energy source. Urine ketone concentration may increase with **severe exercise**, too little **carbohydrate** in the diet, or inability to **utilize carbohydrates** as in diabetes mellitus.	Negative (Brunzel, 1994)
Leukocyte Esterase	The presence of leukocyte (white blood cell) esterase in urine is an indication of **inflammation**, anywhere in the kidneys or in the lower urinary tract.	Negative (Brunzel, 1994)

Urine Assays		
Name of Assay	Relevance to Study	Normal Values
Nitrite	Urinary nitrite is a marker for **urinary tract infections**	Negative (Brunzel, 1994)
Protein	The presence of increased protein in urine is an indication of **renal disease** or an **increase in plasma proteins** which spill into urine. **Strenuous exercise** may cause a transient increase in urinary protein excretion.	Negative (Brunzel, 1994)
Specific Gravity	Specific gravity can be defined as a measure of the density of urine; as it depends on the weight and concentration of particles in solution (osmolality). The close correlation between osmolality and specific gravity warrants its use as a clinical guide to urine osmolality, which is a reflection of renal function. Specific gravity is decreased in conditions that increase glomerular filtration rate (GFR) such as **fever**, or in conditions causing decreased tubular reabsorption such as **acute renal failure**; and increased in conditions such as, **shock**, **dehydration**, and **water deprivation**.	1.003-1.030 units (1 unit = 40 mOsm) (Treseler, 1988)

Urine Assays		
Name of Assay	Relevance to Study	Normal Values
Urobilinogen	Urobilinogen is a product of bilirubin metabolism. Traces of urobilinogen in urine are normal. Urobilinogen concentration is increased in alkaline urine, and is increased when a specimen is collected following meals.	< 1.0 mg/dL (Brunzel, 1994)

Table C2 - Dietary Recall Questionnaire

Prior to beginning the experiment, we are interested in obtaining a record of your diet during the past 24 hours. This will help us better understand some of the biochemical responses we may measure. Please fill out this table as best you can remember concerning what you have eaten, at what times and in what quantities during the past 24 hours. This information will be kept confidential. Please try and remember everything you have consumed, including fluids and alcohol.

Thank-you for your efforts.

Time of day	Food eaten	Quantity of food

Name _____ Date _____

Table C3 - Quality Control

A summary of the method used in each biochemical analysis for blood (A) and urine (B), the normal range reported by Lyster Hospital, and the coefficient of variation (CV) of each method provided by Lyster Hospital and measured by BCRI.

A. BLOOD

Metabolite Name	Technique	Normal Range	CV (%) Lyster Hospital	CV (%) BCRI
Alkaline Phosphatase	Enzymatic - PNPP	Male: 50-136 U/L	4.2	2.8
Blood Urea Nitrogen	Enzymatic	7.0-18 mg/dl	2.6	1.7
CPK (Kinetic)	Enzymatic	35-232 U/L	4.0	3.4
Creatinine	Colorimetry	0.8-1.3 mg/dl	2.1	n/a
Glucose	Hexokinase	70-110 mg/dl	1.0	4.1
Hematocrit	Coulter Instrumentation/ Calculation	Male: 42-52%	0	1.2
Hemoglobin	Coulter Instrumentation	Male:14-18 g/d	0.6	1.5
Lactate	Enzymatic	0.5-2.2 mmol/L	3.0	7.8 *
LDH (Kinetic)	Enzymatic	100-190 U/L	3.1	7.7 *
Total protein	Colorimetry	6.4-8.2 g/dl	1.1	1.4
Uric Acid	Enzymatic	3.5-7.2 mg/dl	2.0	1.4
White blood count	Coulter Instrumentation	4.8-10.8 X 1000/mm3	1.6	3.9

* Low correlation, based on Pearson Correlation Coefficient

B. URINE

Metabolite Name or Characteristic	Technique	Normal value
Appearance (Turbidity)	Visual	Clear
Bilirubin	Reagent Strip	Negative
Blood Cells	Microscope	Negative
Color	Visual	Yellow
Creatinine	Colorimetry	Clearance: 21-26 mg/kg/24 h
Esterase	Reagent Strip	Negative
Glucose	Reagent Strip	Negative
Ketones	Reagent Strip	Negative
Leukocyte Esterase	Reagent Strip	Negative
Nitrite	Reagent Strip	Negative
pH	Reagent Strip	5.0-7.0
Protein	Reagent Strip	Negative
Specific Gravity	Densitometry	1.003-1.035
Urine Volume	Volumetric	0.5-3.0 L/day
Urobilinogin	Reagent Strip	Negative

Appendix D
Multiaxis Ride Simulator (MARS)

1. The MARS consists of the following equipment:

   a. Two large hydraulic pumps in parallel, each pumping hydraulic oil at 85 gpm at up to 3600 psi (3000 psi operating pressure).

   b. Three hydraulic accessory modules for switching the hydraulic oil flow to the actuators.

   c. Three 13.1 kip hydraulic actuators (translational) each having a 3-stage valve system.

   d. Three failsafe valves, each valve capable of shutting down oil flow to the actuator high side within 20 msec of the command to "FAILSAFE".

   e. One multi-channel servo controller (Schenck/Pegasus 5900).

   f. One multi-channel Iterative Transfer Function Compensation Computer (ITFC) with associated anti-aliasing filters, A to D converters, and D to A converters.

2. The MARS capabilities and specifications are as follows:

   a. Up to 600 lbs test load (including test subject).

   b. Frequency response 5 to 40 Hz. Flat about zero +/- 1 dB.

   c. Up to 4 G peak acceleration.

   d. Up to 3.5 inches peak displacement (7 inches peak to peak).

   e. Failsafe shutdown occurs within 20 msec of "FAILSAFE" command from any of the following monitored parameters.

      (1) External paddle switches.

      (2) External safety switches on 5900 servo controller.

      (3) AC power interrupt.

      (4) Preset limit exceedance.

      (5) Anticipation circuit.

      (6) Data signal/reference signal comparison.

      (7) Accelerometer loss.

(8) Inner or outer loop LVDT signal loss.

(9) Safety Officer/NCO close to activate switch.

3. The excitation of the MARS is accomplished as follows:

A command signal (FDRV) is applied to the first stage of the 3-stage valve for the axis excited. The first stage consists of a "force motor" which is a pendulum secured within the field of the force motor transformer. When excitation is applied in the form of a command signal, the pendulum moves back and forth and the end of the pendulum moves between two ports, allowing oil to flow through these ports proportional to the excitation. The oil thus ported is used to move a spool valve which, in turn, ports oil at a higher pressure to move a larger spool valve which, in turn, ports oil at the operating pressure to move the hydraulic actuator RAM. The movement of the RAM thus is proportional in direction to the phase of the excitation and in displacement to the amplitude of the excitation.

4. Excitation to the MARS actuators is output through the multi-channel servo controller from the ITFC computer and created as follow:

a. ITFC differs from a normal control system in that the reduction of the control error is not carried out on-line, but iteratively after the output of a command signal over a specific time (sequence).

b. The actuator command signals (FDRV) are not corrected immediately after the occurrence of a control error, i.e., they are not corrected on-line using the instantaneous control error, but are corrected off-line on the basis of comparison between the recorded achieved response (FIRES) signals and the recorded desired response signals (FSRES) after the command signals have been output for a specified period of time (sequence).

c. The calculation of the corrected drive signals is carried out by transforming the control error with a fast Fourier transform (FFT) into the frequency domain and then multiplying it with the corresponding elements of an inverted frequency response function matrix (acquired during "Identification").

d. The result of this operation, a set of Fourier transformed correction signals, is transformed by inverse FFT into the time domain, is weighted with a selectable factor for each signal, and is added to the previously output drive signal (iteration process). These newly calculated drive signals are then output

for the length of a sequence to the actuators during which time the achieved response signals (accelerometer outputs) required for the calculation of the new drive (FDRV) signals are recorded. If the error signals lie within tolerances specified by the operator for each individual signal, the system is regarded as compensated (or fully iterated).

e. Acquisition, identification, iteration, manipulation, and output of signals is accomplished by a set of versatile software provided in the ITFC computer. In addition to multi-channel signal application, the ITFC computer also can be used to analyze test data or to generate (synthesize) drive signals internally. Most drive signals are provided by researchers, however, and have been recorded on magnetic media in the field. Acquisition of these signals is a function of the ITFC computer and its software.

JOHN M. JENKINS
MARS Technician

Appendix E
Tables

Table E-1
Physical characteristics of subjects in experiment ST1.

ST1 Subjects	Age (years)	Height (inches)	Weight (pounds)
1	23	74.75	198
2	23	73.5	158
3	27	71	165
4	23	71	210
5	24	72	195
6	26	70	140
7	23	70	162
8	28	69	168
9	27	73	178
10	27	68	185
11	24	72	185
Mean	25.2	71.0	174.6
Standard Deviation	2.0	1.7	20.2

Table E-2
Physical characteristics of subjects in experiment LT1.

LT1 Subjects	Age (years)	Height (inches)	Weight (pounds)
1	23	71	176
2	24	67.25	147
3	26	70	174
4	27	71	152
5	24	67	163
6	29	72	190
7	25	73.5	204
8	26	72.5	165
9	25	69	160
10	29	74	179
11	22	70	186
12	26	72.5	165
Mean	25.5	70.8	171.8
Standard Deviation	4.5	2.3	16.4

Table E-3
Physical characteristics of subjects in experiment LT2.

LT2 Subjects	Age (years)	Height (inches)	Weight (pounds)

1	27	70	212
2	32	68	173
3	21	69	196
4	25	72	240
5	19	72	148
6	24	75	198
Mean	24.2	71.2	191.0
Standard Deviation	5.0	2.8	34.1

Table E-4
Physical characteristics of subjects in experiment LT3.

LT3 Subjects	Age (years)	Height (inches)	Weight (pounds)
1	24	72	195
2	30	69	180
3	21	70	165
4	26	72	228
6	23	71	210
7	36	72	175
8	22	73	180
9	33	69	175
10	26	68	171
11	24	69	170
12	22	73	180
13	34	64	154.5
Mean	27	70	180.8
Standard Deviation	5.4	2.6	20.7

Table E-5
Physical characteristics of subjects in experiment LT4.

LT4 Subjects	Age (years)	Height (inches)	Weight (pounds)
1	23	75	190
2	22	68	150
3	22	73	180
4	26	70	183
5	21	69	196
6	21	71	233
9	23	72	185
10	23	68	190
Mean	22.6	70.1	188.1
Standard Deviation	1.7	2.0	24.6

Table E-6
Physical characteristics of subjects in experiment LT5.

LT5 Subjects	Age (years)	Height (inches)	Weight (pounds)
1	40	74	240
2	21	71	233
3	20	72	205
4	25	69	172
5	20	69	170
6	37	70	180
7	25	67	171
8	27	66	183
9	21	71	145
10	37	65	185
Mean	25.9	68.9	182.7
Standard Deviation	6.8	2.4	24.7

Table E-7
Low-pass filter level and correction effects on ratios of peak lumbar (L4) positive z acceleration to peak seat positive 4g z acceleration

Data Set	Frequency (Hz)						
	4	5	6	8	11	15	20
40 Hz	1.975	1.814	1.621	1.491	1.341	1.230	0.983
150 Hz (raw)	2.487	2.487	2.506	2.014	1.618	1.499	1.268
STF (150 Hz)	1.956	1.849	1.975	1.444	1.172	1.025	0.847

Table E-8
Low-pass filter level and correction effects on ratios of peak thoracic (T3) positive z acceleration to peak seat positive 4g z acceleration

Data Set	Frequency (Hz)						
	4	5	6	8	11	15	20
40 Hz	2.632	2.326	1.952	1.482	1.300	1.186	0.958
150 Hz (raw)	3.803	3.618	3.094	2.088	1.626	1.477	1.308
STF (150 Hz)	2.648	2.594	2.205	1.439	1.080	0.965	0.855

Table E-9
Low-pass filter level and correction effects on ratios of peak lumbar (L4) positive z acceleration to peak seat negative 4g z acceleration

Data Set	Frequency (Hz)						
	4	5	6	8	11	15	20
40 Hz	0.941	1.325	1.248	1.011	0.832	0.633	0.461
150 Hz (raw)	3.445	2.566	2.378	1.876	1.462	1.024	0.481
STF (150Hz)	2.983	2.079	1.901	1.371	0.891	0.663	0.316

Table E-10
Low-pass filter level and correction effects on ratios of peak thoracic (T3) positive z acceleration to peak seat negative 4g z acceleration

Data Set	Frequency (Hz)						
	4	5	6	8	11	15	20
40 Hz	1.477	1.402	1.197	0.829	0.630	0.548	0.444
150 Hz (raw)	4.311	4.253	3.888	2.549	1.111	0.571	0.316
STF (150 Hz)	3.428	3.285	2.882	1.930	0.761	0.408	0.238

Table E-11
Statistical summary of the mean frequency (MF) EMG response for pre- and post-exposure test contractions in experiment LT3 for the right and left lumbar (RL and LL) and right and left thoracic (RT and LT) EMG muscles. (n=10, T = 2.26).

Muscle	MF (pre)	MF (post)	paired t	P(T≤t)
RL	70.3	69.6	0.26	0.80
LL	70.77	71.23	-0.26	0.80
RT	59.8	59.5	0.14	0.89
LT	55.3	55.3	-0.015	0.99

Table E-12
Statistical summary of the mean frequency (MF) EMG responsefor pre- and post-exposure test contractions in experiment LT4 on days 1, 3 and 5 for the right and left lumbar (RL and LL) and right and left thoracic (RT and LT) EMG muscles. (n=8, T = 2.36).

Muscle-Day	MF (pre)	MF (post)	paired t	P(T≤t)
RL-1	57.5	56.7	0.38	0.71
RL-3	55.9	58.7	-1.32	0.23
RL-5	59.0	59.3	-0.08	0.93
LL-1	58.4	57.7	0.45	0.67
LL-3	55.9	58.4	-2.62	0.03
LL-5	59.3	59.4	-0.08	0.94
RT-1	74.5	73.0	0.47	0.65
RT-3	72.4	73.3	-0.03	0.77
RT-5	76.4	76.4	0.02	0.98
LT-1	74.4	74.9	-0.17	0.87
LT-3	75.7	75.3	0.15	0.88
LT-5	76.5	76.6	-0.04	0.97

Table E-13
Ratio of peak lumbar (L2) positive x acceleration to peak seat positive x acceleration.

Amplitude (g)	Frequency (Hz)							
	2	4	5	6	8	11	15	20
0.5	0.461	0.490	0.363	0.301	0.325	0.247	0.268	0.327
SD	0.125	0.088	0.069	0.068	0.060	0.028	0.033	0.028
1	0.582	0.444	0.365	0.309	0.247	0.240	0.181	0.196
SD	0.184	0.114	0.102	0.085	0.062	0.061	0.041	0.027
2	n/a	0.392	0.327	0.270	0.175	0.145	0.105	0.085
SD		0.096	0.092	0.055	0.050	0.045	0.029	0.023
3	n/a	0.528	0.476	0.444	0.247	0.131	0.095	0.068
SD		0.154	0.129	0.103	0.067	0.039	0.033	0.031
4	n/a	0.535	0.462	0.381	0.263	0.151	0.108	0.069
SD		0.157	0.127	0.100	0.122	0.070	0.035	0.027
MEAN	0.521	0.477	0.399	0.341	0.251	0.183	0.151	0.149

Table E-14
Ratio of peak thoracic (T1) positive x acceleration to peak seat positive x acceleration.

Amplitude (g)	Frequency (Hz)							
	2	4	5	6	8	11	15	20
0.5	0.421	0.382	0.295	0.256	0.205	0.162	0.160	0.171
SD	0.105	0.084	0.048	0.045	0.052	0.021	0.038	0.048
1	0.670	0.345	0.282	0.176	0.146	0.117	0.104	0.118
SD	0.188	0.069	0.064	0.025	0.028	0.025	0.029	0.023
2	n/a	0.414	0.330	0.239	0.144	0.085	0.092	0.054
SD		0.099	0.075	0.066	0.048	0.024	0.022	0.017
3	n/a	0.466	0.442	0.426	0.230	0.091	0.066	0.049
SD		0.099	0.081	0.092	0.064	0.031	0.023	0.010
4	n/a	0.426	0.359	0.337	0.174	0.082	0.064	0.043
SD		0.092	0.112	0.105	0.055	0.025	0.023	0.015
MEAN	0.545	0.406	0.341	0.287	0.180	0.107	0.097	0.087

Table E-15
Ratio of peak lumbar (L2) negative x acceleration to peak seat negative x acceleration.

Amplitude (g)	Frequency (Hz)							
	2	4	5	6	8	11	15	20
-0.5	0.529	0.438	0.397	0.351	0.232	0.329	0.256	0.252
SD	0.086	0.080	0.076	0.047	0.040	0.049	0.025	0.043
-1	0.514	0.369	0.298	0.252	0.212	0.206	0.168	0.194
SD	0.164	0.041	0.043	0.047	0.044	0.054	0.032	0.032
-2	n/a	0.285	0.257	0.203	0.163	0.100	0.100	0.106
SD		0.092	0.091	0.063	0.063	0.030	0.030	0.031
-3	n/a	0.308	0.247	0.228	0.136	0.102	0.072	0.061
SD		0.144	0.088	0.092	0.059	0.046	0.028	0.015
-4	n/a	0.322	0.269	0.207	0.157	0.121	0.091	0.084
SD		0.139	0.123	0.081	0.084	0.071	0.053	0.052
MEAN	0.522	0.344	0.294	0.248	0.180	0.171	0.137	0.139

Table E-16
Ratio of peak thoracic (T1) negative x acceleration to peak seat negative x acceleration.

Amplitude (g)	Frequency (Hz)							
	2	4	5	6	8	11	15	20
-0.5	0.540	0.334	0.286	0.212	0.191	0.186	0.150	0.140
SD	0.111	0.091	0.066	0.041	0.032	0.028	0.032	0.036
-1	0.457	0.288	0.214	0.194	0.173	0.122	0.101	0.109
SD	0.131	0.065	0.037	0.029	0.021	0.027	0.032	0.024
-2	n/a	0.288	0.266	0.208	0.173	0.103	0.094	0.082
SD		0.070	0.060	0.046	0.082	0.033	0.025	0.027
-3	n/a	0.319	0.246	0.306	0.178	0.126	0.078	0.059
SD		0.106	0.058	0.111	0.083	0.048	0.029	0.018
-4	n/a	0.411	0.325	0.310	0.212	0.120	0.097	0.058
SD		0.164	0.126	0.134	0.074	0.045	0.030	0.016
MEAN	0.498	0.328	0.267	0.246	0.185	0.131	0.104	0.089

Table E-17
Ratio of peak lumbar (L3) positive y acceleration to peak seat positive y acceleration.

Amplitude (g)	Frequency (Hz)							
	2	4	5	6	8	11	15	20
0.5	0.762	0.619	0.479	0.414	0.342	0.294	0.216	0.222
SD	0.124	0.121	0.087	0.075	0.091	0.080	0.060	0.065
1	0.906	0.574	0.493	0.406	0.316	0.226	0.197	0.183
SD	0.140	0.084	0.086	0.077	0.080	0.055	0.043	0.049
2	n/a	0.524	0.459	0.316	0.285	0.173	0.133	0.102
SD		0.106	0.108	0.072	0.054	0.038	0.031	0.032
3	n/a	0.578	0.513	0.510	0.327	0.170	0.129	0.109
SD		0.096	0.102	0.088	0.066	0.038	0.040	0.046
4	n/a	0.646	0.676	0.532	0.266	0.166	0.136	0.102
SD		0.142	0.149	0.109	0.060	0.037	0.050	0.035
MEAN	0.834	0.588	0.524	0.435	0.307	0.206	0.162	0.144

Table E-18
Ratio of peak thoracic (T2) positive y acceleration to peak seat positive y acceleration.

Amplitude (g)	Frequency (Hz)							
	2	4	5	6	8	11	15	20
0.5	0.339	0.222	0.183	0.154	0.113	0.098	0.070	0.066
SD	0.054	0.047	0.036	0.024	0.021	0.029	0.025	0.030
1	0.515	0.236	0.174	0.131	0.105	0.082	0.064	0.058
SD	0.081	0.040	0.028	0.023	0.026	0.024	0.020	0.019
2	n/a	0.262	0.205	0.147	0.109	0.081	0.051	0.048
SD		0.063	0.034	0.042	0.025	0.037	0.007	0.037
3	n/a	0.248	0.223	0.212	0.136	0.060	0.051	0.035
SD		0.052	0.059	0.032	0.031	0.018	0.022	0.008
4	n/a	0.333	0.315	0.253	0.124	0.058	0.045	0.032
SD		0.173	0.121	0.136	0.080	0.021	0.017	0.014
MEAN	0.427	0.260	0.220	0.179	0.117	0.076	0.056	0.048

Table E-19
Ratio of peak lumbar (L4) positive z acceleration to peak seat positive z acceleration.

Amplitude (g)	Frequency (Hz)							
	2	4	5	6	8	11	15	20
0.5	1.057	1.016	0.895	0.846	0.726	0.680	0.611	0.416
SD	0.130	0.082	0.100	0.113	0.137	0.114	0.112	0.091
1	1.154	1.009	0.998	0.936	0.919	0.823	0.702	0.552
SD	0.185	0.122	0.123	0.144	0.133	0.117	0.122	0.104
2	n/a	1.669	1.322	1.162	0.944	0.891	0.838	0.764
SD		0.944	0.521	0.382	0.181	0.252	0.239	0.191
3	n/a	2.215	1.624	1.737	1.415	0.999	0.942	0.868
SD		1.127	0.661	0.919	0.535	0.286	0.290	0.247
4	n/a	1.956	1.849	1.975	1.444	1.172	1.025	0.847
SD		0.525	0.351	0.585	0.361	0.390	0.309	0.223
MEAN	1.106	1.573	1.338	1.331	1.089	0.913	0.824	0.689

Table E-20
Ratio of peak thoracic (T3) positive z acceleration to peak seat positive z acceleration.

Amplitude (g)	Frequency (Hz)							
	2	4	5	6	8	11	15	20
0.5	0.867	0.891	0.750	0.743	0.684	0.641	0.581	0.452
SD	0.085	0.051	0.082	0.092	0.119	0.104	0.073	0.052
1	1.054	0.906	0.904	0.837	0.834	0.799	0.669	0.551
SD	0.221	0.101	0.097	0.108	0.116	0.109	0.077	0.076
2	n/a	1.490	1.335	1.133	1.000	0.872	0.831	0.736
SD		0.623	0.480	0.275	0.241	0.171	0.175	0.177
3	n/a	2.296	1.646	1.593	1.343	0.965	0.868	0.775
SD		1.033	0.666	0.745	0.592	0.326	0.224	0.181
4	n/a	2.648	2.594	2.205	1.439	1.080	0.965	0.855
SD		0.246	0.445	0.653	0.511	0.462	0.386	0.366
MEAN	0.960	1.646	1.446	1.302	1.060	0.871	0.783	0.674

Table E-21
Ratio of peak lumbar (L4) positive z acceleration to peak seat negative z acceleration.

Amplitude (g)	Frequency (Hz)							
	2	4	5	6	8	11	15	20
-0.5	0.850	0.814	0.680	0.571	0.415	0.343	0.282	0.238
SD	0.116	0.266	0.264	0.185	0.092	0.096	0.057	0.041
-1	2.118	2.048	1.734	1.496	0.954	0.414	0.246	0.178
SD	1.546	2.295	1.787	1.403	0.719	0.160	0.056	0.046
-2	n/a	3.216	2.494	2.374	1.410	0.680	0.521	0.231
SD		1.761	1.410	1.435	1.068	0.403	0.485	0.114
-3	n/a	2.524	1.872	1.719	1.288	0.796	0.368	0.309
SD		0.828	0.887	1.117	0.917	0.792	0.248	0.175
-4	n/a	2.983	2.079	1.901	1.371	0.891	0.663	0.316
SD		0.682	0.750	0.777	0.669	0.556	0.535	0.214
MEAN	1.484	2.317	1.772	1.612	1.087	0.625	0.416	0.254

Table E-22
Ratio of peak thoracic (T3) positive z acceleration to peak seat negative z acceleration.

Amplitude (g)	Frequency (Hz)							
	2	4	5	6	8	11	15	20
-0.5	0.692	0.743	0.580	0.528	0.370	0.298	0.249	0.274
SD	0.088	0.146	0.144	0.091	0.105	0.072	0.045	0.056
-1	2.381	1.810	1.444	1.202	0.664	0.357	0.204	0.146
SD	1.527	1.096	0.811	0.626	0.305	0.152	0.046	0.039
-2	n/a	4.931	3.329	2.053	1.140	0.605	0.556	0.282
SD		1.828	0.930	0.678	0.537	0.508	1.010	0.312
-3	n/a	3.560	3.304	2.457	1.288	0.489	0.295	0.219
SD		1.383	0.928	0.965	0.331	0.224	0.177	0.112
-4	n/a	3.428	3.285	2.882	1.930	0.761	0.408	0.238
SD		0.636	0.619	0.413	0.701	0.293	0.191	0.120
MEAN	1.536	2.894	2.388	1.824	1.079	0.502	0.342	0.232

Table E-23
Ratio of second peak of the lumbar (L4) positive z acceleration to a single peak seat positive z acceleration.

Amplitude (g)	Frequency (Hz)						
	4	5	6	8	11	15	20
2	2.123	1.412	0.504	0.286	0.113	0.104	0.079
SD	1.503	1.356	0.400	0.195	0.016	0.022	0.011
3	2.335	1.729	1.671	0.765	0.133	0.078	0.068
SD	0.960	0.915	0.910	0.414	0.026	0.009	0.012
4	2.073	2.148	1.904	1.009	0.207	0.120	0.071
SD	0.422	0.470	0.556	0.625	0.084	0.061	0.008
MEAN	2.177	1.763	1.359	0.687	0.151	0.101	0.073

Table E-24
Ratio of second peak of the thoracic (T3) positive z acceleration to a single peak seat positive z acceleration.

Amplitude (g)	Frequency (Hz)						
	4	5	6	8	11	15	20
2	2.694	1.505	0.503	0.233	0.082	0.086	0.081
SD	1.391	0.811	0.303	0.071	0.013	0.016	0.011
3	3.013	2.117	2.279	1.057	0.120	0.061	0.053
SD	1.010	0.914	0.636	0.678	0.032	0.013	0.008
4	2.798	2.711	2.735	1.374	0.256	0.102	0.057
SD	0.760	0.562	0.783	0.868	0.142	0.054	0.016
MEAN	2.835	2.111	1.839	0.888	0.153	0.083	0.063

Table E-25
Ratio of second peak of the lumbar (L4) positive z acceleration to a single peak seat negative z acceleration.

Amplitude (g)	Frequency (Hz)						
	4	5	6	8	11	15	20
-2	0.720	0.416	0.315	0.146	0.081	0.111	0.054
SD	0.881	0.220	0.162	0.045	0.028	0.141	0.031
-3	0.558	0.465	0.438	0.153	0.098	0.064	0.044
SD	0.196	0.458	0.508	0.034	0.025	0.016	0.013
-4	0.612	0.503	0.398	0.343	0.189	0.137	0.071
SD	0.352	0.317	0.407	0.394	0.182	0.155	0.057
MEAN	0.630	0.461	0.384	0.214	0.123	0.104	0.056

Table E-26
Ratio of second peak of the thoracic (T3) positive z acceleration to a single peak seat negative z acceleration.

Amplitude (g)	Frequency (Hz)						
	4	5	6	8	11	15	20
-2	0.317	0.209	0.185	0.108	0.070	0.065	0.052
SD	0.280	0.135	0.131	0.043	0.024	0.054	0.028
-3	0.496	0.280	0.225	0.093	0.062	0.050	0.026
SD	0.244	0.179	0.134	0.036	0.019	0.020	0.016
-4	0.740	0.553	0.325	0.224	0.107	0.097	0.057
SD	0.661	0.402	0.316	0.204	0.123	0.119	0.044
MEAN	0.517	0.347	0.245	0.142	0.079	0.070	0.045

Table E-27
Time delay (sec) between peak seat positive x acceleration and peak lumbar (L2) positive x acceleration.

Amplitude (g)	Frequency (Hz)							
	2	4	5	6	8	11	15	20
0.5	0.461	0.490	0.363	0.301	0.325	0.247	0.268	0.327
SD	0.125	0.088	0.069	0.068	0.060	0.028	0.033	0.028
1	0.582	0.444	0.365	0.309	0.247	0.240	0.181	0.196
SD	0.184	0.114	0.102	0.085	0.062	0.061	0.041	0.027
2	n/a	0.392	0.327	0.270	0.175	0.145	0.105	0.085
SD		0.096	0.092	0.055	0.050	0.045	0.029	0.023
3	n/a	0.528	0.476	0.444	0.247	0.131	0.095	0.068
SD		0.154	0.129	0.103	0.067	0.039	0.033	0.031
4	n/a	0.535	0.462	0.381	0.263	0.151	0.108	0.069
SD		0.157	0.127	0.100	0.122	0.070	0.035	0.027
MEAN	0.521	0.477	0.399	0.341	0.251	0.183	0.151	0.149

Table E-28
Time delay (sec) between peak seat negative x acceleration and peak lumbar (L2) negative x acceleration.

Amplitude (g)	Frequency (Hz)							
	2	4	5	6	8	11	15	20
0.5	0.106	0.081	0.075	0.087	0.081	0.128	0.146	0.174
SD	0.026	0.028	0.046	0.024	0.024	0.069	0.040	0.024
1	0.087	0.094	0.078	0.095	0.071	0.054	0.033	0.052
SD	0.018	0.013	0.012	0.020	0.008	0.002	0.028	0.001
2	n/a	0.073	0.072	0.060	0.064	0.058	0.063	0.069
SD		0.013	0.015	0.011	0.013	0.035	0.023	0.024
3	n/a	0.087	0.069	0.068	0.061	0.050	0.048	0.094
SD		0.008	0.014	0.012	0.011	0.011	0.027	0.044
4	n/a	0.088	0.086	0.069	0.056	0.056	0.050	0.058
SD		0.008	0.009	0.013	0.008	0.022	0.015	0.036
MEAN	0.097	0.084	0.076	0.076	0.067	0.069	0.068	0.089

Table E-29
Time delay (sec) between peak seat positive x acceleration and peak thoracic (T1) positive x acceleration.

Amplitude (g)	Frequency (Hz)							
	2	4	5	6	8	11	15	20
0.5	0.066	0.053	0.066	0.094	0.108	0.067	0.158	0.143
SD	0.030	0.017	0.031	0.034	0.032	0.023	0.038	0.053
1	0.068	0.081	0.069	0.072	0.095	0.063	0.091	0.079
SD	0.023	0.019	0.019	0.022	0.014	0.012	0.046	0.035
2	n/a	0.078	0.079	0.075	0.080	0.077	0.057	0.053
SD		0.016	0.014	0.023	0.023	0.033	0.019	0.023
3	n/a	0.096	0.077	0.078	0.074	0.082	0.069	0.087
SD		0.022	0.023	0.018	0.015	0.034	0.022	0.029
4	n/a	0.100	0.095	0.085	0.074	0.073	0.073	0.080
SD		0.017	0.021	0.016	0.017	0.020	0.020	0.026
MEAN	0.067	0.082	0.077	0.081	0.086	0.072	0.089	0.088

Table E-30
Time delay (sec) between peak seat negative x acceleration and peak thoracic (T1) negative x acceleration.

Amplitude (g)	Frequency (Hz)							
	2	4	5	6	8	11	15	20
-0.5	0.110	0.070	0.083	0.153	0.074	0.080	0.103	0.116
SD	0.037	0.025	0.020	0.067	0.017	0.026	0.050	0.055
-1	0.091	0.114	0.089	0.105	0.113	0.070	0.063	0.087
SD	0.039	0.041	0.019	0.040	0.019	0.020	0.029	0.026
-2	n/a	0.078	0.074	0.081	0.078	0.078	0.050	0.045
SD		0.017	0.013	0.025	0.030	0.033	0.017	0.008
-3	n/a	0.100	0.066	0.074	0.069	0.069	0.058	0.066
SD		0.051	0.016	0.014	0.018	0.025	0.035	0.033
-4	n/a	0.091	0.090	0.068	0.063	0.063	0.057	0.055
SD		0.030	0.026	0.011	0.014	0.016	0.011	0.023
MEAN	0.101	0.091	0.080	0.096	0.080	0.072	0.066	0.074

Table E-31
Time delay (sec) between peak seat positive x acceleration and peak internal pressure (IP) response.

Amplitude (g)	Frequency (Hz)							
	2	4	5	6	8	11	15	20
0.5	0.039	0.052	0.048	0.068	0.065	0.039	0.158	0.108
SD	0.081	0.084	0.074	0.087	0.065	0.076	0.062	0.090
1	0.037	0.052	0.042	0.049	0.054	0.040	0.080	0.076
SD	0.073	0.075	0.079	0.085	0.083	0.077	0.079	0.080
2	n/a	0.031	0.039	0.036	0.044	0.060	0.027	0.026
SD		0.024	0.023	0.028	0.050	0.079	0.021	0.080
3	n/a	0.053	0.039	0.034	0.031	0.044	0.029	0.044
SD		0.021	0.023	0.013	0.016	0.052	0.022	0.035
4	n/a	0.064	0.059	0.054	0.056	0.053	0.060	0.048
SD		0.019	0.017	0.028	0.031	0.049	0.034	0.037
MEAN	0.038	0.043	0.039	0.043	0.050	0.057	0.056	0.066

Table E-32
Time delay (sec) between peak seat negative x acceleration and peak internal pressure (IP) response.

Amplitude (g)	Frequency (Hz)							
	2	4	5	6	8	11	15	20
-0.5	0.242	0.195	0.197	0.160	0.206	0.200	0.199	0.222
SD	0.028	0.037	0.041	0.038	0.064	0.045	0.049	0.048
-1	0.259	0.206	0.194	0.185	0.199	0.189	0.175	0.215
SD	0.037	0.034	0.024	0.027	0.041	0.057	0.075	0.068
-2	n/a	0.173	0.180	0.177	0.174	0.171	0.136	0.139
SD		0.045	0.042	0.032	0.022	0.059	0.074	0.085
-3	n/a	0.169	0.157	0.174	0.191	0.174	0.182	0.143
SD		0.063	0.046	0.036	0.021	0.052	0.039	0.077
-4	n/a	0.147	0.159	0.181	0.176	0.154	0.142	0.140
SD		0.053	0.039	0.034	0.055	0.072	0.071	0.056
MEAN	0.251	0.178	0.177	0.176	0.189	0.178	0.166	0.172

Table E-33
Time delay (sec) between peak seat positive y acceleration and peak lumbar (L3) positive y acceleration.

Amplitude (g)	Frequency (Hz)							
	2	4	5	6	8	11	15	20
0.5	0.082	0.080	0.083	0.081	0.068	0.072	0.083	0.140
SD	0.024	0.021	0.022	0.015	0.016	0.030	0.022	0.087
1	0.089	0.078	0.075	0.086	0.069	0.059	0.053	0.053
SD	0.036	0.026	0.022	0.022	0.006	0.015	0.016	0.017
2	n/a	0.080	0.069	0.069	0.074	0.059	0.053	0.049
SD		0.012	0.011	0.014	0.020	0.018	0.020	0.021
3	n/a	0.076	0.067	0.066	0.068	0.058	0.053	0.052
SD		0.013	0.013	0.014	0.013	0.017	0.022	0.020
4	n/a	0.079	0.078	0.072	0.062	0.056	0.054	0.049
SD		0.012	0.015	0.015	0.012	0.016	0.019	0.015
MEAN	0.086	0.079	0.074	0.075	0.068	0.061	0.059	0.069

Table E-34
Time delay (sec) between peak seat positive y acceleration and peak thoracic (T2) positive y acceleration.

Amplitude (g)	Frequency (Hz)							
	2	4	5	6	8	11	15	20
0.5	0.054	0.056	0.058	0.065	0.089	0.061	0.124	0.082
SD	0.023	0.015	0.012	0.020	0.040	0.020	0.045	0.055
1	0.059	0.066	0.065	0.078	0.069	0.059	0.047	0.063
SD	0.043	0.018	0.016	0.017	0.010	0.017	0.010	0.026
2	n/a	0.072	0.068	0.069	0.066	0.060	0.056	0.048
SD		0.019	0.017	0.012	0.010	0.011	0.007	0.012
3	n/a	0.067	0.068	0.068	0.070	0.066	0.054	0.079
SD		0.008	0.010	0.012	0.015	0.016	0.010	0.046
4	n/a	0.069	0.074	0.067	0.075	0.065	0.062	0.065
SD		0.015	0.012	0.013	0.010	0.014	0.017	0.041
MEAN	0.056	0.066	0.067	0.070	0.074	0.062	0.068	0.067

Table E-35
Time delay (sec) between peak seat positive y acceleration and peak internal pressure (IP) response.

Amplitude (g)	Frequency (Hz)							
	2	4	5	6	8	11	15	20
0.5	0.132	0.079	0.082	0.135	0.119	0.109	0.192	0.152
SD	0.089	0.099	0.057	0.080	0.037	0.057	0.048	0.057
1	0.126	0.123	0.119	0.108	0.137	0.102	0.145	0.064
SD	0.064	0.064	0.074	0.073	0.050	0.066	0.046	0.049
2	n/a	0.130	0.114	0.093	0.154	0.108	0.100	0.124
SD		0.052	0.059	0.056	0.046	0.080	0.076	0.055
3	n/a	0.097	0.084	0.114	0.123	0.130	0.122	0.102
S		0.066	0.045	0.065	0.059	0.080	0.078	0.056
4	n/a	0.066	0.069	0.113	0.121	0.103	0.134	0.099
SD		0.020	0.024	0.047	0.068	0.068	0.069	0.047
MEAN	0.129	0.099	0.094	0.112	0.131	0.110	0.138	0.108

Table E-36
Time delay (sec) between peak seat positive z acceleration and peak lumbar (L4) positive z acceleration.

Amplitude (g)	Frequency (Hz)							
	2	4	5	6	8	11	15	20
0.5	0.014	0.016	0.022	0.022	0.027	0.020	0.019	0.020
SD	0.012	0.010	0.005	0.005	0.023	0.005	0.005	0.006
1	0.009	0.029	0.020	0.020	0.021	0.021	0.020	0.020
SD	0.003	0.010	0.005	0.005	0.006	0.005	0.005	0.005
2	n/a	0.015	0.016	0.015	0.019	0.021	0.019	0.018
SD		0.010	0.007	0.005	0.004	0.005	0.005	0.004
3	n/a	0.018	0.015	0.015	0.017	0.020	0.019	0.021
SD		0.009	0.007	0.008	0.004	0.004	0.004	0.004
4	n/a	0.026	0.025	0.022	0.021	0.021	0.022	0.022
SD		0.008	0.008	0.006	0.004	0.004	0.004	0.004
MEAN	0.011	0.021	0.019	0.019	0.021	0.021	0.020	0.020

Table E-37
Time delay (sec) between peak seat negative z acceleration and peak lumbar (L4) negative x acceleration.

Amplitude (g)	Frequency (Hz)							
	2	4	5	6	8	11	15	20
-0.5	0.189	0.156	0.144	0.143	0.108	0.111	0.143	0.105
SD	0.017	0.018	0.020	0.020	0.030	0.025	0.036	0.037
-1	0.175	0.158	0.138	0.135	0.119	0.123	0.129	0.139
SD	0.024	0.035	0.020	0.030	0.020	0.040	0.018	0.051
-2	n/a	0.161	0.146	0.134	0.115	0.098	0.118	0.121
SD		0.010	0.018	0.011	0.014	0.016	0.031	0.040
-3	n/a	0.183	0.162	0.151	0.129	0.110	0.109	0.108
SD		0.017	0.021	0.011	0.009	0.014	0.020	0.024
-4	n/a	0.162	0.175	0.164	0.144	0.117	0.114	0.114
SD		0.036	0.016	0.012	0.012	0.017	0.018	0.027
MEAN	0.182	0.164	0.153	0.145	0.123	0.112	0.122	0.117

Table E-38
Time delay (sec) between peak seat positive z acceleration and peak thoracic (T3) positive z acceleration.

Amplitude (g)	Frequency (Hz)							
	2	4	5	6	8	11	15	20
0.5	0.011	0.017	0.018	0.020	0.018	0.019	0.017	0.018
SD	0.012	0.007	0.005	0.006	0.004	0.003	0.002	0.002
1	0.008	0.024	0.019	0.019	0.021	0.021	0.019	0.019
SD	0.007	0.010	0.004	0.005	0.011	0.003	0.002	0.002
2	n/a	0.018	0.015	0.016	0.019	0.021	0.018	0.017
SD		0.014	0.005	0.003	0.004	0.003	0.002	0.003
3	n/a	0.014	0.014	0.017	0.017	0.019	0.019	0.020
SD		0.005	0.005	0.011	0.004	0.002	0.002	0.002
4	n/a	0.028	0.026	0.022	0.021	0.022	0.022	0.022
SD		0.006	0.007	0.005	0.004	0.004	0.004	0.003
MEAN	0.009	0.020	0.018	0.019	0.020	0.020	0.019	0.019

Table E-39
Time delay (sec) between peak seat negative z acceleration and peak thoracic (T3) negative z acceleration.

Amplitude (g)	Frequency (Hz)							
	2	4	5	6	8	11	15	20
-0.5	0.185	0.136	0.126	0.139	0.092	0.107	0.124	0.138
SD	0.020	0.018	0.010	0.003	0.007	0.034	0.035	0.022
-1	0.155	0.142	0.128	0.115	0.108	0.102	0.103	0.088
SD	0.012	0.019	0.015	0.008	0.011	0.026	0.010	0.050
-2	n/a	0.163	0.150	0.137	0.118	0.098	0.115	0.092
SD		0.007	0.015	0.011	0.013	0.016	0.033	0.029
-3	n/a	0.185	0.168	0.150	0.132	0.111	0.107	0.104
SD		0.015	0.017	0.027	0.014	0.021	0.018	0.031
-4	n/a	0.167	0.176	0.166	0.148	0.123	0.119	0.104
SD		0.032	0.016	0.013	0.010	0.011	0.013	0.019
MEAN	0.170	0.158	0.150	0.141	0.120	0.108	0.114	0.105

Table E-40
Time delay (sec) between peak seat positive z acceleration and peak internal pressure (IP) response.

Amplitude (g)	Frequency (Hz)							
	2	4	5	6	8	11	15	20
0.5	0.035	0.055	0.039	0.023	0.027	0.018	0.021	0.033
SD	0.048	0.056	0.034	0.021	0.023	0.018	0.032	0.037
1	0.005	0.024	0.027	0.024	0.021	0.012	0.009	0.008
SD	0.005	0.011	0.019	0.019	0.017	0.004	0.002	0.002
2	n/a	0.032	0.025	0.038	0.019	0.012	0.008	0.007
SD		0.016	0.006	0.037	0.008	0.004	0.004	0.002
3	n/a	0.018	0.025	0.024	0.025	0.016	0.010	0.009
SD		0.006	0.004	0.006	0.004	0.005	0.003	0.002
4	n/a	0.021	0.027	0.018	0.025	0.017	0.012	0.011
SD		0.011	0.009	0.011	0.016	0.007	0.003	0.003
MEAN	0.020	0.030	0.029	0.025	0.024	0.015	0.012	0.014

Table E-41
Time delay (sec) between peak seat negative z acceleration and peak internal pressure (IP) response.

Amplitude (g)	Frequency (Hz)							
	2	4	5	6	8	11	15	20
-0.5	0.182	0.136	0.137	0.118	0.109	0.130	0.105	0.126
SD	0.015	0.027	0.025	0.037	0.037	0.048	0.043	0.019
-1	0.168	0.151	0.135	0.133	0.132	0.102	0.077	0.081
SD	0.021	0.013	0.016	0.020	0.031	0.030	0.044	0.042
-2	n/a	0.148	0.137	0.134	0.112	0.108	0.115	0.089
SD		0.013	0.024	0.045	0.046	0.050	0.049	0.045
-3	n/a	0.166	0.151	0.135	0.129	0.122	0.090	0.119
SD		0.025	0.027	0.031	0.036	0.039	0.040	0.050
-4	n/a	0.155	0.161	0.153	0.142	0.116	0.111	0.107
SD		0.030	0.014	0.011	0.010	0.030	0.043	0.046
MEAN	0.175	0.151	0.144	0.135	0.125	0.115	0.100	0.104

Table E-42
Ratio of peak internal pressure (IP) response to peak seat positive x acceleration (mm $Hg.m^{-1}.s^2$).

Amplitude (g)	Frequency (Hz)							
	2	4	5	6	8	11	15	20
0.5	2.496	2.129	1.664	1.208	1.233	0.959	0.612	0.596
SD	2.150	2.074	1.183	1.108	0.974	0.598	0.451	0.356
1	4.065	2.411	1.513	1.719	1.288	1.000	0.653	0.548
SD	4.651	2.589	1.782	1.789	1.381	0.945	0.642	0.375
2	n/a	3.111	2.230	1.770	1.209	1.062	0.934	0.549
SD		2.221	1.618	1.179	0.933	0.963	0.869	0.458
3	n/a	2.578	2.256	2.348	1.633	0.848	0.639	0.580
SD		1.091	1.317	1.194	1.198	0.635	0.481	0.508
4	n/a	1.637	1.460	1.333	0.838	0.481	0.354	0.346
SD		0.848	0.644	1.922	2.004	0.522	0.704	0.601
MEAN	3.280	2.373	1.825	1.676	1.240	0.870	0.638	0.524

Table E-43
Ratio of peak internal pressure (IP) response to peak seat negative x acceleration (mm $Hg.m^{-1}.s^2$).

Amplitude (g)	Frequency (Hz)							
	2	4	5	6	8	11	15	20
-0.5	5.476	2.614	1.878	1.606	1.317	1.467	0.841	0.762
SD	7.419	6.067	4.812	3.678	2.903	2.995	1.831	1.150
-1	5.342	3.539	2.014	2.696	1.534	0.797	0.555	0.419
SD	4.620	4.593	3.548	2.584	2.626	2.118	1.574	0.934
-2	n/a	1.947	1.868	1.255	0.917	0.495	0.423	0.284
SD		1.432	1.856	0.931	0.573	0.638	0.296	0.245
-3	n/a	1.063	1.107	1.416	0.710	0.453	0.452	0.314
SD		0.911	0.944	1.138	0.535	0.704	0.598	0.417
-4	n/a	1.783	0.967	1.309	0.795	0.459	0.273	0.232
SD		2.295	0.809	1.663	0.918	0.326	0.126	0.318
MEAN	5.409	2.189	1.567	1.656	1.055	0.734	0.509	0.402

Table E-44
Ratio ofpeak internal pressure (IP) response to peak seat positive y acceleration (mm $Hg.m^{-1}.s^2$).

Amplitude (g)	Frequency (Hz)							
	2	4	5	6	8	11	15	20
0.5	2.862	2.438	1.278	1.162	1.157	0.926	0.997	1.594
SD	3.153	2.755	1.050	1.235	1.034	0.913	0.993	1.696
1	2.249	0.956	0.963	0.668	0.708	0.648	0.652	0.564
SD	2.485	0.956	0.985	0.495	0.575	0.540	0.552	0.456
2	n/a	0.733	0.564	0.484	0.339	0.346	0.316	0.128
SD		0.433	0.339	0.367	0.264	0.318	0.403	0.077
3	n/a	0.793	0.759	0.487	0.376	0.228	0.212	0.147
SD		0.342	0.497	0.214	0.232	0.185	0.156	0.127
4	n/a	0.852	0.842	0.554	0.394	0.285	0.271	0.276
SD		0.617	0.497	0.518	0.405	0.304	0.317	0.351
MEAN	2.556	1.154	0.881	0.671	0.595	0.486	0.490	0.542

Table E-45
Ratio of peak internal pressure (IP) response to peak seat positive z acceleration (mm $Hg.m^{-1}.s^2$).

Amplitude (g)	Frequency (Hz)							
	2	4	5	6	8	11	15	20
0.5	2.194	1.736	1.697	1.659	1.661	1.599	1.252	1.288
SD	0.594	0.659	0.591	0.702	0.497	0.445	0.665	0.780
1	2.829	2.222	1.909	1.795	1.680	1.602	1.378	1.379
SD	0.781	0.494	0.473	0.568	0.580	0.545	0.448	0.508
2	n/a	3.020	2.708	1.974	1.724	1.289	1.281	1.231
SD		0.534	0.445	0.354	0.402	0.363	0.219	0.420
3	n/a	3.483	2.727	2.591	1.922	1.199	1.135	1.104
SD		0.624	0.434	0.355	0.374	0.187	0.155	0.162
4	n/a	3.718	3.378	3.180	2.168	1.295	1.279	1.352
SD		0.661	0.504	0.445	0.544	0.257	0.249	0.497
MEAN	2.511	2.836	2.484	2.240	1.831	1.397	1.265	1.271

Table E-46
Ratio of peak internal pressure (IP) response to peak seat negative z acceleration (mm $Hg.m^{-1}.s^2$).

Amplitude (g)	Frequency (Hz)							
	2	4	5	6	8	11	15	20
-0.5	2.061	1.754	1.378	1.179	0.965	1.139	0.701	0.635
SD	0.689	0.543	0.347	0.398	0.291	0.418	0.348	0.208
-1	3.968	3.070	2.384	1.928	1.301	0.905	0.597	0.555
SD	1.359	0.673	0.740	0.463	0.464	0.341	0.173	0.225
-2	n/a	5.263	3.530	2.631	1.975	1.150	0.775	0.471
SD		1.206	0.959	1.479	1.268	0.945	0.582	0.289
-3	n/a	5.758	4.408	3.002	1.633	1.349	0.785	0.596
SD		0.927	0.554	0.524	0.725	1.046	0.496	0.388
-4	n/a	6.271	4.669	3.652	1.914	1.117	0.775	0.571
SD		1.577	1.054	0.651	0.479	0.355	0.230	0.159
MEAN	3.015	4.423	3.273	2.478	1.557	1.132	0.726	0.565

Table E-47
Ratio of second peak internal pressure (IP) response to single peak seat positive z acceleration (mm Hg.m^{-1}.s^2).

Amplitude (g)	Frequency (Hz)						
	4	5	6	8	11	15	20
2	2.138	1.403	0.829	0.570	0.166	0.153	0.120
SD	0.734	0.695	0.646	0.242	0.112	0.240	0.095
3	2.748	2.025	1.991	1.053	0.300	0.145	0.117
SD	0.722	0.613	0.575	0.455	0.119	0.092	0.049
4	3.127	2.878	2.257	1.122	0.412	0.225	0.191
SD	1.009	0.642	0.511	0.437	0.220	0.111	0.116
MEAN	2.671	2.102	1.692	0.915	0.293	0.174	0.142

Table E-48
Ratio of second peak internal pressure (IP) response to single peak seat negative z acceleration (mm Hg.m^{-1}.s^2).

Amplitude (g)	Frequency (Hz)						
	4	5	6	8	11	15	20
-2	1.056	0.652	0.590	0.576	0.335	0.324	0.248
SD	0.652	0.302	0.225	0.637	0.189	0.147	0.112
-3	1.178	0.814	0.614	0.313	0.202	0.214	0.215
SD	0.573	0.316	0.278	0.093	0.112	0.132	0.130
-4	1.033	0.747	0.556	0.370	0.212	0.212	0.195
SD	0.382	0.348	0.249	0.171	0.136	0.106	0.096
MEAN	1.089	0.738	0.587	0.419	0.250	0.250	0.219

Table E-49
Subjective comfort ratings to LT1 motion exposures.

Motion signature	+y		+x		-x		+z		-z	
	Mean	*Std Dev*	*Mean*	*Std Dev*	*Mean*	*Std Dev*	*Mean*	*Std Dev*	*Mean*	*Std Dev*
1g, 128 min^{-1}	5.90	0.57	5.40	0.70	5.70	0.67	4.80	1.62	4.60	0.52
2g, 8 min^{-1}	6.10	0.99	5.90	1.10	6.00	0.67	5.30	0.67	4.80	1.03
2g, 128 min^{-1}	4.20	0.92	4.10	0.88	3.90	1.20	2.50	1.08	1.80	0.79
4g, 8 min^{-1}	4.20	1.32	4.20	0.63	3.20	1.32	2.00	0.82	1.70	0.67

Table E-50
Subjective predicted tolerance ratings to LT1 motion exposures.

Motion signature	+y		+x		-x		+z		-z	
	Mean	*Std Dev*	*Mean*	*Std Dev*	*Mean*	*Std Dev*	*Mean*	*Std Dev*	*Mean*	*Std Dev*
1g, 128 min^{-1}	5.70	1.44	5.70	1.69	5.60	1.73	4.53	1.92	4.15	1.25
2g, 8 min^{-1}	6.35	2.33	5.90	2.22	6.40	1.66	5.40	1.85	5.20	2.00
2g, 128 min^{-1}	3.15	0.91	3.35	1.36	3.20	2.14	1.30	0.76	1.20	0.83
4g, 8 min^{-1}	3.20	1.03	4.00	1.78	2.95	1.46	1.33	0.60	0.95	0.50

Table E-51
Subjective severity ratings to LT1 motion exposures.

Motion signature	+y		+x		-x		+z		-z	
	Mean	*Std Dev*	*Mean*	*Std Dev*	*Mean*	*Std Dev*	*Mean*	*Std Dev*	*Mean*	*Std Dev*
1g, 128 min^{-1}	2.20	0.63	2.70	0.48	2.40	0.84	3.70	1.34	3.30	0.82
2g, 8 min^{-1}	1.70	0.82	2.00	0.94	2.00	0.67	2.70	0.48	2.80	1.03
2g, 128 min^{-1}	4.20	0.63	4.20	0.79	4.40	1.07	5.50	1.27	5.90	0.99
4g, 8 min^{-1}	4.10	1.20	4.50	0.85	4.90	0.99	5.90	0.88	6.00	0.82

Table E-52
The response of blood biochemical data in Experiment LT2 to motion exposures including 4 g shocks in the negative x axis.

A. Alkaline Phosphatase (U/L)

	Mean	*Std Dev*	*Minimum*	*Maximum*	*N*
Baseline	92	20	72	126	6
Pre-	95	15	70	112	6
Post-	98	21	75	133	6
24 Hour	87	23	63	130	6
48 Hour	102	19	81	125	4
72 Hour	101	13	79	109	5
96 Hour	95	16	77	117	4

B. Blood Urea Nitrogen (mg/dl)

	Mean	*Std Dev*	*Minimum*	*Maximum*	*N*
Baseline	12	1	10	14	6
Pre-	13	3	9	17	6
Post-	13	4	9	18	6
24 Hour	14	3	11	17	6
48 Hour	12	3	9	15	4
72 Hour	12	2	9	14	5
96 Hour	13	3	9	15	4

C. Creatine Phosphokinase CPK (U/L)

	Mean	*Std Dev*	*Minimum*	*Maximum*	*N*
Baseline	246	126	72	390	6
Pre-	368	188	57	490	5
Post-	341	196	63	540	6
24 Hour	625	475	124	1482	6
48 Hour	490	548	67	1282	4
72 Hour	379	307	71	794	5
96 Hour	279	217	83	502	4

D. Creatinine (mg/dl)

	Mean	Std Dev	Minimum	Maximum	N
Baseline	1.2	0.2	0.9	1.4	6
Pre-	1.2	0.2	0.9	1.4	6
Post-	1.0	0.2	0.9	1.2	5
24 Hour	1.0	0.2	0.8	1.3	6
48 Hour	1.1	0.1	1.0	1.1	4
72 Hour	1.1	0.2	0.9	1.3	6
96 Hour	1.1	0.2	0.8	1.4	6

E. Glucose (mg/dl)

	Mean	Std Dev	Minimum	Maximum	N
Baseline	86	2	82	87	6
Pre-	88	21	68	127	6
Post-	89	8	83	105	6
24 Hour	93	2	92	97	6
48 Hour	96	14	89	117	4
72 Hour	92	6	86	102	5
96 Hour	105	23	90	131	3

F. Hematocrit (%)

	Mean	Std Dev	Minimum	Maximum	N
Baseline	45.3	2.5	14.1	48.8	6
Pre-	44.6	1.3	43.1	45.9	6
Post-	47.6	3.8	43.2	52.6	6
24 Hour	44.9	3.1	40.9	48.9	6
48 Hour	n/a				
72 Hour	n/a				
96 Hour	n/a				

G. Hemoglobin (g/dl)

	Mean	Std Dev	Minimum	Maximum	N
Baseline	15.1	0.7	14.1	15.9	6
Pre-	14.8	0.5	14.2	15.4	6
Post-	15.8	1.2	14.3	17.0	6
24 Hour	15.1	0.9	13.8	16.0	6
48 Hour	n/a				
72 Hour	n/a				
96 Hour	n/a				

H. Lactate (mEq/L)

	Mean	Std Dev	Minimum	Maximum	N
Baseline	1.3	1.2	0.1	3.5	6
Pre-	1.2	1.0	0.4	2.7	6
Post-	1.2	1.6	0.2	4.1	6
24 Hour	1.6	2.7	1.2	6.3	5
48 Hour	n/a				
72 Hour	n/a				
96 Hour	n/a				

I. Lactate Dehydrogenase (LDH) (U/L)

	Mean	Std Dev	Minimum	Maximum	N
Baseline	162	49	73	214	6
Pre-	180	47	98	222	6
Post-	205	41	138	250	6
24 Hour	176	65	99	273	6
48 Hour	201	47	130	225	4
72 Hour	181	49	113	222	5
96 Hour	196	50	126	243	4

J. Platlets (x1000)

	Mean	Std Dev	Minimum	Maximum	N
Baseline	231	83	123	360	6
Pre-	221	69	122	338	6
Post-	227	66	116	323	6
24 Hour	218	76	116	353	6
48 Hour	n/a				
72 Hour	n/a				
96 Hour	n/a				

K. Total Protein (g/dl)

	Mean	Std Dev	Minimum	Maximum	N
Baseline	7.0	0.5	6.2	7.6	6
Pre-	7.1	0.3	6.7	7.3	6
Post-	7.7	0.7	7.0	8.9	6
24 Hour	7.1	0.6	6.6	8.1	6
48 Hour	7.1	0.3	6.7	7.4	4
72 Hour	7.2	0.4	6.6	7.6	5
96 Hour	7.3	0.3	7.0	7.6	4

L. Uric Acid (mg/dl)

	Mean	*Std Dev*	*Minimum*	*Maximum*	*N*
Baseline	5.2	1.0	4.2	6.4	6
Pre-	5.4	1.5	4.0	8.2	6
Post-	5.2	1.2	3.9	7.2	6
24 Hour	4.7	0.8	3.9	6.0	6
48 Hour	5.1	1.4	3.8	6.8	4
72 Hour	5.5	0.8	4.4	6.5	5
96 Hour	5.5	1.3	4.4	7.1	4

M. WBC (x1000)

	Mean	*Std Dev*	*Minimum*	*Maximum*	*N*
Baseline	4.9	1.9	2.5	7.9	6
Pre-	6.2	3.0	2.5	10.5	6
Post-	6.8	2.9	2.5	11.0	6
24 Hour	6.2	2.5	2.5	8.9	6
48 Hour	n/a				
72 Hour	n/a				
96 Hour	n/a				

Table E-53
The response of blood biochemical data in Experiment LT2 to motion exposures including 4 g shocks in the positive z axis.

A. Alkaline Phosphatase (U/L)

	Mean	*Std Dev*	*Minimum*	*Maximum*	*N*
Baseline	92	20	72	126	6
Pre-	100	14	85	123	6
Post-	97	17	71	113	6
24 Hour	93	11	74	106	6
48 Hour	88	12	77	110	6
72 Hour	100	19	87	131	5
96 Hour	88	12	71	106	6

B. Blood Urea Nitrogen (mg/dl)

	Mean	*Std Dev*	*Minimum*	*Maximum*	*N*
Baseline	12	1	10	14	6
Pre-	13	3	10	16	6
Post-	13	2	10	16	6
24 Hour	12	2	9	15	6
48 Hour	14	3	10	17	6
72 Hour	11	2	7	12	5
96 Hour	12	4	8	16	6

C. Creatine PhosphokinaseCPK (U/L)

	Mean	*Std Dev*	*Minimum*	*Maximum*	*N*
Baseline	246	126	72	390	6
Pre-	362	273	115	756	6
Post-	365	279	117	759	6
24 Hour	319	357	68	1031	6
48 Hour	745	1110	85	2962	6
72 Hour	551	930	73	2214	5
96 Hour	418	520	69	1381	6

D. Creatinine (mg/dl)

	Mean	Std Dev	Minimum	Maximum	N
Baseline	1.2	0.2	0.9	1.4	6
Pre-	1.2	0.2	0.9	1.4	6
Post-	1.1	0.2	0.8	1.4	5
24 Hour	1.1	0.2	0.9	1.4	6
48 Hour	1.1	0.3	0.7	1.6	6
72 Hour	1.1	0.2	0.9	1.3	6
96 Hour	1.1	0.2	0.8	1.3	6

E. Glucose (mg/dl)

	Mean	Std Dev	Minimum	Maximum	N
Baseline	86	2	82	87	6
Pre-	96	11	84	113	6
Post-	87	5	81	93	6
24 Hour	99	28	78	153	6
48 Hour	92	3	88	96	6
72 Hour	90	19	68	119	5
96 Hour	93	9	84	108	6

F. Hematocrit (%)

	Mean	Std Dev	Minimum	Maximum	N
Baseline	45.3	2.5	41.9	48.8	6
Pre-	44.3	1.8	42.5	47.5	6
Post-	45.1	1.7	43.5	47.8	6
24 Hour	44.8	1.6	42.9	46.6	6
48 Hour	n/a				
72 Hour	n/a				
96 Hour	n/a				

G. Hemoglobin (g/dl)

	Mean	Std Dev	Minimum	Maximum	N
Baseline	15.1	0.7	14.1	15.9	6
Pre-	14.8	0.8	14.0	16.1	6
Post-	15.1	0.8	14.4	16.4	6
24 Hour	15.1	0.8	14.3	16.1	6
48 Hour	n/a				
72 Hour	n/a				
96 Hour	n/a				

H. Lactate (mEq/L)

	Mean	Std Dev	Minimum	Maximum	N
Baseline	1.3	1.2	0.1	3.5	6
Pre-	1.2	0.8	0.2	2.1	6
Post-	1.0	0.8	0.1	2.3	6
24 Hour	1.1	0.8	0.1	2.0	6
48 Hour	n/a				
72 Hour	n/a				
96 Hour	n/a				

I. Lactate Dehydrogenase (LDH) (U/L)

	Mean	Std Dev	Minimum	Maximum	N
Baseline	162	49	73	214	6
Pre-	215	69	158	312	6
Post-	212	39	178	276	6
24 Hour	201	21	166	227	6
48 Hour	235	58	171	324	6
72 Hour	202	76	120	303	5
96 Hour	208	79	115	335	6

J. Platlets (x1000)

	Mean	Std Dev	Minimum	Maximum	N
Baseline	231	83	123	360	6
Pre-	237	73	130	350	6
Post-	237	75	119	343	6
24 Hour	228	68	131	342	6
48 Hour	n/a				
72 Hour	n/a				
96 Hour	n/a				

K. Total Protein (g/dl)

	Mean	Std Dev	Minimum	Maximum	N
Baseline	7.0	0.5	6.2	7.6	6
Pre-	7.2	0.4	6.3	7.5	6
Post-	7.5	0.5	6.5	7.9	6
24 Hour	7.3	0.2	7.1	7.6	6
48 Hour	7.2	0.4	6.5	7.6	6
72 Hour	7.1	0.2	6.9	7.4	5
96 Hour	7.2	0.2	7.0	7.5	6

L. Uric Acid (mg/dl)

	Mean	*Std Dev*	*Minimum*	*Maximum*	*N*
Baseline	5.2	1.0	4.2	6.4	6
Pre-	5.4	1.2	3.9	6.9	6
Post-	5.3	1.1	3.7	6.7	6
24 Hour	5.9	1.0	4.9	7.0	6
48 Hour	5.4	1.0	3.8	6.5	6
72 Hour	5.0	0.9	4.3	6.4	5
96 Hour	5.2	0.7	4.3	6.4	6

M. WBC (x1000)

	Mean	*Std Dev*	*Minimum*	*Maximum*	*N*
Baseline	4.9	1.9	2.5	7.9	6
Pre-	6.8	2.9	2.5	10.2	6
Post-	7.0	2.9	2.5	10.1	6
24 Hour	6.4	2.1	3.5	9.4	6
48 Hour	n/a				
72 Hour	n/a				
96 Hour	n/a				

Table E-54
The response of blood biochemical in Experiment LT3 in motion exposures (7 hours per day).

A. Alkaline Phosphatase (U/L)

	Mean	*Std Dev*	*Minimum*	*Maximum*	*N*
Baseline	93	14	72	114	10
Pre-	86	13	68	103	9
Post-	94	15	75	123	9
24 Hour	102	19	77	147	10
48 Hour	92	17	63	113	7
72 Hour	90	13	68	104	7
96 Hour	82	16	68	108	6

B. Blood Urea Nitrogen (mg/dl)

	Mean	*Std Dev*	*Minimum*	*Maximum*	*N*
Baseline	13	3	8	18	10
Pre-	14	4	8	18	9
Post-	15	3	11	20	9
24 Hour	13	4	7	19	10
48 Hour	12	3	7	16	7
72 Hour	13	2	11	16	7
96 Hour	14	4	9	18	6

C1. Creatine Phosphokinase (CPK) (U/L)

	Mean	*Std Dev*	*Minimum*	*Maximum*	*N*
Baseline	255	393	74	1356	10
Pre-	249	419	75	1356	9
Post-	289	344	93	1170	9
24 Hour	269	282	110	1056	10
48 Hour	169	28	128	212	7
72 Hour	164	91	85	292	7
96 Hour	146	67	80	237	6

C2. Creatine Phosphokinase (CPK) (U/L)

*one subject excluded due to elevated measurement

	Mean	*Std Dev*	*Minimum*	*Maximum*	*N*
Baseline	132	74	74	298	9
Pre-	111	60	75	251	8
Post-	178	101	93	395	8
24 Hour	182	60	110	299	9
48 Hour	169	28	128	212	7
72 Hour	164	91	85	292	7
96 Hour	146	67	80	237	6

D. Creatinine (mg/dl)

	Mean	*Std Dev*	*Minimum*	*Maximum*	*N*
Baseline	1.0	0.1	0.9	1.2	10
Pre-	1.0	0.1	0.9	1.2	10
Post-	1.0	0.1	0.9	1.3	7
24 Hour	1.0	0.1	0.9	1.2	9
48 Hour	1.0	0.1	0.8	1.1	8
72 Hour	1.1	0.1	0.9	1.2	9
96 Hour	1.0	0.1	0.9	1.1	8

E. Glucose (mg/dl)

	Mean	*Std Dev*	*Minimum*	*Maximum*	*N*
Baseline	95	19	66	127	10
Pre-	100	12	84	127	9
Post-	96	26	57	155	10
24 Hour	94	15	65	119	10
48 Hour	90	7	78	100	7
72 Hour	88	9	77	102	7
96 Hour	109	27	87	152	6

F. Hematocrit (%)

	Mean	Std Dev	Minimum	Maximum	N
Baseline	46.5	3.6	42.7	54.8	10
Pre-	46.3	4.0	39.5	54.3	9
Post-	47.6	4.0	39.6	52.8	10
24 Hour	45.8	3.9	41.0	53.6	10
48 Hour	n/a				
72 Hour	n/a				
96 Hour	n/a				

G. Hemoglobin (g/dl)

	Mean	Std Dev	Minimum	Maximum	N
Baseline	15.7	1.3	14.1	18.2	10
Pre-	15.5	1.4	12.9	18.1	9
Post-	16.0	1.5	13.1	17.8	10
24 Hour	15.5	1.5	13.4	18.0	10
48 Hour	n/a				
72 Hour	n/a				
96 Hour	n/a				

H. Lactate (mEq/L)

	Mean	Std Dev	Minimum	Maximum	N
Baseline	1.0	0.4	0.4	1.9	9
Pre-	0.8	0.5	0.2	2.0	9
Post-	0.9	0.4	0.5	1.9	10
24 Hour	1.2	0.5	0.5	2.0	10
48 Hour	n/a				
72 Hour	n/a				
96 Hour	n/a				

I. Lactate Dehydrogenase (LDH) (U/L)

	Mean	Std Dev	Minimum	Maximum	N
Baseline	173	52	117	269	10
Pre-	154	31	108	199	9
Post-	177	45	106	242	9
24 Hour	157	23	127	198	10
48 Hour	175	39	115	233	7
72 Hour	168	36	110	210	7
96 Hour	160	34	119	215	6

J. Platlets (x1000)

	Mean	Std Dev	Minimum	Maximum	N
Baseline	218	35	138	257	10
Pre-	225	18	190	247	9
Post-	225	38	128	258	10
24 Hour	221	32	141	252	10
48 Hour	n/a				
72 Hour	n/a				
96 Hour	n/a				

K. Total Protein (g/dl)

	Mean	Std Dev	Minimum	Maximum	N
Baseline	7.4	0.2	7.0	7.8	10
Pre-	7.4	0.2	7.0	7.8	9
Post-	7.6	0.4	6.8	8.2	10
24 Hour	7.4	0.4	6.7	8.2	10
48 Hour	7.6	0.3	7.1	7.9	7
72 Hour	7.5	0.4	6.8	8.0	7
96 Hour	7.5	0.4	6.9	8.1	6

L. Uric Acid (mg/dl)

	Mean	Std Dev	Minimum	Maximum	N
Baseline	5.7	1.0	4.6	7.6	10
Pre-	5.4	1.0	4.3	7.6	9
Post-	5.5	1.1	3.9	7.3	10
24 Hour	5.7	1.1	3.7	7.7	10
48 Hour	5.5	0.9	3.9	6.4	7
72 Hour	5.8	1.4	3.8	7.3	7
96 Hour	5.5	1.0	4.0	6.9	6

M. WBC (x1000)

	Mean	Std Dev	Minimum	Maximum	N
Baseline	5.3	0.7	3.9	6.2	10
Pre-	5.6	0.9	4.4	7.5	9
Post-	7.8	2.4	4.1	11.1	10
24 Hour	5.9	1.6	4.4	8.9	10
48 Hour	n/a				
72 Hour	n/a				
96 Hour	n/a				

Table E-55
The response of blood biochemical data in Experiment LT4 (5 days of 4 hours per day).

A. Alkaline Phosphatase (U/L)

	Mean	*Std Dev*	*Minimum*	*Maximum*	*N*
Baseline	97	21	72	131	8
Pre 1-	91	13	72	112	7
Post 1-	92	12	73	107	7
Pre 2-	89	13	71	111	8
Post 2-	98	14	76	121	8
Pre 3-	91	16	69	115	8
Post 3-	96	23	70	136	7
Pre 4-	87	7	75	100	8
Post 4-	98	21	73	138	8
Pre 5-	90	11	75	107	8
Post 5-	91	13	73	112	8
24 Hour	98	20	70	139	8
48 Hour	96	23	72	144	8
72 Hour	88	7	82	101	6
96 Hour	92	14	76	113	8

B. Blood Urea Nitrogen (mg/dl)

	Mean	*Std Dev*	*Minimum*	*Maximum*	*N*
Baseline	14	5	8	21	7
Pre 1-	14	3	8	19	8
Post 1-	14	3	9	17	8
Pre 2-	15	3	11	20	8
Post 2-	14	3	10	19	8
Pre 3-	13	3	10	18	8
Post 3-	13	3	10	18	8
Pre 4-	15	2	13	20	8
Post 4-	14	3	9	20	7
Pre 5-	14	2	11	17	8
Post 5-	13	4	8	18	8
24 Hour	13	3	7	16	8
48 Hour	13	5	7	21	8
72 Hour	16	5	13	27	6
96 Hour	15	3	11	20	8

C. Creatine Phosphokinase (CPK) (U/L)

	Mean	*Std Dev*	*Minimum*	*Maximum*	*N*
Baseline	272	199	98	627	8
Pre 1-	325	314	91	1038	8
Post 1-	332	302	96	1024	8
Pre 2-	410	414	107	1132	8
Post 2-	429	432	124	1226	8
Pre 3-	332	319	102	953	8
Post 3-	309	267	108	786	8
Pre 4-	280	258	99	787	8
Post 4-	320	289	101	875	7
Pre 5-	239	195	98	646	8
Post 5-	233	181	102	620	8
24 Hour	200	123	92	451	8
48 Hour	369	451	128	1270	6
72 Hour	252	183	78	541	6
96 Hour	211	106	85	339	8

D. Creatinine (mg/dl)

	Mean	*Std Dev*	*Minimum*	*Maximum*	*N*
Baseline	1.1	0.2	0.8	1.3	8
Pre 1-	1.1	0.1	0.8	1.3	8
Pre 2-	1.0	0.1	0.9	1.2	8
Pre 3-	1.1	0.1	0.8	1.2	8
Pre 4-	1.1	0.1	0.9	1.3	8
Pre 5-	1.0	0.1	0.7	1.1	8
24 Hour	1.1	0.2	0.8	1.5	8
48 Hour	1.0	0.2	0.9	1.3	8
72 Hour	1.0	0.2	0.8	1.2	7
96 Hour	1.0	0.1	0.8	1.2	8

E. Glucose (mg/dl)

	Mean	Std Dev	Minimum	Maximum	N
Baseline	88	10	72	101	8
Pre 1-	110	23	88	152	8
Post 1-	92	3	86	96	8
Pre 2-	110	22	77	137	8
Post 2-	90	2	85	93	8
Pre 3-	98	14	88	131	8
Post 3-	90	7	75	95	8
Pre 4-	120	25	87	154	8
Post 4-	87	3	82	91	7
Pre 5-	98	23	70	144	8
Post 5-	89	2	87	92	8
24 Hour	93	7	87	108	8
48 Hour	91	9	69	97	8
72 Hour	94	17	79	125	6
96 Hour	91	21	65	134	8

F. Hematocrit (%)

	Mean	Std Dev	Minimum	Maximum	N
Baseline	45.7	2.2	43.7	49.3	7
Pre 1-	44.2	2.6	41.5	48.5	8
Post 1-	45.9	1.9	43.2	49.0	8
Pre 2-	44.7	1.8	43.1	48.0	8
Post 2-	45.2	2.3	41.4	49.0	8
Pre 3-	43.7	1.7	41.3	47.0	8
Post 3-	45.4	1.7	43.5	48.6	8
Pre 4-	43.3	1.5	40.5	45.8	8
Post 4-	44.6	1.5	43.5	47.7	7
Pre 5-	44.4	1.7	41.2	46.3	7
Post 5-	45.0	1.5	42.9	47.7	8
24 Hour	44.8	1.9	13.1	49.3	8
48 Hour	n/a				
72 Hour	n/a				
96 Hour	n/a				

G. Hemoglobin (g/dl)

	Mean	*Std Dev*	*Minimum*	*Maximum*	*N*
Baseline	15.4	0.6	14.8	16.5	7
Pre 1-	15.0	1.0	13.8	16.6	8
Post 1-	15.5	0.8	14.4	16.9	8
Pre 2-	15.2	0.7	14.4	16.3	8
Post 2-	15.3	0.8	14.1	16.5	8
Pre 3-	15.0	0.7	14.1	16.1	8
Post 3-	15.3	0.6	14.3	16.2	8
Pre 4-	14.8	0.6	13.7	15.9	8
Post 4-	15.0	0.6	14.1	16.1	7
Pre 5-	15.0	0.6	14.1	15.8	7
Post 5-	15.1	0.6	14.4	16.0	8
24 Hour	15.1	0.6	14.6	16.5	8
48 Hour	n/a				
72 Hour	n/a				
96 Hour	n/a				

H. Lactate (mEq/L)

	Mean	*Std Dev*	*Minimum*	*Maximum*	*N*
Baseline	1.4	1.1	0.1	3.6	7
Pre 1-	2.0	0.9	1.3	4.0	8
Post 1-	1.3	0.7	0.4	2.6	7
Pre 2-	1.7	1.2	0.3	3.8	8
Post 2-	1.3	0.8	0.4	2.7	8
Pre 3-	1.9	0.9	0.6	3.2	8
Post 3-	1.4	0.8	0.6	3.2	8
Pre 4-	1.9	0.9	0.7	3.6	8
Post 4-	1.1	0.5	0.5	1.9	8
Pre 5-	1.6	0.7	0.5	2.5	8
Post 5-	1.5	0.8	0.6	2.8	8
24 Hour	1.3	0.5	1.6	1.9	8
48 Hour	n/a				
72 Hour	n/a				
96 Hour	n/a				

I. Lactate Dehydrogenase (LDH) (U/L)

	Mean	*Std Dev*	*Minimum*	*Maximum*	*N*
Baseline	173	18	139	194	8
Pre 1-	176	35	133	245	8
Post 1-	187	42	129	243	8
Pre 2-	182	30	125	221	8
Post 2-	192	25	141	218	8
Pre 3-	202	36	171	246	8
Post 3-	185	36	135	226	8
Pre 4-	184	26	139	224	8
Post 4-	189	62	130	288	8
Pre 5-	197	71	114	319	8
Post 5-	180	44	133	270	8
24 Hour	178	22	142	201	8
48 Hour	184	35	140	243	8
72 Hour	195	67	127	308	6
96 Hour	191	55	123	298	8

J. Platlets (x1000)

	Mean	*Std Dev*	*Minimum*	*Maximum*	*N*
Baseline	224	59	136	301	7
Pre 1-	228	65	119	299	8
Post 1-	252	61	136	316	8
Pre 2-	230	71	111	316	8
Post 2-	231	82	114	321	8
Pre 3-	226	65	116	308	8
Post 3-	244	64	139	322	8
Pre 4-	216	62	109	291	8
Post 4-	245	61	131	304	7
Pre 5-	233	74	116	304	7
Post 5-	239	64	129	305	8
24 Hour	217	63	129	291	8
48 Hour	n/a				
72 Hour	n/a				
96 Hour	n/a				

K. Total Protein (g/dl)

	Mean	*Std Dev*	*Minimum*	*Maximum*	*N*
Baseline	7.6	0.3	7.3	8.0	8
Pre 1-	7.3	0.4	6.8	8.0	8
Post 1-	7.7	0.4	7.2	8.5	8
Pre 2-	7.2	0.3	7.0	7.7	8
Post 2-	7.7	0.4	7.0	8.2	8
Pre 3-	7.3	0.4	6.7	7.7	8
Post 3-	7.6	0.3	7.3	8.2	8
Pre 4-	7.3	0.3	6.8	7.6	8
Post 4-	7.6	0.4	7.1	8.1	8
Pre 5-	7.4	0.3	7.1	7.7	8
Post 5-	7.5	0.2	7.2	7.7	8
24 Hour	7.3	0.3	6.9	7.7	8
48 Hour	7.3	0.3	6.9	7.7	8
72 Hour	7.3	0.2	7.1	7.6	6
96 Hour	7.6	0.3	7.2	7.8	8

L. Uric Acid (mg/dl)

	Mean	*Std Dev*	*Minimum*	*Maximum*	*N*
Baseline	5.8	0.9	4.1	6.8	8
Pre 1-	5.8	1.0	4.6	7.5	8
Post 1-	5.7	1.2	4.4	8.0	8
Pre 2-	5.7	1.0	4.4	7.7	7
Post 2-	5.4	0.9	3.9	6.9	8
Pre 3-	5.7	0.9	4.1	6.9	8
Post 3-	5.6	0.8	4.7	7.2	8
Pre 4-	5.9	0.8	4.9	7.0	8
Post 4-	5.4	0.6	4.5	6.3	8
Pre 5-	6.1	0.8	4.8	7.0	8
Post 5-	5.6	0.8	4.5	6.8	8
24 Hour	5.9	0.8	4.9	7.5	8
48 Hour	6.0	0.7	4.7	6.9	8
72 Hour	5.9	0.8	4.9	7.2	6
96 Hour	6.1	1.2	4.7	7.8	8

M. White Blood Cell Profile (x1000)

	Mean	*Std Dev*	*Minimum*	*Maximum*	*N*
Baseline	5.3	1.7	2.6	8.0	7
Pre 1-	5.4	1.8	2.7	7.9	8
Post 1-	6.0	2.1	3.0	9.2	8
Pre 2-	4.9	1.3	2.8	6.7	8
Post 2-	5.6	1.7	2.8	7.6	8
Pre 3-	4.6	1.4	2.3	6.5	8
Post 3-	5.5	1.2	2.9	7.2	8
Pre 4-	4.7	1.5	2.3	7.1	8
Post 4-	5.5	1.7	2.7	7.6	7
Pre 5-	4.4	1.4	2.2	6.6	7
Post 5-	5.2	1.4	2.7	6.9	8
24 Hour	4.7	1.5	2.4	7.0	8
48 Hour	n/a				
72 Hour	n/a				
96 Hour	n/a				

Table E-56

The response of urinary biochemical measurements in Experiment LT2 to motion exposures including 4 g shocks in the negative x axis.

A. Urine Appearance

	Clear		Cloudy		Hazy		Tubid		Missing	
	Freq.	%	Freq.	%	Freq.	%	Freq.	%	Freq.	%
Baseline	6	100	0	0	0	0	0	0	0	0
Pre-	6	100	0	0	0	0	0	0	0	0
Post-	5	83.3	1	16.7	0	0	0	0	0	0
24 Hour	5	83.3	0	0	1	16.7	0	0	0	0
48 Hour	3	50	0	0	0	0	1	16.7	2	33.3
72 Hour	5	83.3	1	16.7	0	0	0	0	0	0
96 Hour	5	83.3	1	16.7	0	0	0	0	0	0

B. Bilirubin

	Negative		Missing	
	Freq.	%	Freq.	%
Baseline	6	100	0	0
Pre-	6	100	0	0
Post-	6	100	0	0
24 Hour	6	100	0	0
48 Hour	6	100	0	0
72 Hour	6	100	0	0
96 Hour	6	100	0	0

C. Blood Cells

	Negative		Trace		Small		Large		Missing	
	Freq.	%	Freq.	%	Freq.	%	Freq.	%	Freq.	%
Baseline	6	100	0	0	0	0	0	0	0	0
Pre-	6	100	0	0	0	0	0	0	0	0
Post-	6	100	0	0	0	0	0	0	0	0
24 Hour	6	100	0	0	0	0	0	0	0	0
48 Hour	6	100	0	0	0	0	0	0	0	0
72 Hour	4	66.7	1	16.7	0	0	1	16.7	0	0
96 Hour	6	100	0	0	0	0	0	0	0	0

D. Color

	No color		Yellow		Amber	
	Freq.	%	Freq.	%	Freq.	%
Baseline	0	0	6	100	0	0
Pre-	0	0	6	100	0	0
Post-	0	0	6	100	0	0
24 Hour	1	16.7	5	83.3	0	0
48 Hour	0	0	3	50	0	0
72 Hour	1	16.7	4	66.7	1	16.7
96 Hour	0	0	6	100	0	0

	Orange		Straw		Missing	
	Freq.	%	Freq.	%	Freq.	%
Baseline	0	0	0	0	0	0
Pre-	0	0	0	0	0	0
Post-	0	0	0	0	0	0
24 Hour	0	0	0	0	0	0
48 Hour	0	0	1	16.7	2	33.3
72 Hour	0	0	0	0	0	0
96 Hour	0	0	0	0	0	0

E. Creatinine (mg/dl)

	Mean	*Std Dev*	*Minimum*	*Maximum*	*N*
Baseline	178.5	87.6	65.1	286.4	6
Pre-	201.1	75.7	91.0	286.4	5
Post-	n/a				
24 Hour	213.2	153.8	111.0	522.0	6
48 Hour	167.0	99.6	110.0	316.0	4
72 Hour	156.7	69.0	75.0	246.0	6
96 Hour	137.5	81.3	40.0	260.0	6

F. Creatine Clearance (ml/min)

	Mean	*Std Dev*	*Minimum*	*Maximum*	*N*
Baseline	118.5	18.4	94.1	143.5	6
Pre-	120.9	19.6	94.1	143.5	5
Post-	n/a				
24 Hour	98.4	36.7	31.9	129.5	6
48 Hour	115.3	56.7	50.1	179.9	4
72 Hour	131.5	22.1	97.0	155.3	6
96 Hour	104.2	38.1	63.1	153.8	6

G. Creatine Clearance/ BSA (ml/min/1.73m2)

	Mean	*Std Dev*	*Minimum*	*Maximum*	*N*
Baseline	71.4	14.8	56.9	93.0	6
Pre-	73.2	15.8	56.9	93.0	5
Post-	n/a				
24 Hour	57.8	19.5	21.3	74.2	6
48 Hour	67.7	27.5	32.5	95.7	4
72 Hour	78.4	11.2	64.7	94.0	6
96 Hour	63.7	27.4	35.7	99.7	6

H. Glucose

	Negative		"50"		"100"		Missing	
	Freq.	%	Freq.	%	Freq.	%	Freq.	%
Baseline	6	100	0	0	0	0	0	0
Pre-	6	100	0	0	0	0	0	0
Post-	6	100	0	0	0	0	0	0
24 Hour	6	100	0	0	0	0	0	0
48 Hour	4	66.7	0	0	0	0	2	33.3
72 Hour	6	100	0	0	0	0	0	0
96 Hour	6	100	0	0	0	0	0	0

I. Ketones

	Negative		Trace		Missing	
	Freq.	%	Freq.	%	Freq.	%
Baseline	6	100	0		0	0
Pre-	6	100	0	0	0	0
Post-	6	100	0	0	0	0
24 Hour	6	100	0	0	0	0
48 Hour	4	66.7	0	0	2	33.3
72 Hour	6	100	0	0	0	0
96 Hour	6	100	0	0	0	0

J. Esterase

	Negative		Trace		Missing	
	Freq.	%	Freq.	%	Freq.	%
Baseline	6	100	0	0	0	0
Pre-	6	100	0	0	0	0
Post-	6	100	0	0	0	0
24 Hour	5	83.3	1	16.7	0	0
48 Hour	4	66.7	0	0	2	33.3
72 Hour	5	83.3	1	16.7	0	0
96 Hour	6	100	0	0	0	0

K. Nitrite

	Negative		Missing	
	Freq.	%	Freq.	%
Baseline	6	100	0	0
Pre-	6	100	0	0
Post-	6	100	0	0
24 Hour	6	100	0	0
48 Hour	4	66.7	2	33.3
72 Hour	6	100	0	0
96 Hour	6	100	0	0

L. pH

	Mean	Std Dev	Minimum	Maximum	N
Baseline	6.4	0.5	6.0	7.0	6.0
Pre-	6.4	0.5	6.0	7.0	6.0
Post-	6.3	0.4	6.0	7.0	6.0
24 Hour	6.2	0.3	6.0	6.5	6.0
48 Hour	6.3	0.5	6.0	7.0	4.0
72 Hour	6.3	0.8	5.0	7.0	6.0
96 Hour	6.3	0.8	6.0	8.0	6.0

M. Protein

	Negative		Trace		"30"		Missing	
	Freq.	%	Freq.	%	Freq.	%	Freq.	%
Baseline	4	66.7	2	33.3	0	0	0	0
Pre-	4	66.7	2	33.3	0	0	0	0
Post-	6	100	0	0	0	0	0	0
24 Hour	6	100	0	0	0	0	0	0
48 Hour	4	66.7	0	0	0	0	2	33.3
72 Hour	5	83.3	1	16.7	0	0	0	0
96 Hour	6	100	0	0	0	0	0	0

N. Specific Gravity

	Mean	Std Dev	Minimum	Maximum	N
Baseline	1.021	0.005	1.012	1.026	6
Pre-	1.021	0.005	1.012	1.026	6
Post-	1.023	0.007	1.012	1.033	6
24 Hour	1.022	0.009	1.004	1.030	6
48 Hour	1.016	0.011	1.002	1.027	4
72 Hour	1.022	0.007	1.010	1.030	6
96 Hour	1.021	0.007	1.009	1.029	6

O. Urine Total Volume (ml)

	Mean	Std Dev	Minimum	Maximum	N
Baseline	1372.5	719.9	740.0	2600.0	6
Pre-	1127.0	442.4	740.0	1880.0	5
Post-	n/a				
24 Hour	814.2	427.6	275.0	1480.0	6
48 Hour	1175.0	592.4	620.0	1950.0	4
72 Hour	1525.0	815.5	1000.0	2940.0	6
96 Hour	1541.7	915.9	440.0	2900.0	6

P. Urobilinogen

	Normal		1		4		Missing	
	Freq.	%	Freq.	%	Freq.	%	Freq.	%
Baseline	6	100	0	0	0	0	0	0
Pre-	6	100	0	0	0	0	0	0
Post-	6	100	0	0	0	0	0	0
24 Hour	5	83.3	0	0	1	16.7	0	0
48 Hour	4	66.7	0	0	0	0	2	33.3
72 Hour	5	83.3	0	0	1	16.7	0	0
96 Hour	5	83.3	1	16.7	0	0	0	0

Q. 24 Urine Creatinine (g/24hr)

	Mean	*Std Dev*	*Minimum*	*Maximum*	*N*
Baseline	2.0	0.3	1.7	2.6	6
Pre-	2.0	0.3	1.7	2.6	5
Post-	n/a				
24 Hour	1.5	0.6	0.5	2.2	6
48 Hour	1.8	0.8	0.8	2.6	4
72 Hour	2.0	0.4	1.5	2.5	6
96 Hour	1.5	0.5	0.9	2.0	6

Table E-57
The response of urinary biochemical measurements in Experiment LT2 to motion exposures including 4 g shocks in the positive z axis.

A. Appearance (Turbidity)

	Clear		Cloudy		Hazy		Tubid		Missing	
	Freq.	%	Freq.	%	Freq.	%	Freq.	%	Freq.	%
Baseline	6	100	0	0	0	0	0	0	0	0
Pre-	5	83.3	1	16.7	0	0	0	0	0	0
Post-	5	83.3	0	0	1	16.7	0	0	0	0
24 Hour	5	83.3	0	0	0	0	1	16.7	0	0
48 Hour	3	50	2	33.3	0	0	0	0	1	16.7
72 Hour	5	83.3	0	0	0	0	1	16.7	0	0
96 Hour	6	100	0	0	0	0	0	0	0	0

B. Bilirubin

	Negative		Missing	
	Freq.	%	Freq.	%
Baseline	6	100	0	0
Pre-	6	100	0	0
Post-	6	100	0	0
24 Hour	6	100	0	0
48 Hour	6	100	0	0
72 Hour	6	100	0	0
96 Hour	6	100	0	0

C. Blood Cells

	Negative		Trace		Small		Large		Missing	
	Freq.	%	Freq.	%	Freq.	%	Freq.	%	Freq.	%
Baseline	6	100	0	0	0	0	0	0	0	0
Pre-	6	100	0	0	0	0	0	0	0	0
Post-	6	100	0	0	0	0	0	0	0	0
24 Hour	6	100	0	0	0	0	0	0	0	0
48 Hour	5	83.3	0	0	0	0	0	0	1	16.7
72 Hour	6	100	0	0	0	0	0	0	0	0
96 Hour	6	100	0	0	0	0	0	0	0	0

D. Color

	No color		Yellow		Amber	
	Freq.	%	Freq.	%	Freq.	%
Baseline	0	0	6	100	0	0
Pre-	1	16.7	5	83.3	0	0
Post-	2	33.3	4	66.7	0	0
24 Hour	0	0	4	66.7	0	0
48 Hour	0	0	5	83.3	0	0
72 Hour	0	0	5	83.3	0	0
96 Hour	0	0	6	100	0	0

	Orange		Straw		Missing	
	Freq.	%	Freq.	%	Freq.	%
Baseline	0	0	0	0	0	0
Pre-	0	0	0	0	0	0
Post-	0	0	0	0	0	0
24 Hour	0	0	2	33.3	0	0
48 Hour	0	0	0	0	1	16.7
72 Hour	0	0	1	16.7	0	0
96 Hour	0	0	0	0	0	0

E. Creatinine (mg/dl)

	Mean	*Std Dev*	*Minimum*	*Maximum*	*N*
Baseline	178.5	87.6	65.1	286.4	6
Pre-	201.1	75.7	91.0	286.4	5
Post-	92.0	n/a	92.0	92.0	1
24 Hour	176.8	117.0	66.0	390.0	6
48 Hour	122.2	72.0	48.0	242.0	5
72 Hour	205.0	130.3	49.0	380.0	6
96 Hour	164.5	155.8	53.0	394.0	6

F. Creatinine Clearance (ml/min)

	Mean	*Std Dev*	*Minimum*	*Maximum*	*N*
Baseline	118.5	18.4	94.1	143.5	6
Pre-	120.9	19.6	94.1	143.5	5
Post-	107.5	n/a	107.5	107.5	1
24 Hour	103.0	39.1	29.8	135.4	6
48 Hour	118.2	55.8	32.2	170.9	5
72 Hour	96.4	31.9	34.6	121.8	6
96 Hour	83.1	40.2	8.7	126.4	6

G. Creatinine Clearance/BSA (ml/min/1.73 m2)+A104

	Mean	*Std Dev*	*Minimum*	*Maximum*	*N*
Baseline	71.4	14.8	56.9	93.0	6
Pre-	73.2	15.8	56.9	93.0	5
Post-	62.8	n/a	62.8	62.8	1
24 Hour	60.5	21.2	19.9	73.7	6
48 Hour	71.9	34.6	21.5	110.8	5
72 Hour	57.2	18.6	23.1	73.7	6
96 Hour	49.3	25.1	5.8	81.9	6

H. Glucose

	Negative		"50"		"100"		Missing	
	Freq.	%	Freq.	%	Freq.	%	Freq.	%
Baseline	6	100	0	0	0	0	0	0
Pre-	6	100	0	0	0	0	0	0
Post-	6	100	0	0	0	0	0	0
24 Hour	6	100	0	0	0	0	0	0
48 Hour	5	83.3	0	0	0	0	1	16.7
72 Hour	6	100	0	0	0	0	0	0
96 Hour	6	100	0	0	0	0	0	0

I. Ketones

	Negative		Trace		Missing	
	Freq.	%	Freq.	%	Freq.	%
Baseline	6	100	0		0	0
Pre-	6	100	0	0	0	0
Post-	6	100	0	0	0	0
24 Hour	6	100	0	0	0	0
48 Hour	5	83.3	0	0	1	16.7
72 Hour	6	100	0	0	0	0
96 Hour	6	100	0	0	0	0

J. Leukocyte Esterase

	Negative		Trace		Missing	
	Freq.	%	Freq.	%	Freq.	%
Baseline	6	100	0	0	0	0
Pre-	6	100	0	0	0	0
Post-	6	100	0	0	0	0
24 Hour	6	100	0	0	0	0
48 Hour	5	83.3	0	0	1	16.7
72 Hour	4	66.7	2	33.3	0	0
96 Hour	5	83.3	1	16.7	0	0

K. Nitrite

	Negative		Missing	
	Freq.	%	Freq.	%
Baseline	6	100	0	0
Pre-	6	100	0	0
Post-	6	100	0	0
24 Hour	6	100	0	0
48 Hour	5	83.3	1	16.7
72 Hour	6	100	0	0
96 Hour	6	100	0	0

L. pH

	Mean	Std Dev	Minimum	Maximum	N
Baseline	6.4	0.5	6.0	7.0	6
Pre-	6.2	0.8	5.0	7.0	6
Post-	6.3	0.5	6.0	7.0	6
24 Hour	6.1	0.7	5.0	7.0	6
48 Hour	6.2	0.5	6.0	7.0	5
72 Hour	6.7	0.4	6.0	7.0	6
96 Hour	6.4	0.5	6.0	7.0	6

M. Protein

	Negative		Trace		"30"		Missing	
	Freq.	%	Freq.	%	Freq.	%	Freq.	%
Baseline	4	66.7	2	33.3	0	0	0	0
Pre-	6	100	0	0	0	0	0	0
Post-	6	100	0	0	0	0	0	0
24 Hour	6	100	0	0	0	0	0	0
48 Hour	5	83.3	0	0	0	0	1	16.7
72 Hour	6	100	0	0	0	0	0	0
96 Hour	6	100	0	0	0	0	0	0

N. Specific Gravity

	Mean	Std Dev	Minimum	Maximum	N
Baseline	1.021	0.005	1.012	1.026	6
Pre-	1.021	0.010	1.006	1.031	6
Post-	1.020	0.009	1.008	1.034	6
24 Hour	1.022	0.009	1.005	1.033	6
48 Hour	1.021	0.009	1.006	1.030	5
72 Hour	1.020	0.009	1.007	1.030	6
96 Hour	1.019	0.011	1.001	1.028	6

O. Urine Volume (ml)

	Mean	Std Dev	Minimum	Maximum	N
Baseline	1372.5	719.9	740.0	2600.0	6
Pre-	1127.0	442.4	740.0	1880.0	5
Post-	2020.0	n/a	2020.0	2020.0	1
24 Hour	1210.0	833.5	280.0	2630.0	6
48 Hour	1408.0	567.1	870.0	2285.0	5
72 Hour	1178.3	996.5	200.0	2760.0	6
96 Hour	1303.3	1123.7	190.0	2830.0	6

P. Urobilinogen

	Normal		1		4		Missing	
	Freq.	%	Freq.	%	Freq.	%	Freq.	%
Baseline	6	100	0	0	0	0	0	0
Pre-	5	83.3	0	0	1	16.7	0	0
Post-	5	83.3	0	0	1	16.7	0	0
24 Hour	6	100	0	0	0	0	0	0
48 Hour	5	83.3	0	0	0	0	1	16.7
72 Hour	6	100	0	0	0	0	0	0
96 Hour	6	100	0	0	0	0	0	0

Q. 24 Hr. Urine Creatinine (g/24hr)

	Mean	*Std Dev*	*Minimum*	*Maximum*	*N*
Baseline	2.0	0.3	1.7	2.6	6
Pre-	2.0	0.3	1.7	2.6	5
Post-	1.9	n/a	1.9	1.9	1
24 Hour	1.6	0.7	0.4	2.7	6
48 Hour	1.7	0.8	0.4	2.4	5
72 Hour	1.6	0.6	0.5	2.3	6
96 Hour	1.3	0.6	0.1	1.9	6

Table E-58
The response of urinary biochemical measurements in Experiment LT3 (7 hours per day).

A. Urine Appearance

	Clear		Cloudy		Hazy		Tubid		Missing	
	Freq.	%	Freq.	%	Freq.	%	Freq.	%	Freq.	%
Baseline	8	80	2	20	0	0	0	0	0	0
Pre-	6	60	4	40	0	0	0	0	0	0
Post-	8	80	0	0	1	10	1	10	0	0
24 Hour	8	80	2	20	0	0	0	0	0	0
48 Hour	7	70	2	20	0	0	0	0	1	10
72 Hour	6	60	3	30	0	0	0	0	1	10
96 Hour	6	60	20	0	0	0	2	20	2	20

B. Bilirubin

	Negative		Missing	
	Freq.	%	Freq.	%
Baseline	10	100	0	0
Pre-	10	100	0	0
Post-	10	100	0	0
24 Hour	10	100	0	0
48 Hour	9	90	1	10
72 Hour	9	90	1	10
96 Hour	8	80	2	20

C. Blood

	Negative		Trace		Small		Large		Missing	
	Freq.	%	Freq.	%	Freq.	%	Freq.	%	Freq.	%
Baseline	9	90	0	0	1	10	0	0	0	0
Pre-	8	80	1	10	1	10	0	0	0	0
Post-	9	90	0	0	1	10	0	0	0	0
24 Hour	9	90	1	10	0	0	0	0	0	0
48 Hour	8	80	1	10	0	0	0	0	1	10
72 Hour	7	70	2	20	0	0	0	0	1	10
96 Hour	8	80	0	0	0	0	0	0	2	20

D. Color

	No color		Yellow		Amber	
	Freq.	%	Freq.	%	Freq.	%
Baseline	0	0	8	80	1	10
Pre-	0	0	7	70	1	10
Post-	0	0	10	100	0	0
24 Hour	0	0	9	90	0	0
48 Hour	2	20	5	50	1	10
72 Hour	0	0	7	70	0	0
96 Hour	0	0	8	80	0	0

	Orange		Straw		Missing	
	Freq.	%	Freq.	%	Freq.	%
Baseline	0	0	1	10	0	0
Pre-	0	0	2	20	0	0
Post-	0	0	0	0	0	0
24 Hour	1	10	0	0	0	0
48 Hour	0	0	1	10	0	0
72 Hour	0	0	2	20	0	0
96 Hour	0	0	0	0	2	20

E. Creatinine (mg/dl)

	Mean	*Std Dev*	*Minimum*	*Maximum*	*N*
Baseline	126.9	70.0	23.0	280.0	10
Pre-	126.9	70.0	23.0	280.0	10
Post-	n/a				
24 Hour	135.3	72.4	34.0	258.0	9
48 Hour	118.6	63.1	14.0	201.0	8
72 Hour	151.4	53.7	58.0	203.0	9
96 Hour	157.4	88.8	45.0	284.0	8

F. Creatinine Clearance (ml/min)

	Mean	*Std Dev*	*Minimum*	*Maximum*	*N*
Baseline	98.8	34.3	20.9	140.1	10
Pre-	98.8	34.3	20.9	140.1	10
Post-	n/a				
24 Hour	91.1	44.9	25.0	150.5	9
48 Hour	107.8	48.4	12.7	172.5	8
72 Hour	97.4	21.5	57.2	133.5	9
96 Hour	96.9	27.4	39.4	137.5	8

G. Creatinine Clearance/BSA (ml/min/1.73m2)

	Mean	*Std Dev*	*Minimum*	*Maximum*	*N*
Baseline	60.6	21.3	14.8	88.7	10
Pre-	60.6	21.3	14.8	88.7	10
Post-	n/a				
24 Hour	55.8	27.0	17.7	87.7	9
48 Hour	66.0	30.8	9.0	109.3	8
72 Hour	60.3	13.0	36.7	84.5	9
96 Hour	60.5	16.3	27.8	86.0	8

H. Glucose

	Negative		"50"		"100"		Missing	
	Freq.	%	Freq.	%	Freq.	%	Freq.	%
Baseline	10	100	0	0	0	0	0	0
Pre-	10	100	0	0	0	0	0	0
Post-	10	100	0	0	0	0	0	0
24 Hour	10	100	0	0	0	0	0	0
48 Hour	9	90	0	0	0	0	1	10
72 Hour	9	90	0	0	0	0	1	10
96 Hour	8	80	0	0	0	0	2	20

I. Ketones

	Negative		Trace		Missing	
	Freq.	%	Freq.	%	Freq.	%
Baseline	10	100	0	0	0	0
Pre-	10	100	0	0	0	0
Post-	10	100	0	0	0	0
24 Hour	10	100	0	0	0	0
48 Hour	9	90	0	0	1	10
72 Hour	9	90	0	0	1	10
96 Hour	8	80	0	0	2	20

J. Leukocyte Esterase

	Negative		Trace		Missing	
	Freq.	%	Freq.	%	Freq.	%
Baseline	10	100	0	0	0	0
Pre-	10	100	0	0	0	0
Post-	9	90	9	90	0	0
24 Hour	8	80	2	20	0	0
48 Hour	9	90	0	0	1	10
72 Hour	8	80	1	10	1	10
96 Hour	6	60	2	20	2	20

K. Nitrite

	Negative		Missing	
	Freq.	%	Freq.	%
Baseline	10	100	0	0
Pre-	10	100	0	0
Post-	10	100	0	0
24 Hour	10	100	0	0
48 Hour	9	90	1	10
72 Hour	9	90	1	10
96 Hour	8	80	2	20

L. pH

	Mean	Std Dev	Minimum	Maximum	N
Baseline	6.2	0.8	5.0	8.0	10
Pre-	5.7	0.5	5.0	6.0	10
Post-	6.4	0.8	5.0	8.0	10
24 Hour	6.3	0.6	5.0	7.0	10
48 Hour	6.2	0.3	6.0	6.5	9
72 Hour	6.0	0.7	5.0	7.0	9
96 Hour	6.0	0.7	5.0	7.0	8

M. Protein

	Negative		Trace		"30"		Missing	
	Freq.	%	Freq.	%	Freq.	%	Freq.	%
Baseline	10	100	0	0	0	0	0	0
Pre-	10	100	0	0	0	0	0	0
Post-	9	90	1	10	0	0	0	0
24 Hour	10	100	0	0	0	0	0	0
48 Hour	9	90	1	10	0	0	0	0
72 Hour	9	90	1	10	0	0	0	0
96 Hour	7	70	0	0	1	10	2	20

N. Specific Gravity

	Mean	Std Dev	Minimum	Maximum	N
Baseline	1.023	0.007	1.007	1.034	10
Pre-	1.020	0.008	1.010	1.035	10
Post-	1.023	0.009	1.008	1.036	10
24 Hour	1.021	0.009	1.005	1.034	10
48 Hour	1.021	0.008	1.011	1.036	9
72 Hour	1.021	0.006	1.011	1.030	9
96 Hour	1.023	0.007	1.012	1.034	8

O. Urine Volume (ml)

	Mean	Std Dev	Minimum	Maximum	N
Baseline	1308.0	491.9	670.0	2320.0	10
Pre-	1308.0	491.9	670.0	2320.0	10
Post-	n/a				
24 Hour	1174.4	714.3	370.0	2830.0	9
48 Hour	1455.6	551.8	865.0	2650.0	8
72 Hour	1221.1	768.3	490.0	2825.0	9
96 Hour	1130.0	543.7	560.0	2150.0	8

P. Urobilinogen

	Normal		1		4		Missing	
	Freq.	%	Freq.	%	Freq.	%	Freq.	%
Baseline	10	100	0	0	0	0	0	0
Pre-	10	100	0	0	0	0	0	0
Post-	10	100	0	0	0	0	0	0
24 Hour	10	100	0	0	0	0	0	0
48 Hour	8	80	0	0	1	10	1	10
72 Hour	9	90	0	0	0	0	1	10
96 Hour	8	80	0	0	0	0	2	20

Table E-59
The response of urinary biochemical measurements in Experiment LT4 (5 days of 4 hours per day).

A. Urine Appearance

	Clear		Cloudy		Hazy		Tubid		Missing	
	Freq.	%	Freq.	%	Freq.	%	Freq.	%	Freq.	%
Baseline	7	87.5	0	0	1	12.5	0	0	0	0
Pre 1-	7	87.5	0	0	0	0	1	12.5	0	0
Post 1-	8	100	0	0	0	0	0	0	0	0
Pre 2-	7	87.5	1	12.5	0	0	0	0	0	0
Post 2-	7	87.5	1	12.5	0	0	0	0	0	0
Pre 3-	7	87.5	1	12.5	0	0	0	0	0	0
Post 3-	5	62.5	1	12.5	1	12.5	1	12.5	0	0
Pre 4-	7	87.5	0	0	0	0	1	12.5	0	0
Post 4-	7	87.5	0	0	0	0	0	0	1	12.5
Pre 5-	7	87.5	1	12.5	0	0	0	0	0	0
Post 5-	6	75	2	25	0	0	0	0	0	0
24 Hour	8	100	0	0	0	0	0	0	0	0
48 Hour	8	100	0	0	0	0	0	0	0	0
72 Hour	7	87.5	1	12.5	0	0	0	0	0	0
96 Hour	6	75	2	25	0	0	0	0	0	0

B. Bilirubin

	Negative		Missing	
	Freq.	%	Freq.	%
Baseline	8	100	0	0
Pre 1-	8	100	0	0
Post 1-	8	100	0	0
Pre 2-	8	100	0	0
Post 2-	8	100	0	0
Pre 3-	8	100	0	0
Post 3-	8	100	0	0
Pre 4-	8	100	0	0
Post 4-	7	87.5	1	12.5
Pre 5-	8	100	0	0
Post 5-	8	100	0	0
24 Hour	8	100	0	0
48 Hour	8	100	0	0
72 Hour	8	100	0	0
96 Hour	8	100	0	0

C. Blood Cells

	Negative		Trace		Small		Large		Missing	
	Freq.	%	Freq.	%	Freq.	%	Freq.	%	Freq.	%
Baseline	8	100	0	0	0	0	0	0	0	0
Pre 1-	8	100	0	0	0	0	0	0	0	0
Post 1-	8	100	0	0	0	0	0	0	0	0
Pre 2-	8	100	0	0	0	0	0	0	0	0
Post 2-	8	100	0	0	0	0	0	0	0	0
Pre 3-	8	100	0	0	0	0	0	0	0	0
Post 3-	8	100	0	0	0	0	0	0	0	0
Pre 4-	8	100	0	0	0	0	0	0	0	0
Post 4-	7	87.5	0	0	0	0	0	0	1	12.5
Pre 5-	8	100	0	0	0	0	0	0	0	0
Post 5-	8	100	0	0	0	0	0	0	0	0
24 Hour	8	100	0	0	0	0	0	0	0	0
48 Hour	7	87.5	1	12.5	0	0	0	0	0	0
72 Hour	8	100	0	0	0	0	0	0	0	0
96 Hour	8	100	0	0	0	0	0	0	0	0

D. Color

	No color		Yellow		Amber		Orange		Straw	
	Freq.	%	Freq.	%	Freq.	%	Freq.	%	Freq.	%
Baseline	0	0	8	80	0	0	0	0	0	0
Pre 1-	0	0	8	80	0	0	0	0	0	0
Post 1-	0	0	8	80	0	0	0	0	0	0
Pre 2-	1	12.5	7	87.5	0	0	0	0	0	0
Post 2-	0	0	8	80	0	0	0	0	0	0
Pre 3-	0	0	8	80	0	0	0	0	0	0
Post 3-	0	0	8	80	0	0	0	0	0	0
Pre 4-	0	0	8	80	0	0	0	0	0	0
Post 4-	0	0	7	87.5	0	0	0	0	0	0
Pre 5-	0	0	8	80	0	0	0	0	0	0
Post 5-	0	0	8	80	0	0	0	0	0	0
24 Hour	0	0	7	87.5	0	0	0	0	1	12.5
48 Hour	0	0	7	87.5	0	0	0	0	1	12.5
72 Hour	0	0	8	80	0	0	0	0	0	0
96 Hour	0	0	8	80	0	0	0	0	0	0

E. Creatinine (mg/dl)

	Mean	*Std Dev*	*Minimum*	*Maximum*	*N*
Baseline	172.4	75.2	38.0	253.0	8
Pre 1-	173.5	76.6	38.0	262.0	8
Pre 2-	219.8	100.0	85.0	336.0	8
Pre 3-	216.5	83.0	117.0	330.0	8
Pre 4-	215.7	98.2	92.0	378.0	7
Pre 5-	180.9	68.5	88.0	247.0	7
24 Hour	180.6	78.1	61.9	303.0	8
48 Hour	151.7	88.0	36.0	306.0	8
72 Hour	207.0	72.6	69.8	291.0	7
96 Hour	170.3	73.4	62.0	259.0	7

F. Creatinine Clearance (ml/min)

	Mean	*Std Dev*	*Minimum*	*Maximum*	*N*
Baseline	117.1	41.8	68.4	190.9	8
Pre 1-	109.5	44.8	67.8	190.9	8
Pre 2-	92.1	35.9	44.4	147.0	8
Pre 3-	90.6	37.7	25.0	140.9	8
Pre 4-	98.8	35.3	55.6	155.9	7
Pre 5-	119.7	41.6	55.7	160.5	7
24 Hour	113.0	53.0	37.6	201.8	8
48 Hour	95.9	29.2	47.1	135.0	8
72 Hour	126.3	17.3	109.2	158.6	7
96 Hour	89.6	33.2	32.2	119.8	7

G. Creatinine Clearance/BSA (ml/min/1.73m2)

	Mean	*Std Dev*	*Minimum*	*Maximum*	*N*
Baseline	70.4	22.0	46.0	109.9	8
Pre 1-	65.7	23.7	42.0	109.9	8
Pre 2-	55.8	20.7	27.2	84.7	8
Pre 3-	55.2	23.1	15.5	86.1	8
Pre 4-	60.2	21.0	31.5	89.8	7
Pre 5-	72.7	24.0	34.1	90.4	7
24 Hour	69.3	33.3	23.0	123.4	8
48 Hour	58.8	19.6	28.8	82.8	8
72 Hour	77.5	10.7	65.5	97.2	7
96 Hour	55.4	21.3	19.3	81.0	7

H. Glucose

	Negative		"50"		"100"		Missing	
	Freq.	%	Freq.	%	Freq.	%	Freq.	%
Baseline	8	100	0	0	0	0	0	0
Pre 1-	8	100	0	0	0	0	0	0
Post 1-	8	100	0	0	0	0	0	0
Pre 2-	7	87.5	0	0	1	12.5	0	0
Post 2-	8	100	0	0	0	0	0	0
Pre 3-	8	100	0	0	0	0	0	0
Post 3-	8	100	0	0	0	0	0	0
Pre 4-	8	100	0	0	0	0	0	0
Post 4-	7	87.5	0	0	0	0	1	12.5
Pre 5-	8	100	0	0	0	0	0	0
Post 5-	8	100	0	0	0	0	0	0
24 Hour	8	100	0	0	0	0	0	0
48 Hour	8	100	0	0	0	0	0	0
72 Hour	8	100	0	0	0	0	0	0
96 Hour	7	87.5	1	12.5	0	0	0	0

I. Ketones

	Negative		Trace		Missing	
	Freq.	%	Freq.	%	Freq.	%
Baseline	8	100	0	0	0	0
Pre 1-	8	100	0	0	0	0
Post 1-	8	100	0	0	0	0
Pre 2-	7	87.5	1	12.5	0	0
Post 2-	8	100	0	0	0	0
Pre 3-	8	100	0	0	0	0
Post 3-	8	100	0	0	0	0
Pre 4-	8	100	0	0	0	0
Post 4-	7	87.5	0	0	1	12.5
Pre 5-	8	100	0	0	0	0
Post 5-	8	100	0	0	0	0
24 Hour	8	100	0	0	0	0
48 Hour	8	100	0	0	0	0
72 Hour	8	100	0	0	0	0
96 Hour	8	100	0	0	0	0

J. Leukocyte Esterase

	Negative		Trace		Missing	
	Freq.	%	Freq.	%	Freq.	%
Baseline	8	100	0	0	0	0
Pre 1-	8	100	0	0	0	0
Post 1-	8	100	0	0	0	0
Pre 2-	8	100	0	0	0	0
Post 2-	8	100	0	0	0	0
Pre 3-	6	75	2	25	0	0
Post 3-	8	100	0	0	0	0
Pre 4-	7	87.5	1	12.5	0	0
Post 4-	7	87.5	0	0	1	12.5
Pre 5-	8	100	0	0	0	0
Post 5-	7	87.5	1	12.5	0	0
24 Hour	6	75	2	25	0	0
48 Hour	7	87.5	1	12.5	0	0
72 Hour	8	100	0	0	0	0
96 Hour	8	100	0	0	0	0

K. Nitrite

	Negative		Missing	
	Freq.	%	Freq.	%
Baseline	8	100	0	0
Pre 1-	8	100	0	0
Post 1-	8	100	0	0
Pre 2-	8	100	0	0
Post 2-	8	100	0	0
Pre 3-	8	100	0	0
Post 3-	8	100	0	0
Pre 4-	8	100	0	0
Post 4-	7	87.5	1	12.5
Pre 5-	8	100	0	0
Post 5-	8	100	0	0
24 Hour	8	100	0	0
48 Hour	8	100	0	0
72 Hour	8	100	0	0
96 Hour	8	100	0	0

L. pH

	Mean	Std Dev	Minimum	Maximum	N
Baseline	6.3	0.7	5.0	7.0	8
Pre 1-	5.8	0.7	5.0	6.5	8
Post 1-	6.4	0.7	6.0	8.0	8
Pre 2-	5.9	0.7	5.0	7.0	8
Post 2-	6.0	0.5	5.0	7.0	8
Pre 3-	5.7	0.6	5.0	6.5	8
Post 3-	6.4	0.7	5.0	7.0	8
Pre 4-	6.0	0.9	5.0	8.0	8
Post 4-	6.9	0.8	6.0	8.0	7
Pre 5-	5.6	0.5	5.0	6.0	8
Post 5-	6.4	0.7	5.0	7.0	8
24 Hour	6.4	0.9	5.0	8.0	8
48 Hour	6.1	0.6	5.0	7.0	8
72 Hour	6.0	0.8	5.0	7.0	8
96 Hour	5.9	0.8	5.0	7.0	8

M. Protein

	Negative		Trace		"30"		Missing	
	Freq.	%	Freq.	%	Freq.	%	Freq.	%
Baseline	8	100	0	0	0	0	0	0
Pre 1-	8	100	0	0	0	0	0	0
Post 1-	8	100	0	0	0	0	0	0
Pre 2-	7	87.5	1	12.5	0	0	0	0
Post 2-	8	100	0	0	0	0	0	0
Pre 3-	8	100	0	0	0	0	0	0
Post 3-	8	100	0	0	0	0	0	0
Pre 4-	7	87.5	1	12.5	0	0	0	0
Post 4-	7	87.5	0	0	0	0	1	12.5
Pre 5-	7	87.5	1	12.5	0	0	0	0
Post 5-	8	100	0	0	0	0	0	0
24 Hour	8	100	0	0	0	0	0	0
48 Hour	6	75	2	25	0	0	0	0
72 Hour	7	87.5	1	12.5	0	0	0	0
96 Hour	7	87.5	1	12.5	0	0	0	0

N. Specific Gravity

	Mean	Std Dev	Minimum	Maximum	N
Baseline	1.025	0.005	1.017	1.034	8
Pre 1-	1.026	0.005	1.020	1.034	8
Post 1-	1.021	0.007	1.009	1.030	8
Pre 2-	1.025	0.008	1.007	1.035	8
Post 2-	1.023	0.005	1.019	1.033	8
Pre 3-	1.027	0.003	1.022	1.031	8
Post 3-	1.026	0.004	1.020	1.034	8
Pre 4-	1.025	0.004	1.020	1.032	8
Post 4-	1.026	0.004	1.021	1.034	7
Pre 5-	1.022	0.008	1.010	1.034	8
Post 5-	1.022	0.006	1.010	1.031	8
24 Hour	1.022	0.006	1.017	1.032	8
48 Hour	1.024	0.008	1.012	1.035	8
72 Hour	1.027	0.004	1.020	1.035	8
96 Hour	1.025	0.005	1.015	1.032	8

O. Urine Volume (ml)

	Mean	Std Dev	Minimum	Maximum	N
Baseline	1415.0	1083.2	600.0	3360.0	8
Pre 1-	1383.8	1111.3	410.0	3360.0	8
Pre 2-	892.5	808.4	190.0	2740.0	8
Pre 3-	793.8	542.4	140.0	1730.0	8
Pre 4-	904.3	698.4	380.0	2440.0	7
Pre 5-	1081.4	641.3	340.0	2100.0	7
24 Hour	1250.0	931.1	320.0	2740.0	8
48 Hour	1309.4	1131.3	570.0	3980.0	8
72 Hour	1032.9	542.9	710.0	2220.0	7
96 Hour	1082.9	959.9	260.0	3060.0	7

P. Urobilinogen

	Normal		1		4		Missing	
	Freq.	%	Freq.	%	Freq.	%	Freq.	%
Baseline	8	100	0	0	0	0	0	0
Pre 1-	8	100	0	0	0	0	0	0
Post 1-	8	100	0	0	0	0	0	0
Pre 2-	8	100	0	0	0	0	0	0
Post 2-	8	100	0	0	0	0	0	0
Pre 3-	8	100	0	0	0	0	0	0
Post 3-	8	100	0	0	0	0	0	0
Pre 4-	7	87.5	0	0	1	12.5	0	0
Post 4-	6	75	0	0	1	12.5	1	12.5
Pre 5-	7	87.5	0	0	1	12.5	0	0
Post 5-	8	100	0	0	0	0	0	0
24 Hour	8	100	0	0	0	0	0	0
48 Hour	7	87.5	1	12.5	0	0	0	0
72 Hour	8	100	0	0	0	0	0	0
96 Hour	8	100	0	0	0	0	0	0

Q. 24 Hr Urine Creatinine (g/24hr)

	Mean	*Std Dev*	*Minimum*	*Maximum*	*N*
Baseline	1.8	0.7	1.1	3.0	8
Pre 1-	1.7	0.7	1.1	3.0	8
Pre 2-	1.4	0.6	0.6	2.3	8
Pre 3-	1.4	0.6	0.4	2.2	8
Pre 4-	1.5	0.5	1.0	2.2	7
Pre 5-	1.6	0.6	0.8	2.4	7
24 Hour	1.7	0.8	0.6	3.2	8
48 Hour	1.4	0.4	0.9	1.9	8
72 Hour	1.8	0.3	1.5	2.1	7
96 Hour	1.3	0.5	0.5	1.9	7

Appendix F
Figures

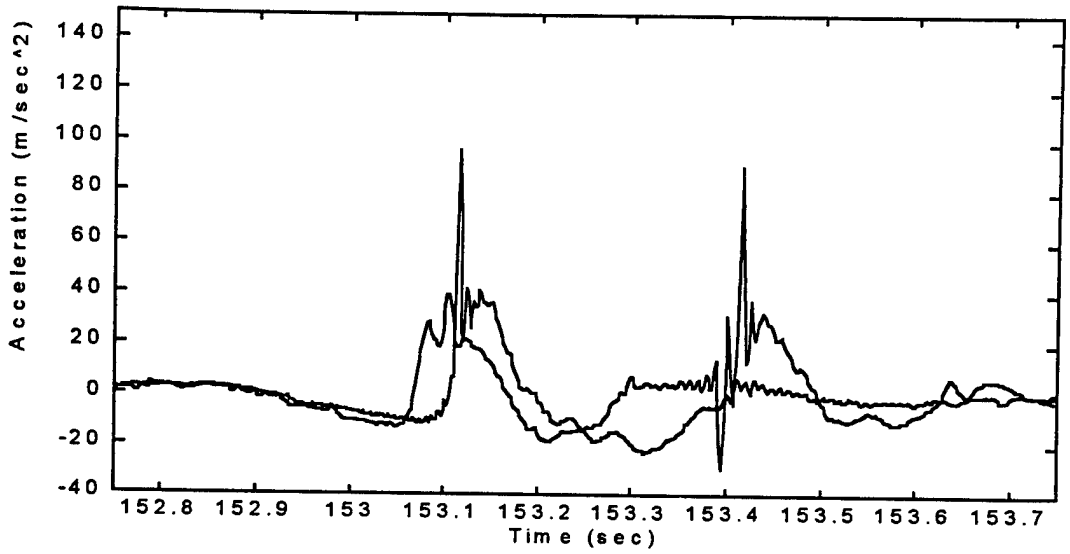

Figure F-1. Acceleration measured at the seat and lumbar spine for a +4 g, 4 Hz z axis shock. Dotted line: Lumbar L4 z; solid line: Seat Sz.

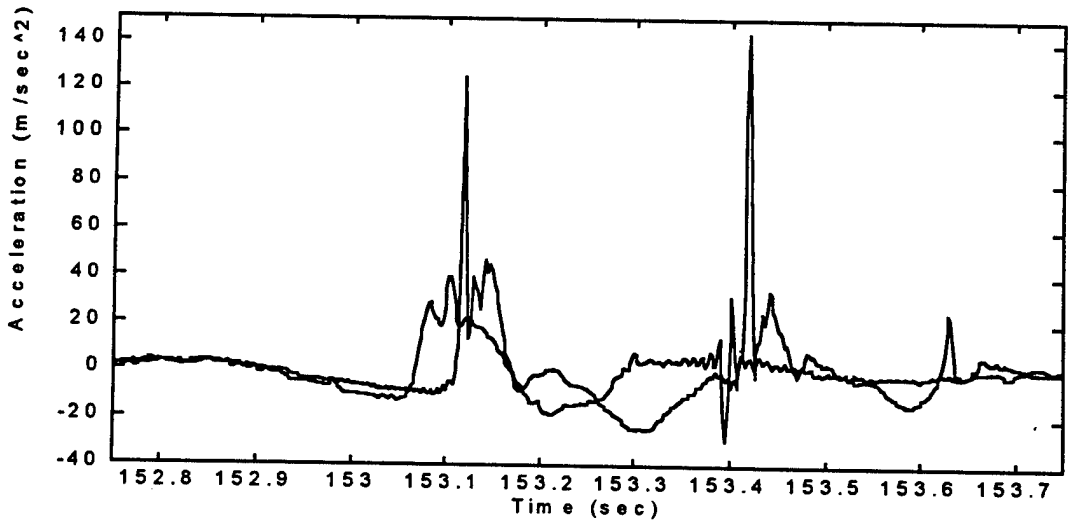

Figure F-2. Acceleration measured at the seat and thoracic spine for a +4 g, 4 Hz z axis shock. Dotted line: Thoracic T3 z; solid line: Seat Sz.

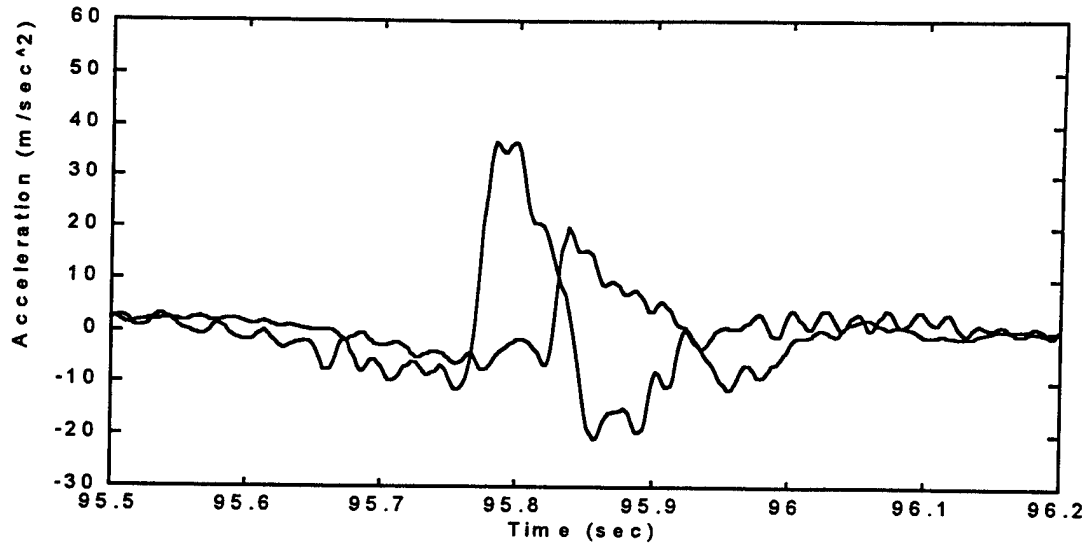

Figure F-3. Acceleration measured at the seat and lumbar spine for a +4 g, 4 Hz y axis shock. Dotted line: Lumbar L3 y; solid line: Seat Sy.

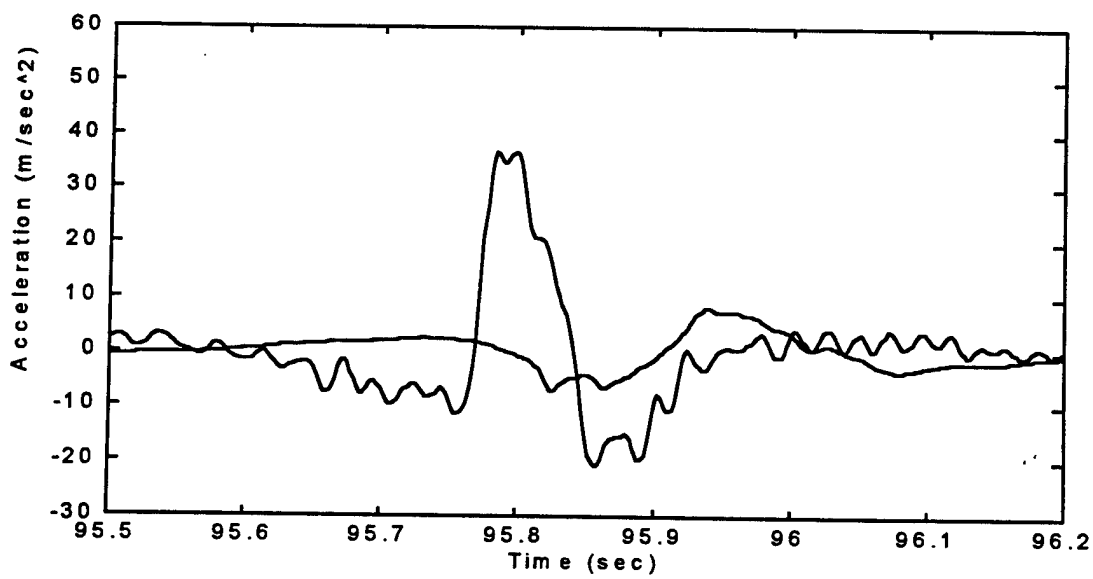

Figure F-4. Acceleration measured at the seat and thoracic spine for a +4 g, 4 Hz y axis shock. Dotted line: Thoracic T2 y; solid line: Seat Sy.

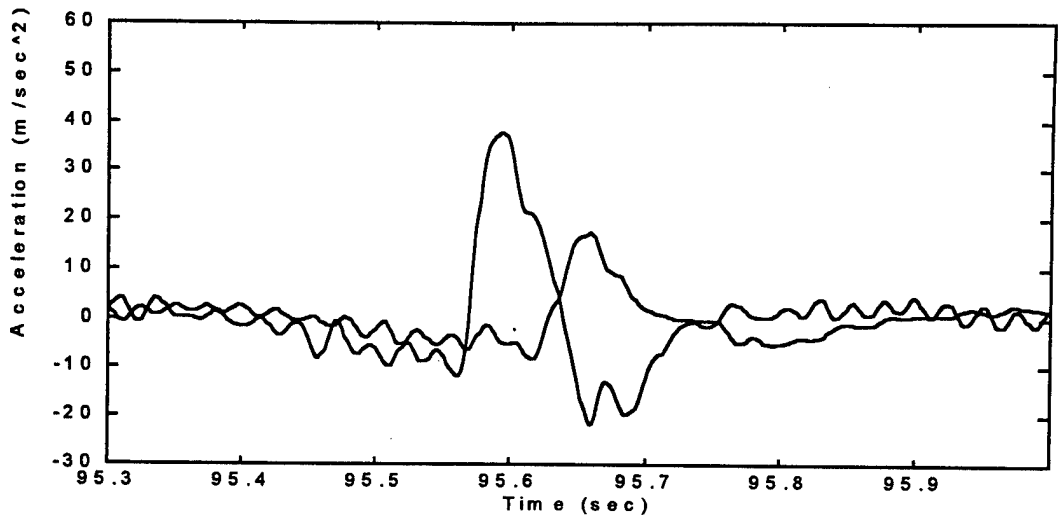

Figure F-5. Acceleration measured at the seat and lumbar spine for a +4 g, 4 Hz x axis shock. Dotted line: Lumbar L2 x; solid line: Seat Sx.

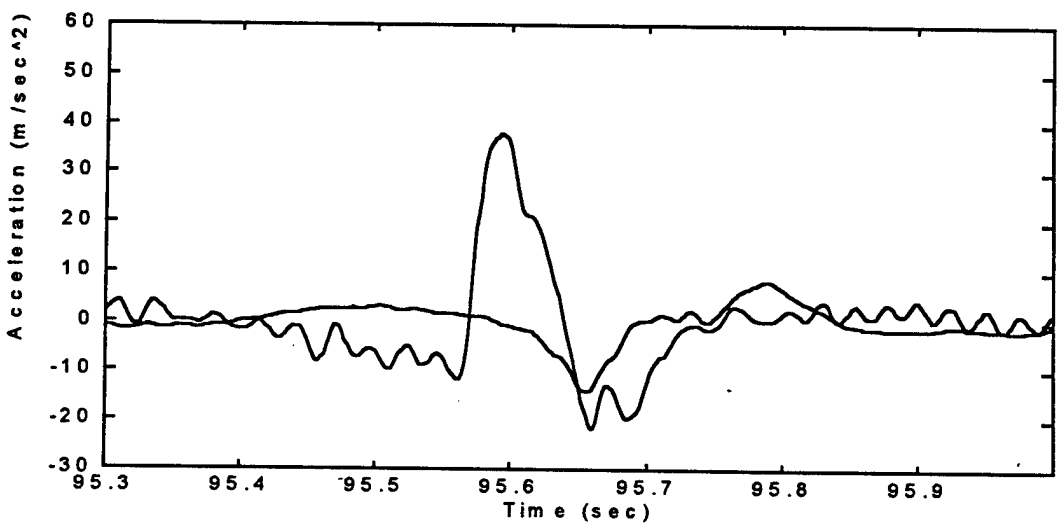

Figure F-6. Acceleration measured at the seat and thoracic spine for a +4 g, 4 Hz x axis shock. Dotted line: Thoracic T1 x; solid line: Seat Sx.

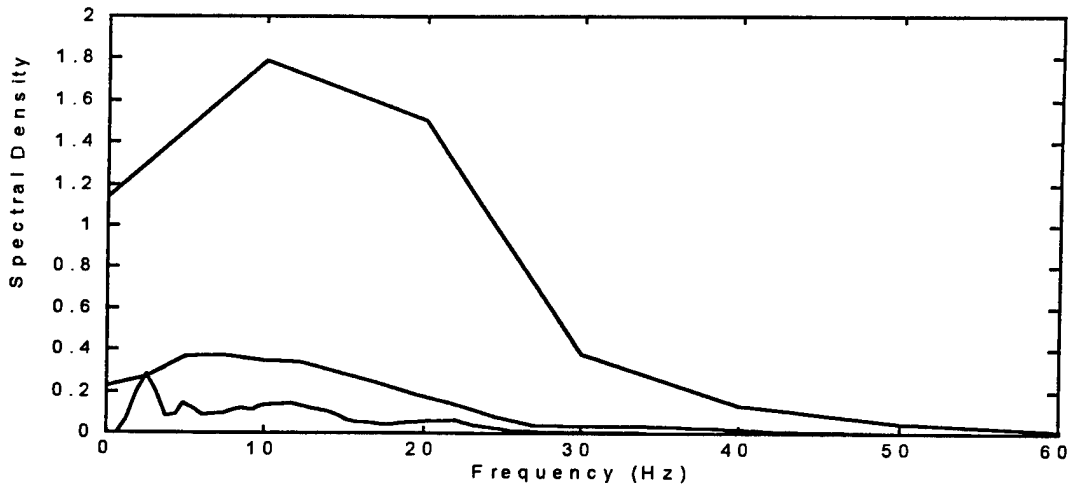

Figure F-7. Spectral density of acceleration measured at seat, lumbar and thoracic spine for a +4 g, 20 Hz z axis shock. Solid line: Seat Sz; dashed line: Lumbar L4 z; dotted line: Thoracic T3 z.

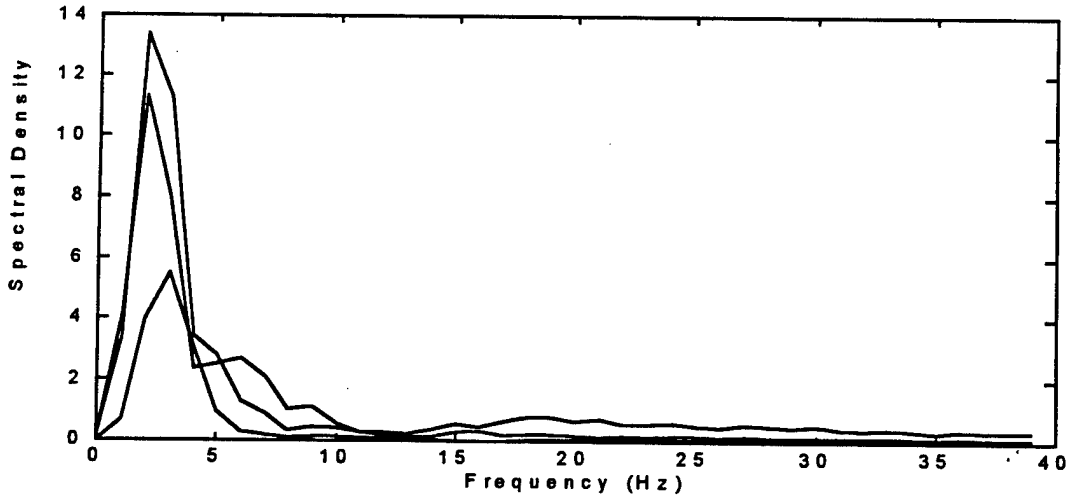

Figure F-8. Spectral density of acceleration measured at seat, lumbar and thoracic spine for a +4 g, 4 Hz z axis shock. Solid line: Seat Sz; dashed line: Lumbar L4 z; dotted line: Thoracic T3 z.

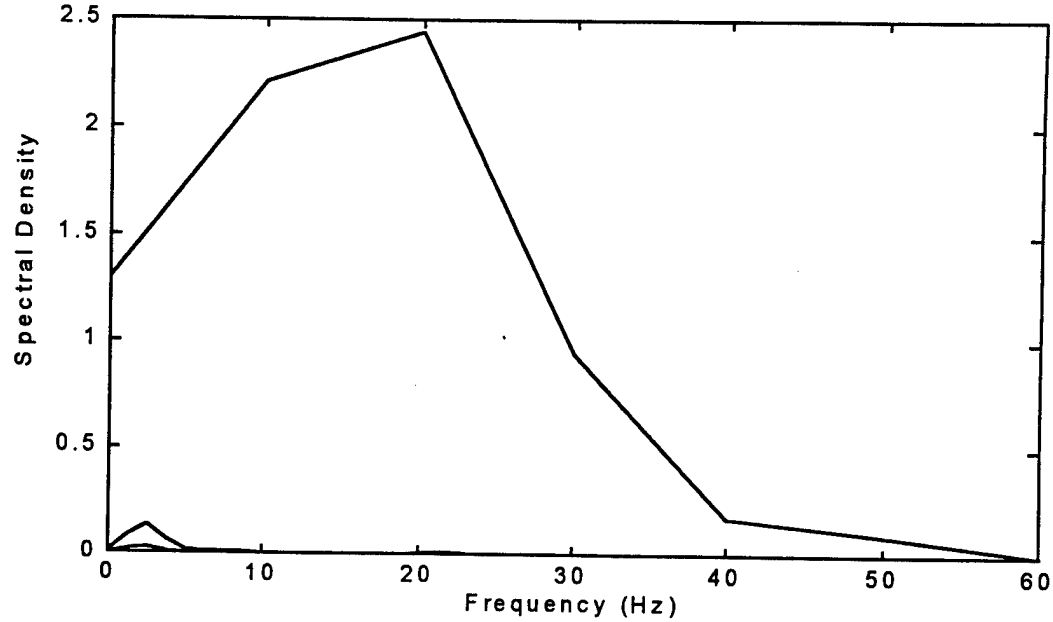

Figure F-9. Spectral density of acceleration measured at seat, lumbar and thoracic spine for a +4 g, 20 Hz y axis shock. Solid line: Seat Sy; dashed line: Lumbar L3 y; dotted line: Thoracic T2 y.

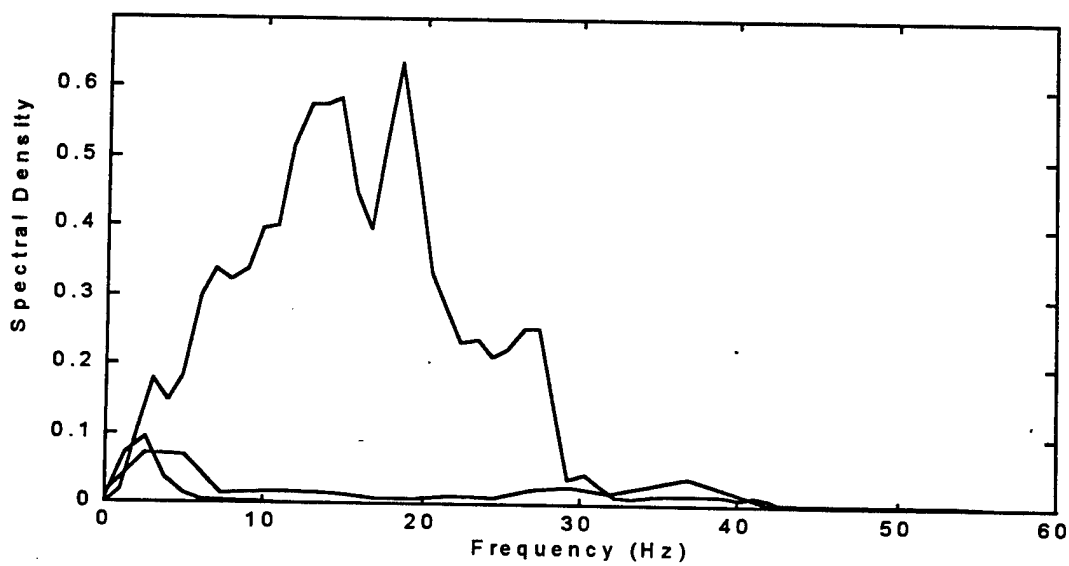

Figure F-10. Spectral density of acceleration measured at seat, lumbar and thoracic spine for a +4 g, 20 Hz x axis shock. Solid line: Seat Sx; dashed line: Lumbar L2 x; dotted line: Thoracic T1 x

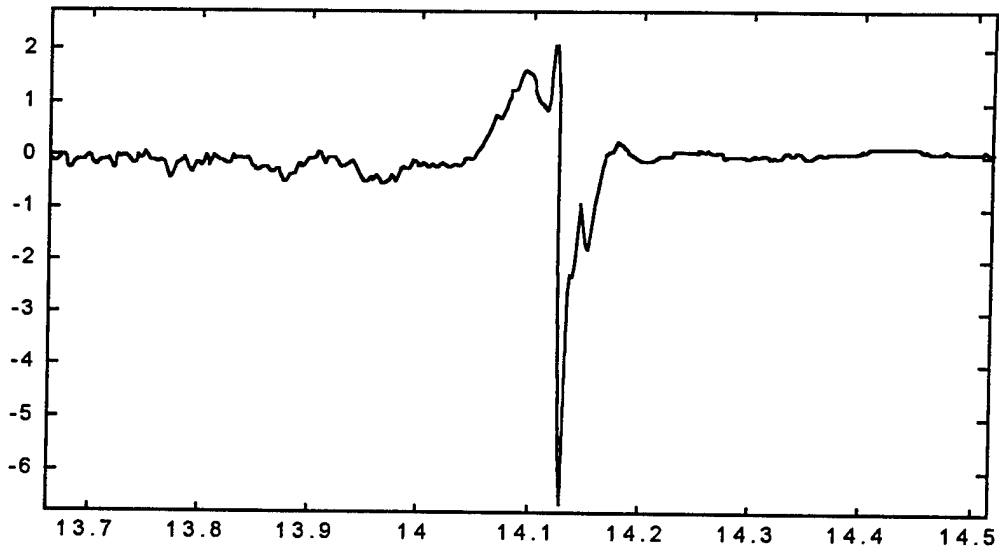

Figure F-11. Example of a free damped oscillation of the L3 accelerometer (y axis) in response to perturbation of the skin.

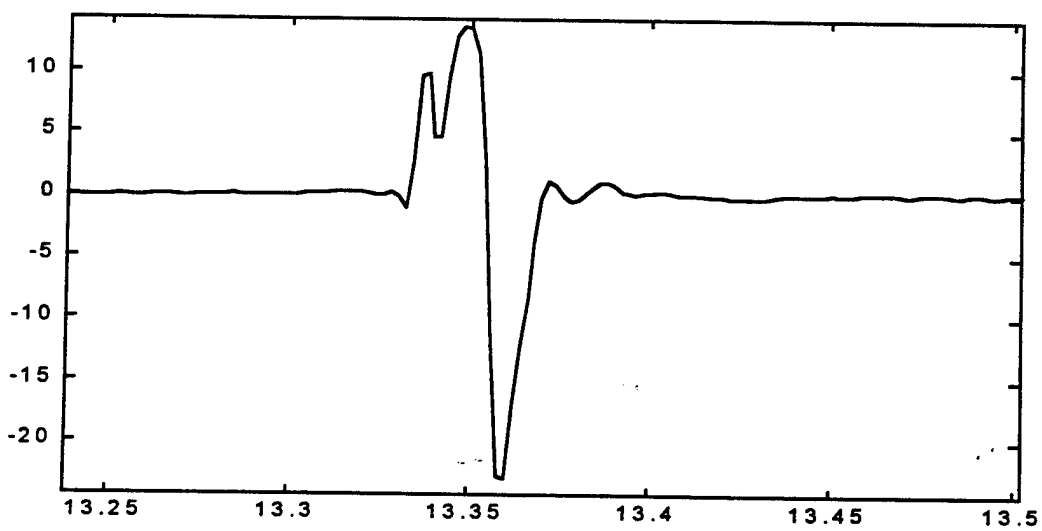

Figure F-12. Example of a free damped oscillation of the L4 accelerometer (z axis) in response to perturbation of the skin.

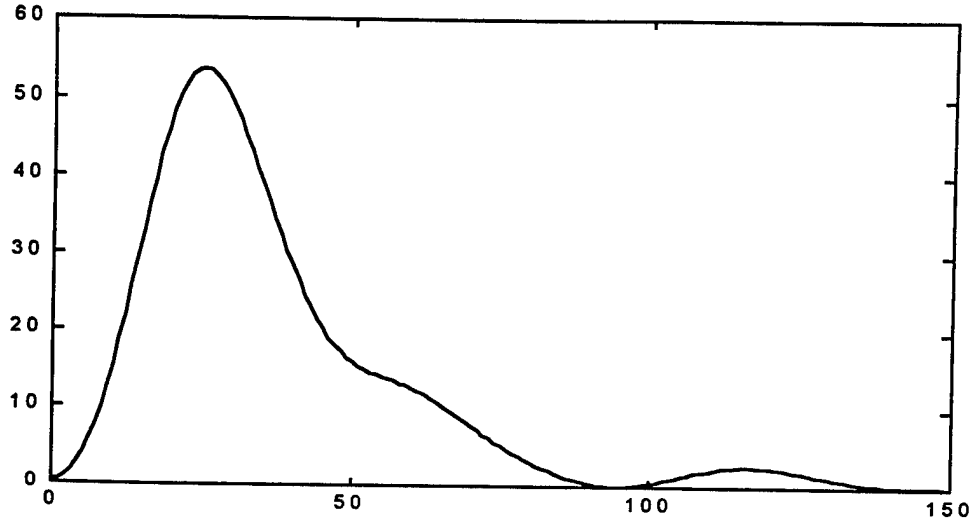

Figure F-13. Spectral density of a free damped oscillation of the skin-accelerometer system at L4 (z axis).

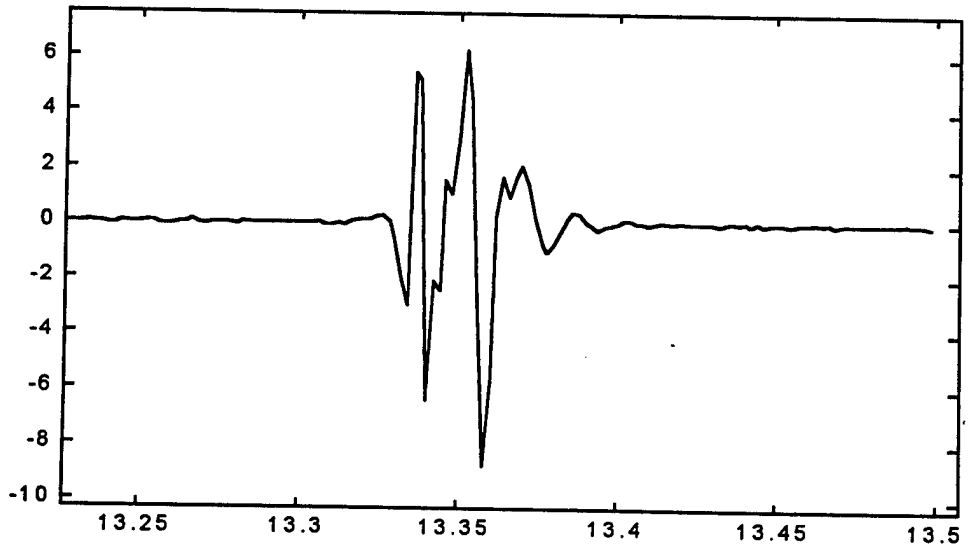

Figure F-14. The high pass acceleration component of a skin perturbation.

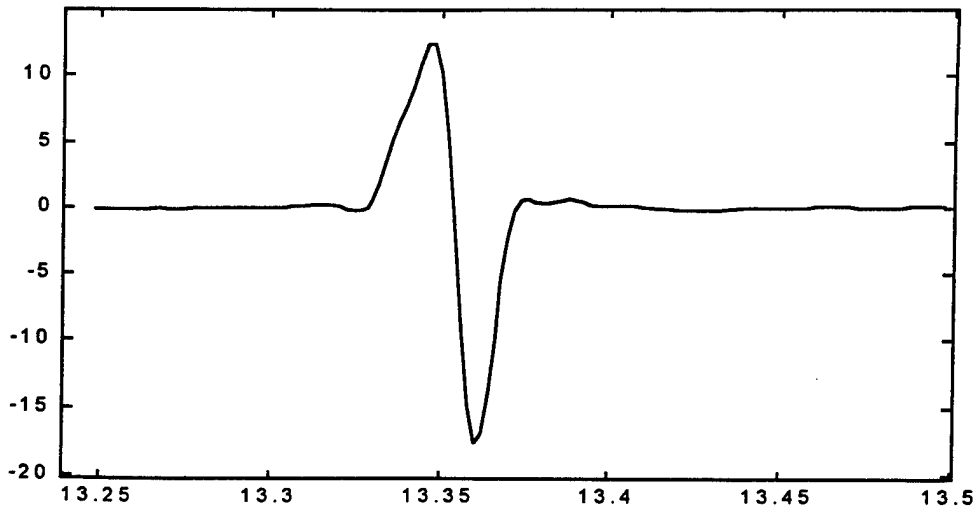

Figure F-15. The low pass acceleration component of a skin perturbation.

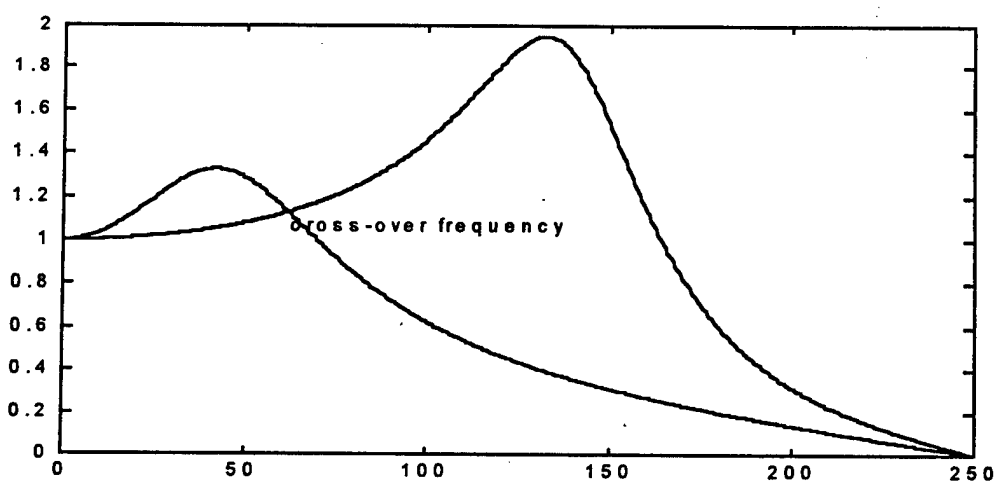

Figure F-16. The amplitude components of low frequency (dotted line) and high frequency (solid line) bone-skin transfer functions derived from a free damped oscillation. The cross-over frequency (fi) was used to establish the cut-off frequency for low pass and high pass filtering of the measured acceleration signal.

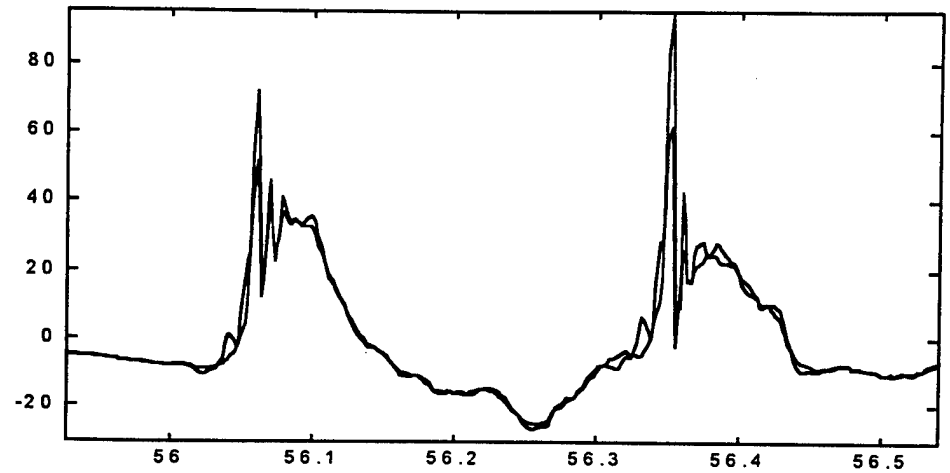

Figure F-17. Recorded L4 accelerometer response to a -4 g, z axis shock at the seat and the predicted acceleration at the spinous process after correction by the skin transfer function. Dotted line = recorded L4 response; Solid line = corrected response.

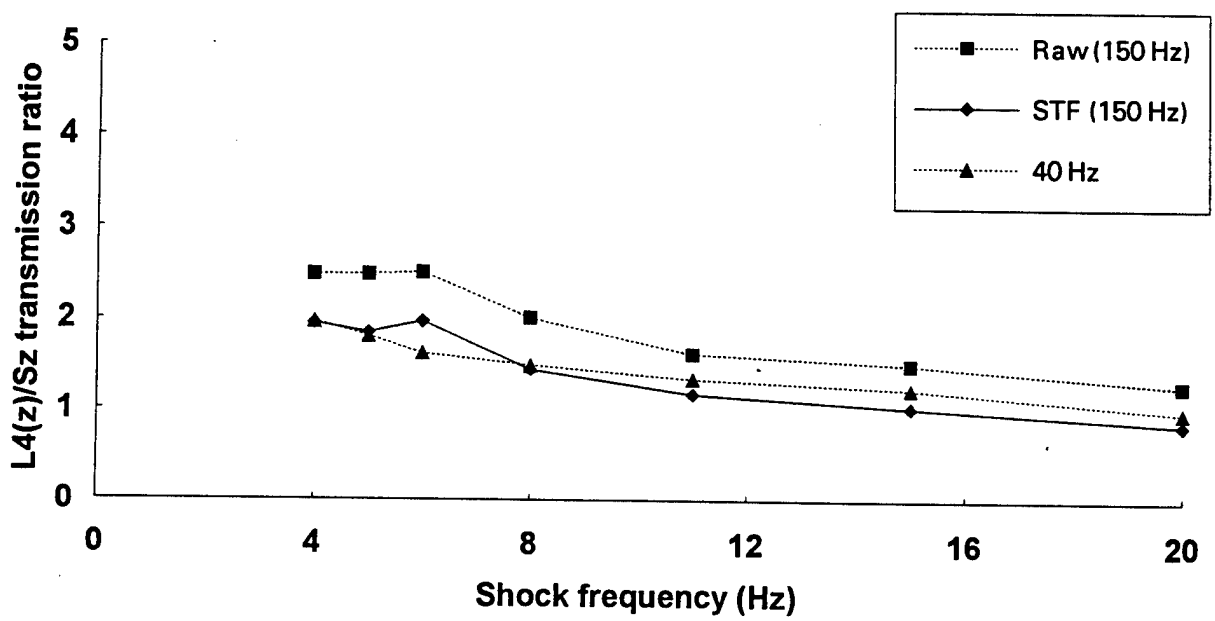

Figure F-18. Spine (L4) z acceleration to seat z acceleration for 4 g shocks using 40 Hz, 150 Hz, and Skin Transfer Function analysis.

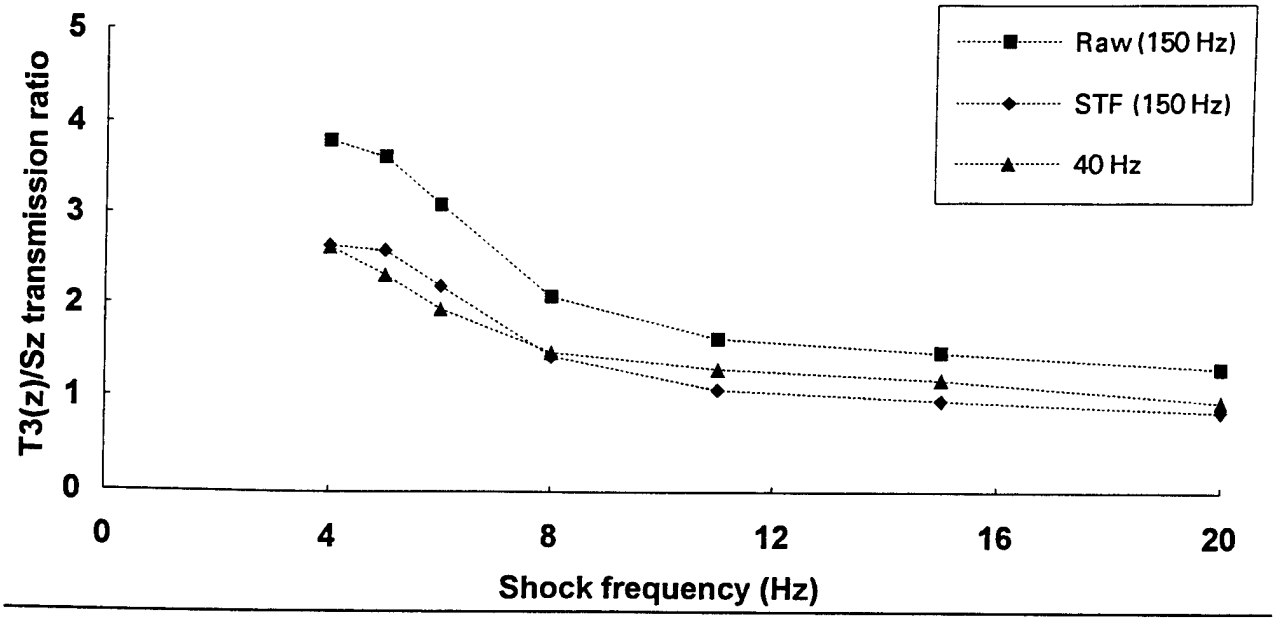

Figure F-19. Spine (T3) z acceleration to seat z acceleration for 4 g shocks using 40 Hz, 150 Hz, and Skin Transfer Function analysis.

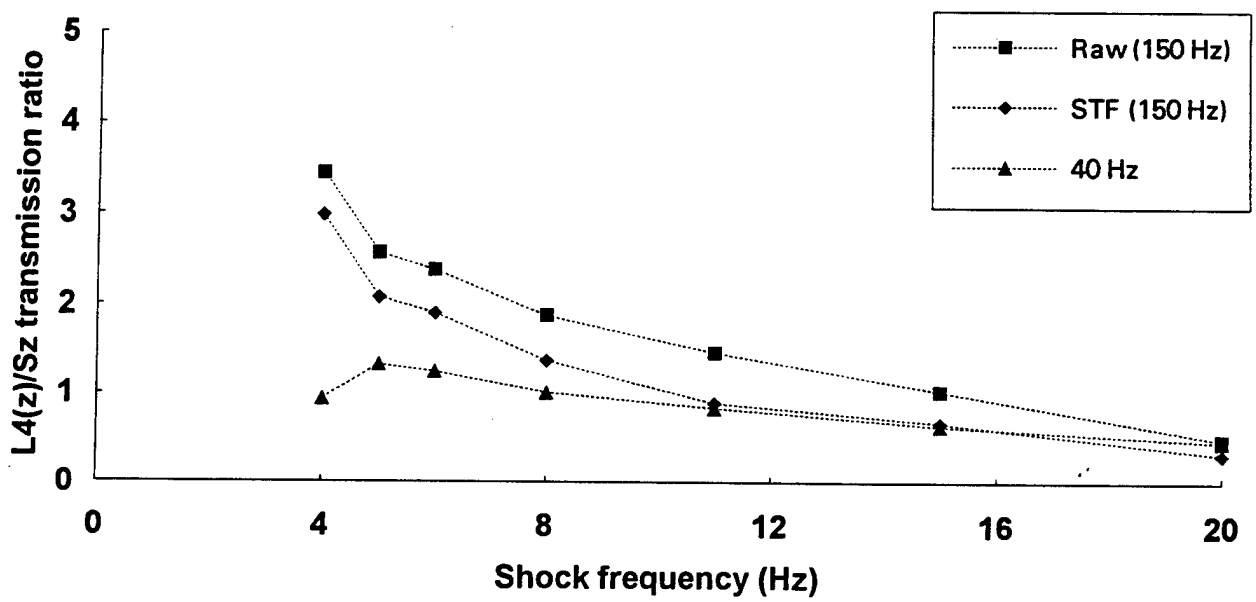

Figure F-20. Spine (L4) z acceleration to seat z acceleration for -4 g shocks using 40 Hz, 150 Hz, and Skin Transfer Function analysis.

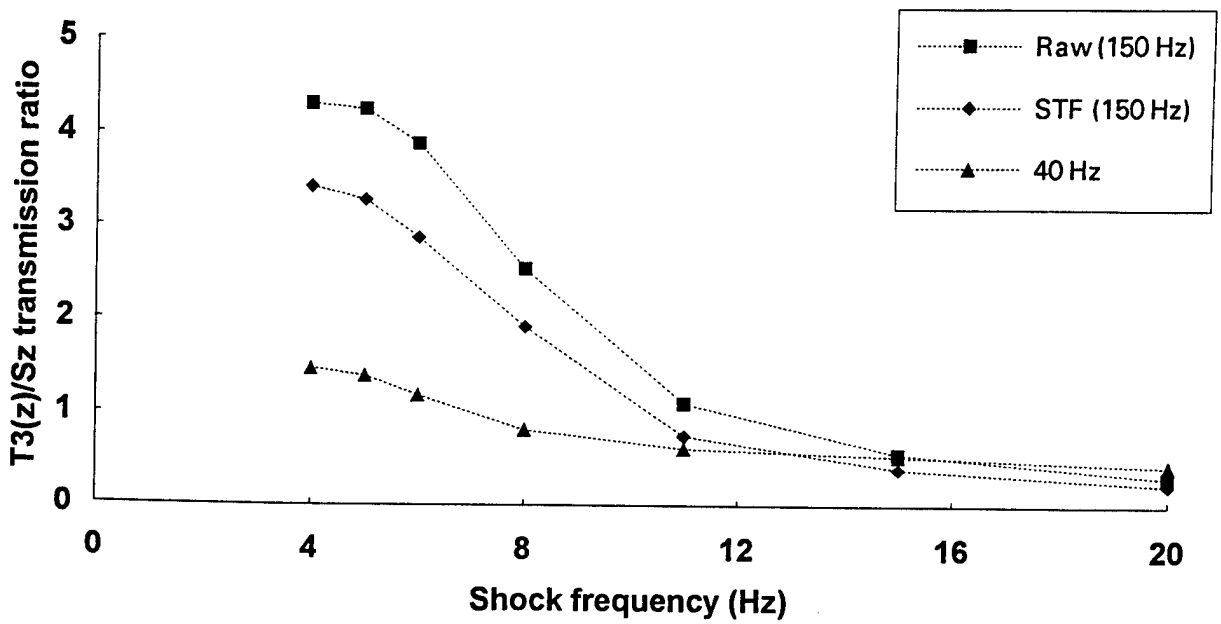

Figure F-21. Spine (T3) z acceleration to seat z acceleration for -4 g shocks using 40 Hz, 150 Hz (Raw), and Skin Transfer Function (STF) analysis.

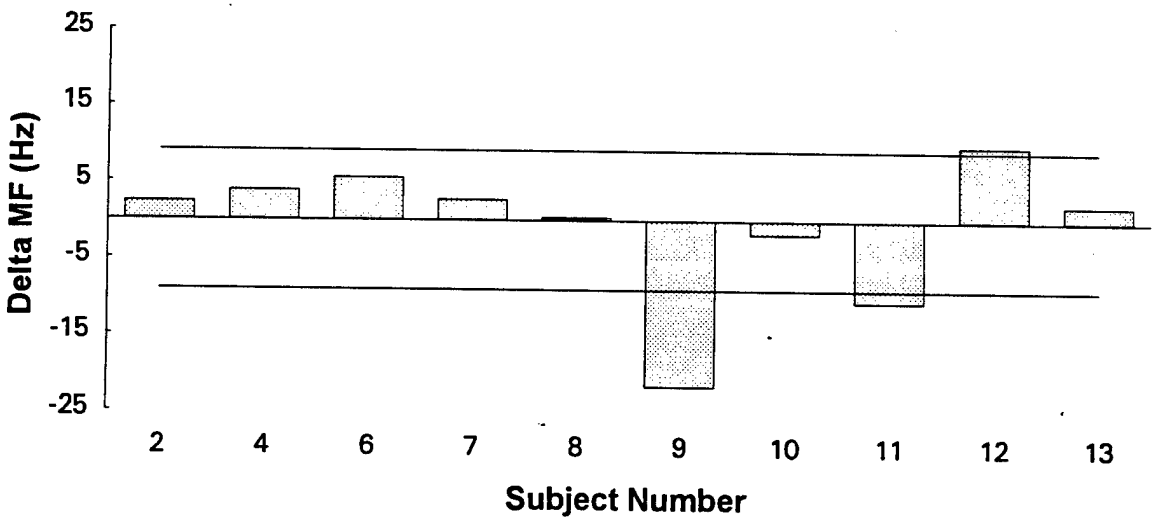

Figure F-22. Change in mean frequency (delta MF) at right lumbar muscle site (L3) after exposure to motion during experiment LT3. Lines represent ± 1 standard deviation.

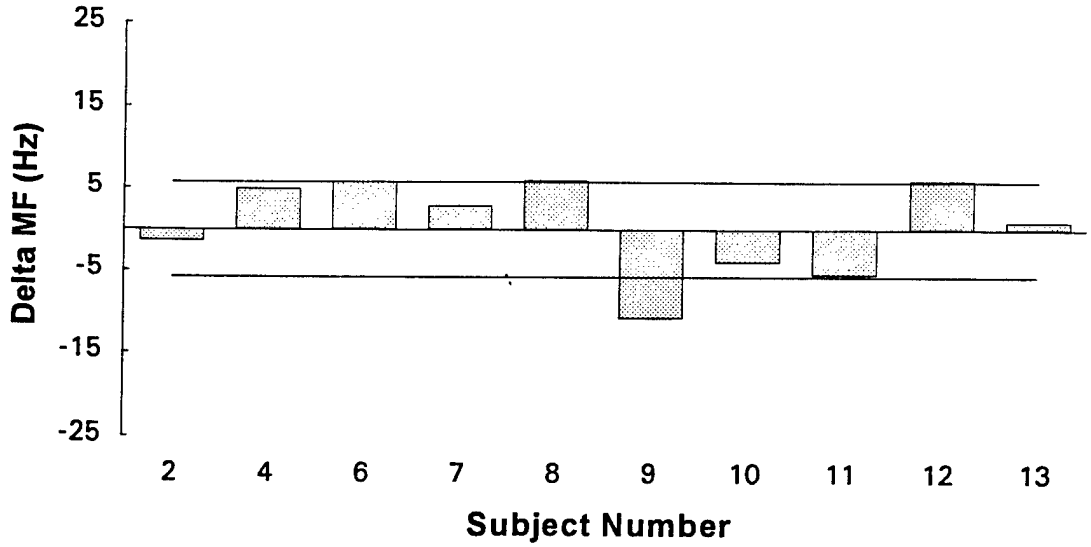

Figure F-23. Change in mean frequency (delta MF) at left lumbar muscle site (L3) after exposure to motion during experiment LT3. Lines represent ± 1 standard deviation.

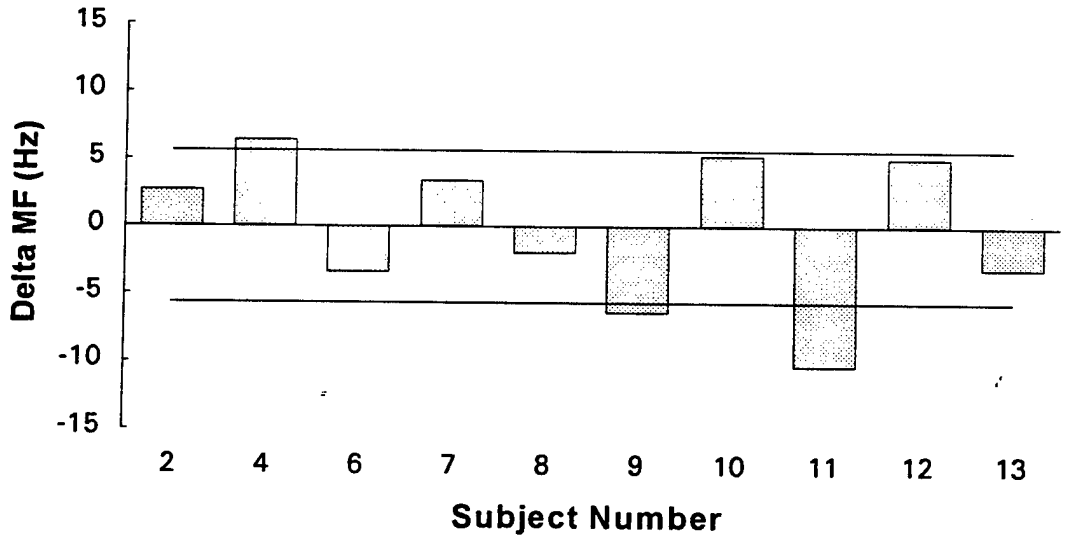

Figure F-24. Change in mean frequency (delta MF) at right thoracic muscle site (T9) after exposure to motion during experiment LT3. Lines represent ± 1 standard deviation.

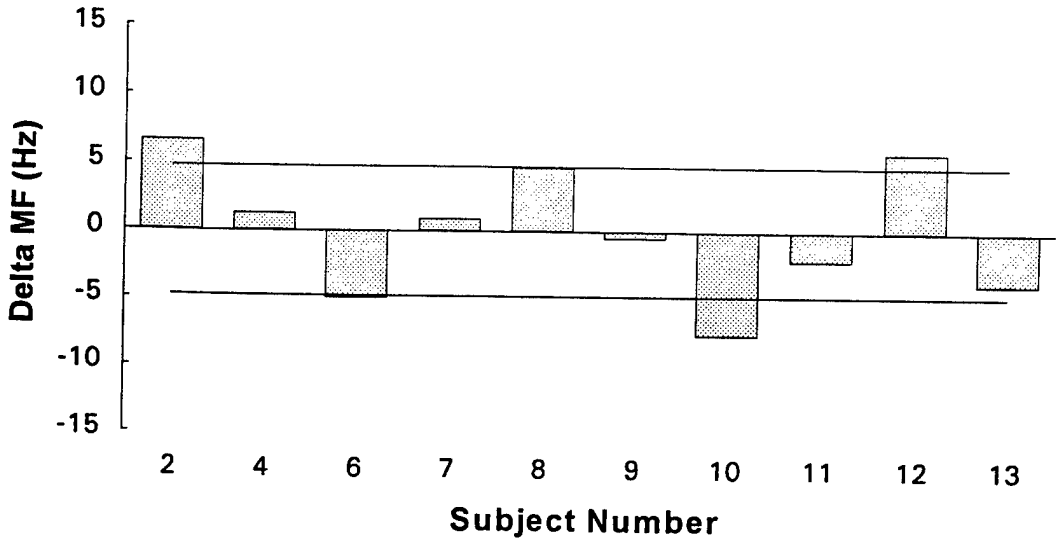

Figure F-25. Change in mean frequency (delta MF) at left thoracic muscle site (T9) after exposure to motion during experiment LT3. Lines represent ± 1 standard deviation.

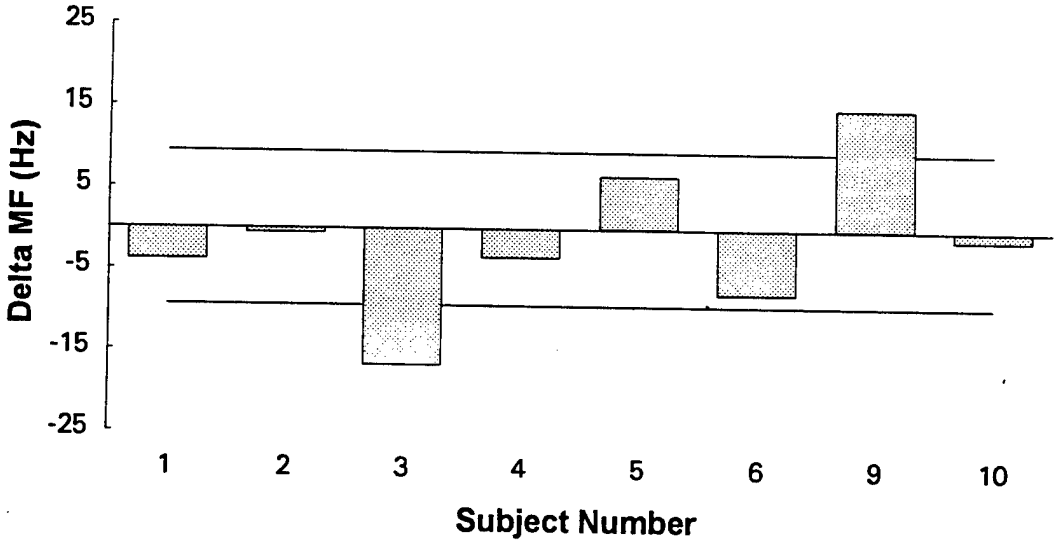

Figure F-26. Change in mean frequency (delta MF) at right lumbar muscle site (L3) after exposure to motion on day 1 of experiment LT4. Lines represent ± 1 standard deviation.

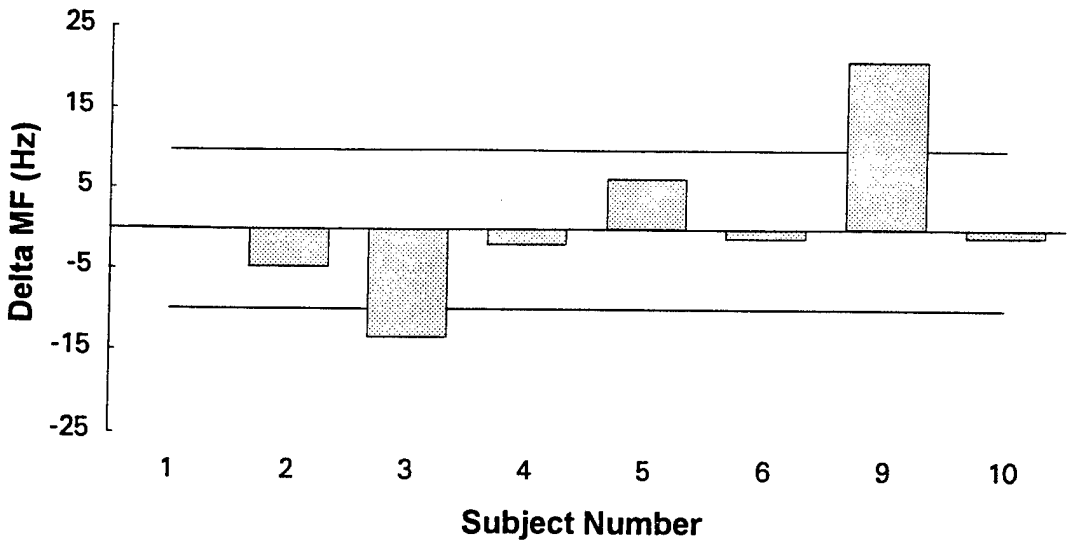

Figure F-27. Change in mean frequency (delta MF) at left lumbar muscle site (L3) after exposure to motion on day 1 of experiment LT4. Lines represent ± 1 standard deviation.

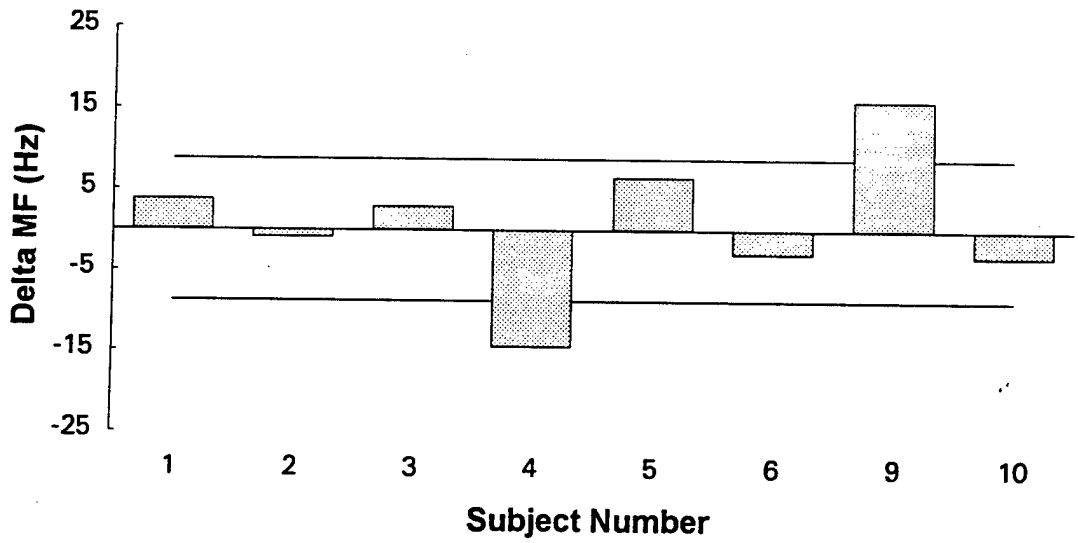

Figure F-28. Change in mean frequency (delta MF) at right lumbar muscle site (L3) after exposure to motion on day 3 of experiment LT4. Lines represent ± 1 standard deviation.

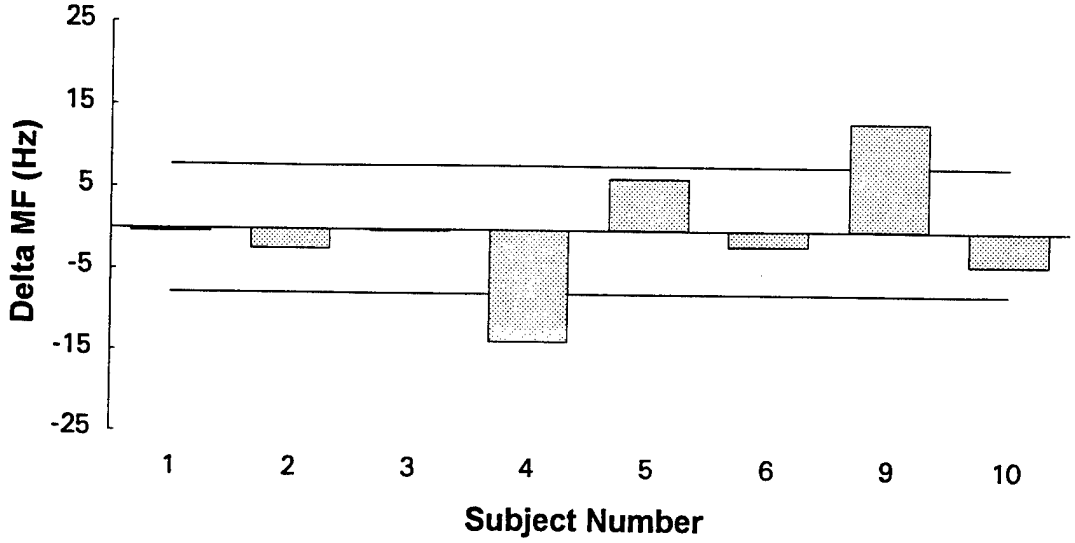

Figure F-29. Change in mean frequency (delta MF) at left lumbar muscle site (L3) after exposure to motion on day 3 of experiment LT4. Lines represent ± 1 standard deviation.

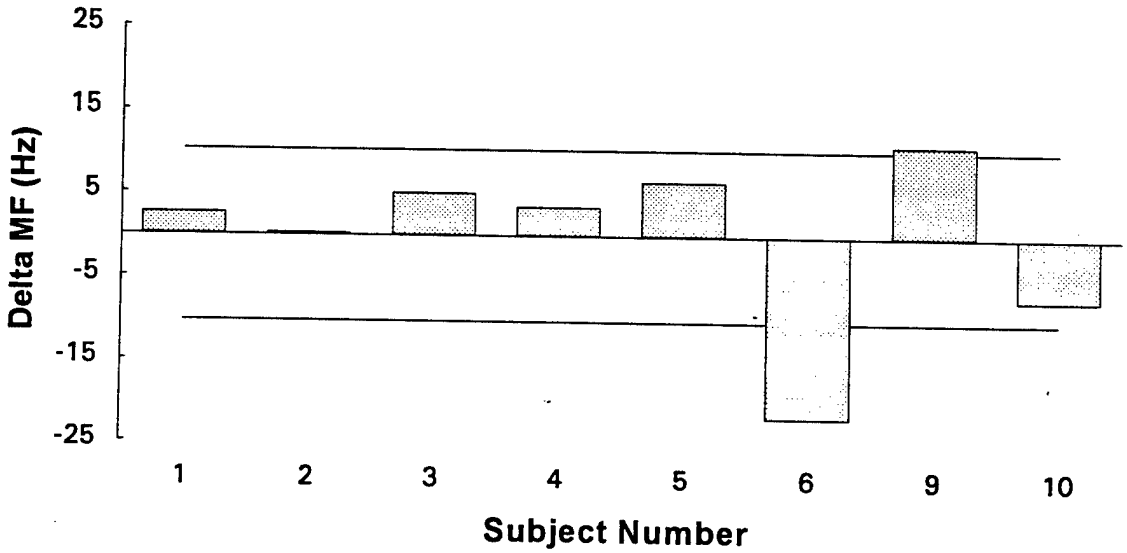

Figure F-30. Change in mean frequency (delta MF) at right lumbar muscle site (L3) after exposure to motion on day 5 of experiment LT4. Lines represent ± 1 standard deviation.

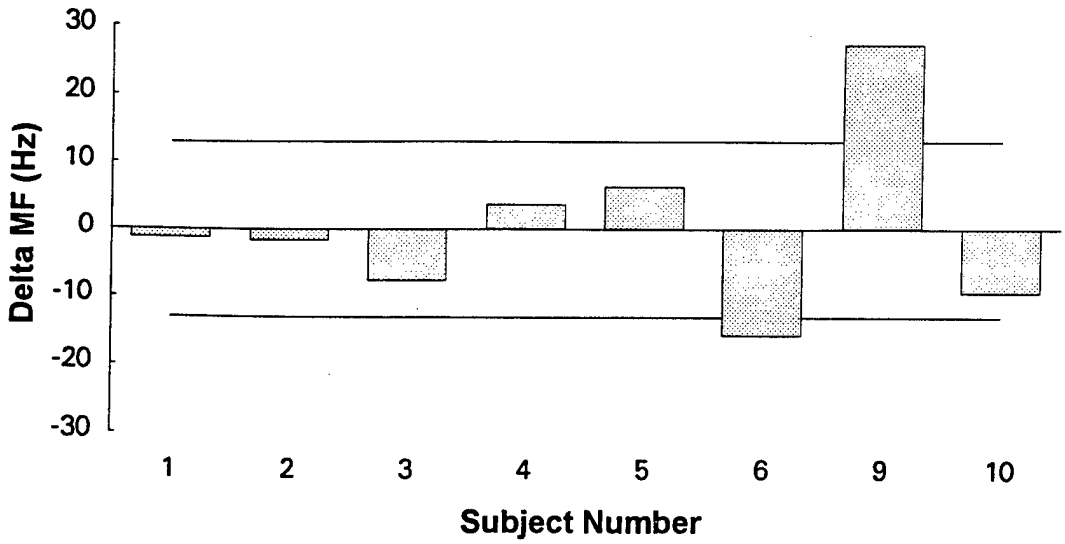

Figure F-31. Change in mean frequency (delta MF) at left lumbar muscle site (L3) after exposure to motion on day 5 of experiment LT4. Lines represent ± 1 standard deviation.

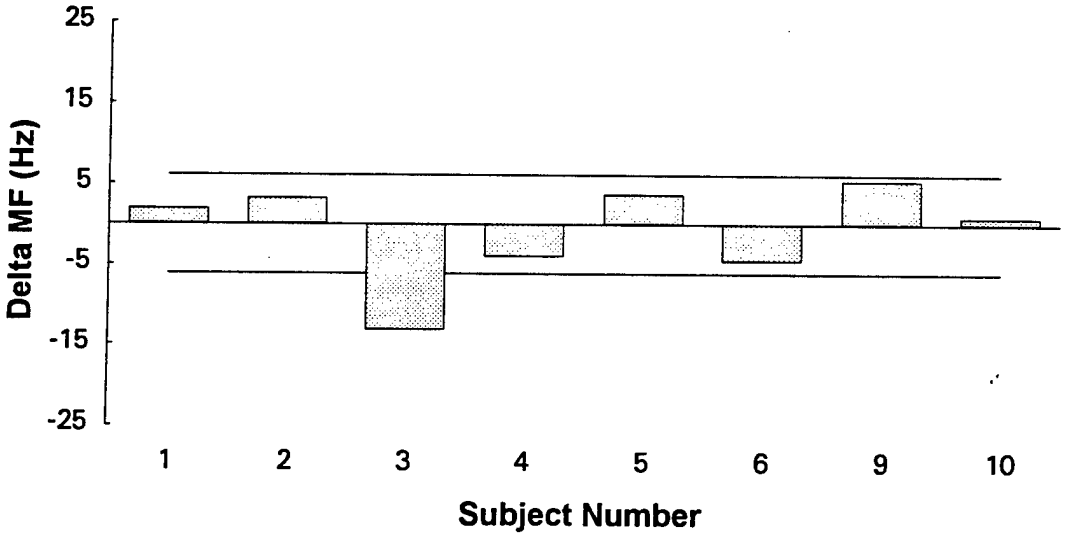

Figure F-32. Change in mean frequency (delta MF) at right thoracic muscle site (T9) after exposure to motion on day 1 of experiment LT4. Lines represent ± 1 standard deviation.

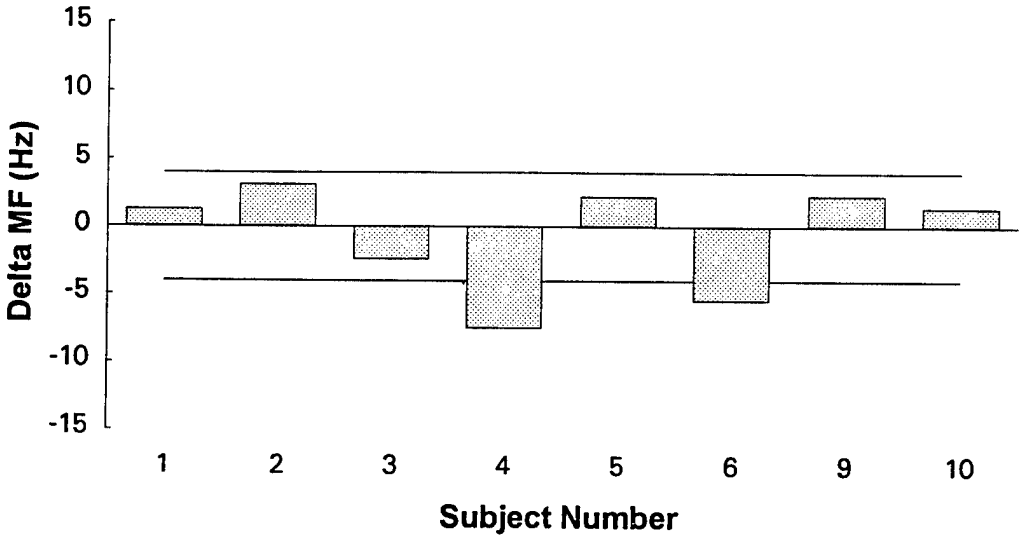

Figure F-33. Change in mean frequency (delta MF) at left thoracic muscle site (T9) after exposure to motion on day 1 of experiment LT4. Lines represent ± 1 standard deviation.

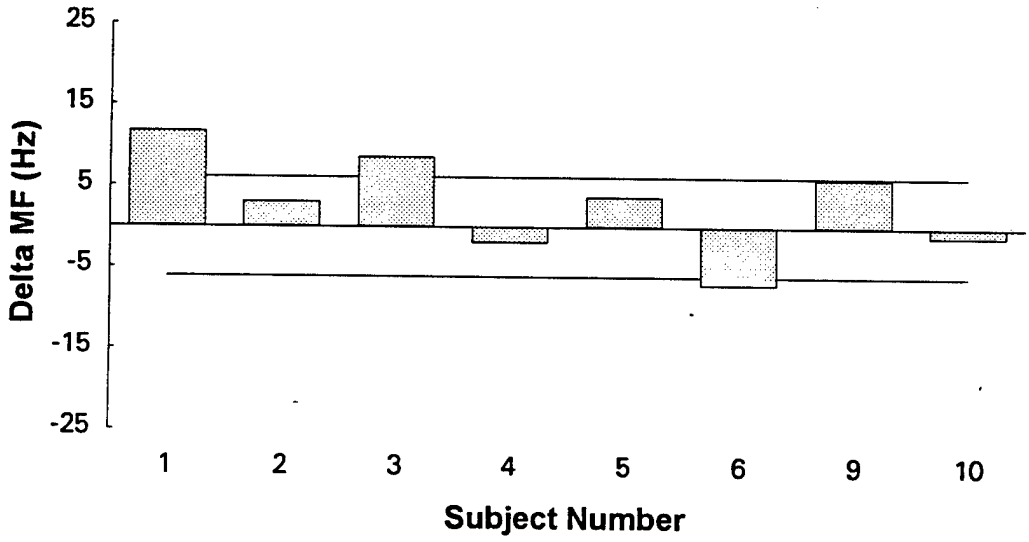

Figure F-34. Change in mean frequency (delta MF) at right thoracic muscle site (T9) after exposure to motion on day 3 of experiment LT4. Lines represent ± 1 standard deviation.

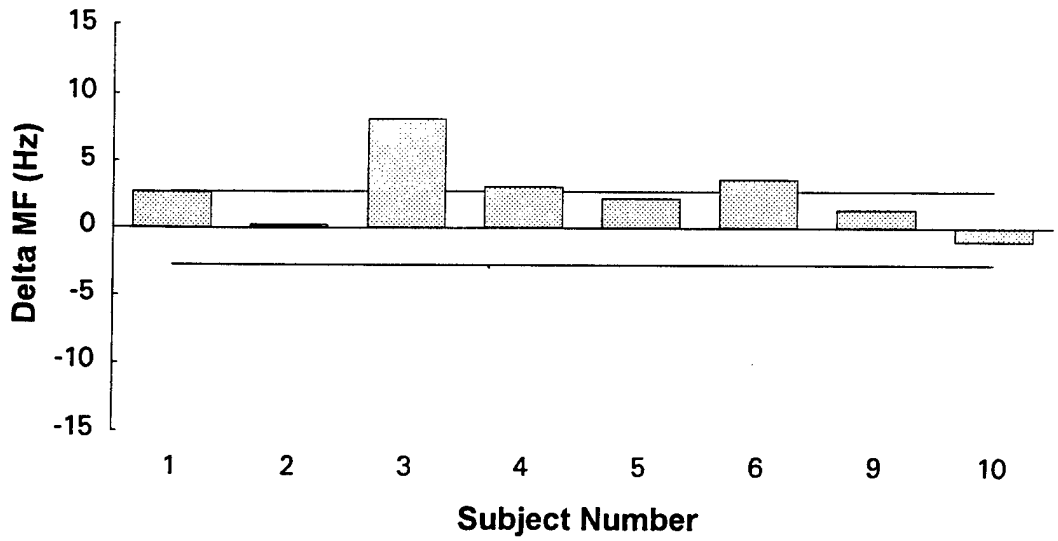

Figure F-35. Change in mean frequency (delta MF) at left thoracic muscle site (T9) after exposure to motion on day 3 of experiment LT4. Lines represent ± 1 standard deviation.

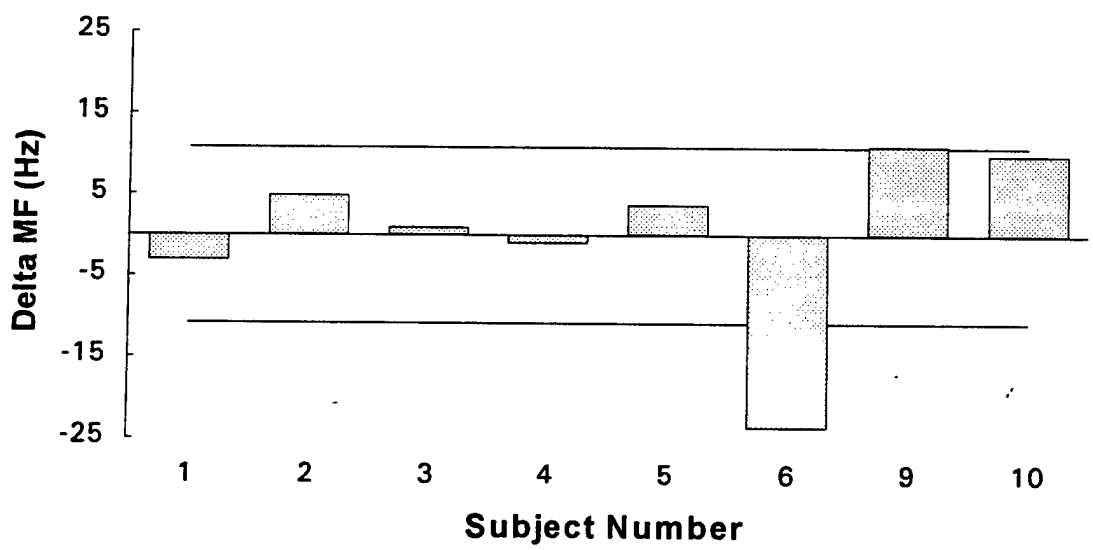

Figure F-36. Change in mean frequency (delta MF) at right thoracic muscle site (T9) after exposure to motion on day 5 of experiment LT4. Lines represent ± 1 standard deviation.

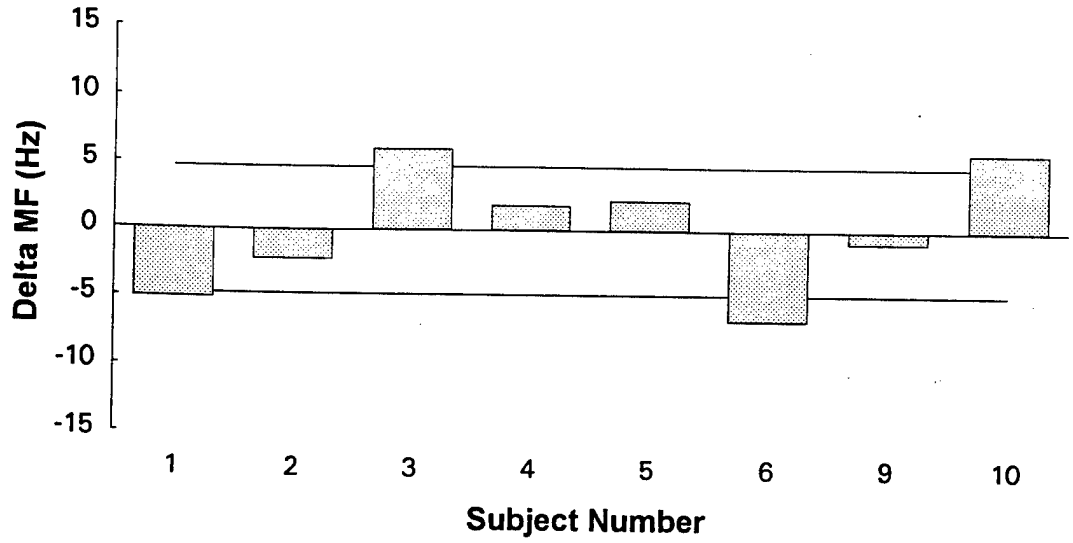

Figure F-37. Change in mean frequency (delta MF) at left thoracic muscle site (T9) after exposure to motion on day 5 of experiment LT4. Lines represent ± 1 standard deviation.

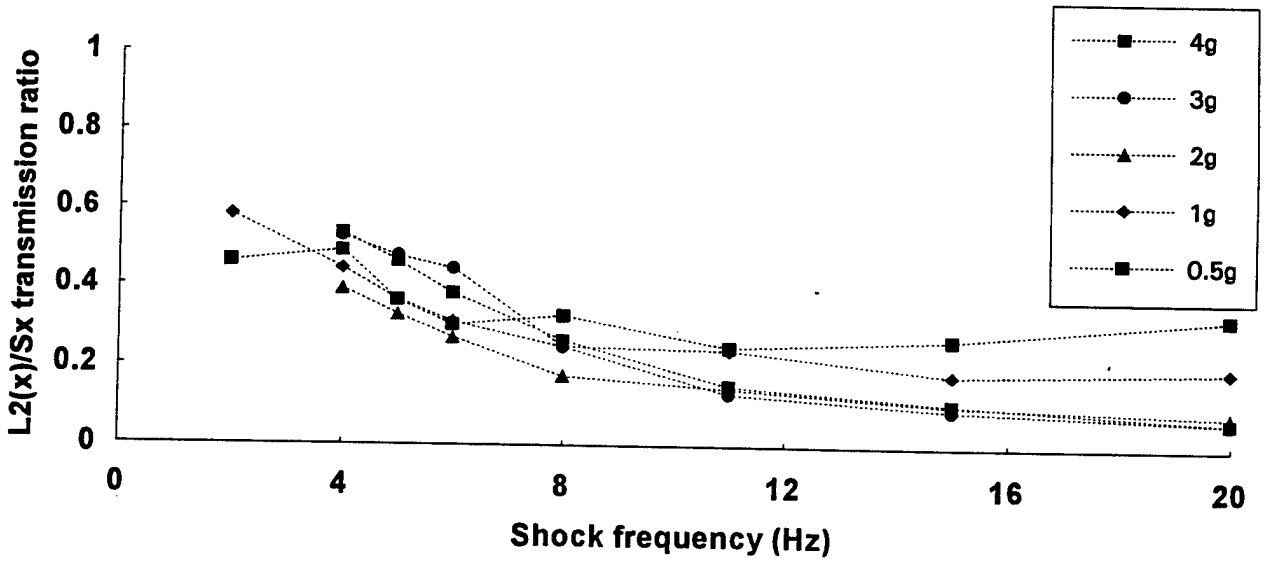

Figure F-38. Spine (L2) x acceleration to seat x acceleration for 0.5, 1, 2, 3, 4 g shocks.

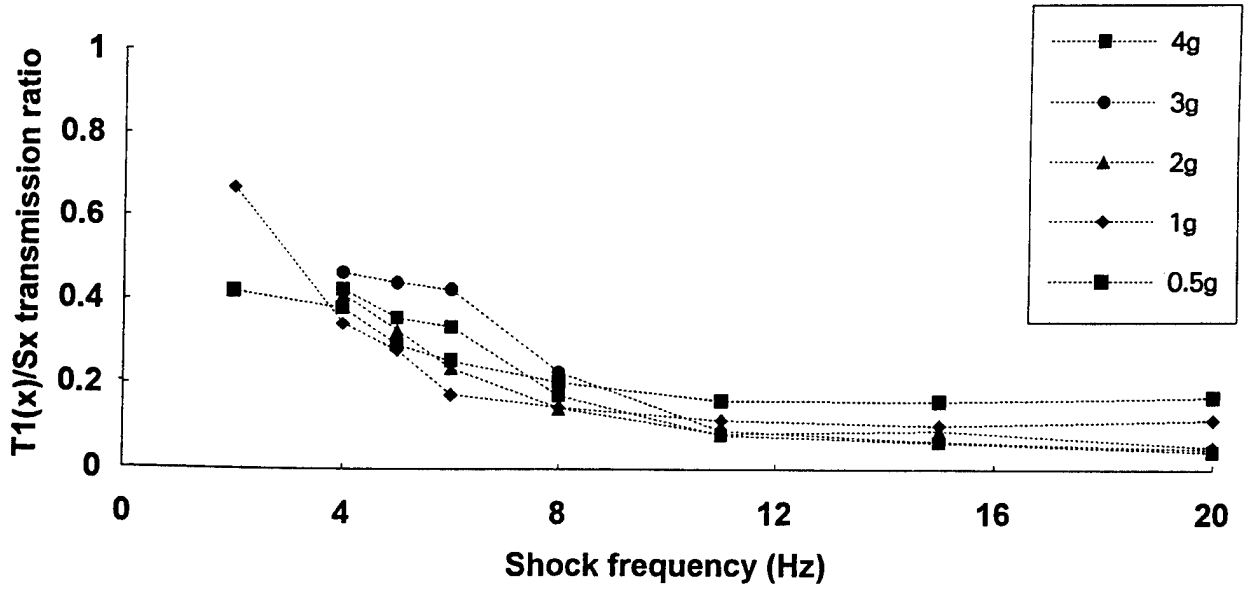

Figure F-39. Spine (T1) x acceleration to seat x acceleration for 0.5, 1, 2, 3, 4 g shocks.

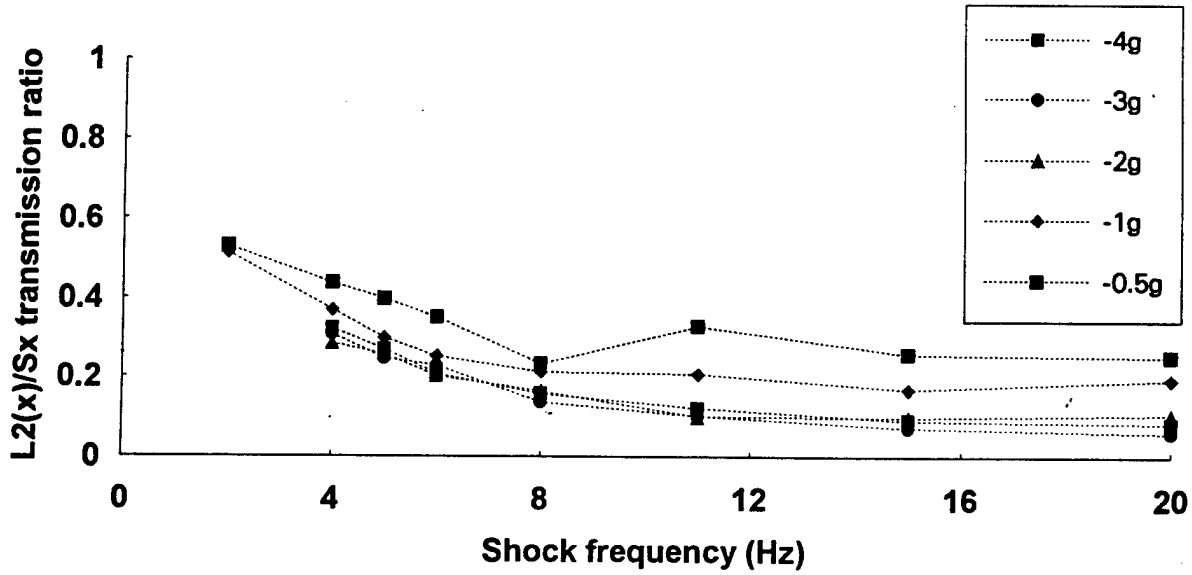

Figure F-40. Spine (L2) x acceleration to seat x acceleration for -0.5, -1, -2, -3, -4 g shocks.

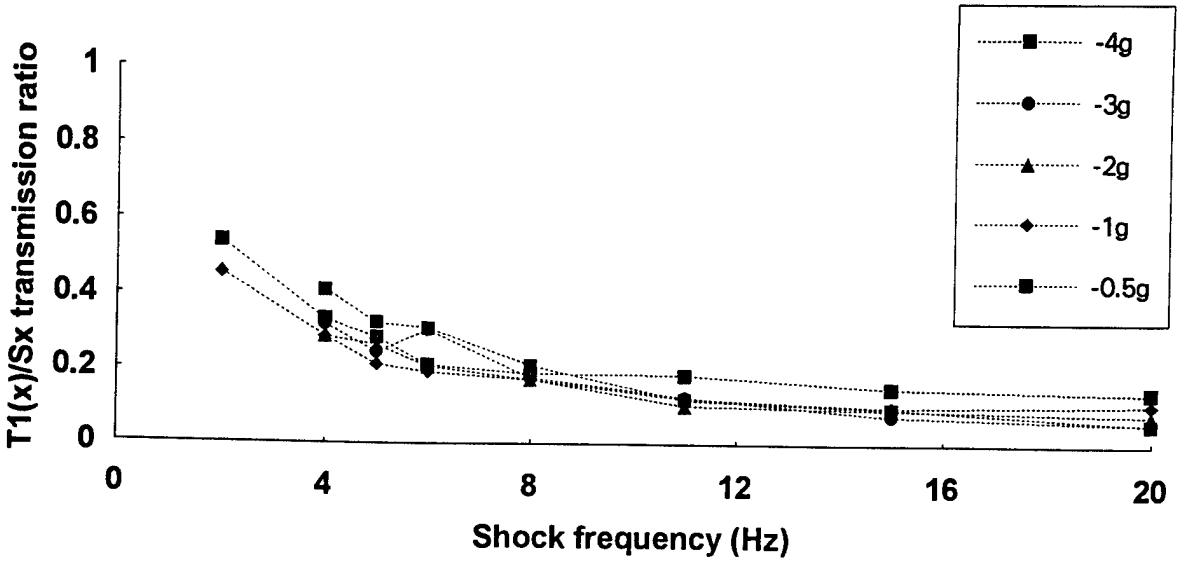

Figure F-41. Spine (T1) x acceleration to seat x acceleration for -0.5, -1, -2, -3, -4 g shocks.

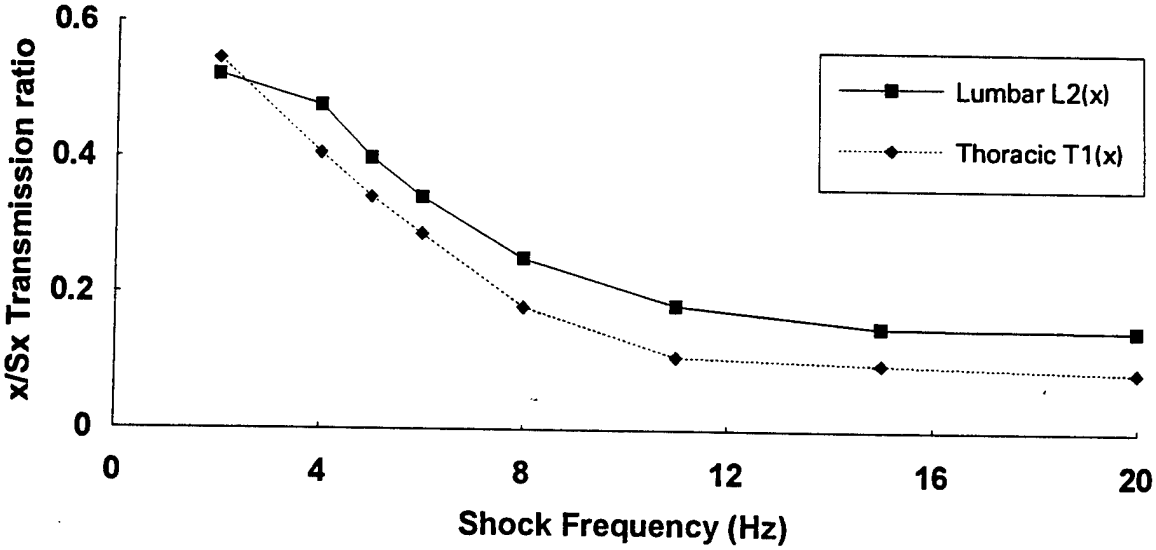

Figure F-42. Comparison of the mean transmission ratios of all shock amplitudes measured at the lumbar (L2) and thoracic (T1) spine in response to positive x axis shocks.

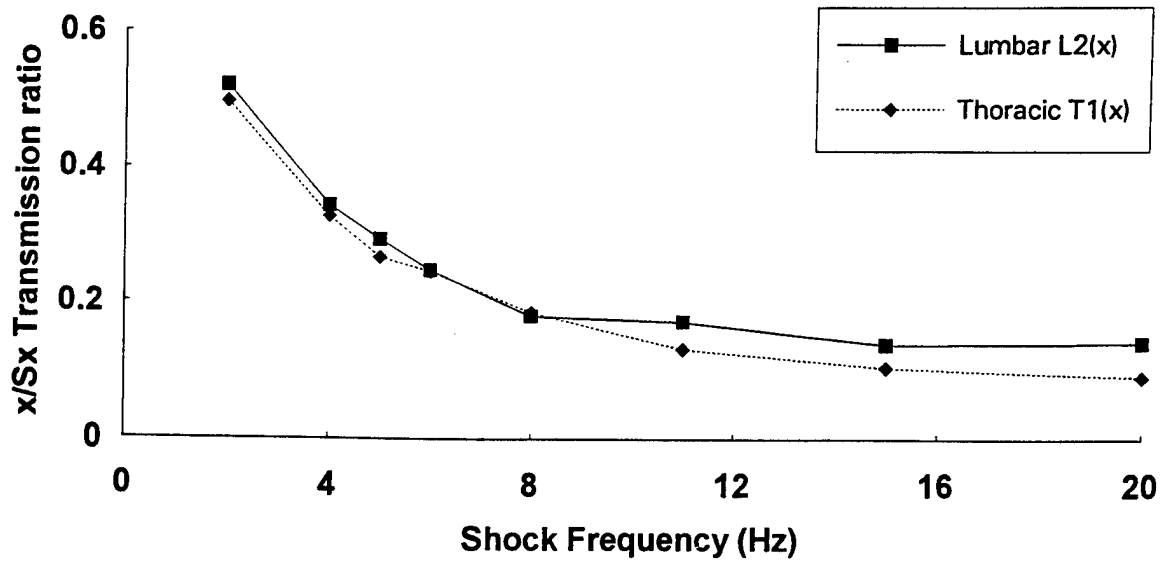

Figure F-43. Comparison of the mean transmission ratios of all shock amplitudes measured at the lumbar (L2) and thoracic (T1) spine in response to negative x axis shocks.

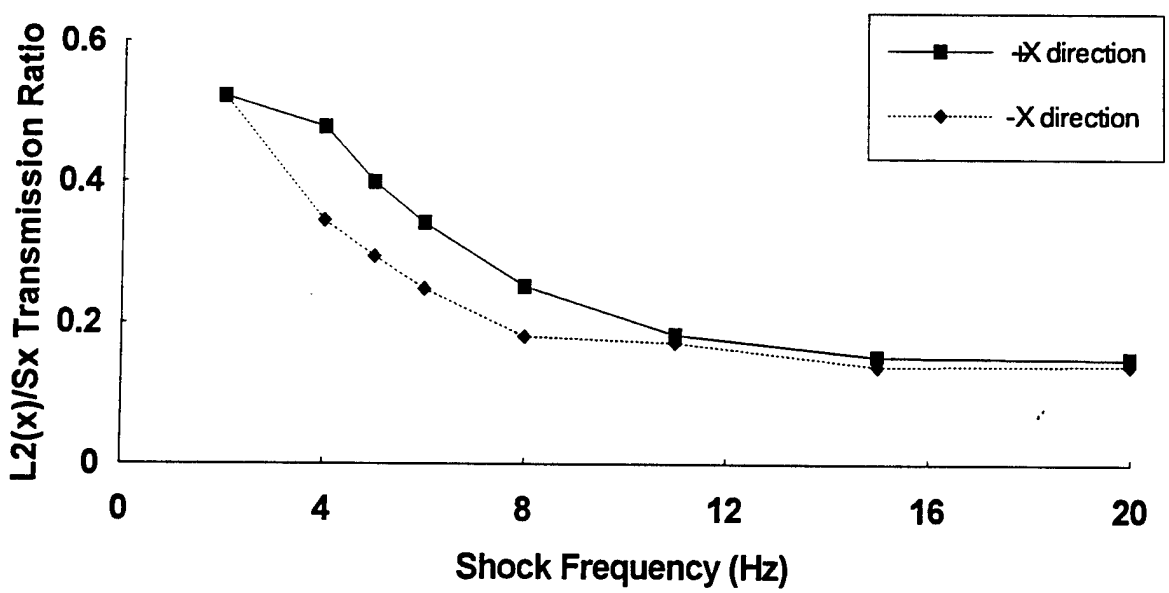

Figure F-44. Comparison of the mean transmission ratios of all shock amplitudes measured at the lumbar (L2) spine in response to positive and negative x axis shocks.

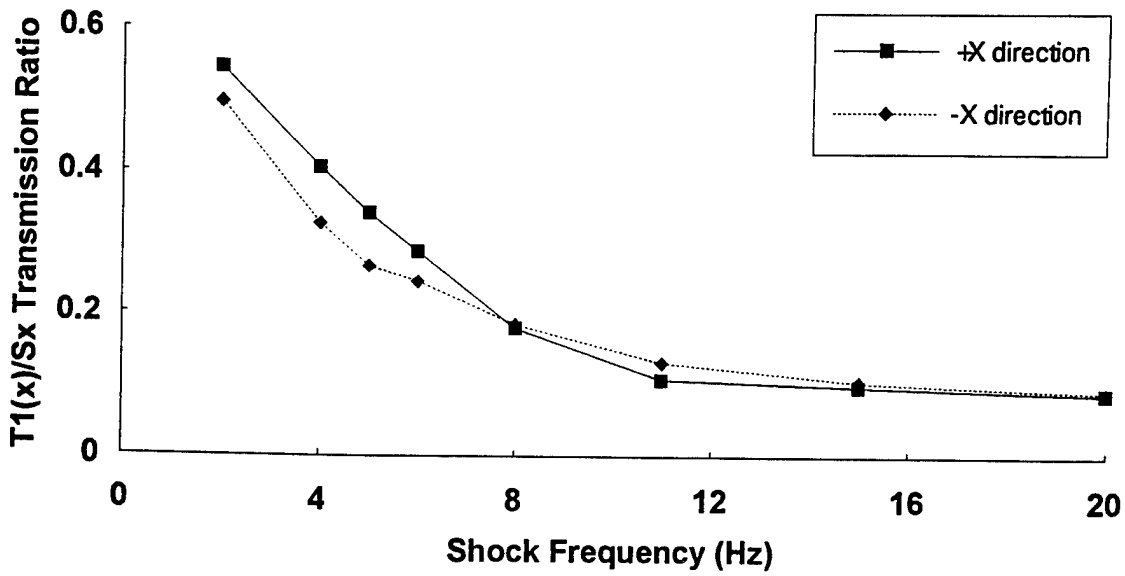

Figure F-45. Comparison of the mean transmission ratios of all shock amplitudes measured at the lumbar (T1) spine in response to positive and negative x axis shocks.

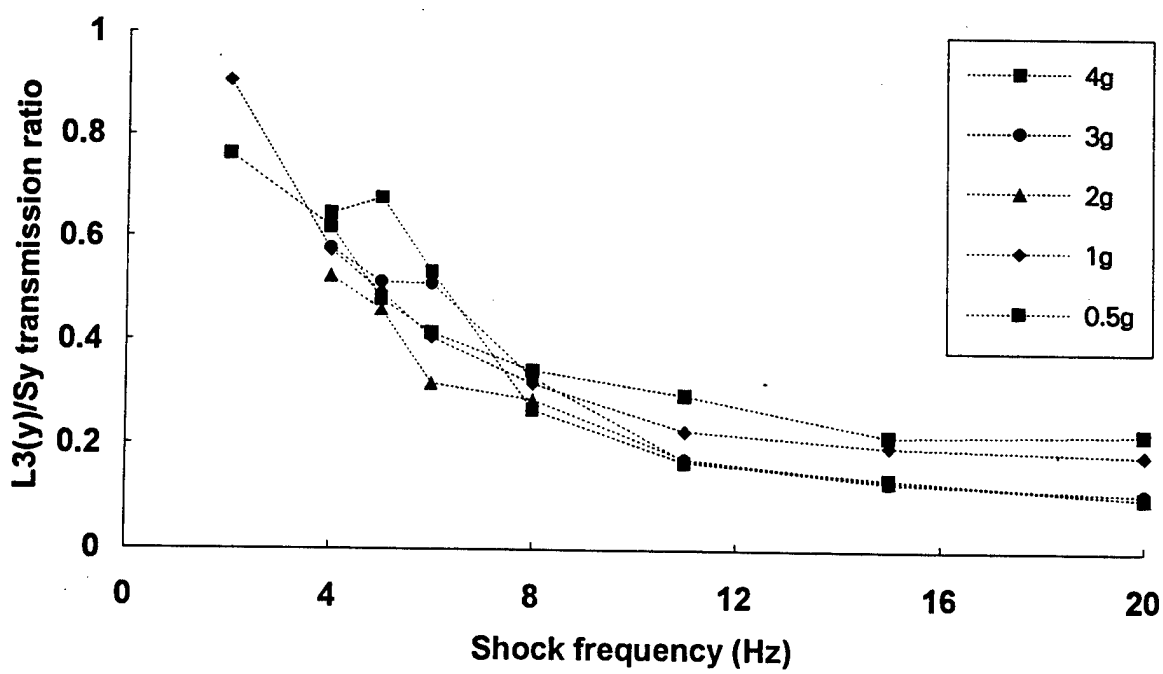

Figure F-46. Spine (L3) y acceleration to seat y acceleration for 0.5, 1, 2, 3, 4 g shocks.

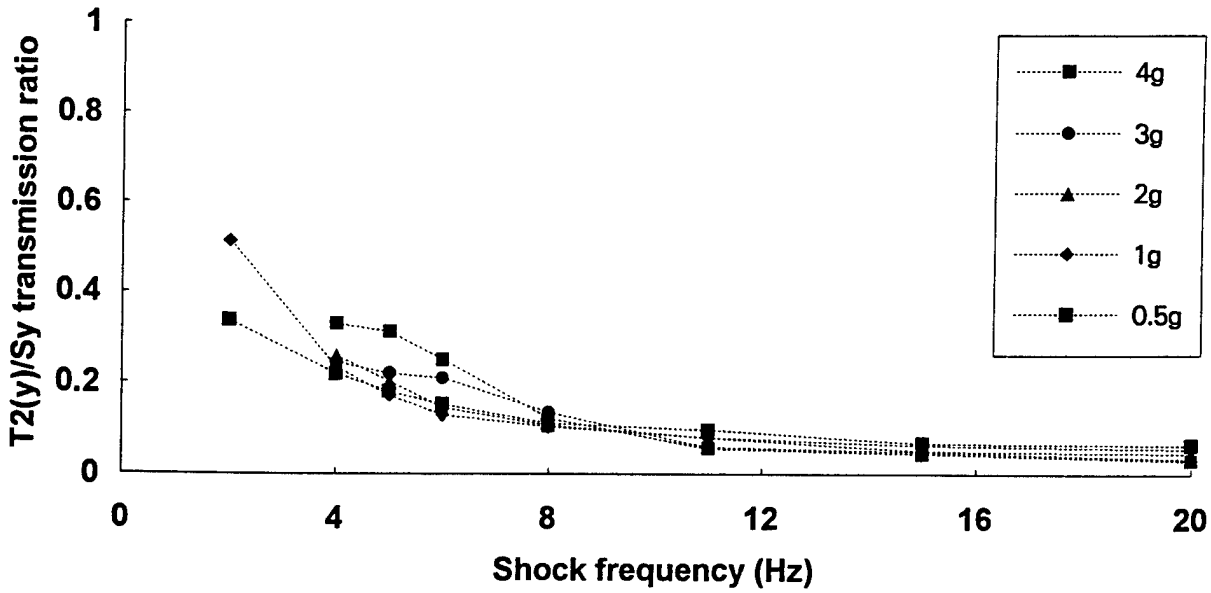

Figure F-47. Spine (T2) negative y acceleration to seat y acceleration for -0.5, -1, -2, -3, -4 g shocks.

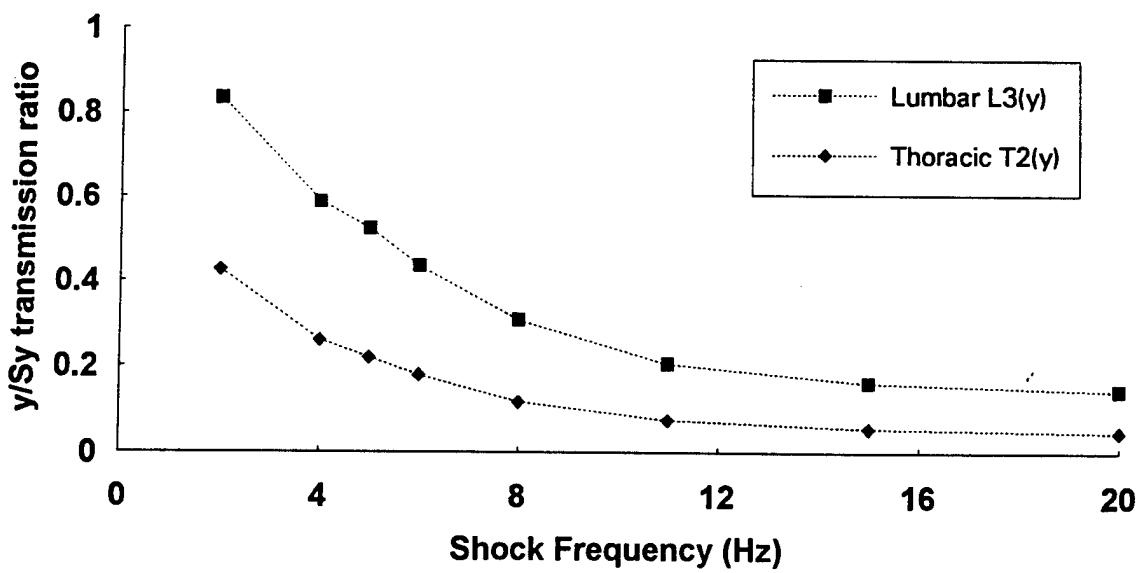

Figure F-48. Comparison of the mean transmission ratios of all shock amplitudes measured at the lumbar (L3) and thoracic (T2) spine in response to positive y axis shocks.

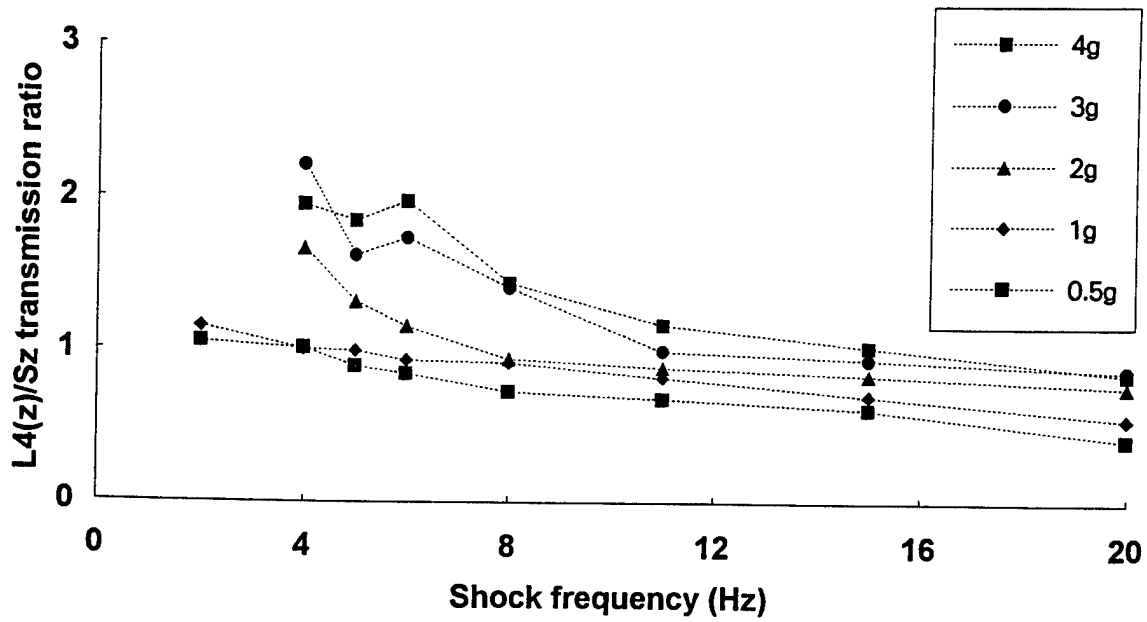

Figure F-49. Spine (L4) z acceleration to seat z acceleration for 0.5, 1, 2, 3, 4 g shocks.

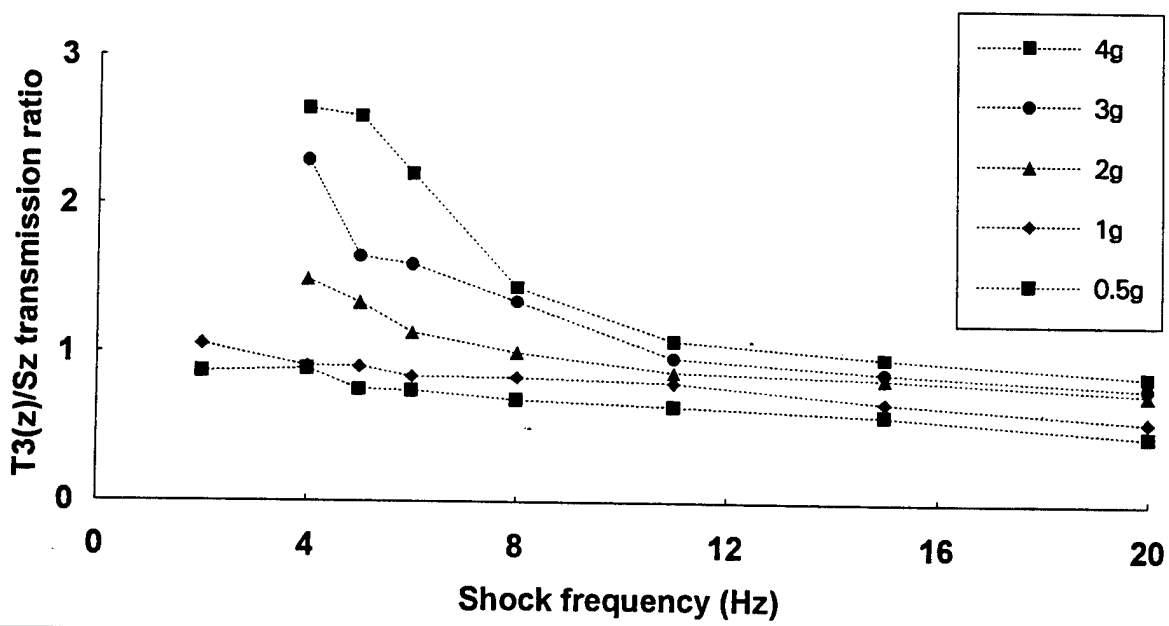

Figure F-50. Spine (T3) z acceleration to seat z acceleration for 0.5, 1, 2, 3, 4 g shocks.

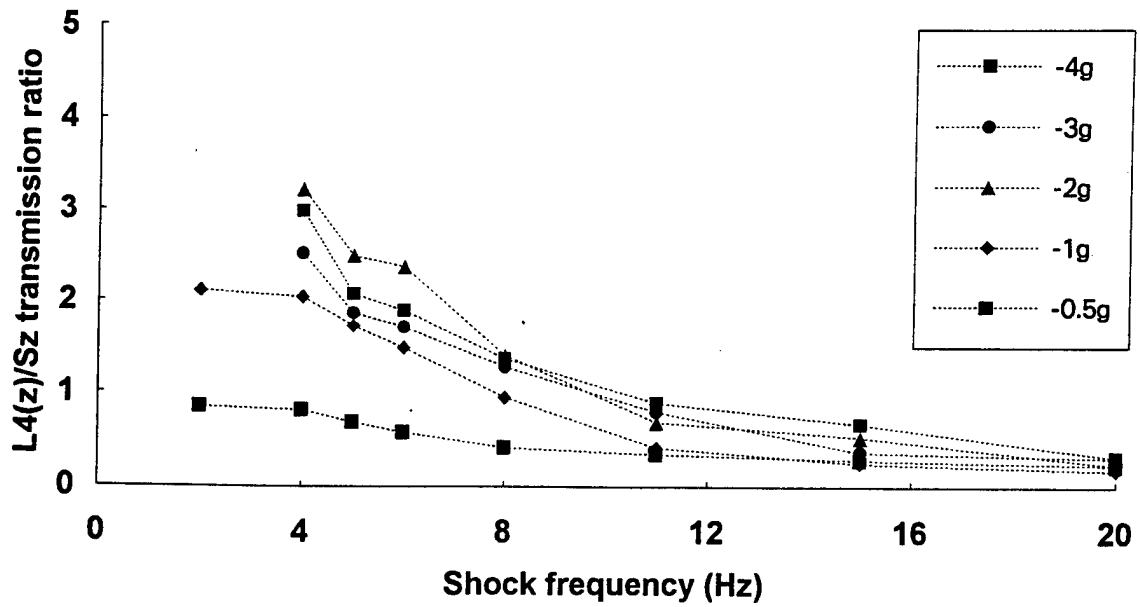

Figure F-51. Spine (L4) positive z acceleration to seat z acceleration for -0.5, -1, -2, -3, -4 g shocks.

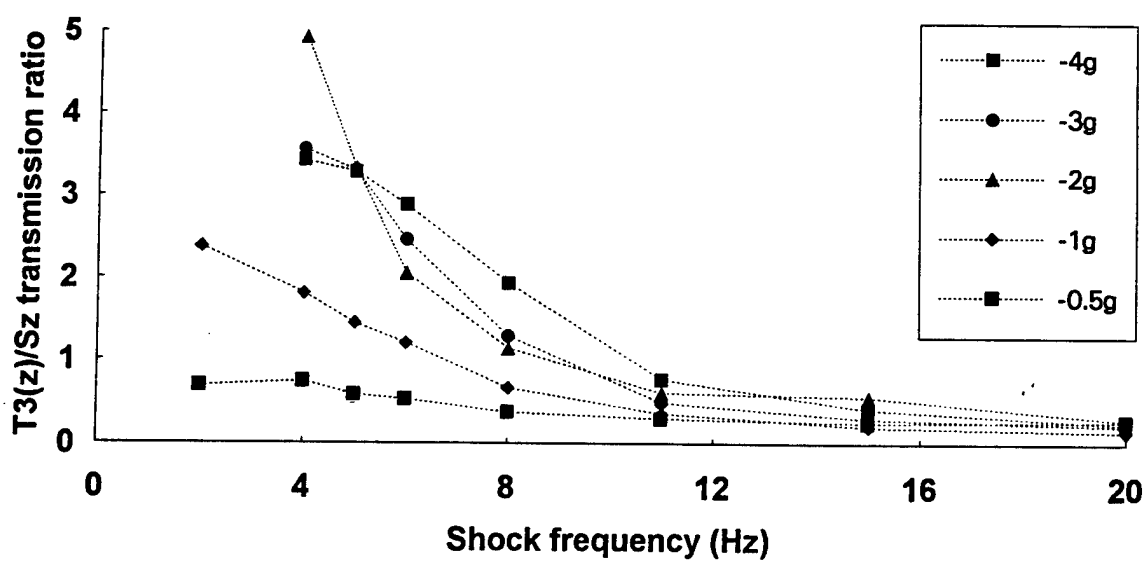

Figure F-52. Spine (T3) positive z acceleration to seat z acceleration for -0.5, -1, -2, -3, -4 g shocks.

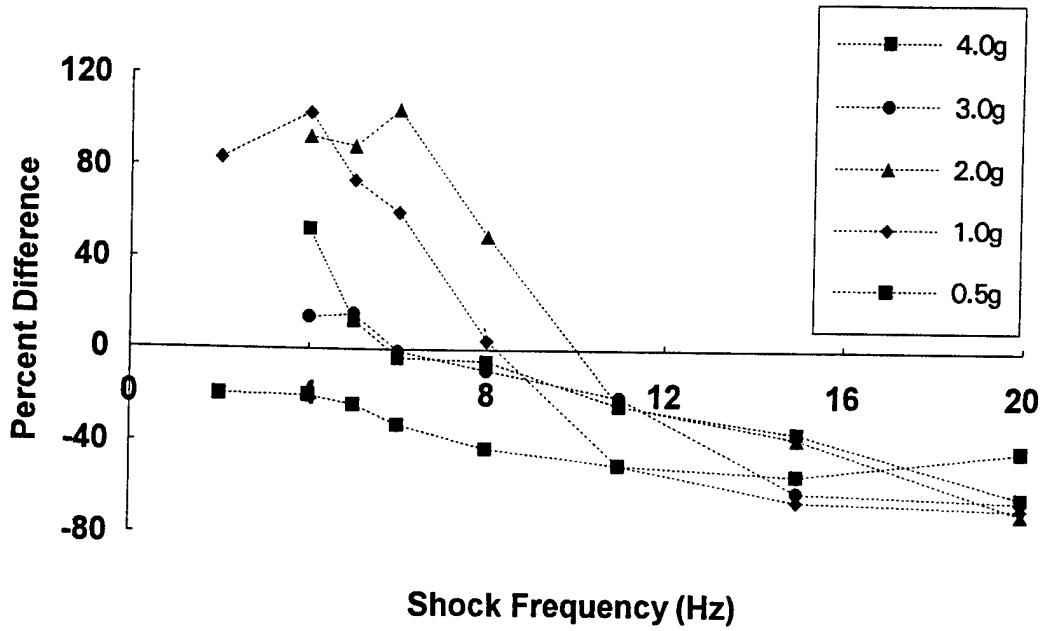

Figure F-53. Percent difference of spine (L4) z acceleration to seat z acceleration.

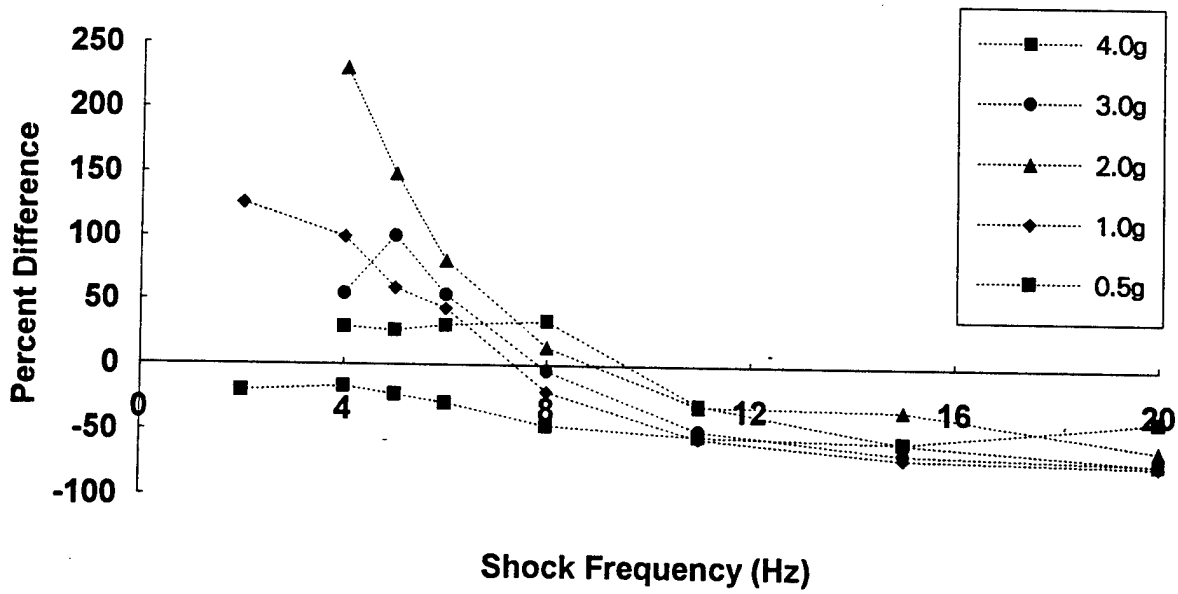

Figure F-54. Percent difference of spine (T3) z acceleration to seat z acceleration.

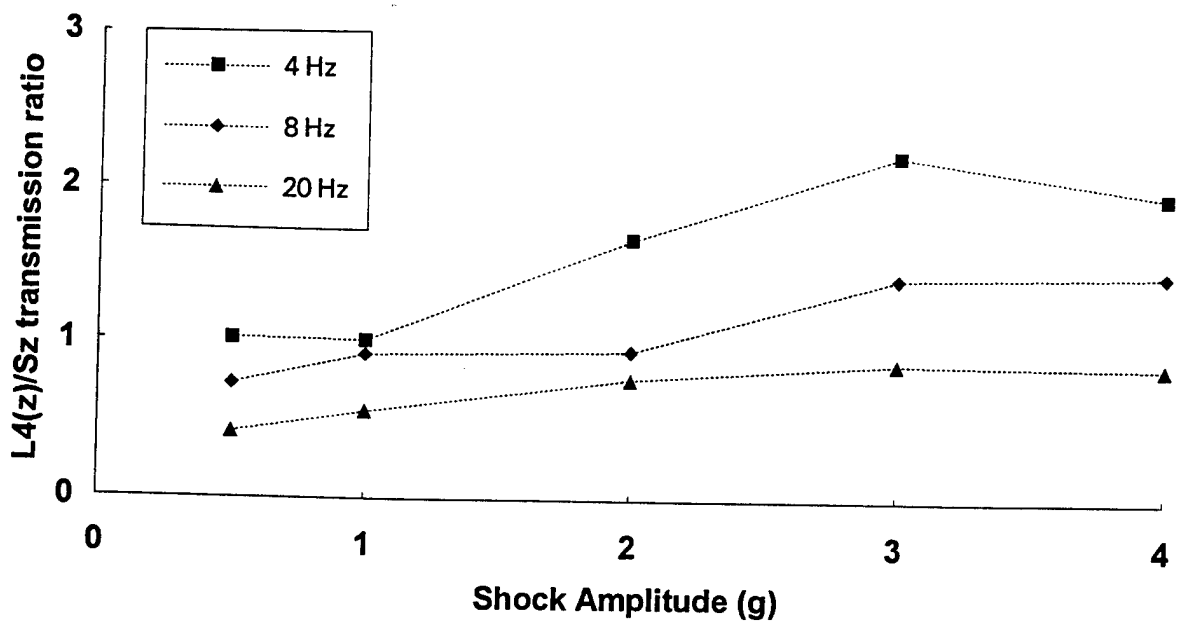

Figure F-55. Spine (L4) z acceleration to seat z positive acceleration for 4, 8 and 20 Hz shocks.

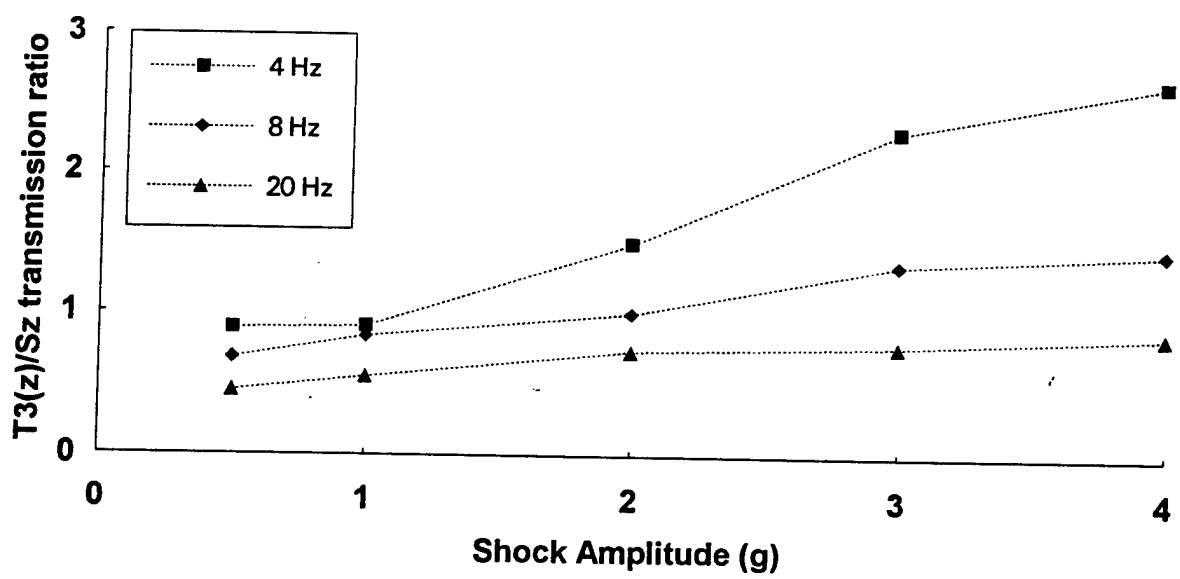

Figure F-56. Spine (T3) positive z acceleration to seat z positive acceleration for 4, 8 and 20 Hz shocks.

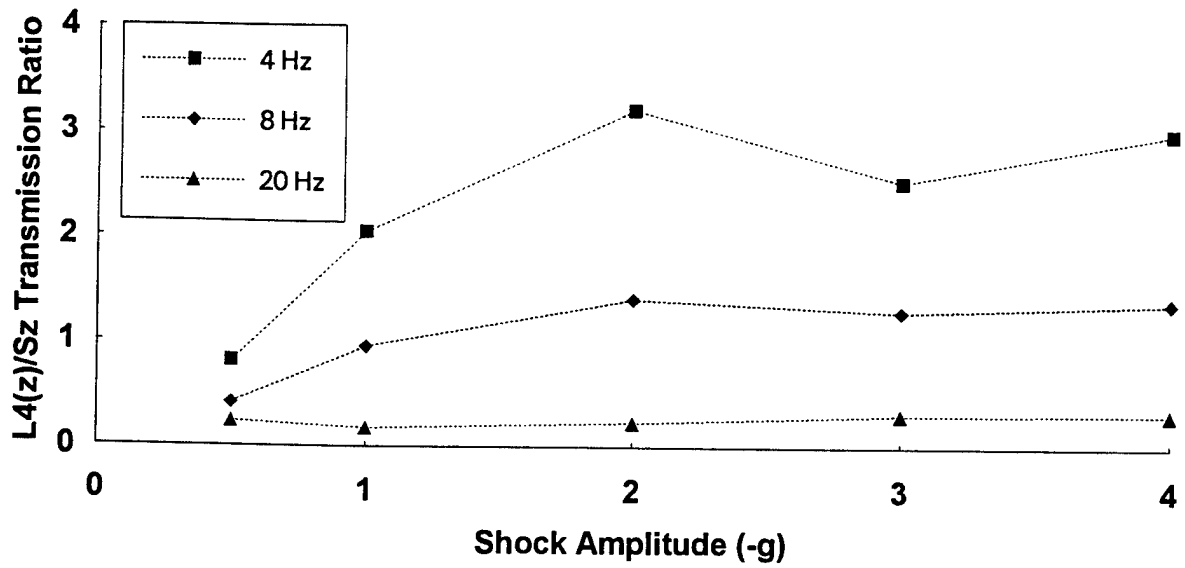

Figure F-57. Spine (L4) positive z acceleration to seat z negative acceleration for 4, 8 and 20 Hz shocks.

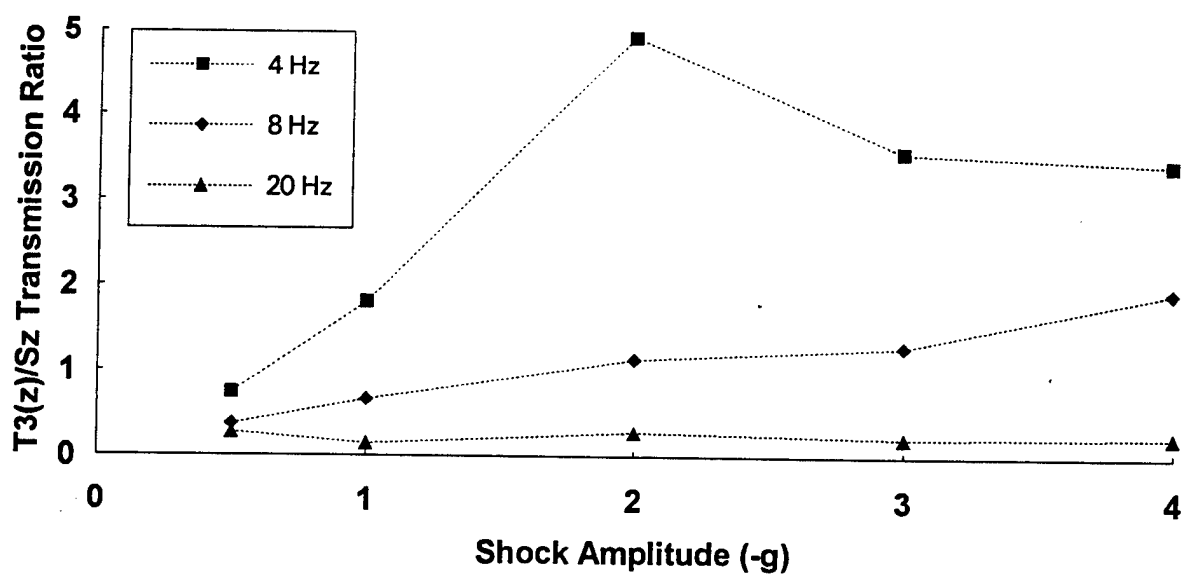

Figure F-58. Spine (T3) positive z acceleration to seat negative z acceleration for 4, 8 and 20 Hz shocks.

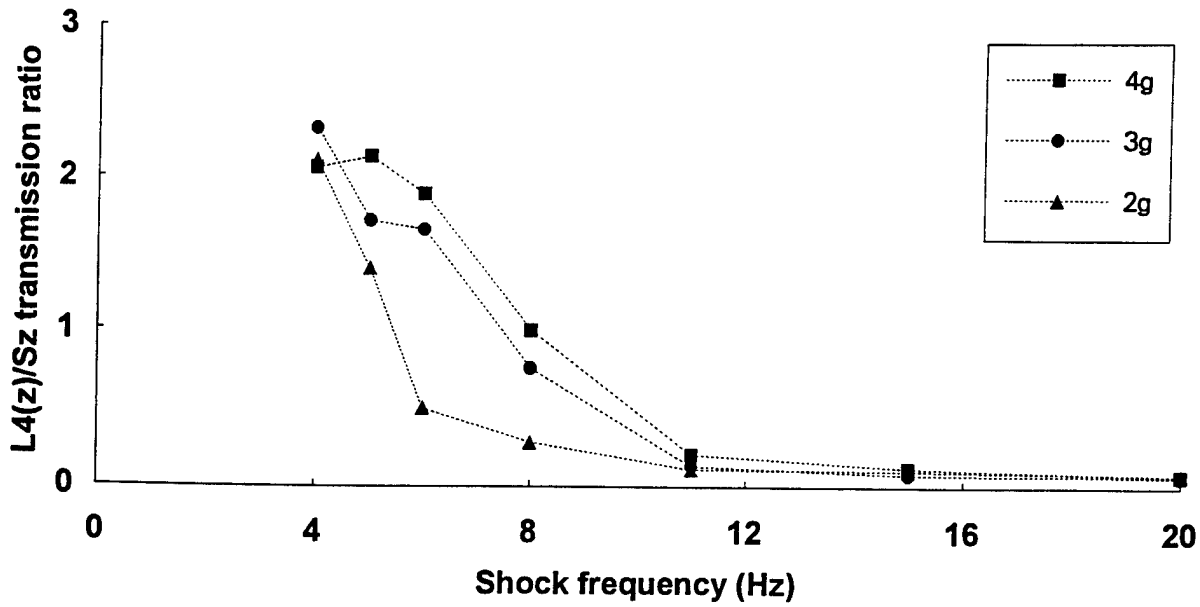

Figure F-59. Second peak of the spinal (L4) z acceleration to a single seat z acceleration for 2, 3, 4 g shocks.

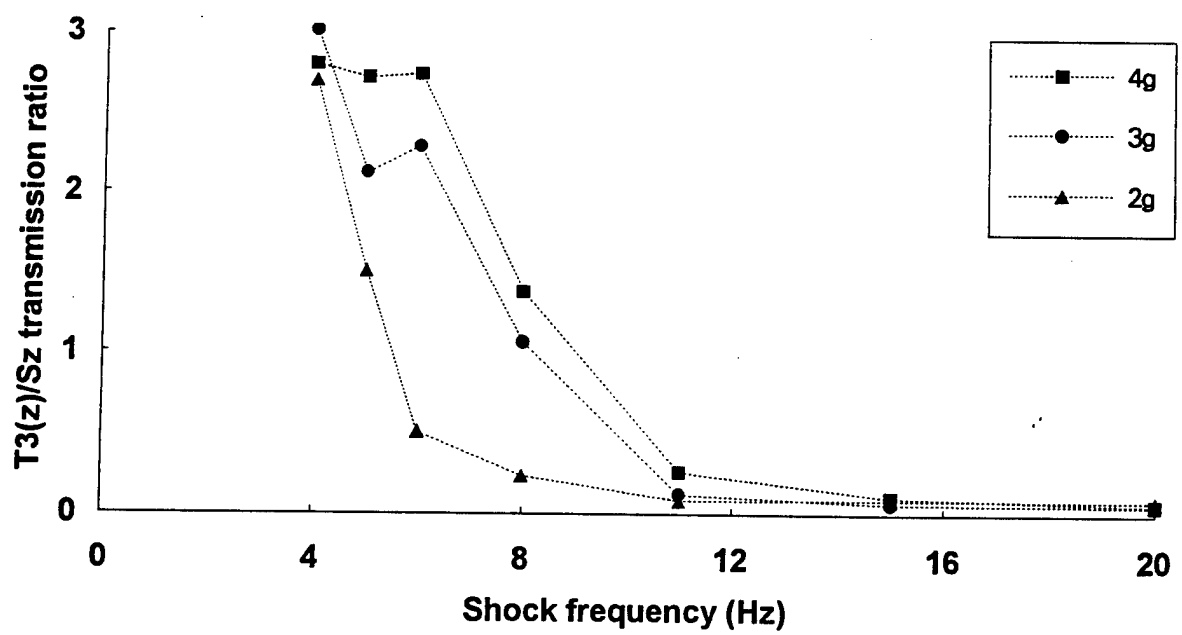

Figure F-60. Second peak of the spinal (T3) z acceleration to a single seat z acceleration for 2, 3, 4 g shocks.

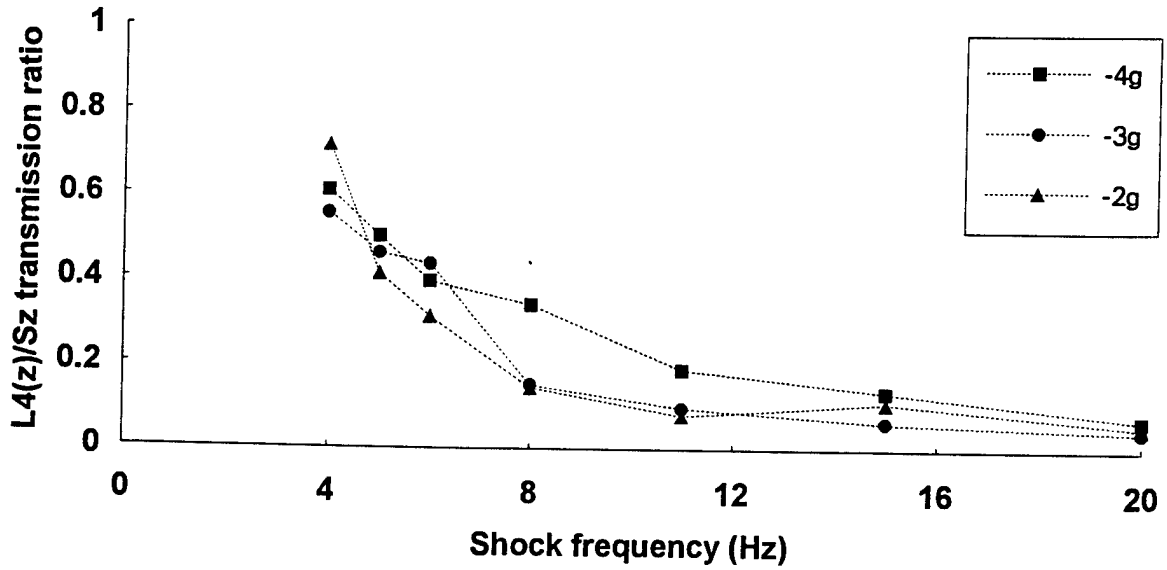

Figure F-61. Second peak of the spinal (L4) positive z acceleration to a single seat z acceleration for -2, -3, and -4 g shocks.

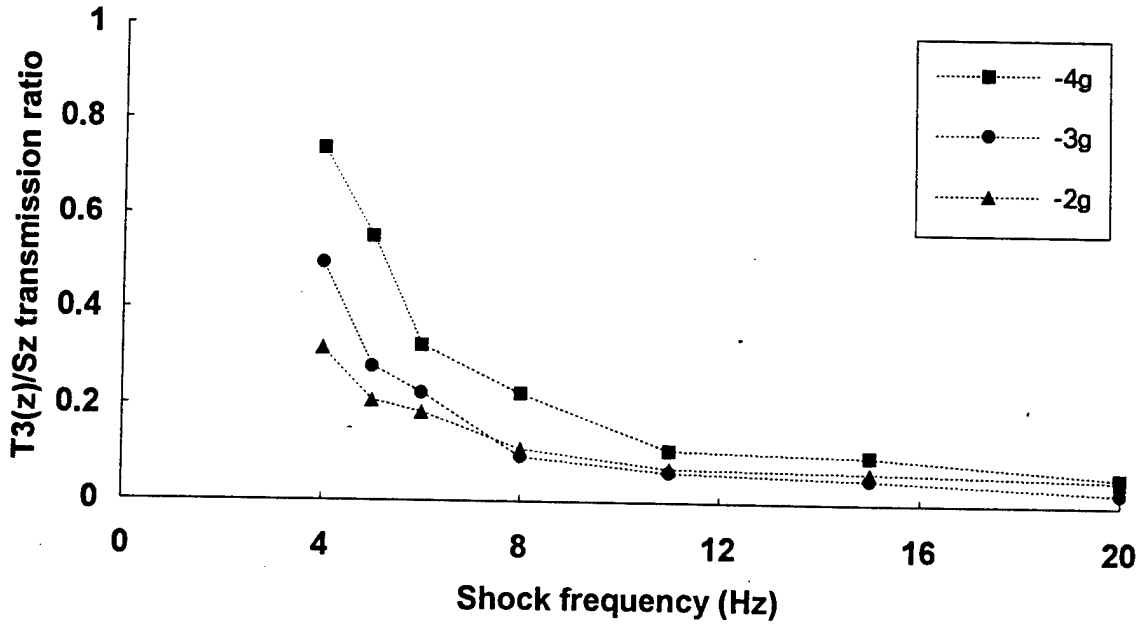

Figure F-62. Second peak of the spinal (T3) positive z acceleration to a single seat z acceleration for -2, -3, and -4 g shocks.

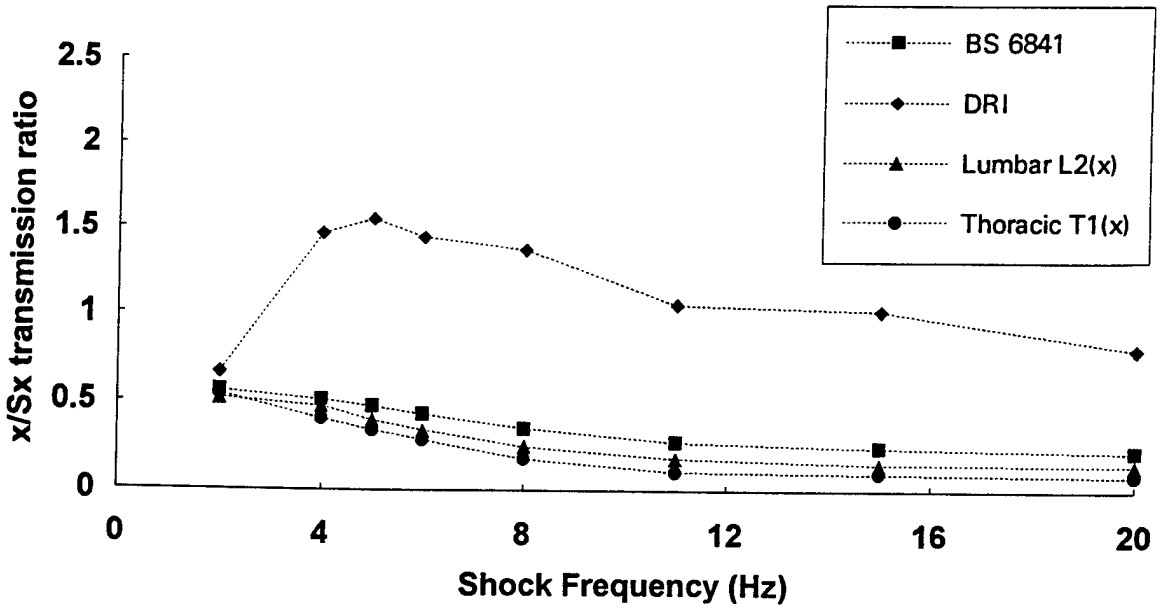

Figure F-63. Comparison of measured spine x transmission ratio (positive shocks) with predicted transmission ratios using BS 6841 filter and DRI models.

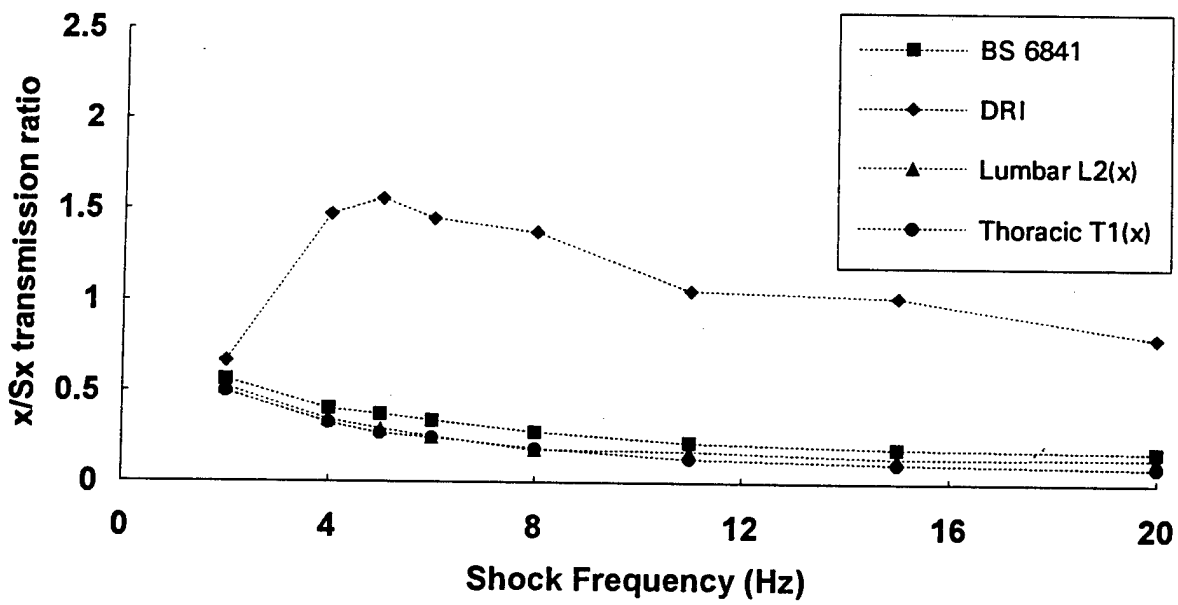

Figure F-64. Comparison of measured spine x transmission ratio (negative shocks) with predicted transmission ratios using BS 6841 filter and DRI model.

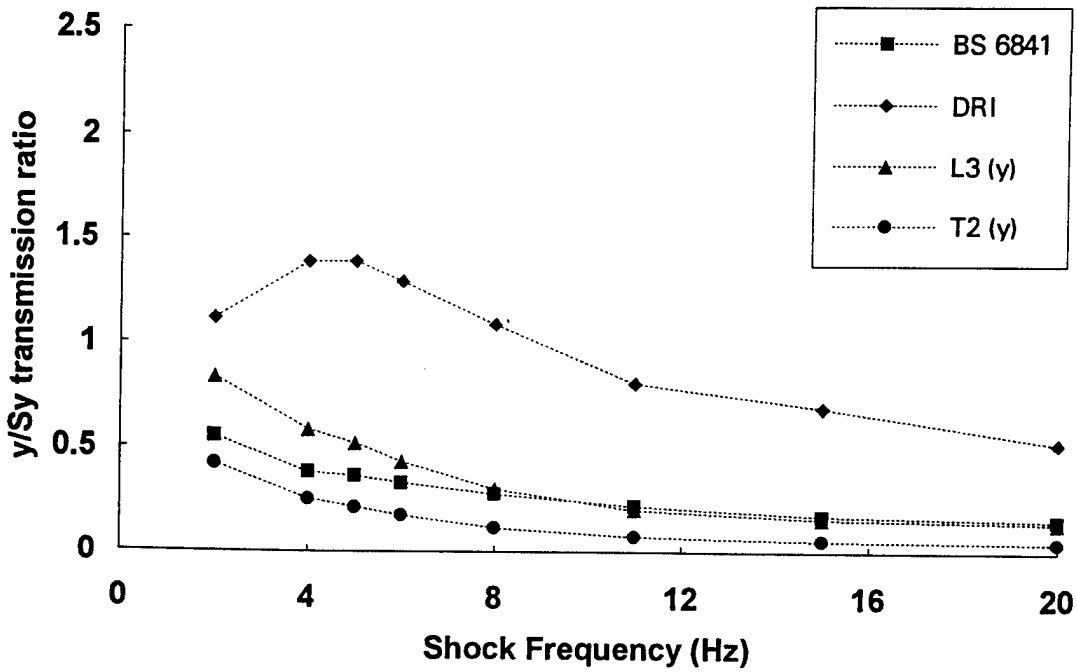

Figure F-65. Comparison of measured spine y transmission ratio (positive shocks) with predicted transmission ratios using BS 6841 filter and DRI model.

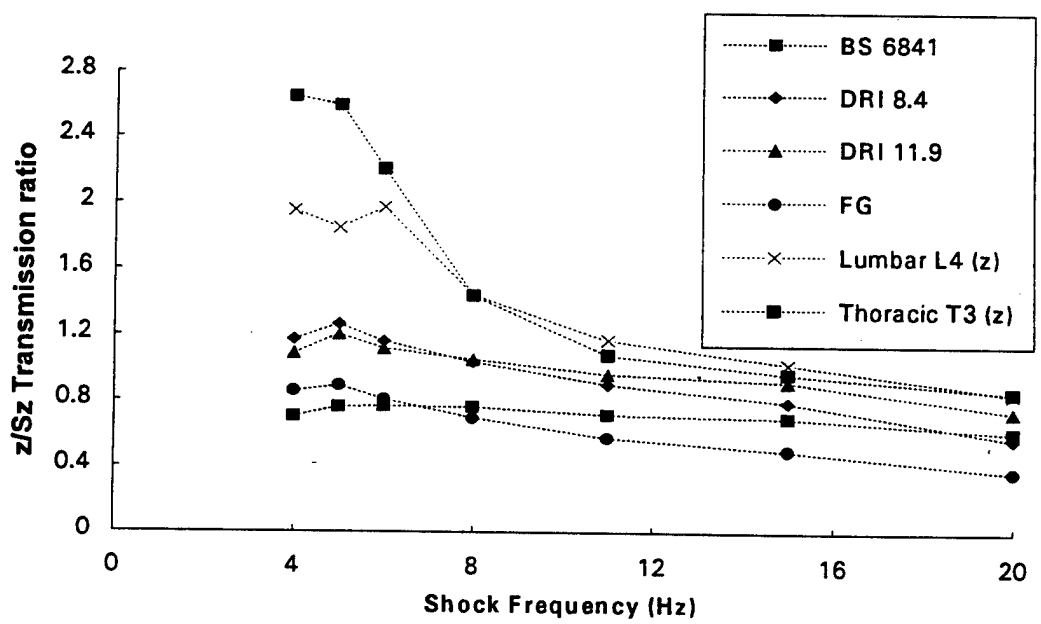

Figure F-66. Comparison of measured spine z transmission ratio (4g shocks) with predicted transmission ratios using BS 6841 filter, Fairley-Griffin (FG) model and DRI model.

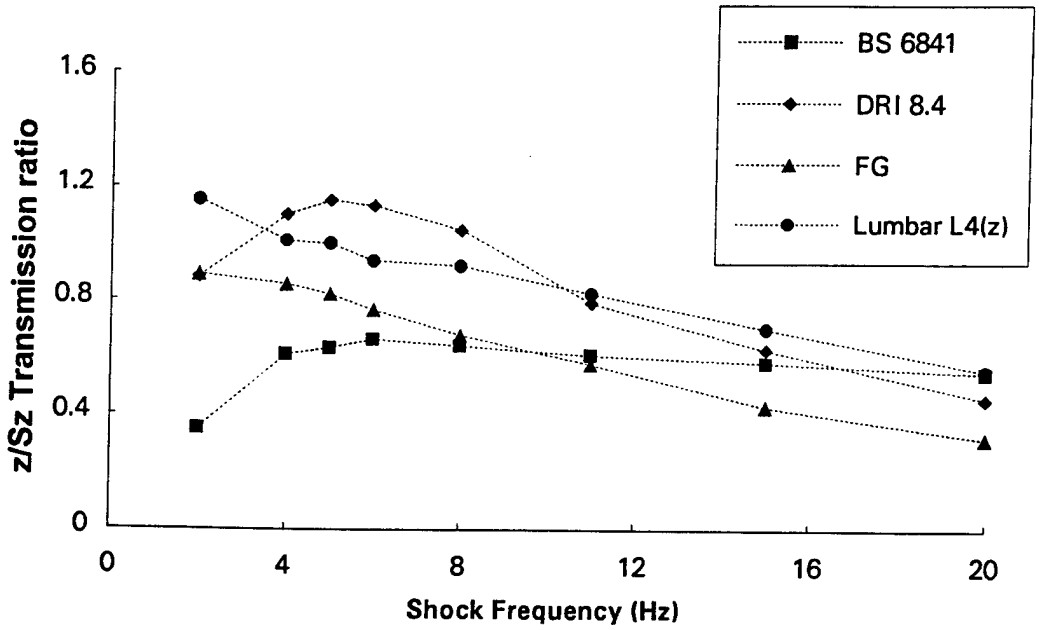

Figure F-67. Comparison of measured spine z transmission ratio (1 g shocks) with predicted transmission ratios using BS 6841 filter, Fairley-Griffin (FG) model and DRI model.

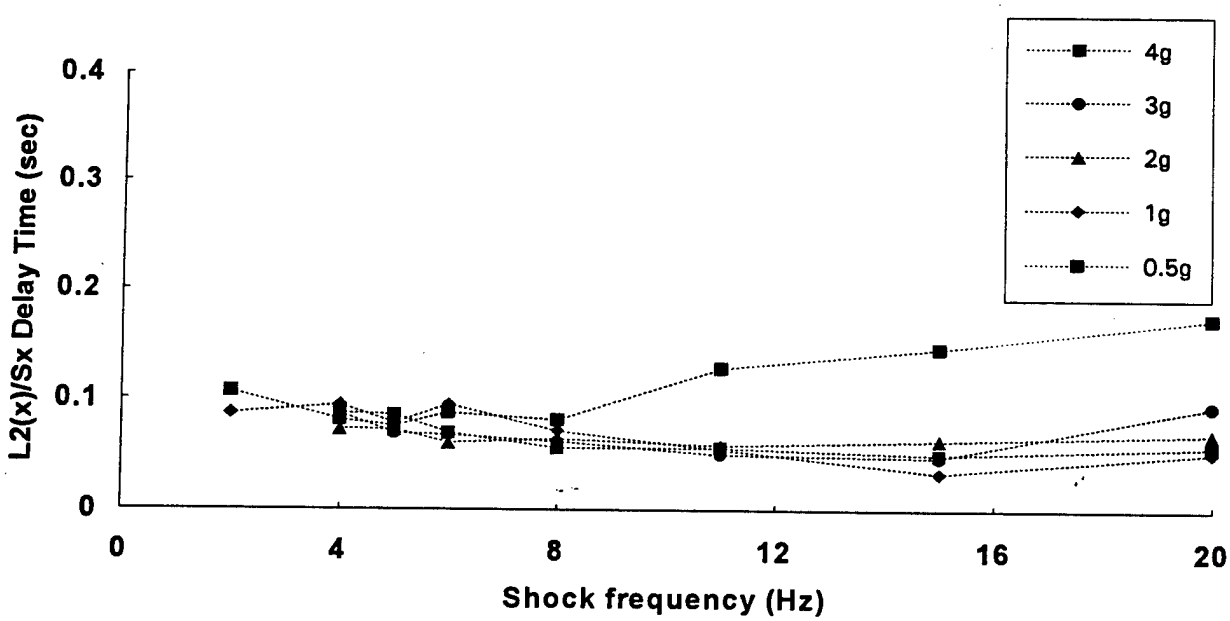

Figure F-68. Delay time for peak acceleration measured at spine (L2) to seat x acceleration for 0.5, 1, 2, 3, and 4 g shocks.

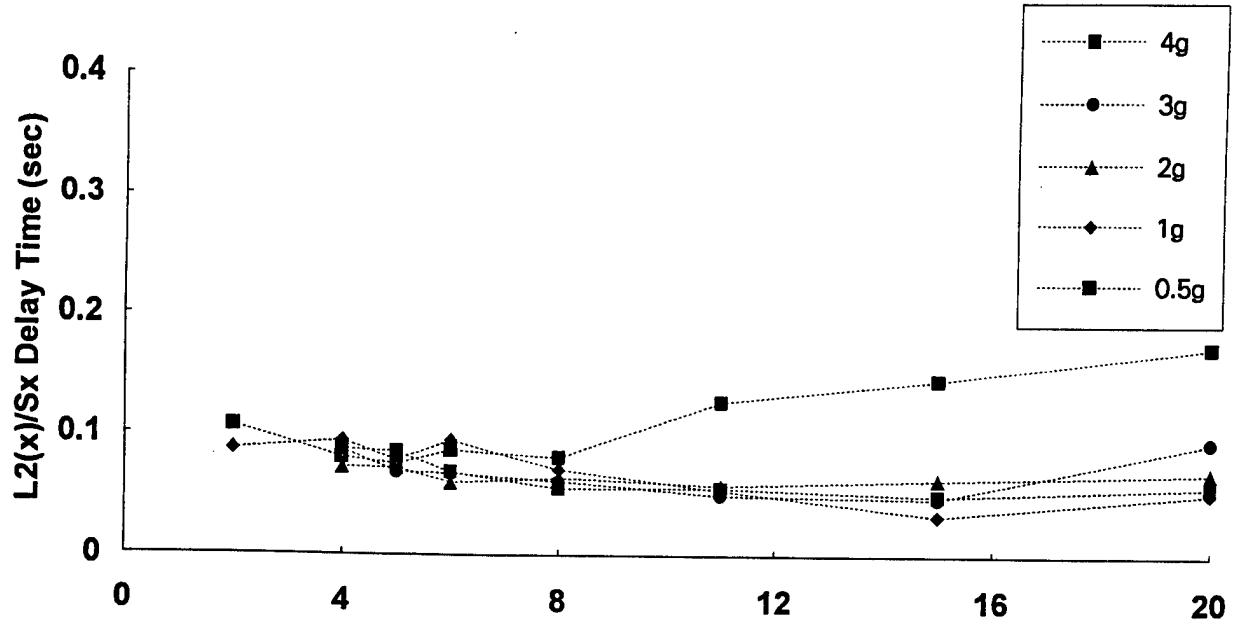

Figure F-69. Delay time for peak acceleration measured at spine (L2) to seat x acceleration for -0.5, -1, -2, -3, and -4 g shocks.

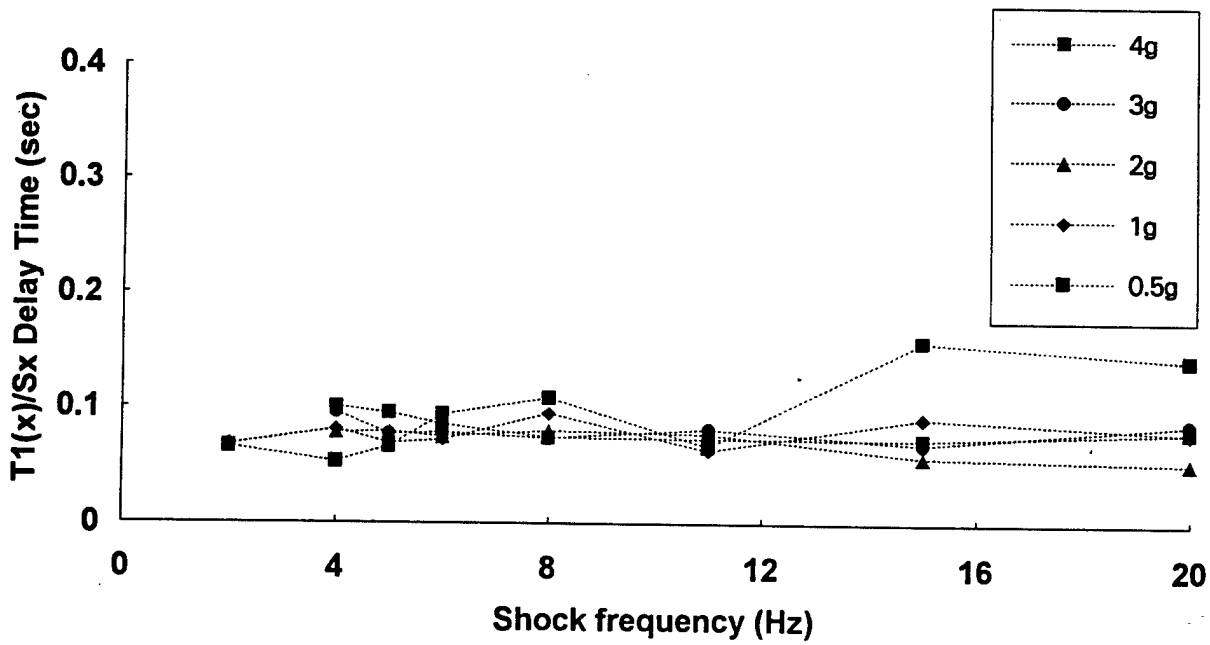

Figure F-70. Delay time for peak acceleration measured at spine (T1) to seat x acceleration for 0.5, 1, 2, 3, and 4 g shocks.

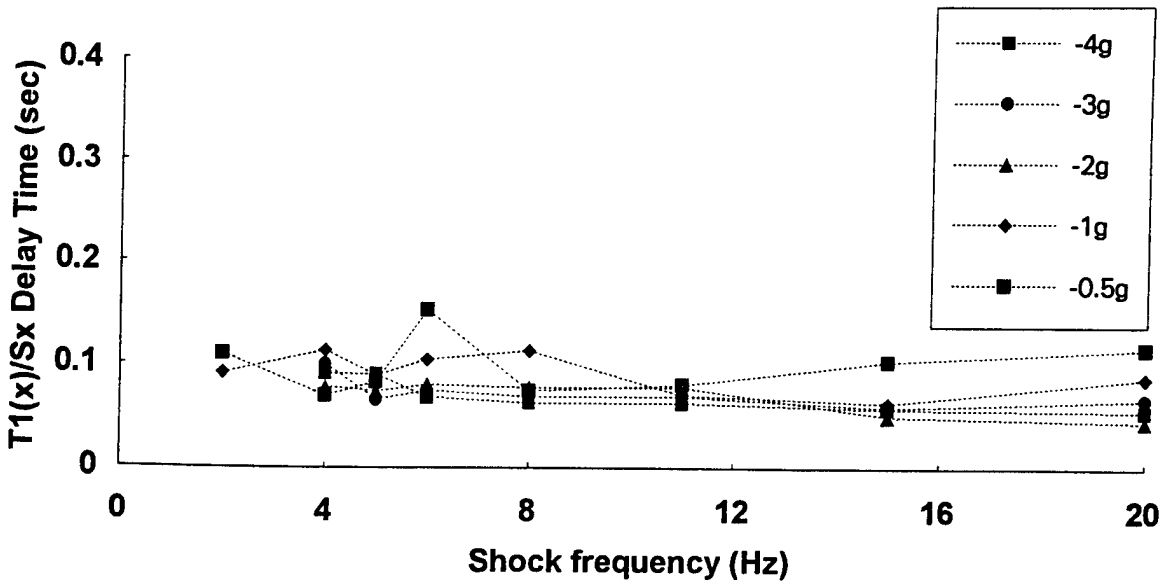

Figure F-71. Delay time for peak acceleration measured at spine (T1) to seat x acceleration for -0.5, -1, -2, -3, and -4 g shocks.

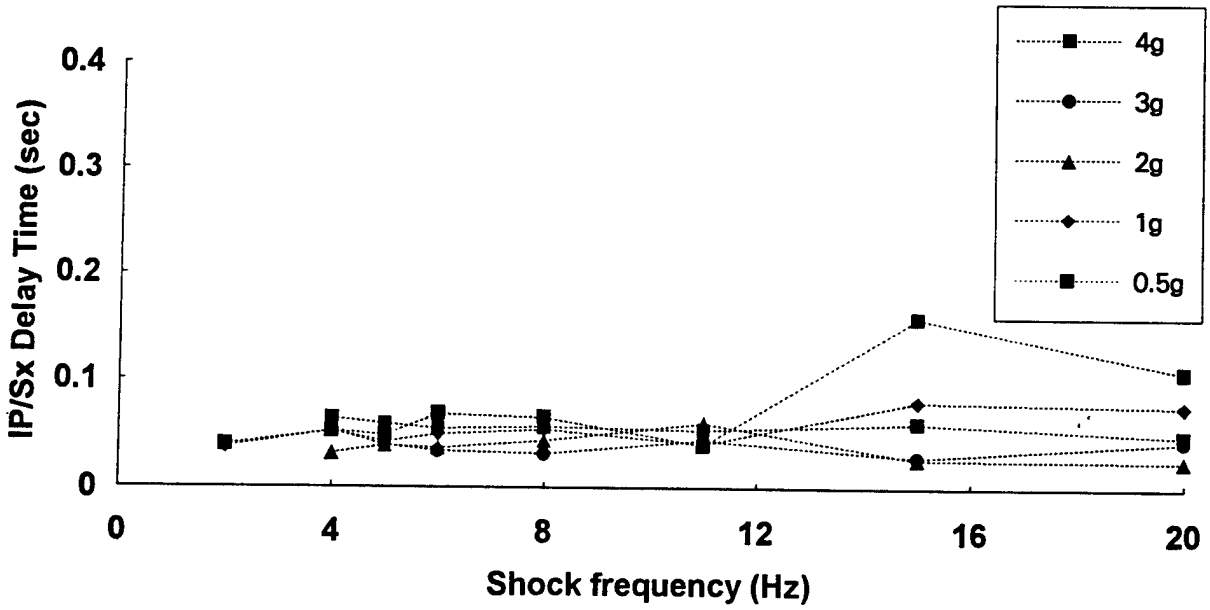

Figure F-72. Delay time for peak internal pressure response to seat x acceleration for 0.5, 1, 2, 3, and 4 g shocks.

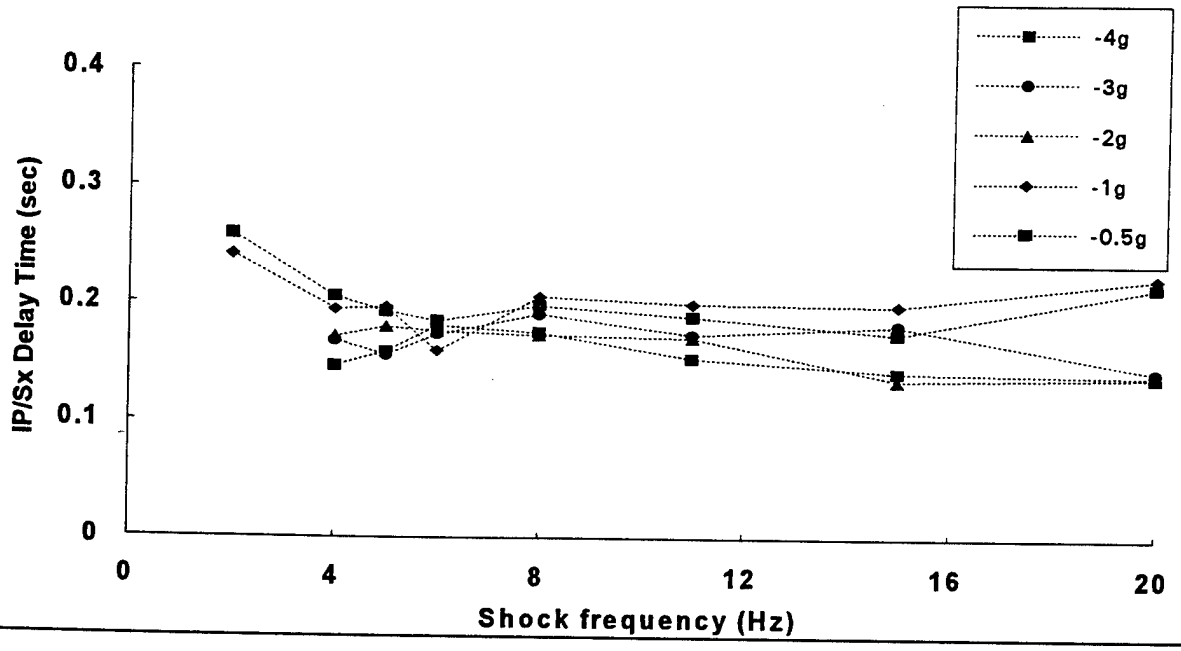

Figure F-73. Delay time for peak internal pressure response to seat x acceleration for -0.5, -1, -2, -3, and -4 g shocks.

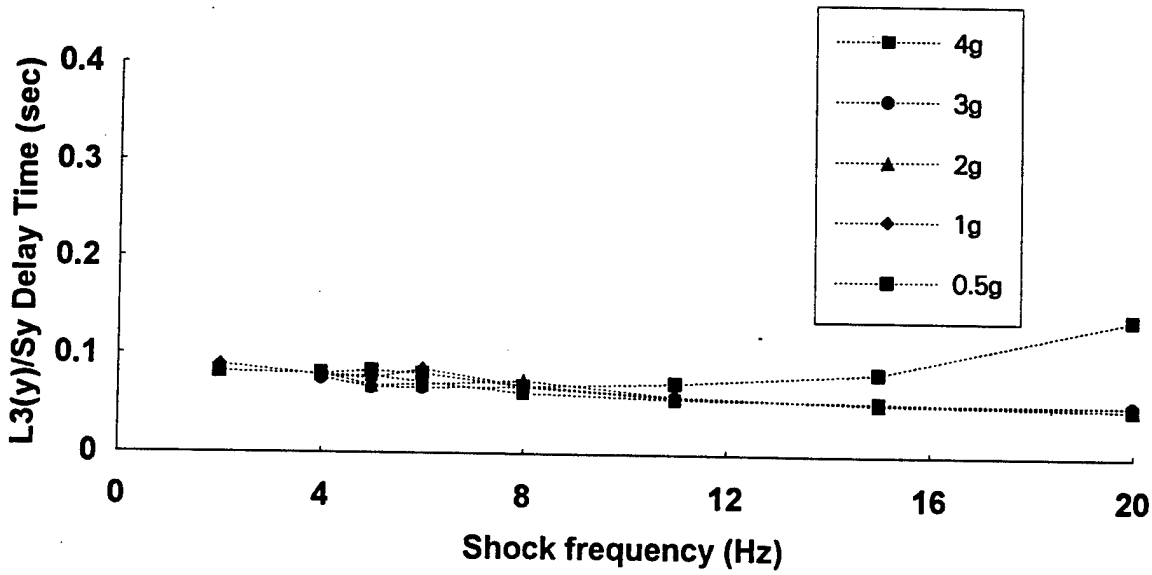

Figure F-74. Delay time for peak acceleration measured at spine (L3) to seat y acceleration for 0.5, 1, 2, 3, and 4 g shocks.

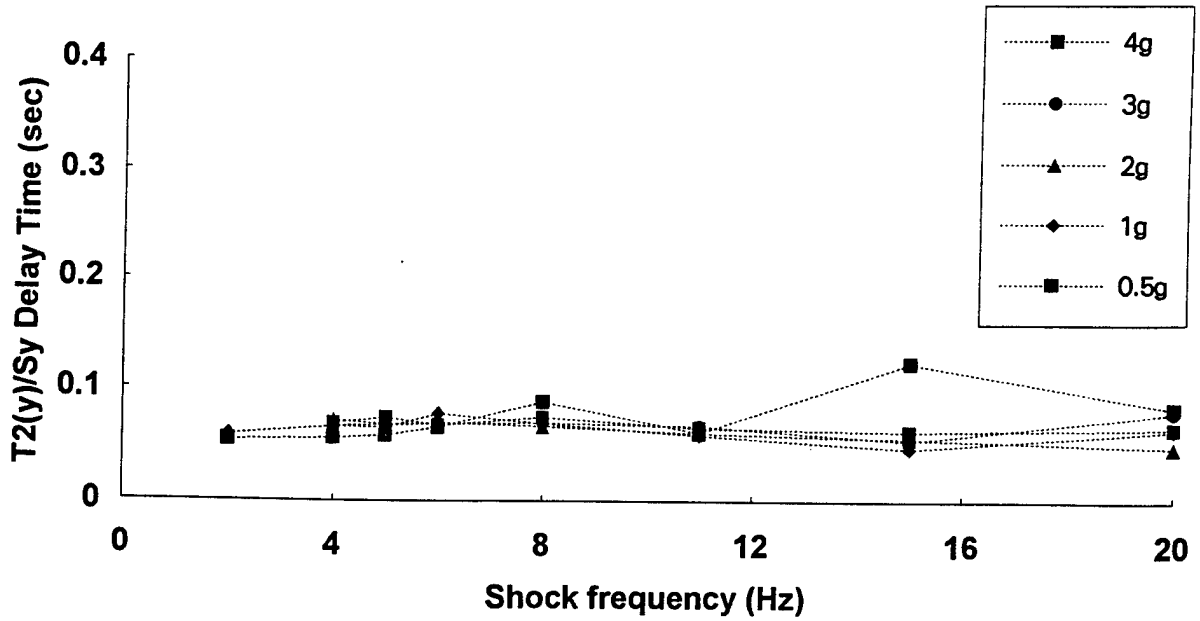

Figure F-75. Delay time for peak acceleration measured at spine (T2) to seat y acceleration for 0.5, 1, 2, 3, and 4 g shocks.

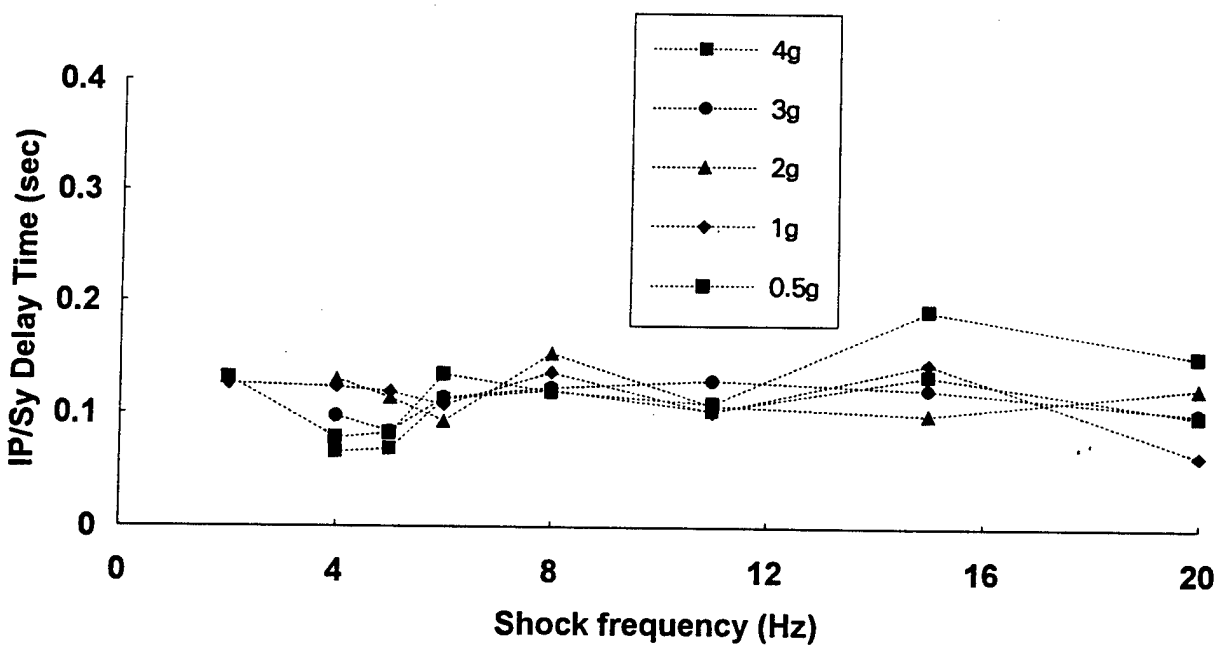

Figure F-76. Delay time for peak internal pressure response to seat y acceleration for 0.5, 1, 2, 3, and 4 g shocks.

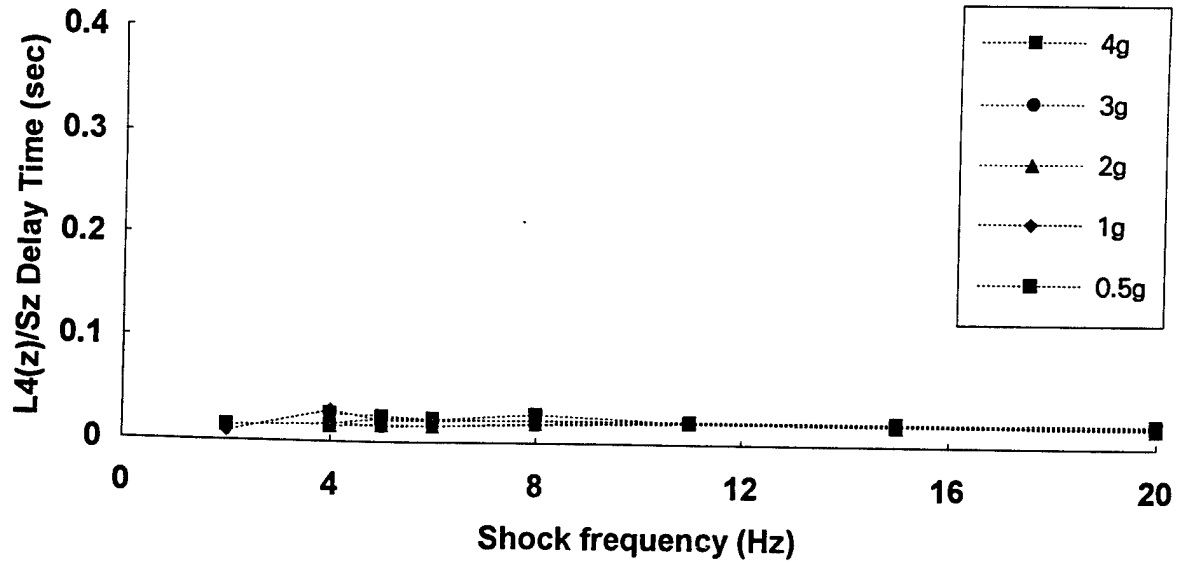

Figure F-77. Delay time for peak acceleration measured at spine (L4) to seat z acceleration for 0.5, 1, 2, 3, and 4 g shocks.

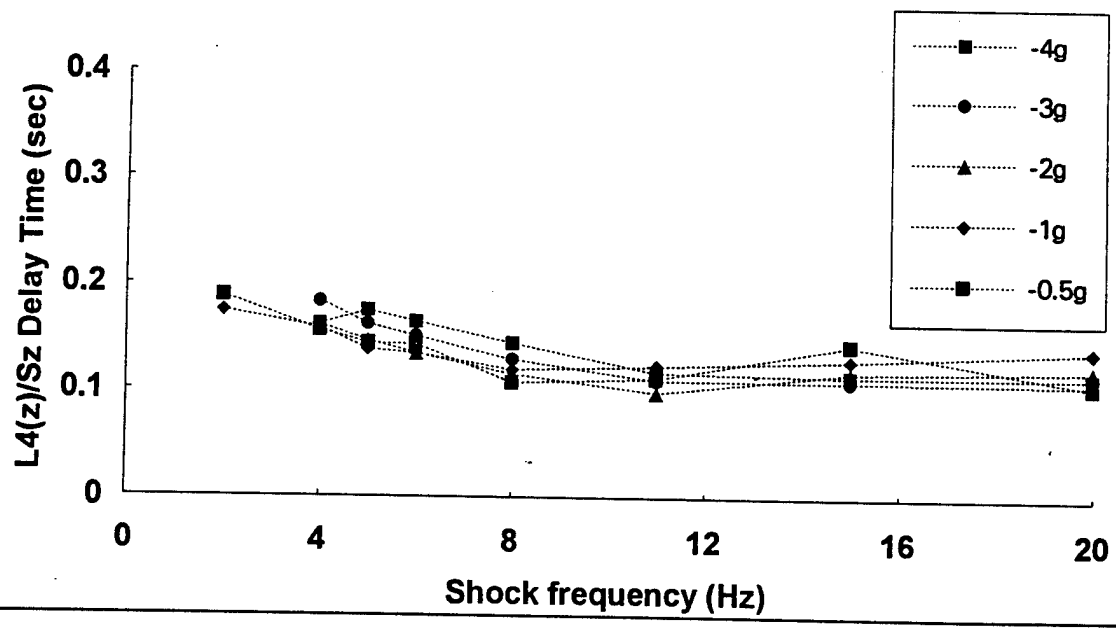

Figure F-78. Delay time for peak acceleration measured at spine (L4) to seat z acceleration for -0.5, -1, -2, -3, and -4 g shocks.

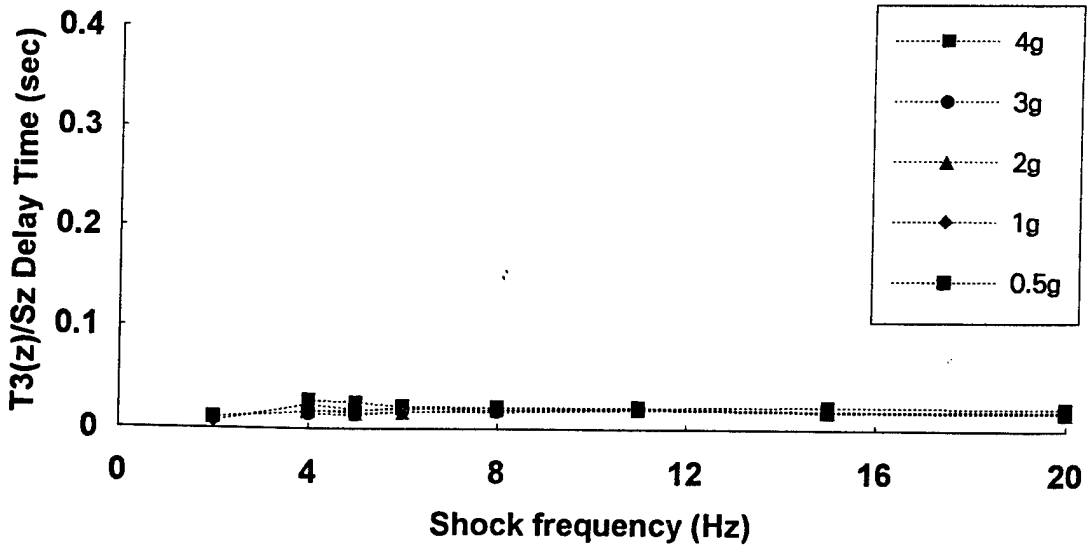

Figure F-79. Delay time for peak acceleration measured at spine (T3) to seat z acceleration for 0.5, 1, 2, 3, and 4 g shocks.

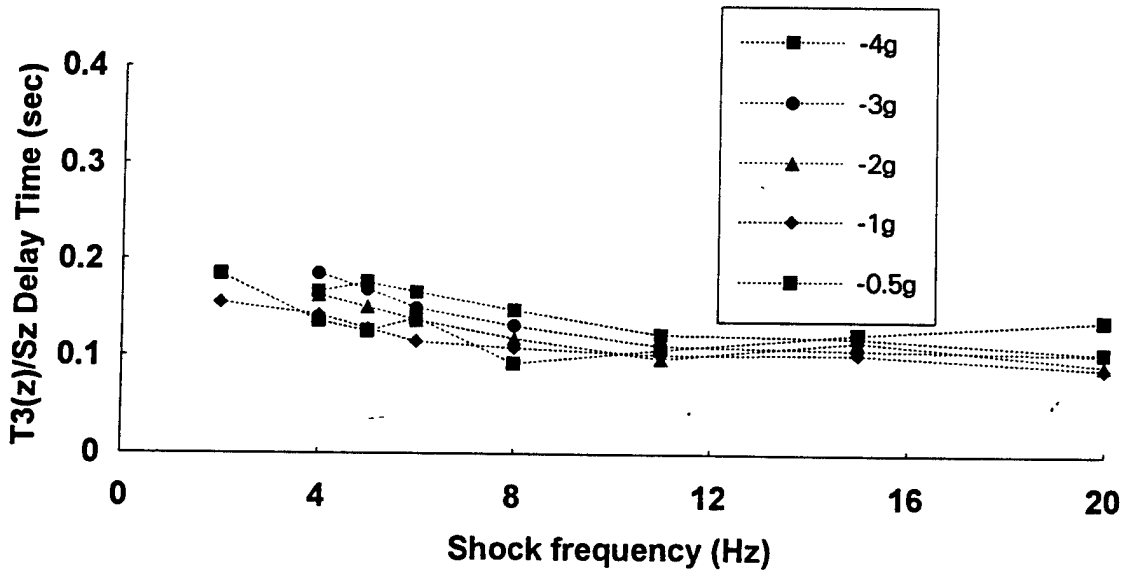

Figure F-80. Delay time for peak acceleration measured at spine (T3) to seat z acceleration for -0.5, -1, -2, -3, and -4 g shocks.

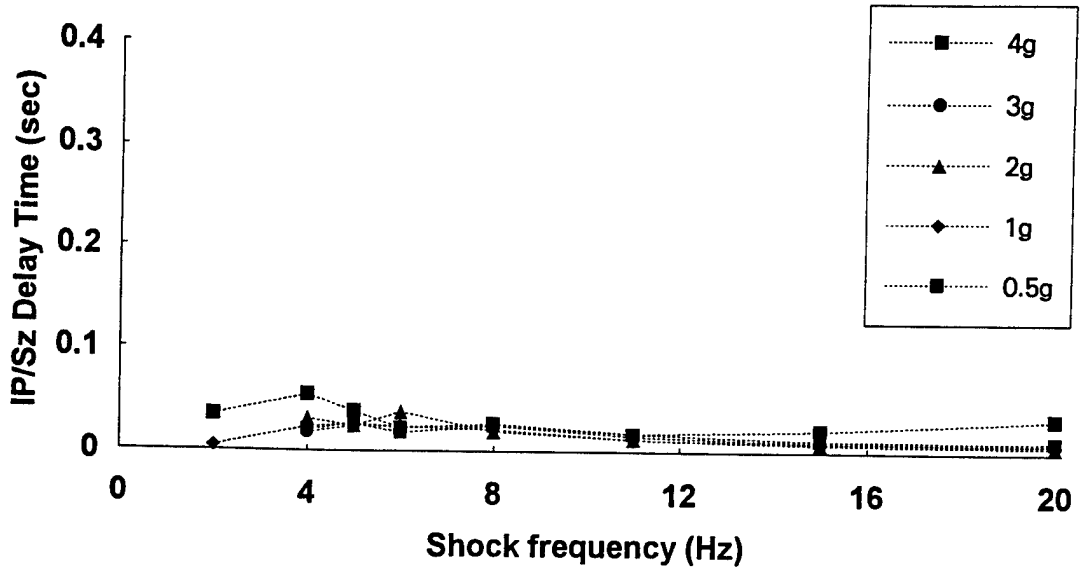

Figure F-81. Delay time for peak internal pressure response to seat z acceleration for 0.5, 1, 2, 3, and 4 g shocks.

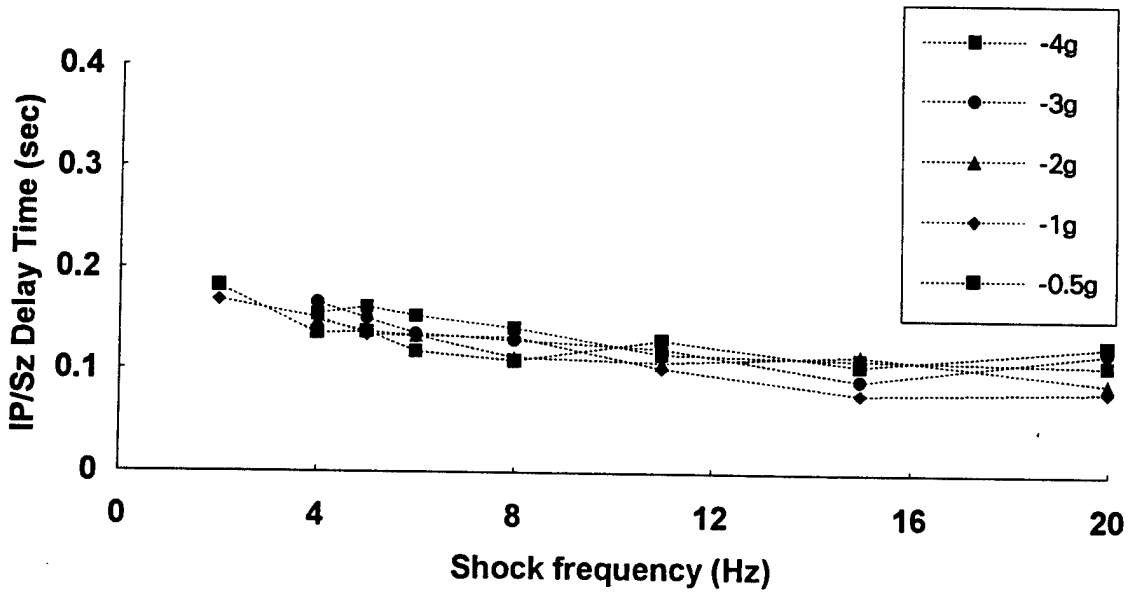

Figure F-82. Delay time for peak internal pressure response to seat z acceleration for -0.5, -1, -2, -3, and -4 g shocks.

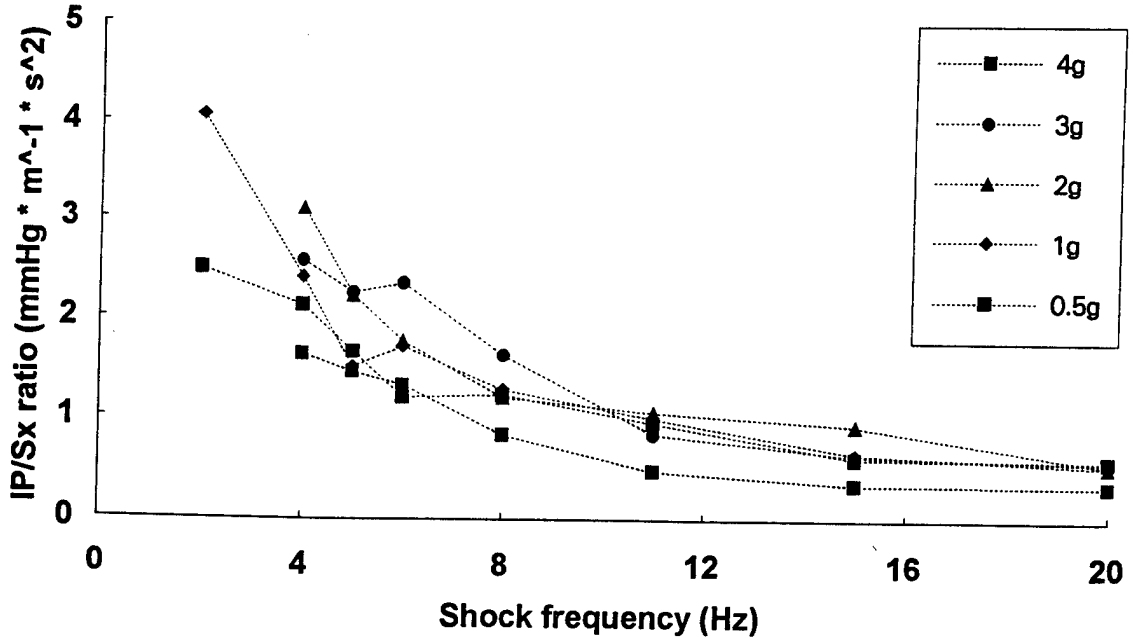

Figure F-83. Internal pressure response to seat x acceleration for 0.5, 1, 2, 3, and 4 g shocks.

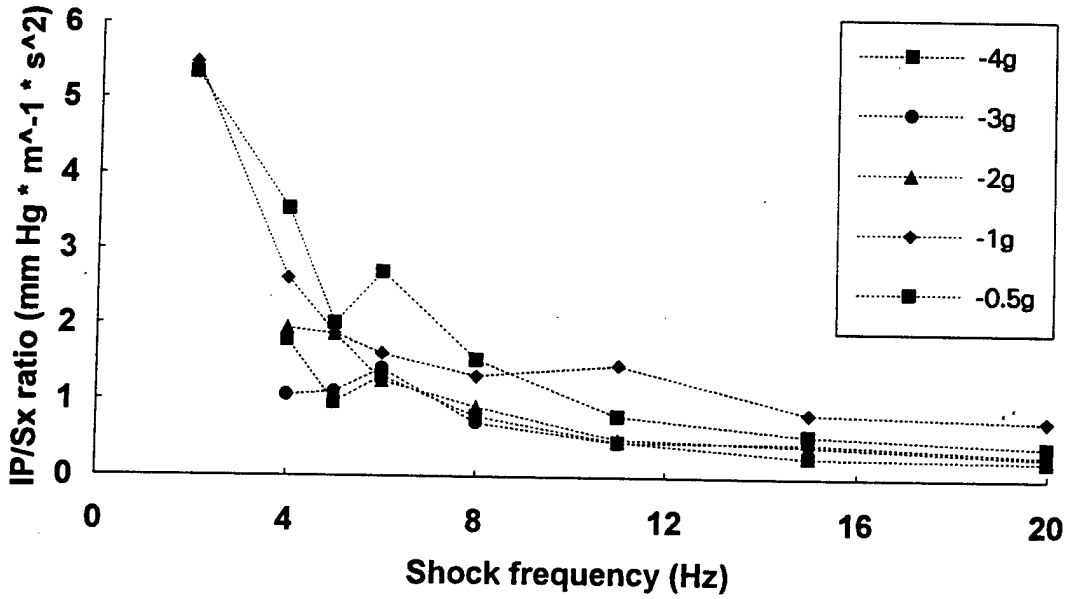

Figure F-84. Internal pressure response to seat x acceleration for -0.5, -1, -2, -3, and -4 g shocks.

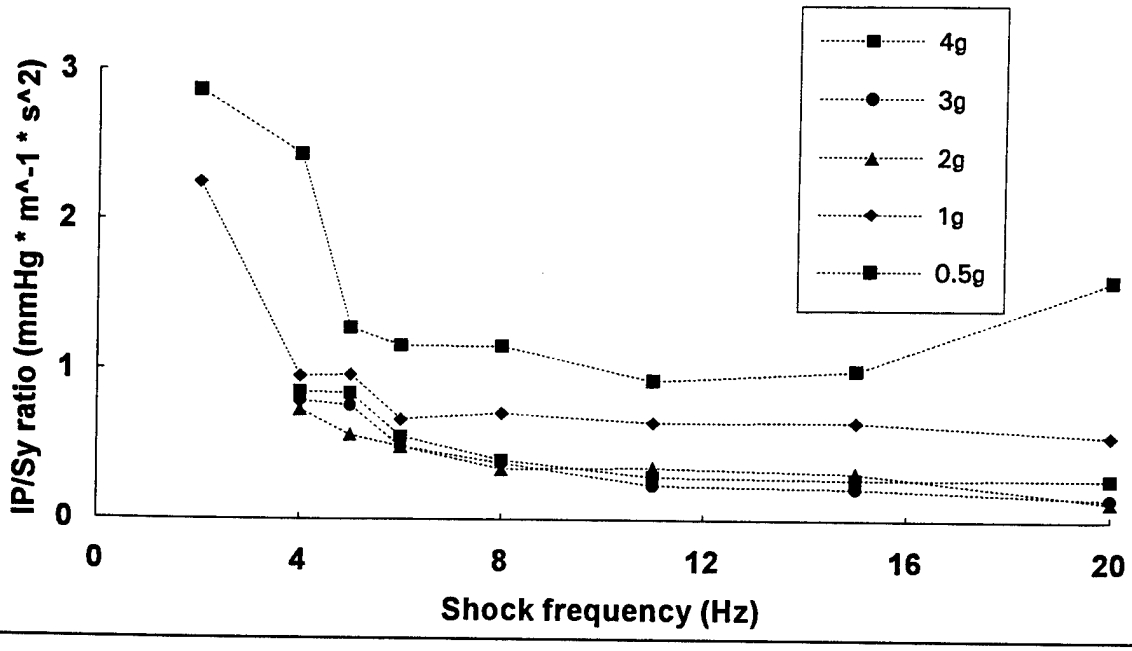

Figure F-85. Internal pressure response to seat y acceleration for 0.5, 1, 2, 3, and 4 g shocks.

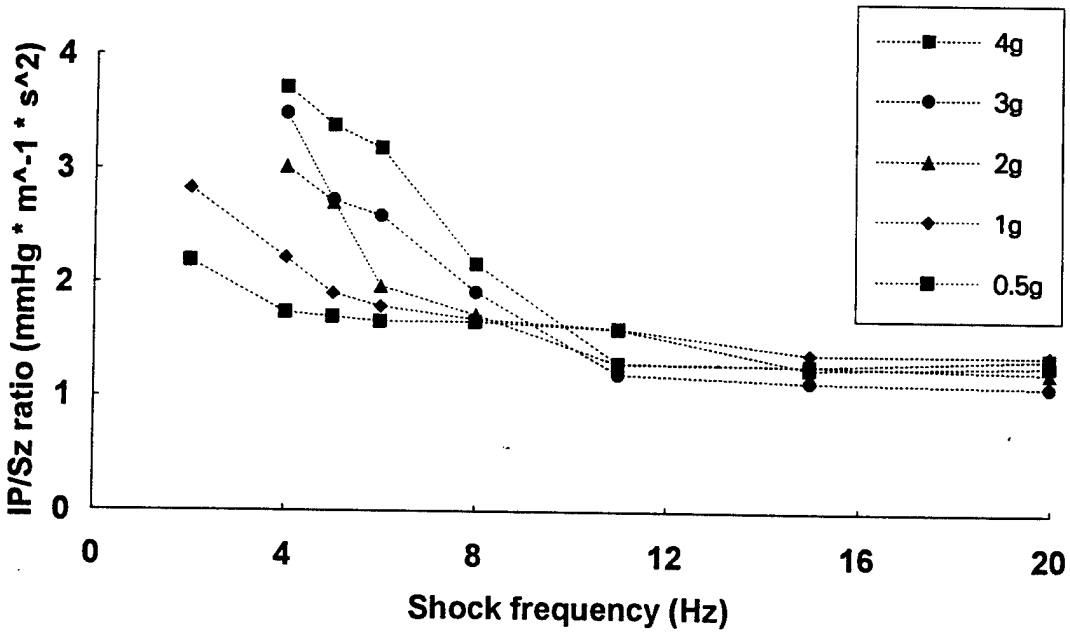

Figure F-86. Internal pressure response to seat z acceleration for 0.5, 1, 2, 3, and 4 g shocks.

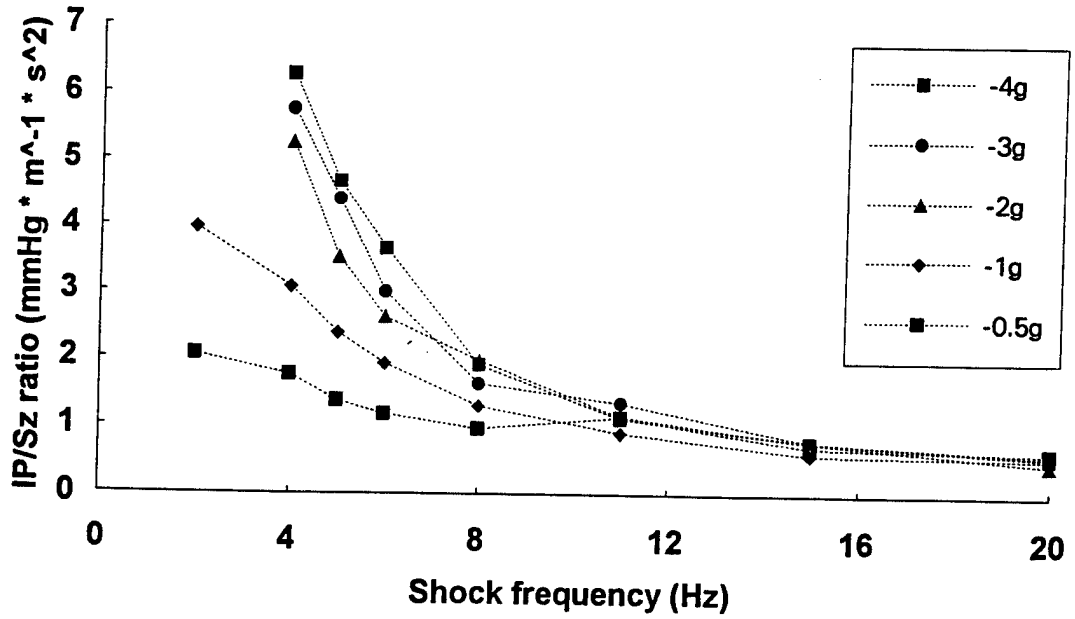

Figure F-87. Internal pressure response to seat z acceleration for -0.5, -1, -2, -3, and -4 g shocks.

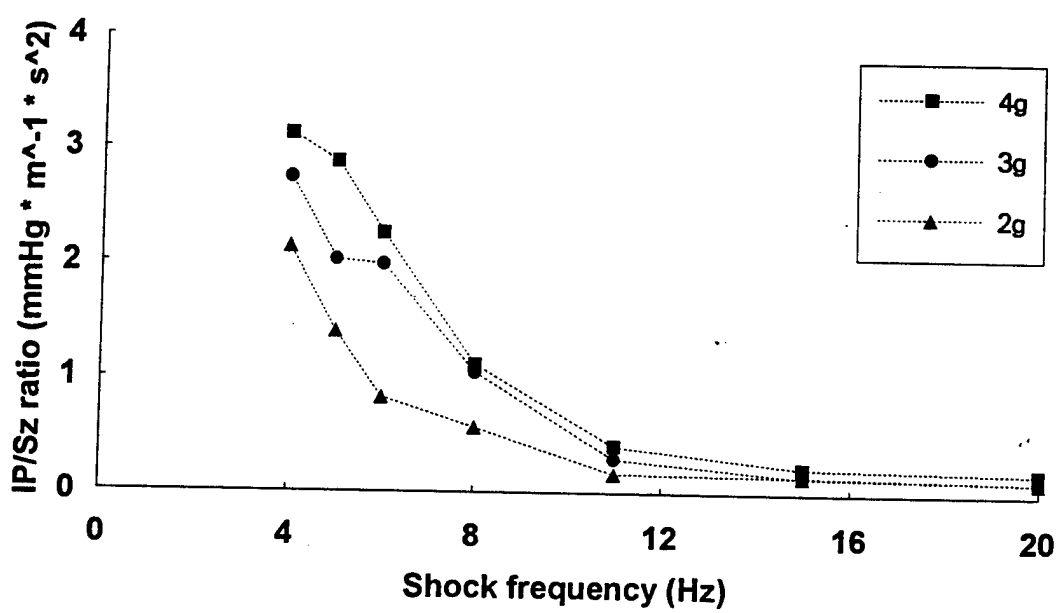

Figure F-88. Second internal pressure response to a single seat z acceleration for 2, 3, and 4 g shocks.

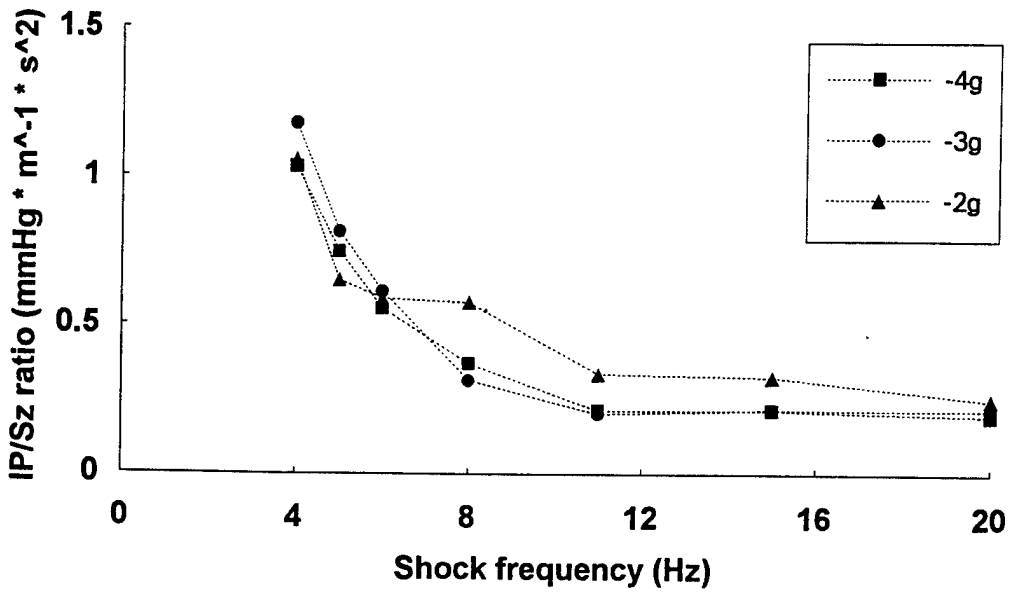

Figure F-89. Second internal pressure response to a single seat z acceleration for -2, -3, and -4 g shocks.

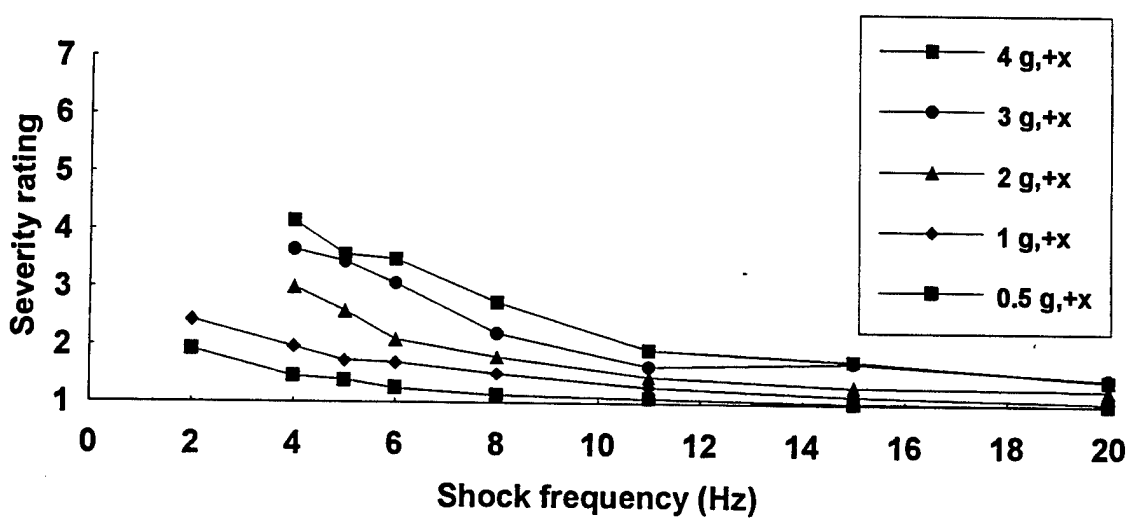

Figure F-90. Subjective severity ratings to single shocks in the positive x axis as a function of shock frequency and amplitude.

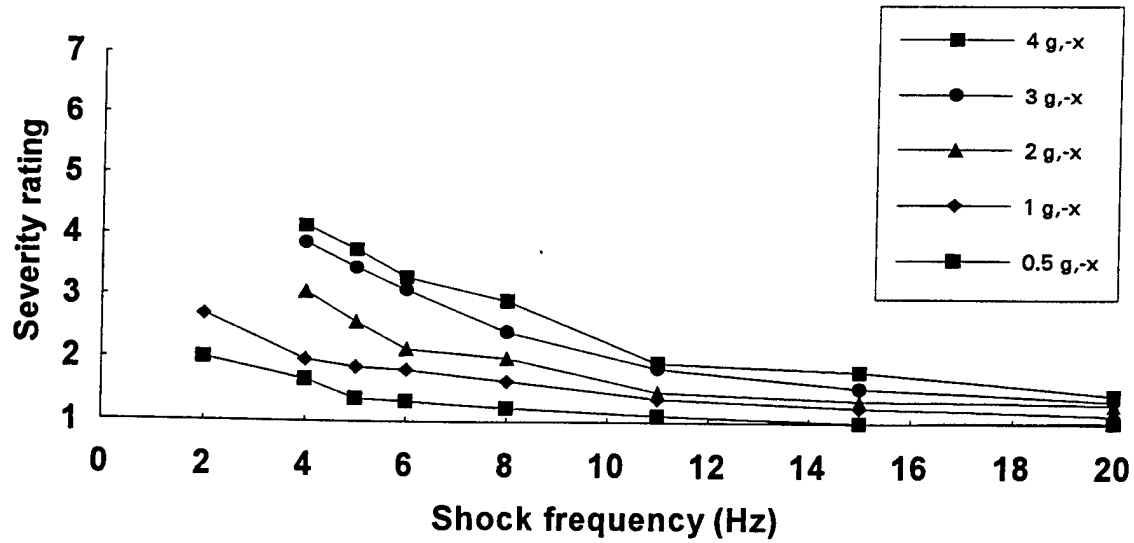

Figure F-91. Subjective severity ratings to single shocks in the negative x axis as a function of shock frequency and amplitude.

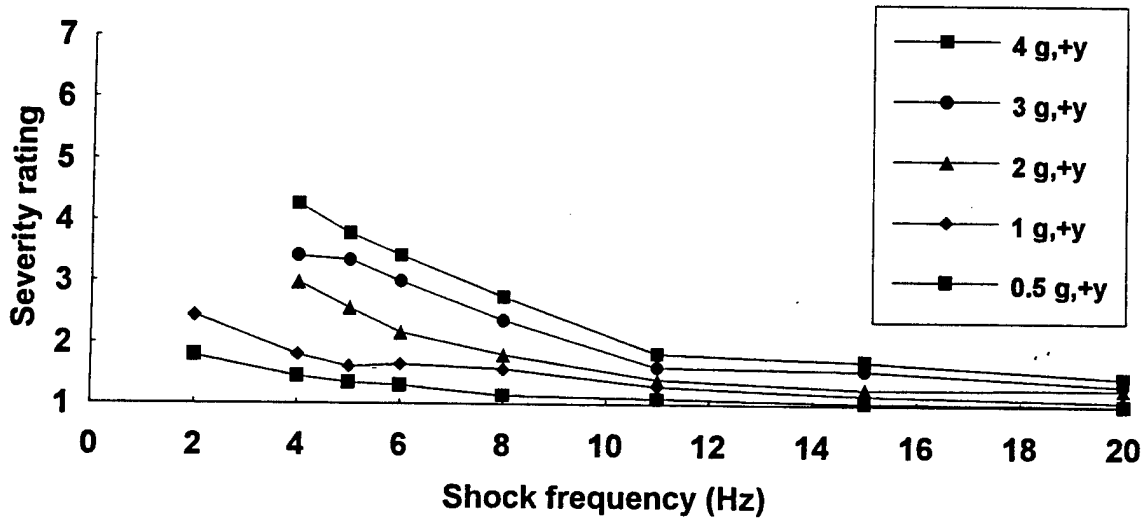

Figure F-92. Subjective severity ratings to single shocks in the y axis as a function of shock frequency and amplitude.

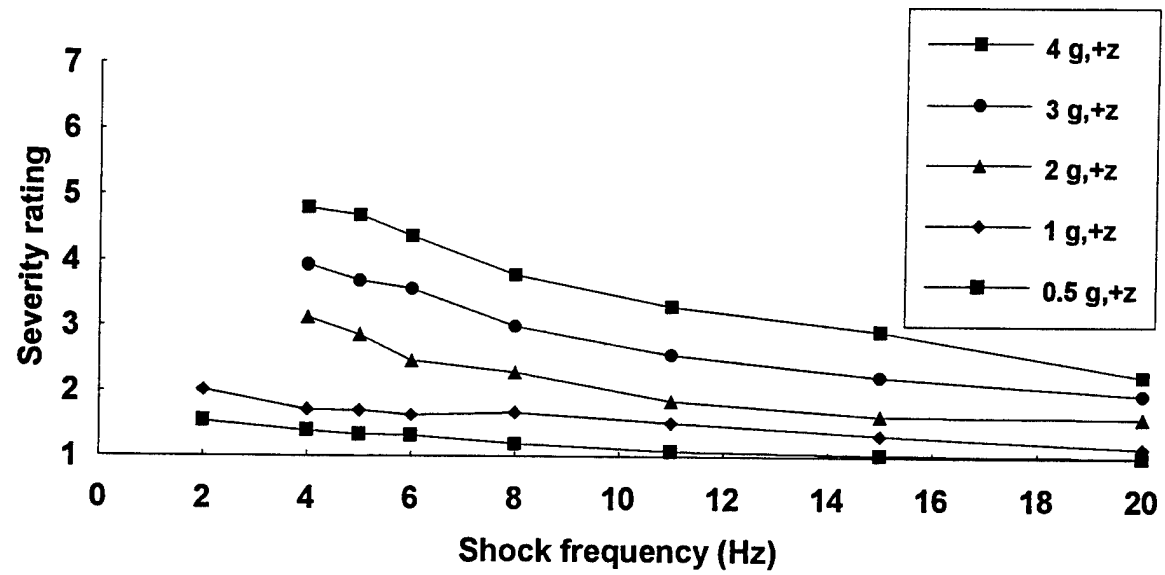

Figure F-93. Subjective severity ratings to single shocks in the positive z axis as a function of shock frequency and amplitude.

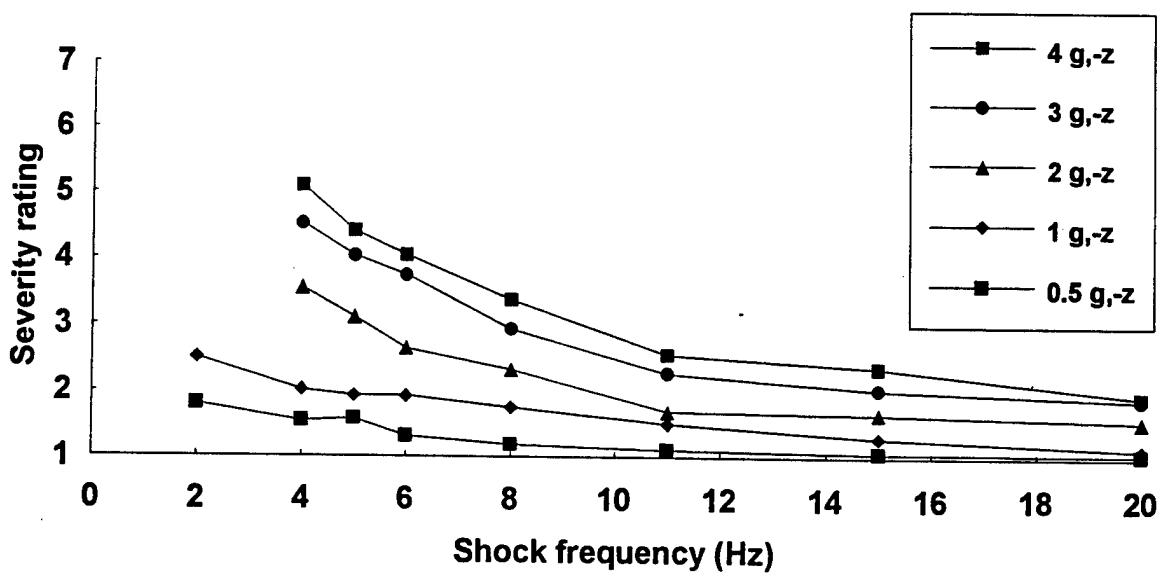

Figure F-94. Subjective severity ratings to single shocks in the negative z axis as a function of shock frequency and amplitude.

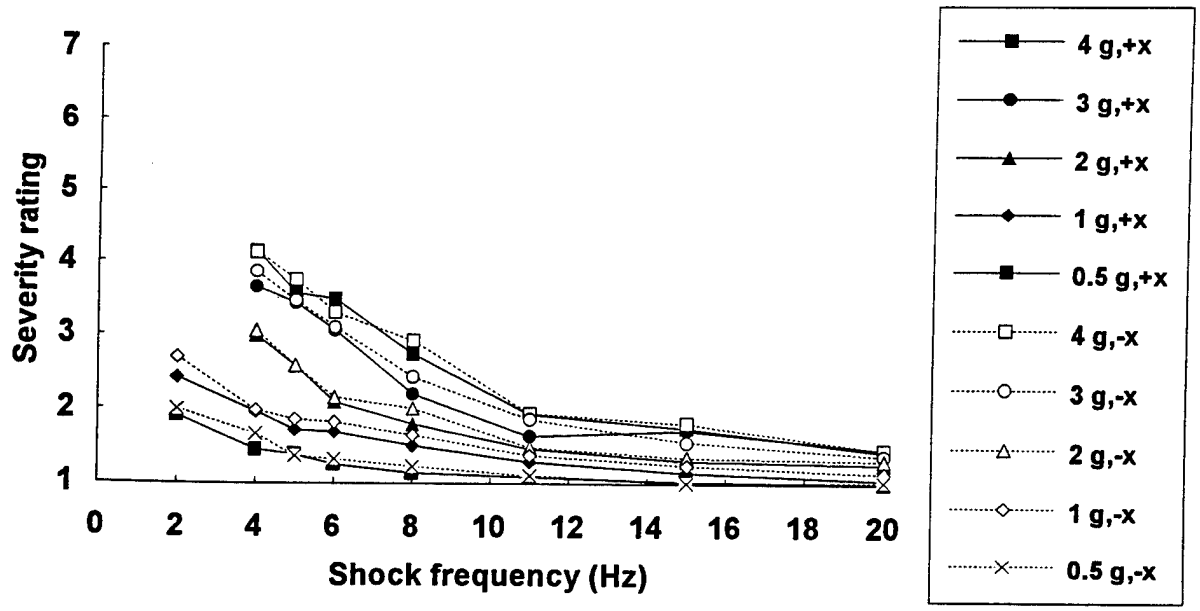

Figure F-95. Comparison between subjective severity ratings to single shocks in the positive and negative x axis as a function of shock frequency and amplitude.

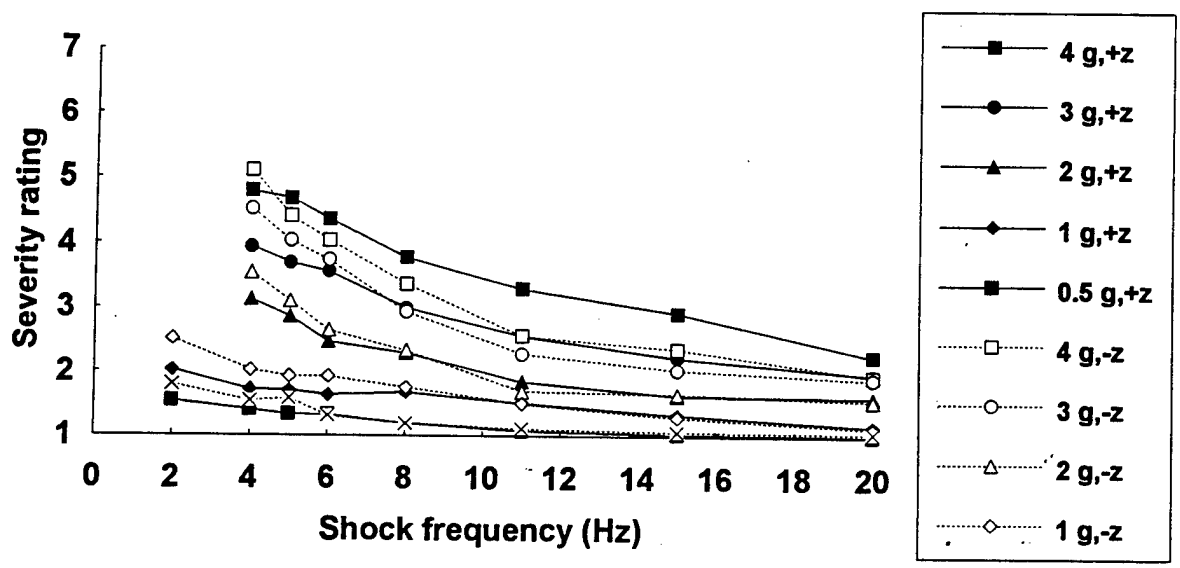

Figure F-96. Comparison between subjective severity ratings to single shocks in the positive and negative z axis as a function of shock frequency and amplitude.

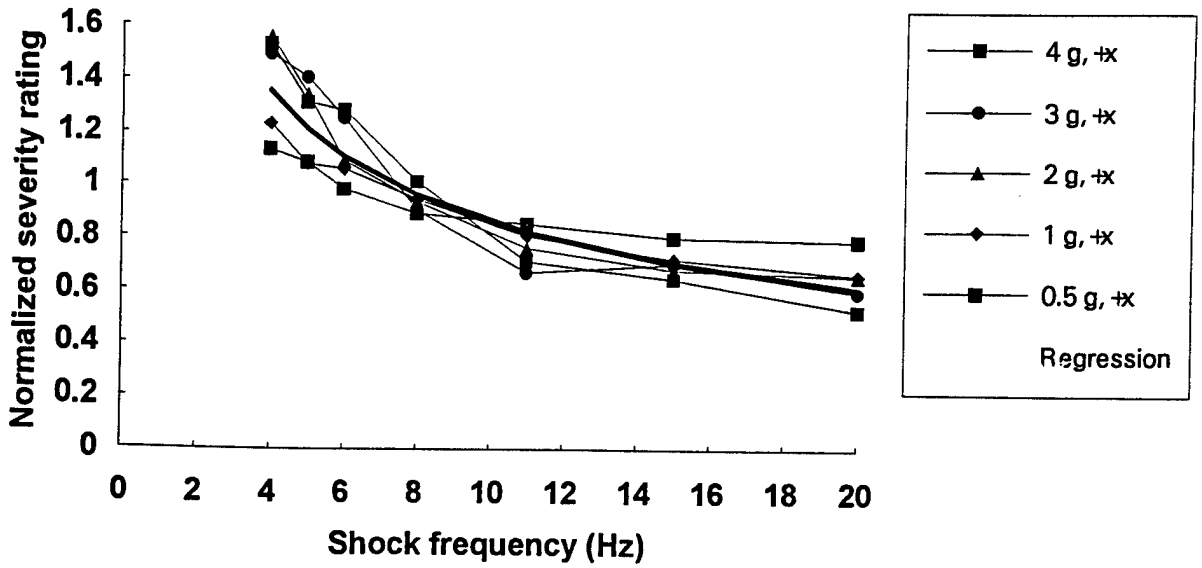

Figure F-97. Comparison of normalized subjective severity ratings to single shocks in the positive x axis for different shock magnitudes. The solid line represents the regression line for all data.

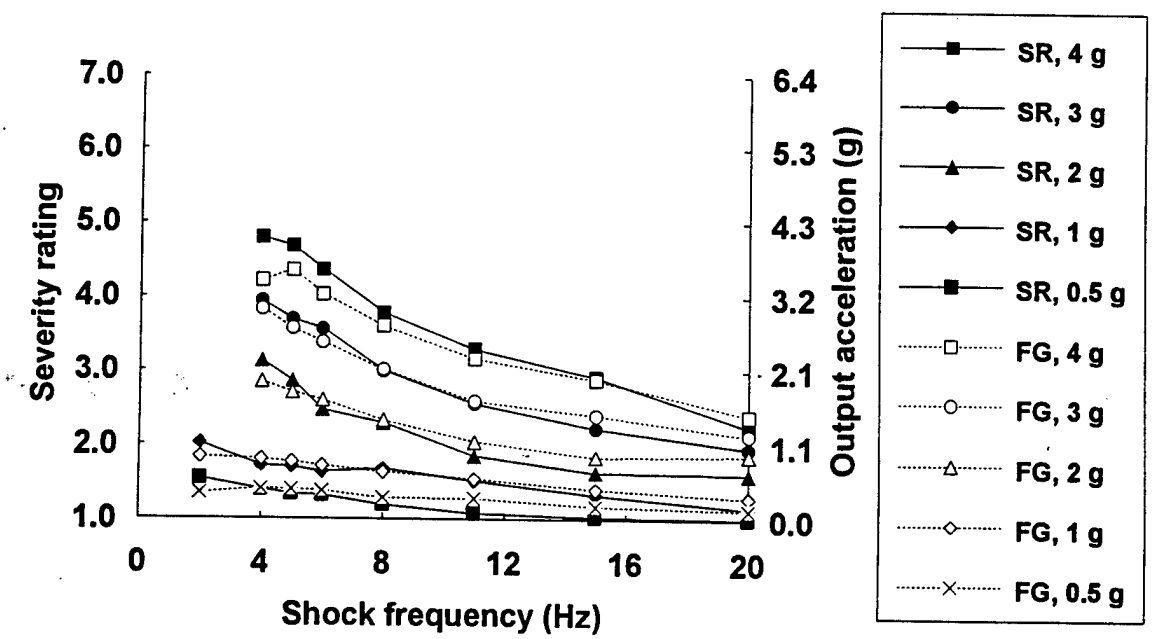

Figure F-98. Comparison between severity ratings (SR) and expected output from the Fairley-Griffin (FG) model to positive z axis shocks.

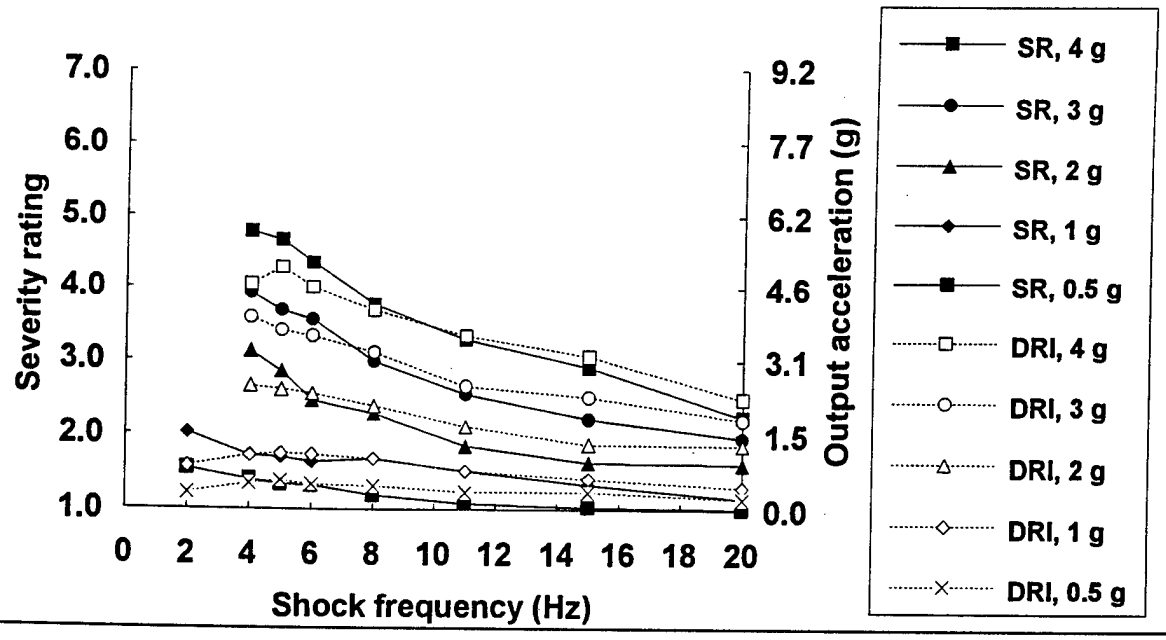

Figure F-99. Comparison between severity ratings (SR) and expected output from the DRI model (8.4 Hz) to positive z axis shocks.

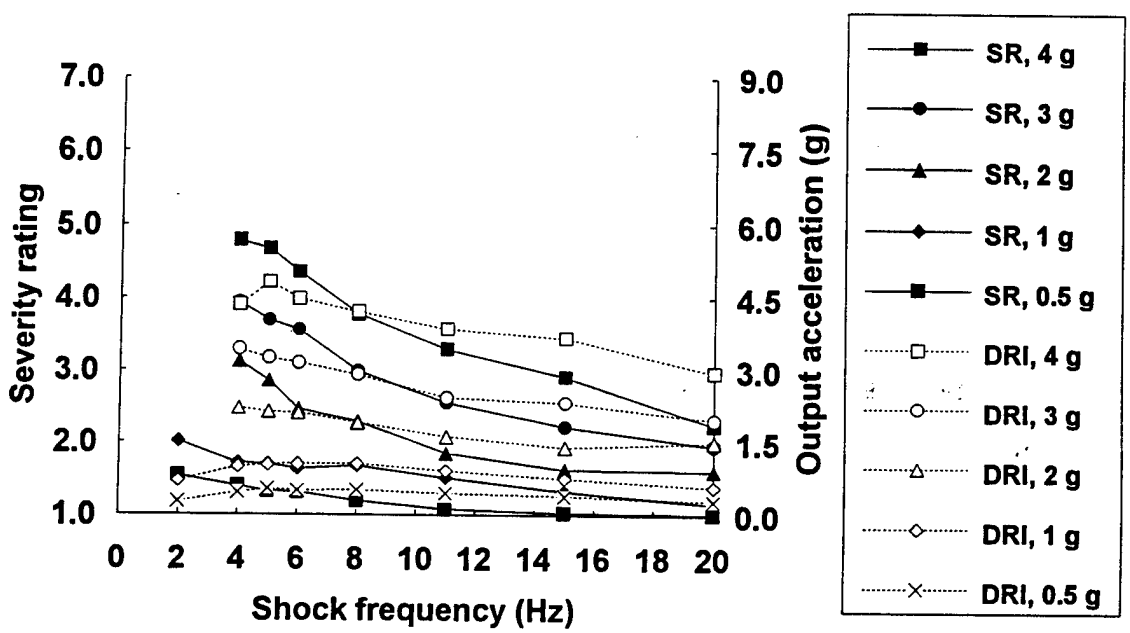

Figure F-100. Comparison between severity ratings (SR) and expected output from the DRI model (11.9 Hz) to positive z axis shocks.

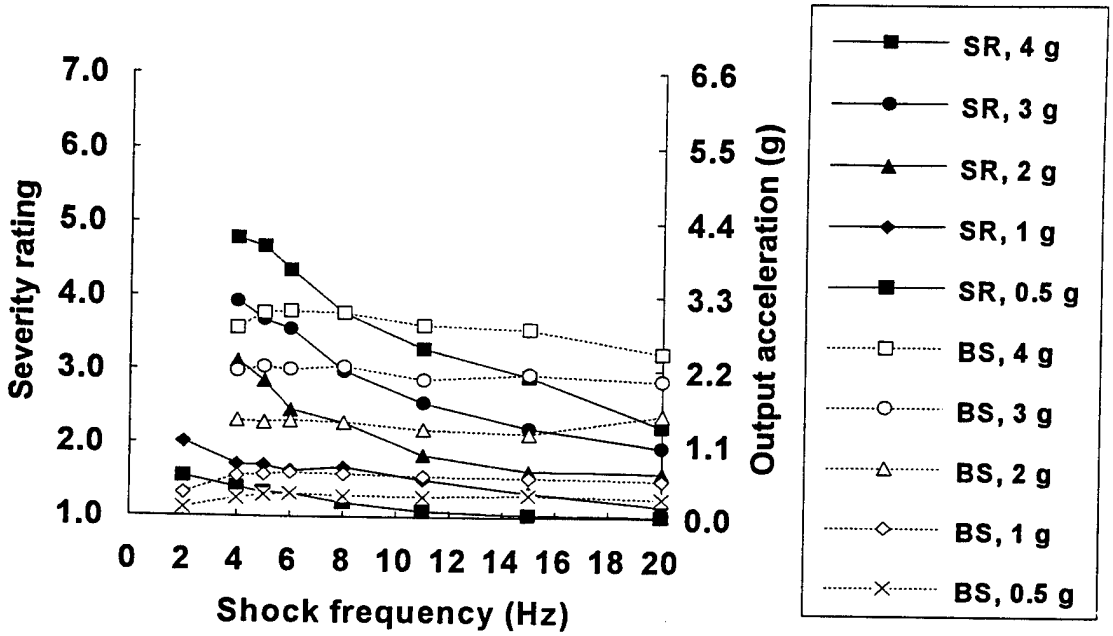

Figure F-101. Comparison between severity ratings (SR) and expected output from the BS 6841 W_b filter to positive z axis shocks.

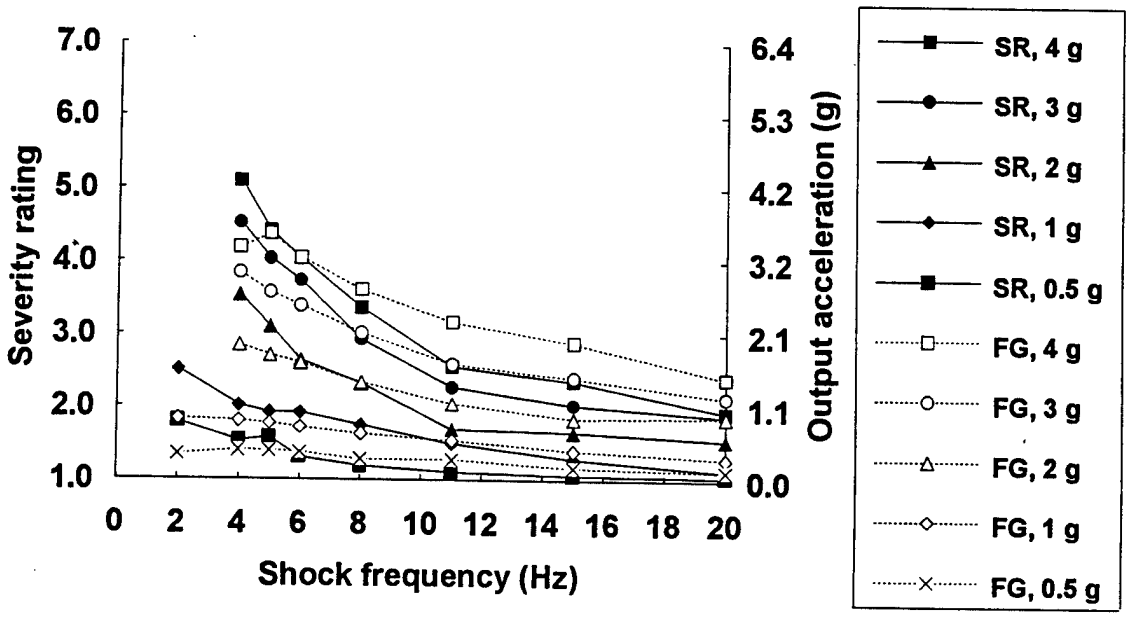

Figure F-102. Comparison between severity ratings (SR) and expected output from the Fairley-Griffin (FG) model to negative z axis shocks.

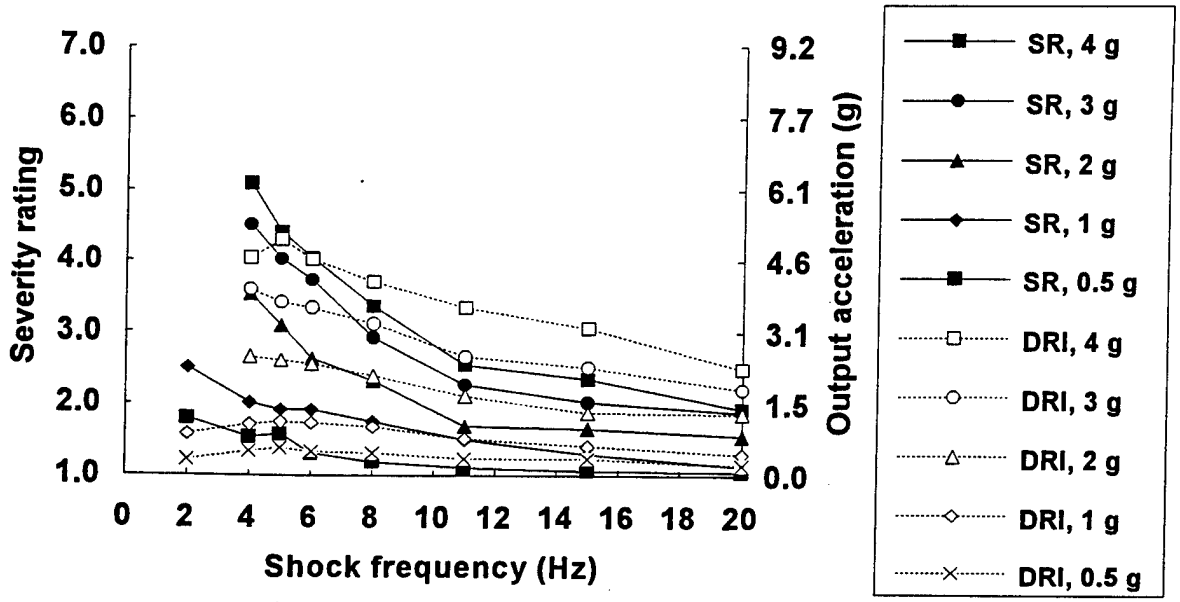

Figure F-103. Comparison between severity ratings (SR) and expected output from the DRI model (8.4 Hz) to negative z axis shocks.

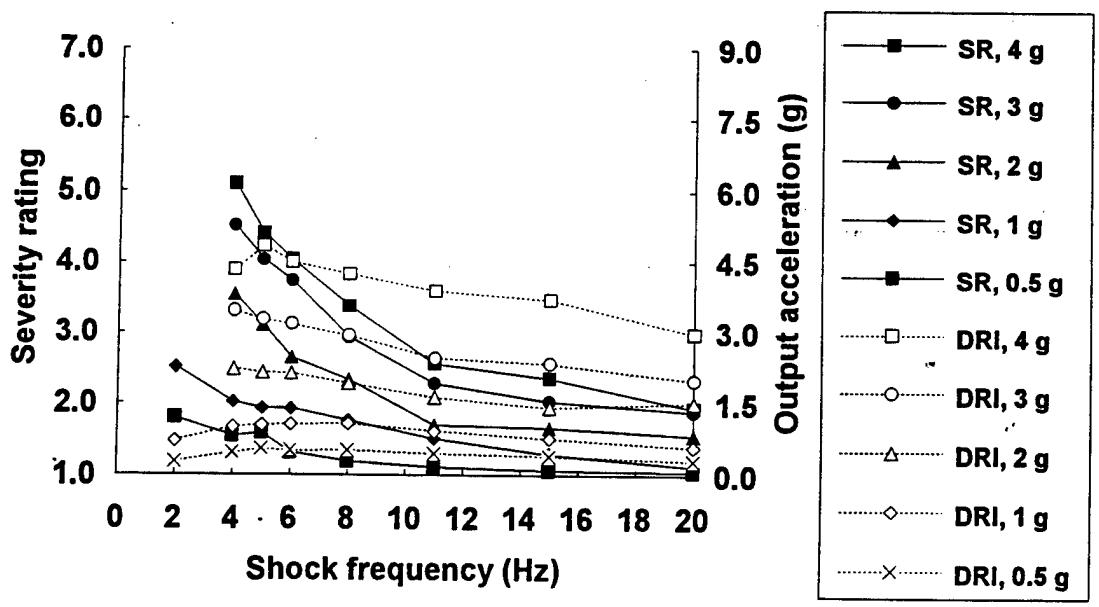

Figure F-104. Comparison between severity ratings (SR) and expected output from the DRI model (11.9 Hz) to negative z axis shocks.

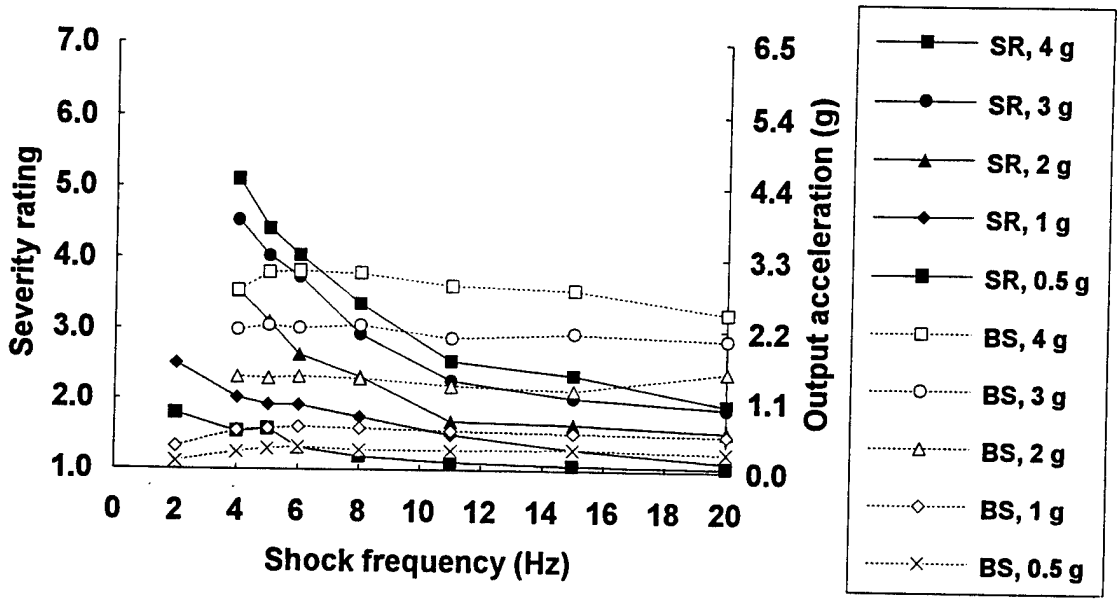

Figure F-105. Comparison between severity ratings (SR) and expected output from the BS 6841 W_b filter to negative z axis shocks.

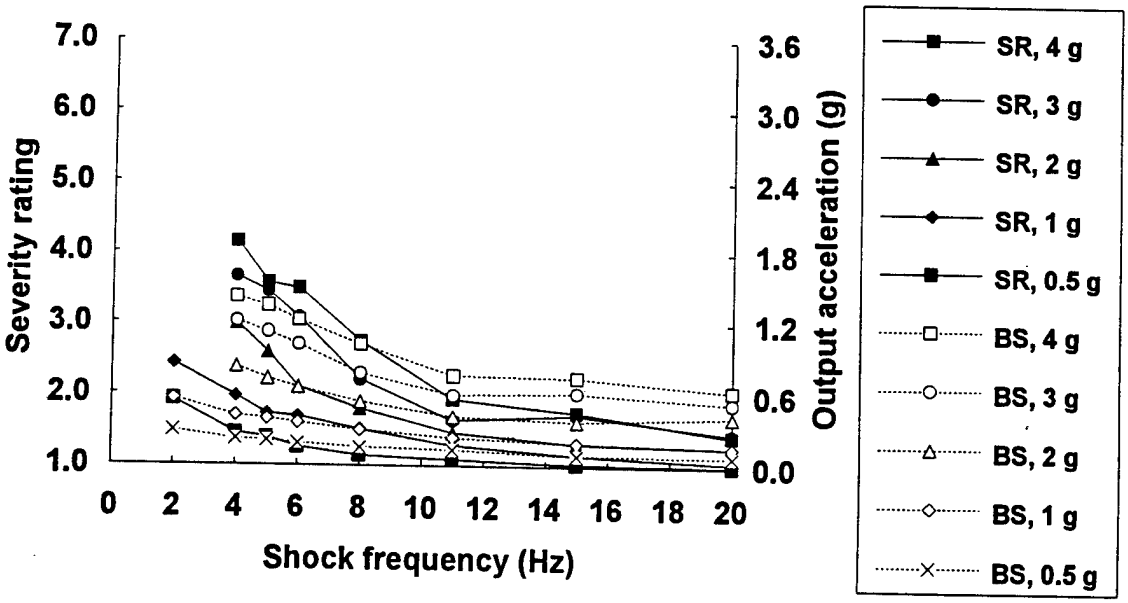

Figure F-106. Comparison between severity ratings (SR) and expected output from the BS 6841 W_d filter to positive x axis shocks.

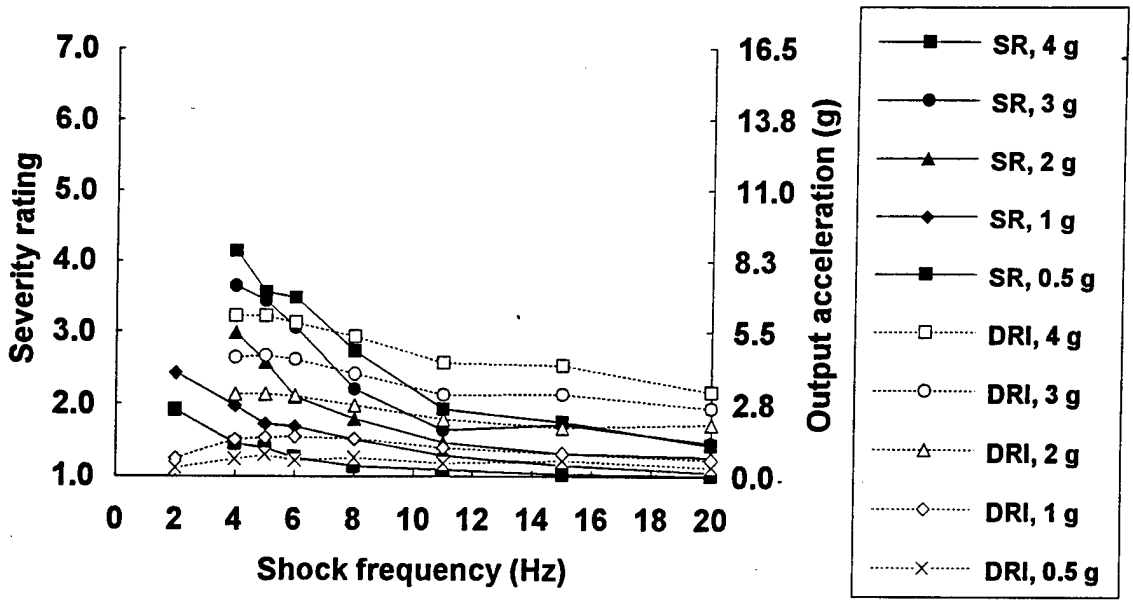

Figure F-107. Comparison between severity ratings (SR) and expected output from the DRI model (10 Hz) to positive x axis shocks.

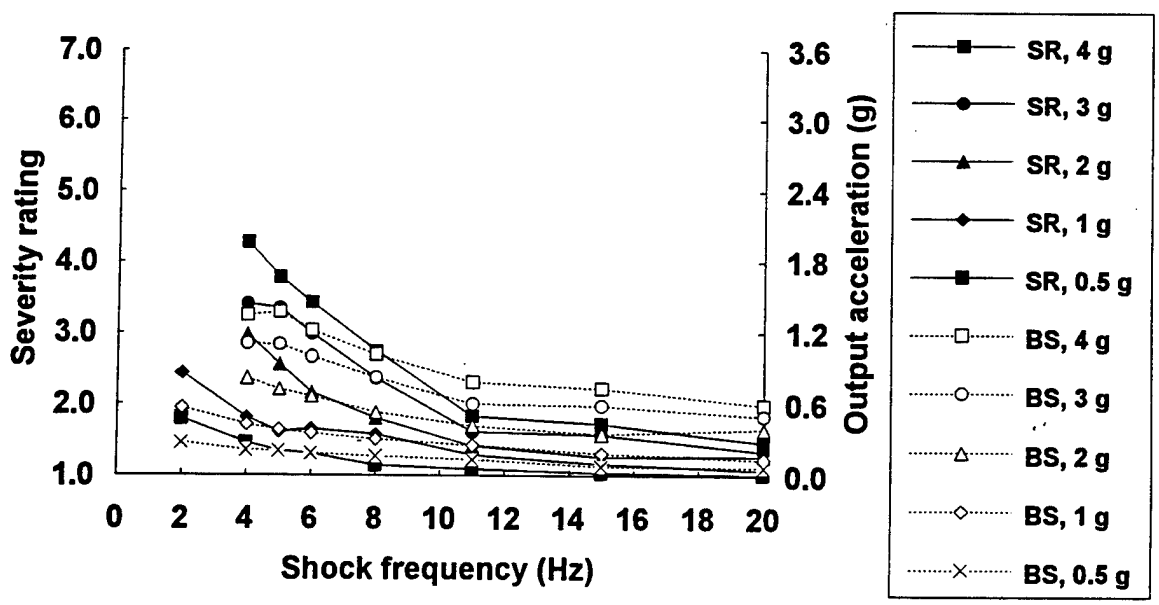

Figure F-108. Comparison between severity ratings (SR) and expected output from the BS 6841 W_d filter to positive y axis shocks.

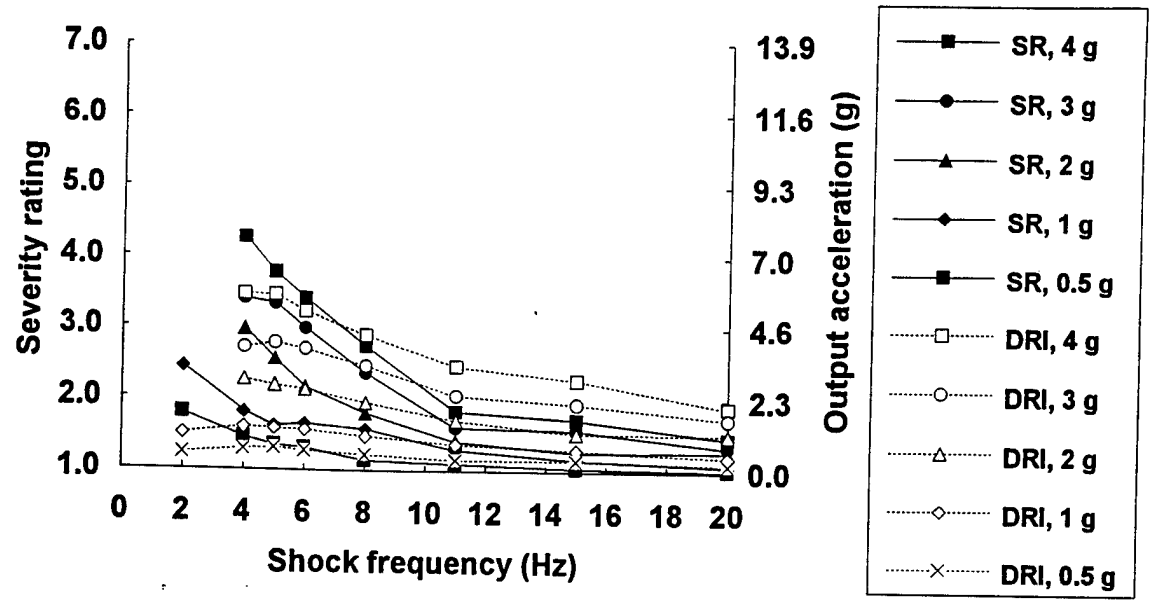

Figure F-109. Comparison between severity ratings (SR) and expected output from the DRI model (10 Hz) to positive y axis shocks.

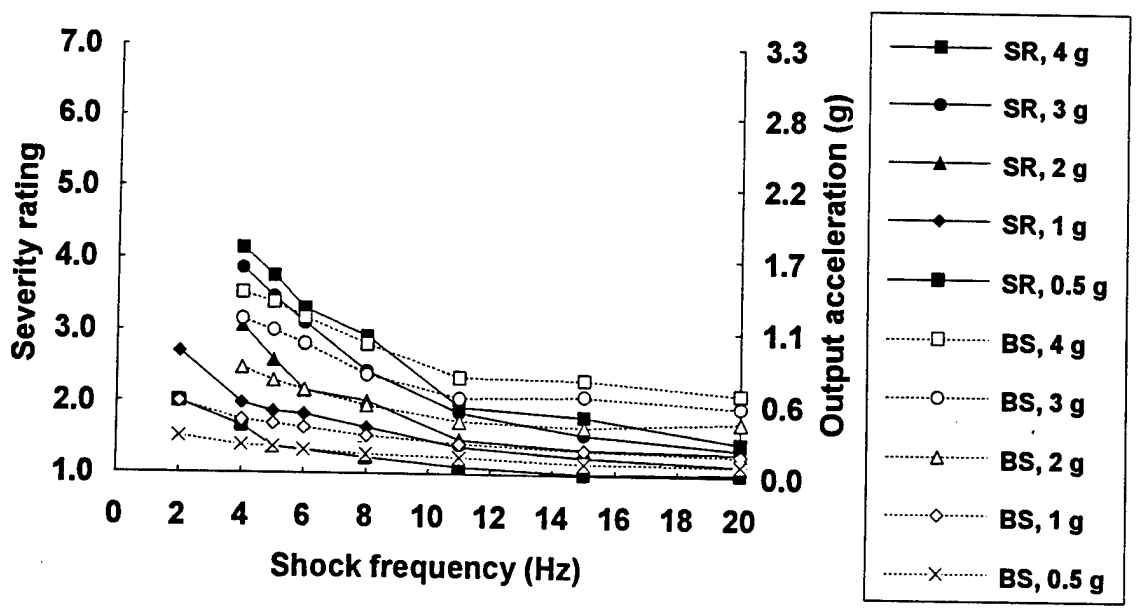

Figure F-110. Comparison between severity ratings (SR) and expected output from the BS 6841 W_d filter to negative x axis shocks.

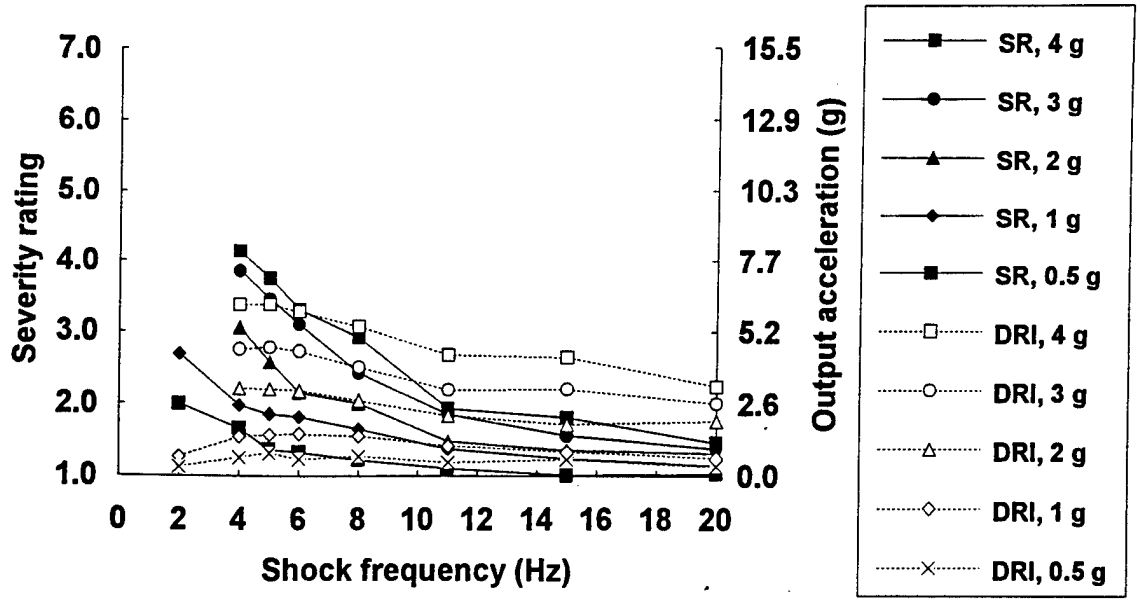

Figure F-111. Comparison between severity ratings (SR) and expected output from the DRI model (10 Hz) to negative x axis shocks.

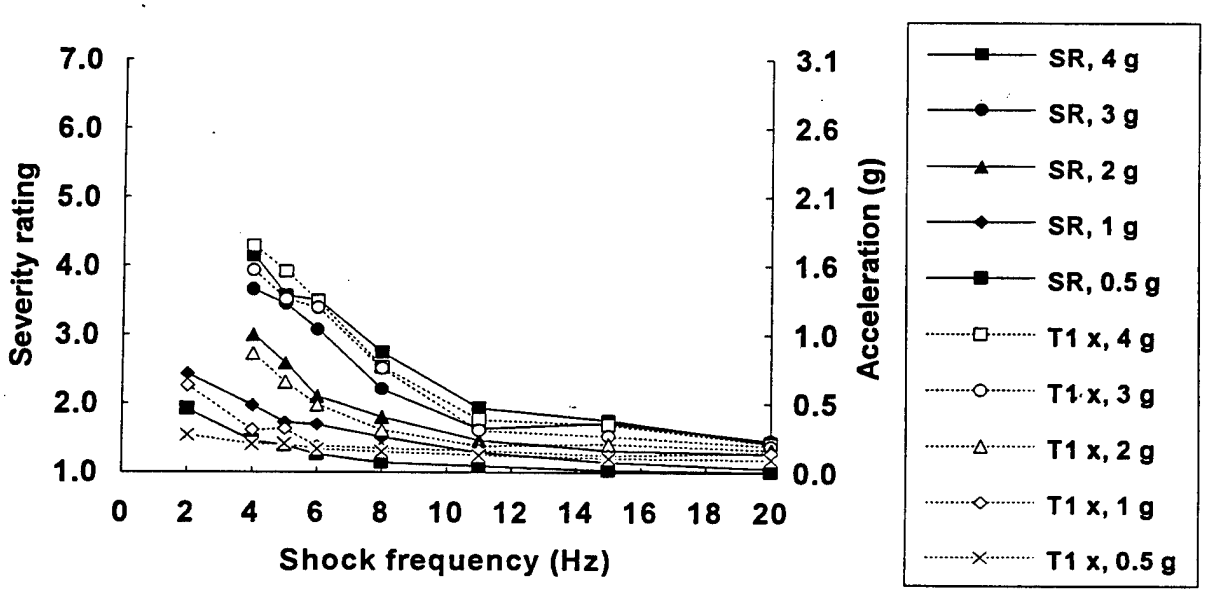

Figure F-112. Comparison between severity ratings (SR) and acceleration measured at the thoracic spine (T1) in response to positive x axis shocks (T1 x).

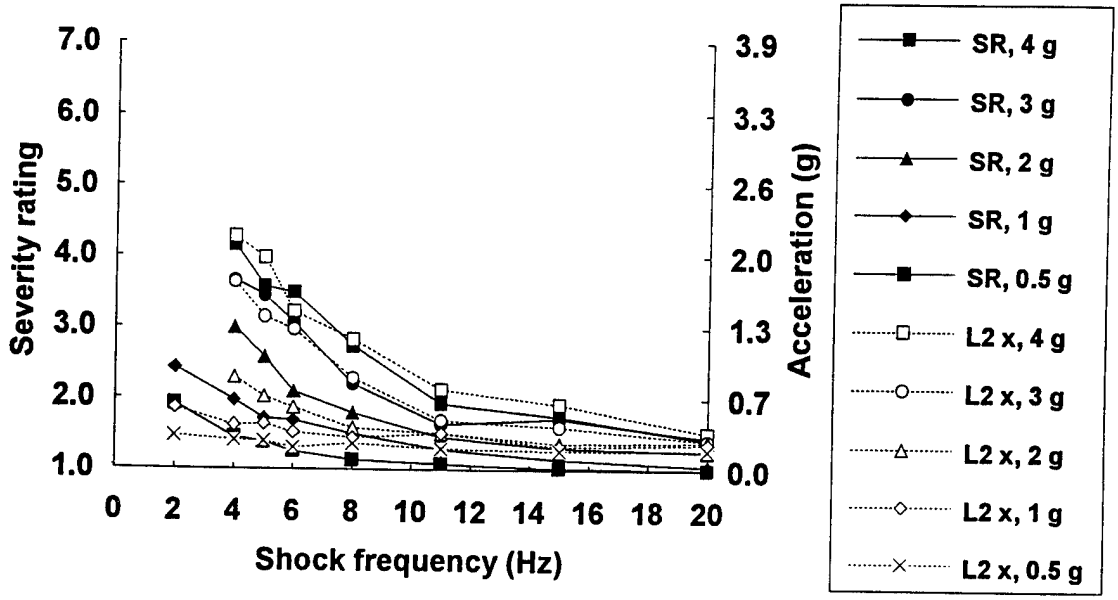

Figure F-113. Comparison between severity ratings (SR) and acceleration measured at the lumbar spine (L2) in response to positive x axis shocks (L2 x).

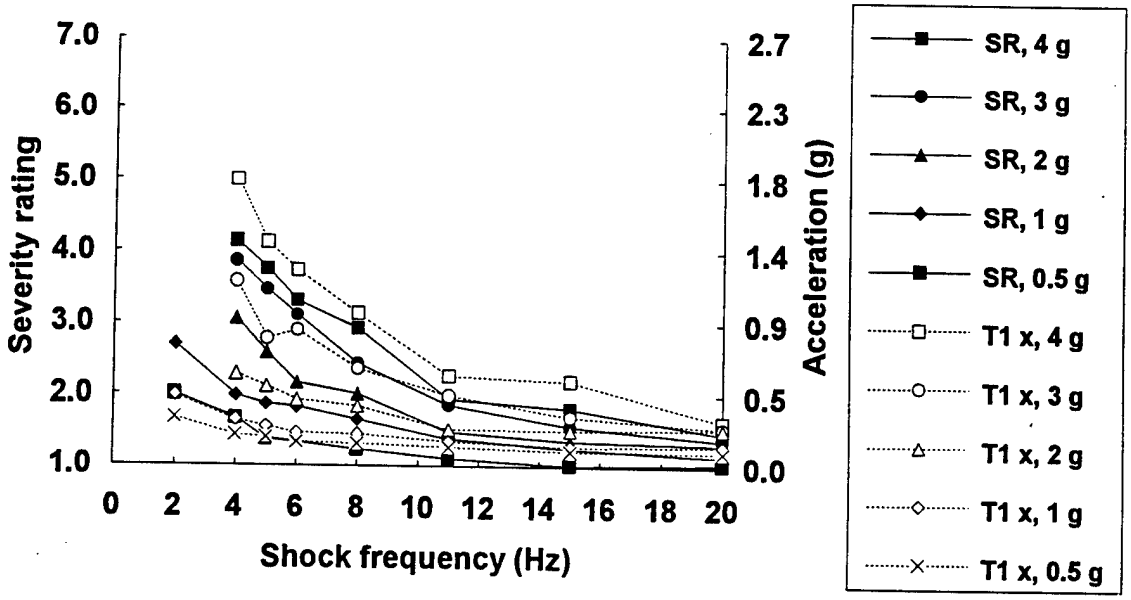

Figure F-114. Comparison between severity ratings (SR) and acceleration measured at the thoracic spine (T1) in response to negative x axis shocks (T1 x).

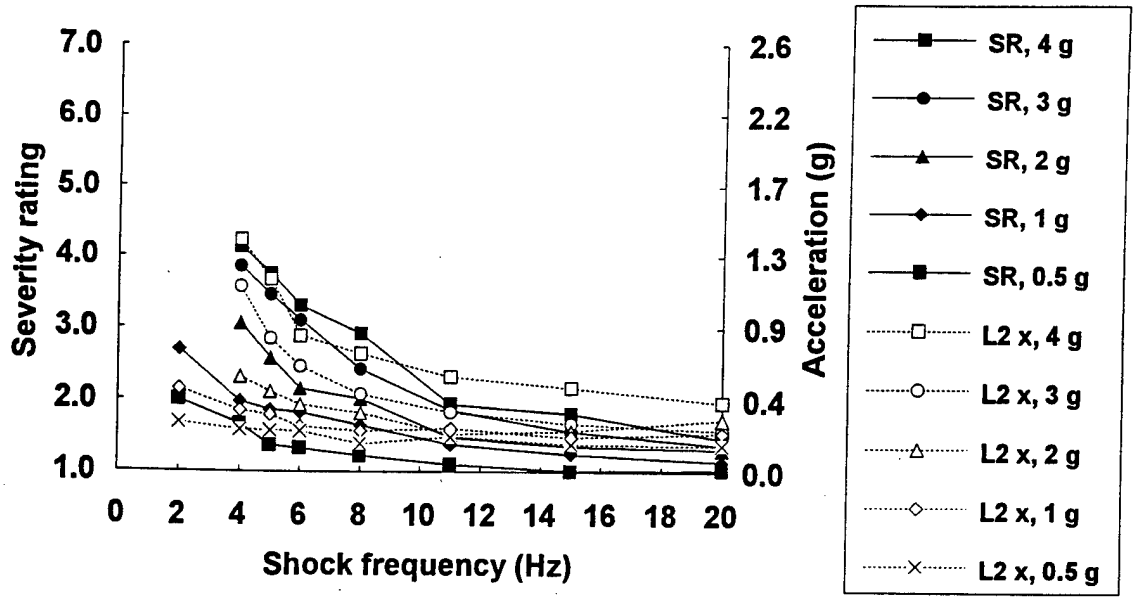

Figure F-115A. Comparison between severity ratings (SR) and acceleration measured at the lumbar spine (L2) in response to negative x axis shocks (L2 x).

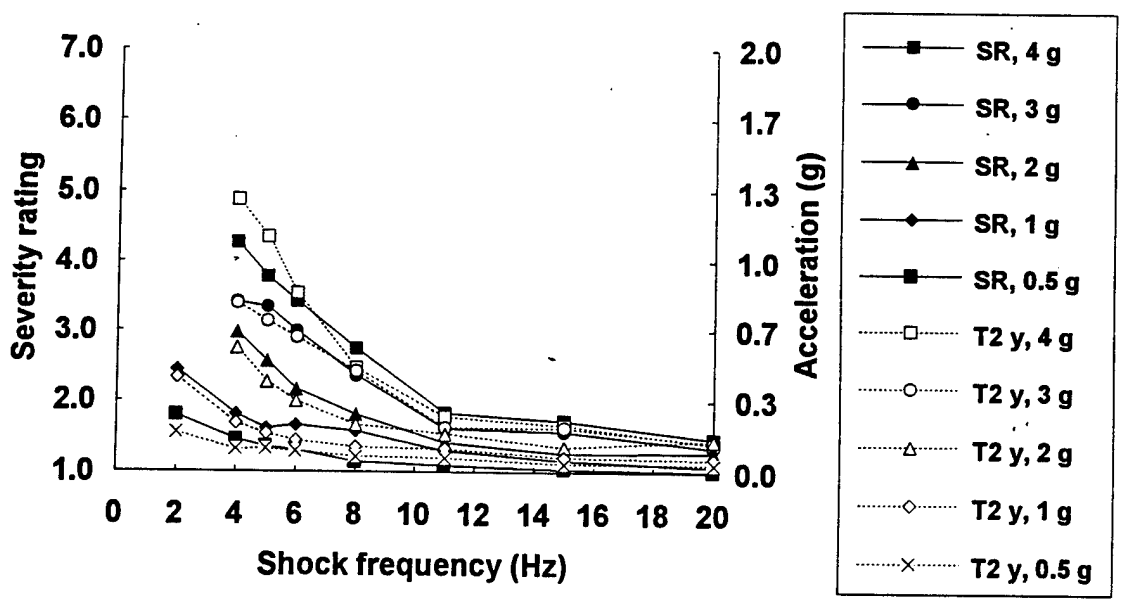

Figure F-115B. Comparison between severity ratings (SR) and acceleration measured at the thoracic spine (T2) in response to positive y axis shocks (T2 y).

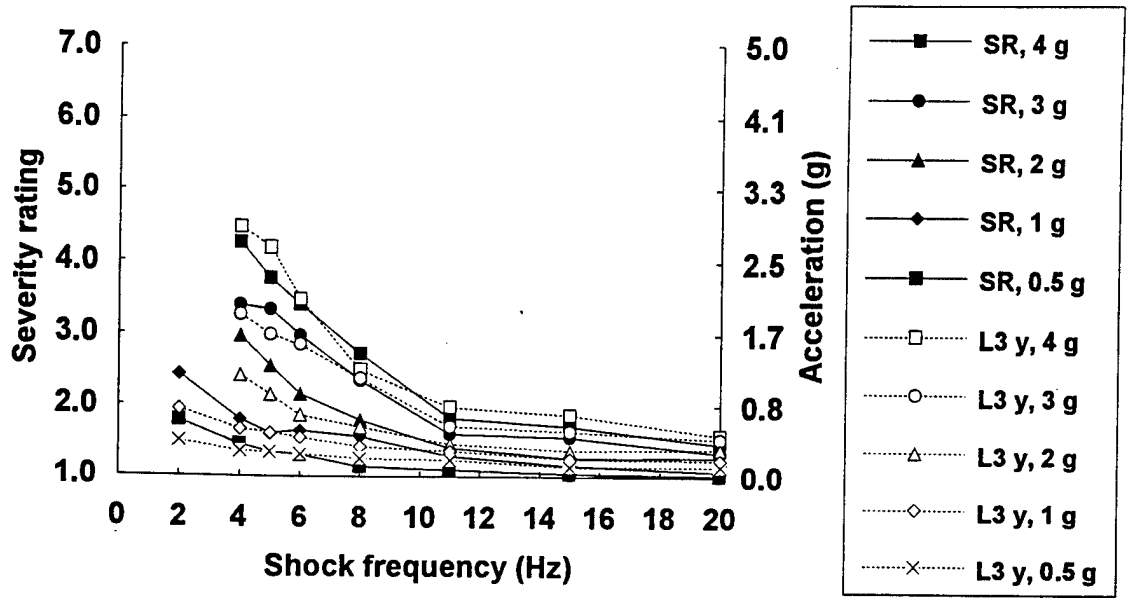

Figure F-115C. Comparison between severity ratings (SR) and acceleration measured at the lumbar spine (L3) in response to positive y axis shocks (L3 y).

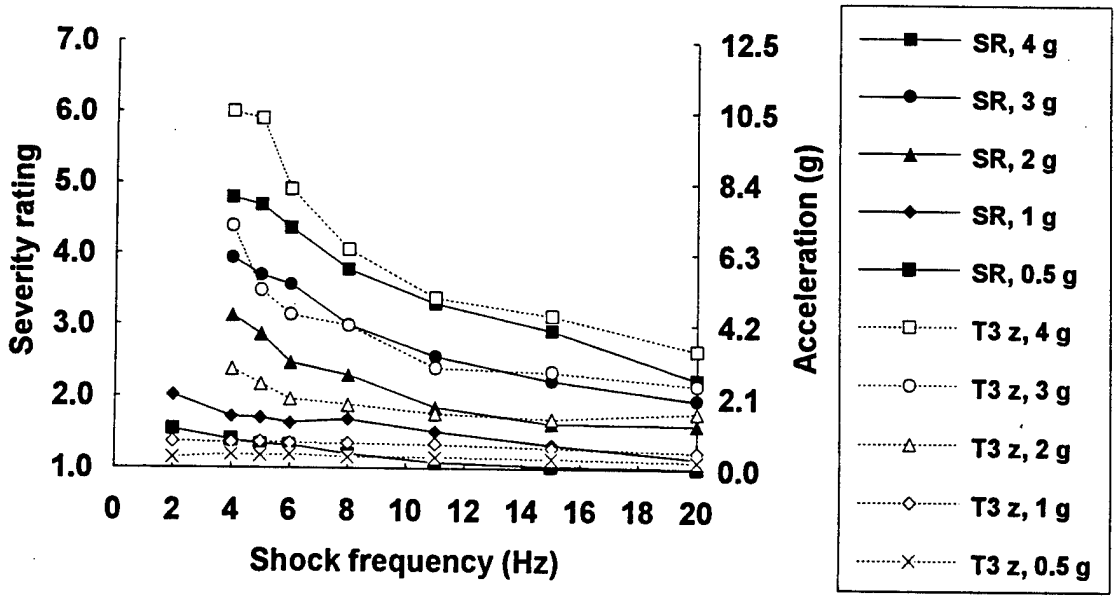

Figure F-116. Comparison between severity ratings (SR) and acceleration measured at the thoracic spine (T3) in response to positive z axis shocks (T3 z).

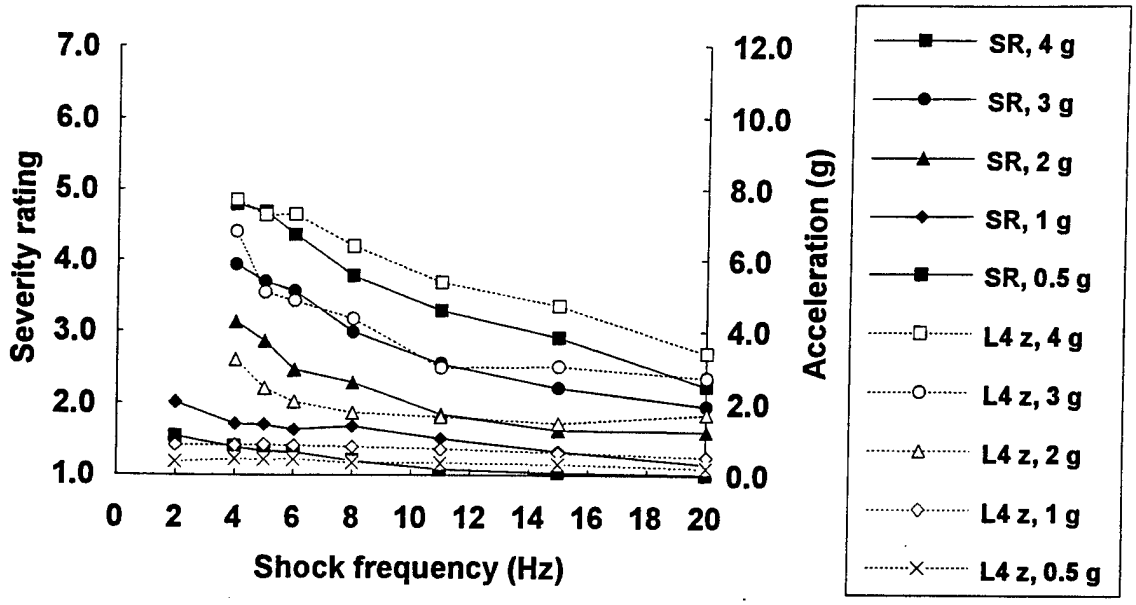

Figure F-117. Comparison between severity ratings (SR) and acceleration measured at the lumbar spine (L4) in response to positive z axis shocks (L4 z).

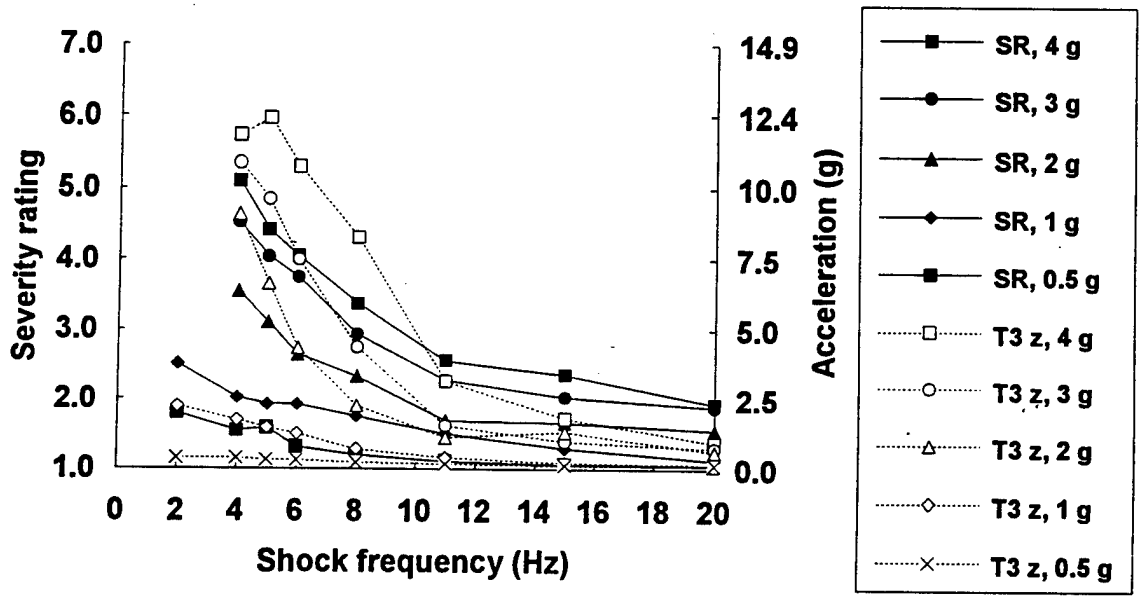

Figure F-118. Comparison between severity ratings (SR) and acceleration measured at the thoracic spine (T3) in response to negative z axis shocks (T3 z).

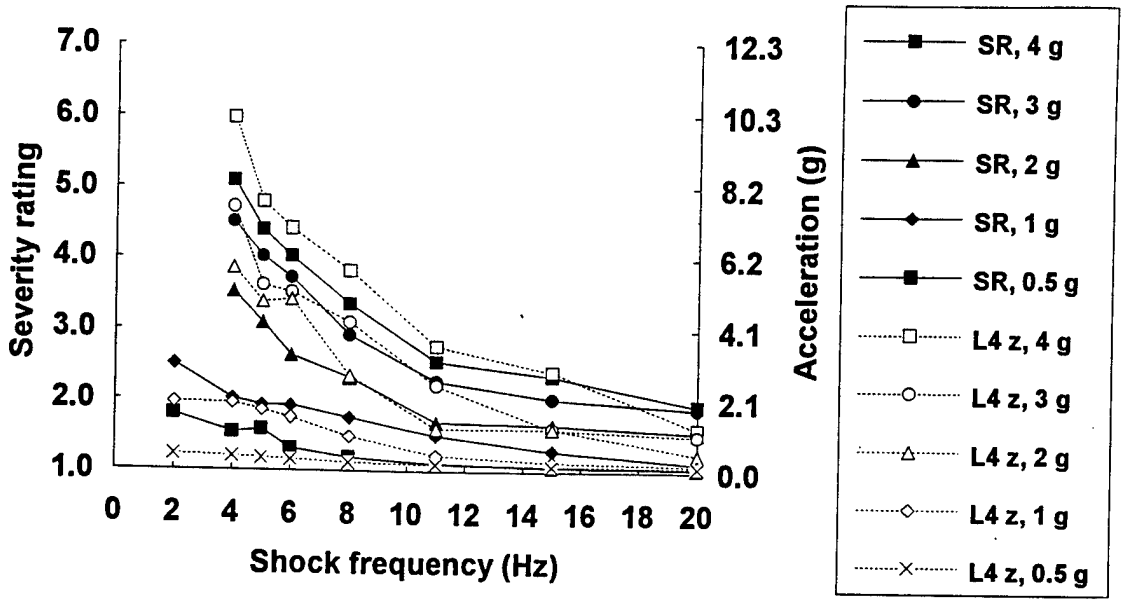

Figure F-119. Comparison between severity ratings (SR) and acceleration measured at the lumbar spine (L4) in response to negative z axis shocks (L4 z).

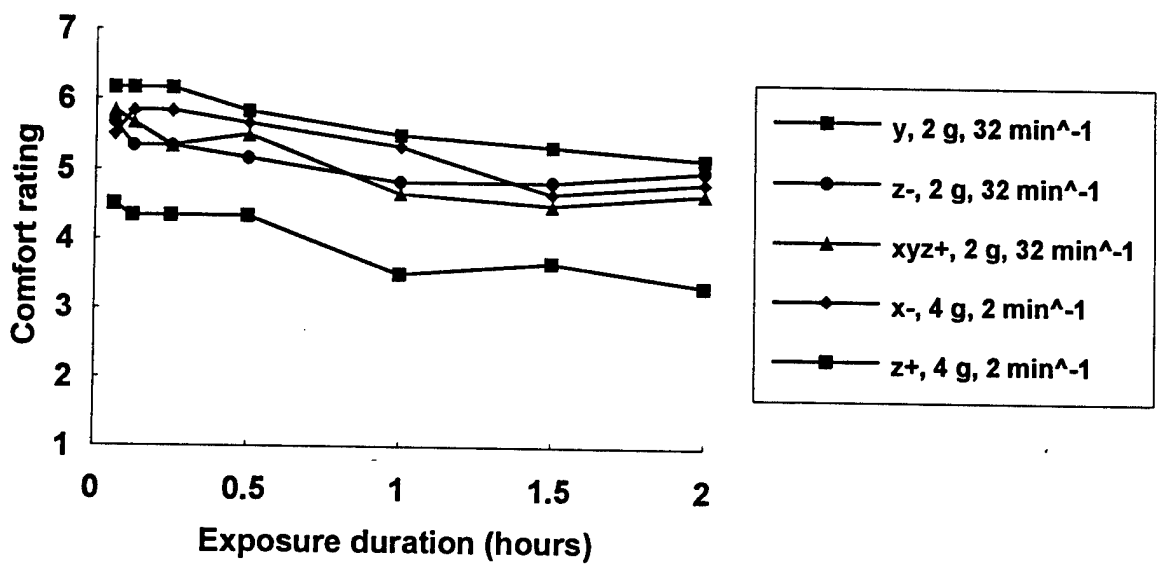

Figure F-120. Subjective comfort ratings as a function of exposure duration for 2 hour repeated shock exposures.

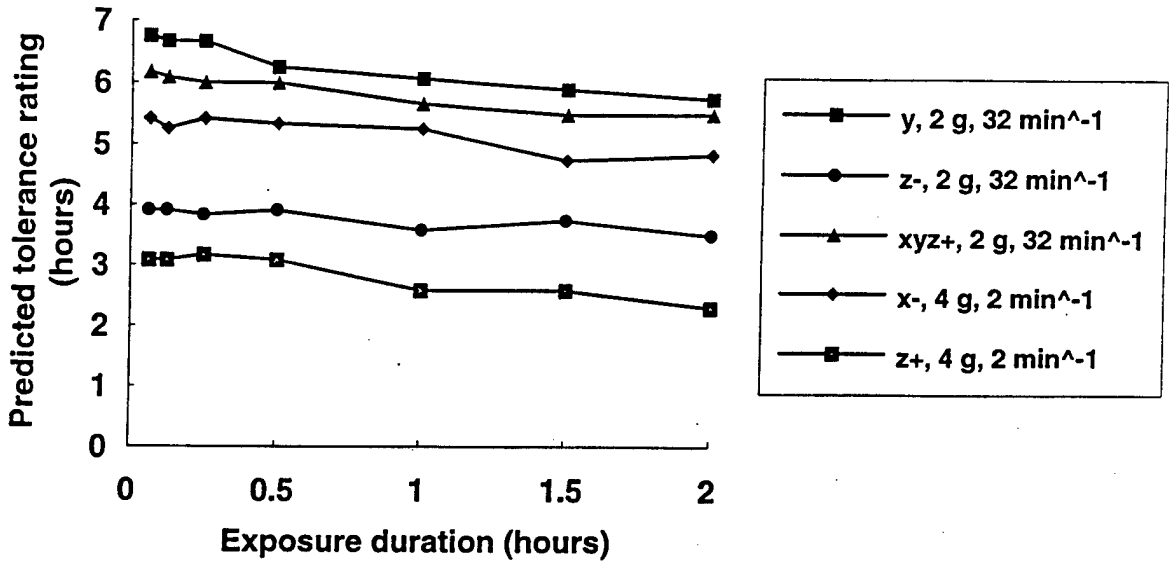

Figure F-121. Subjective predicted tolerance ratings as a function of exposure duration for 2 hour repeated shock exposures.

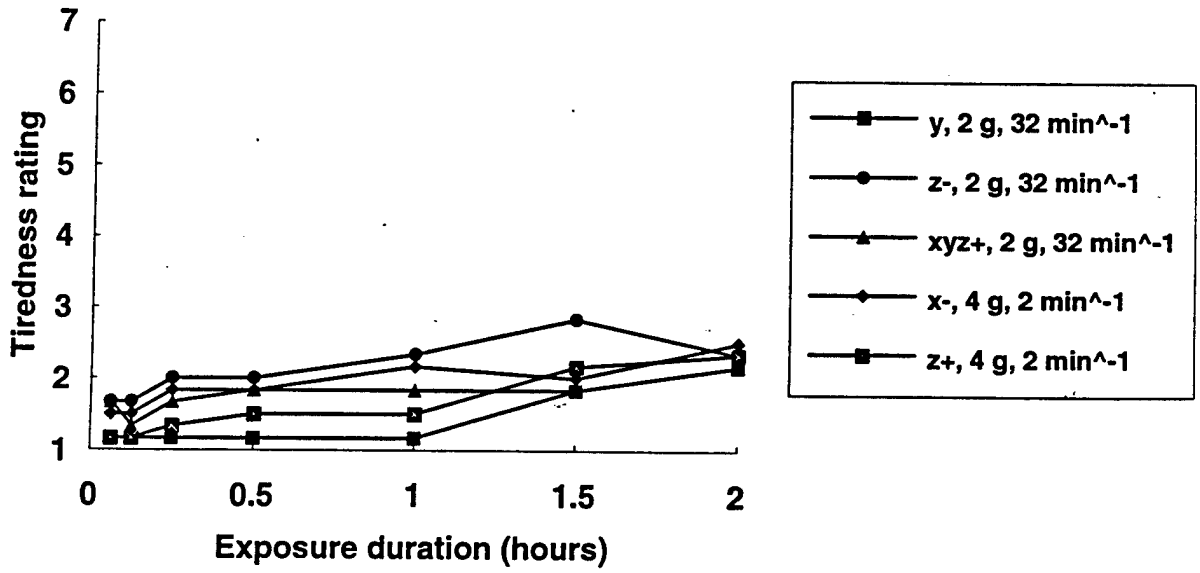

Figure F-122. Subjective tiredness ratings as a function of exposure duration for 2 hour repeated shock exposures.

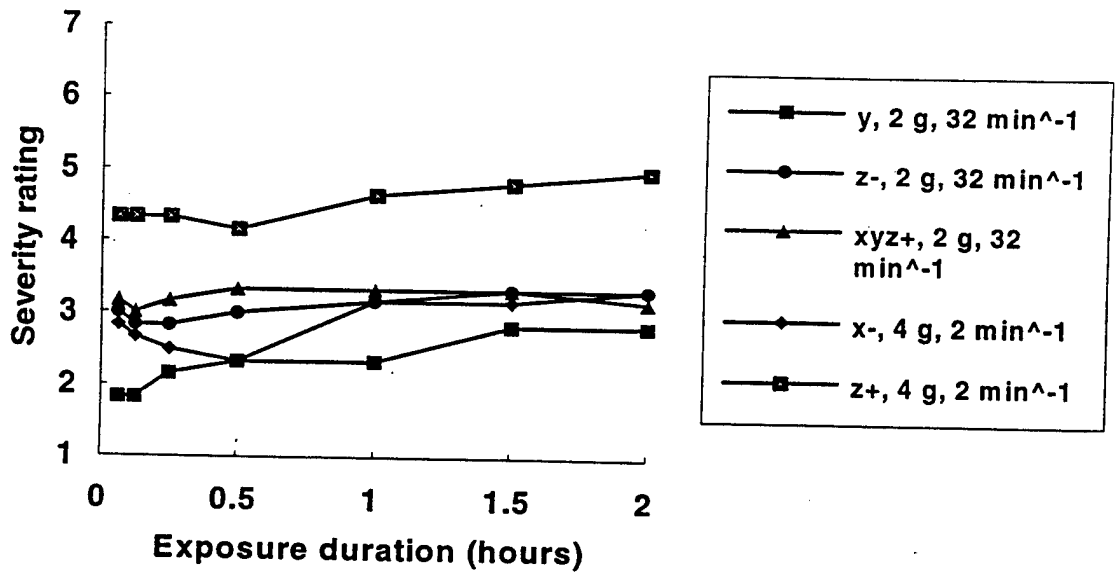

Figure F-123. Subjective severity ratings as a function of exposure duration for 2 hour repeated shock exposures.

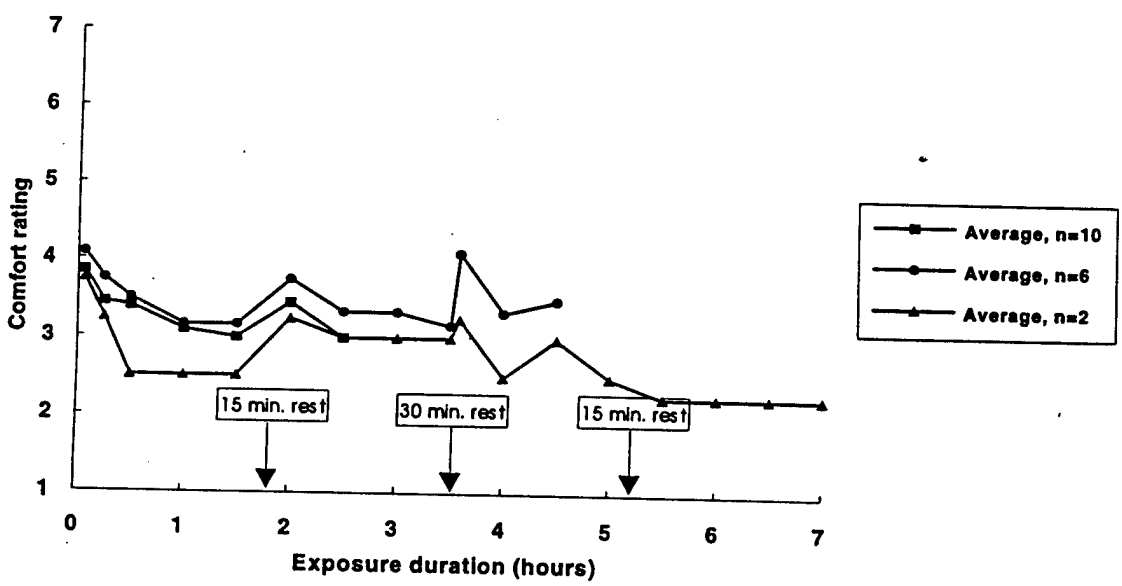

Figure F-124. Subjective comfort ratings as a function of exposure duration for a 7 hour repeated shock exposure.

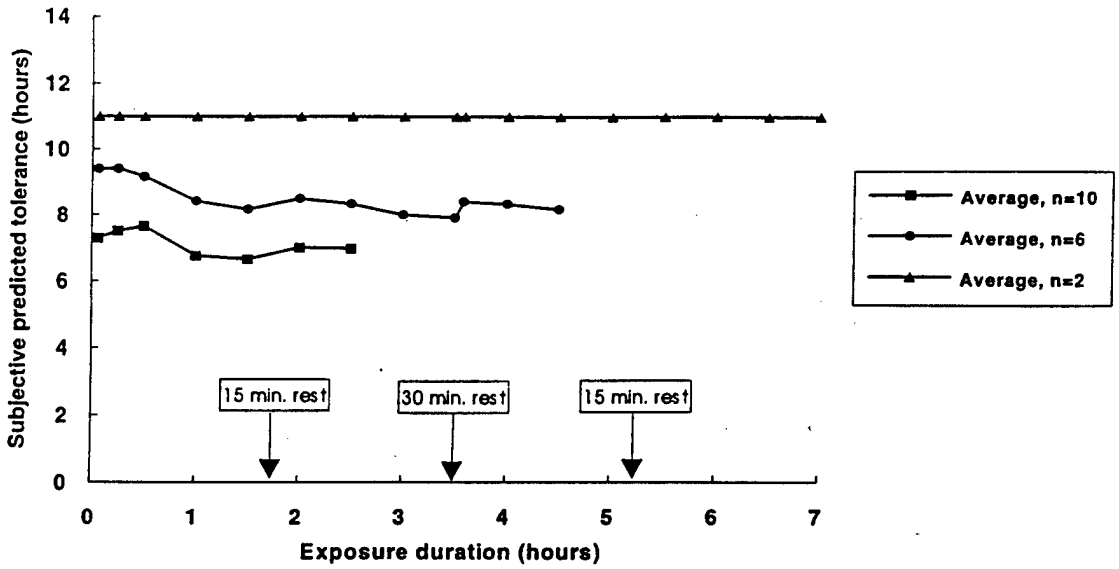

Figure F-125. Subjective predicted tolerance ratings as a function of exposure duration for a 7 hour repeated shock exposure.

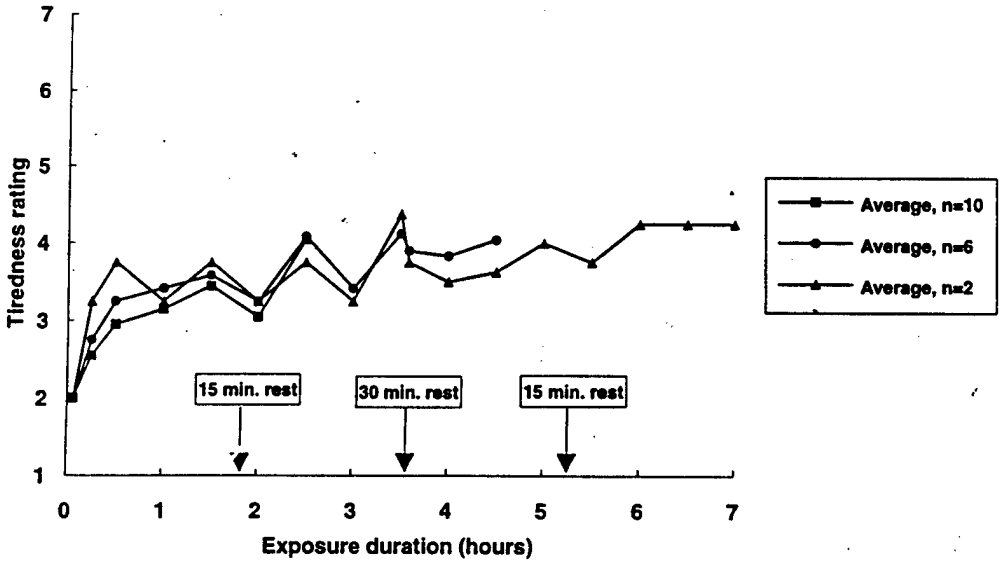

Figure F-126. Subjective tiredness ratings as a function of exposure duration for a 7 hour repeated shock exposure.

Figure F-126. Subjective tiredness ratings as a function of exposure duration for a 7 hour repeated shock exposure.

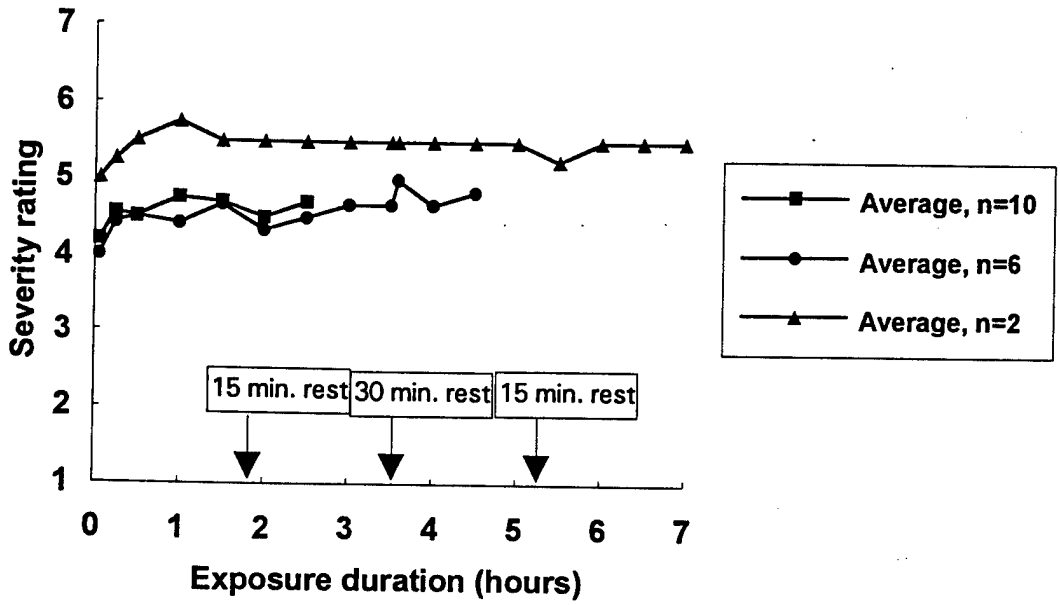

Figure F-127. Subjective severity ratings as a function of exposure duration for a 7 hour repeated shock exposure.

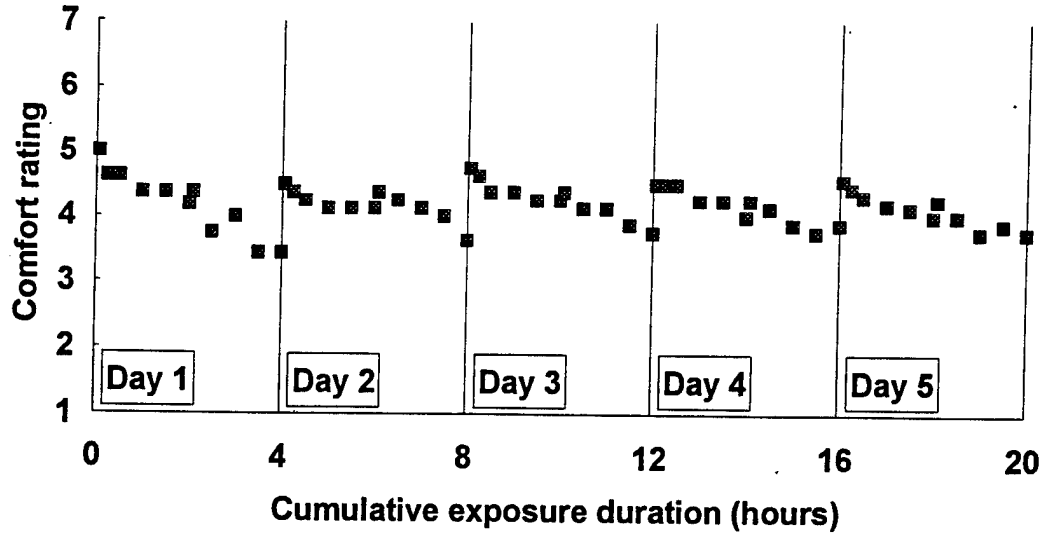

Figure F-128. Subjective comfort ratings as a function of cumulative exposure duration for 4 hour repeated shock exposures in five consecutive days.

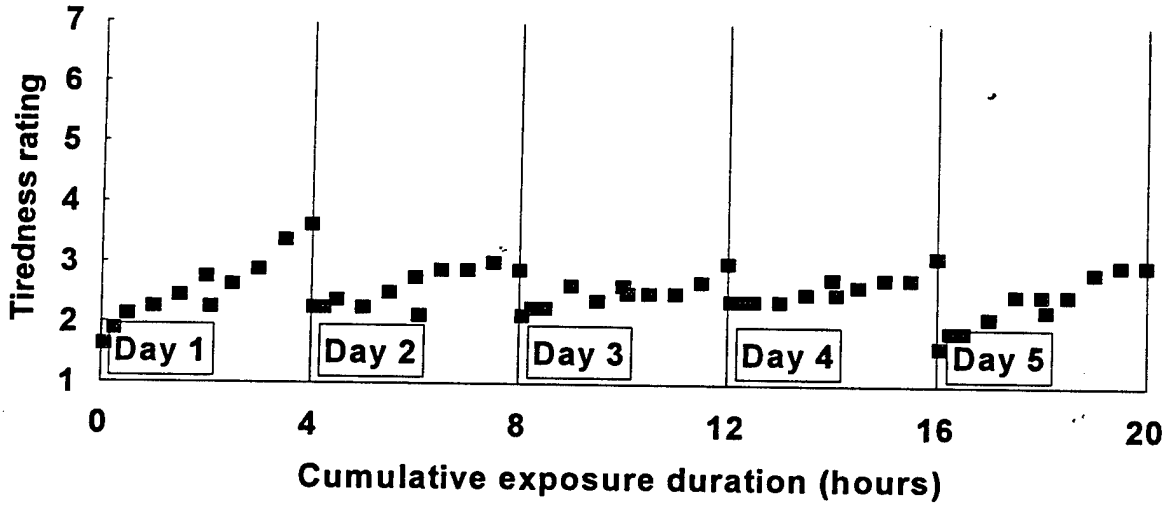

Figure F-129. Subjective tiredness ratings as a function of cumulative exposure duration for 4 hour repeated shock exposures in five consecutive days.

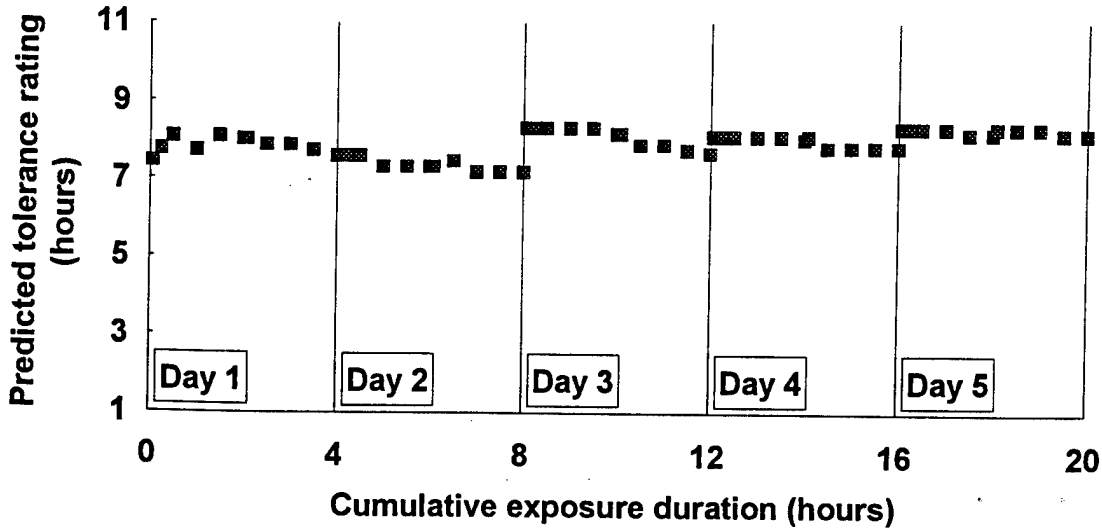

Figure F-130. Subjective predicted tolerance ratings as a function of cumulative exposure duration for 4 hour repeated shock exposures in five consecutive days.

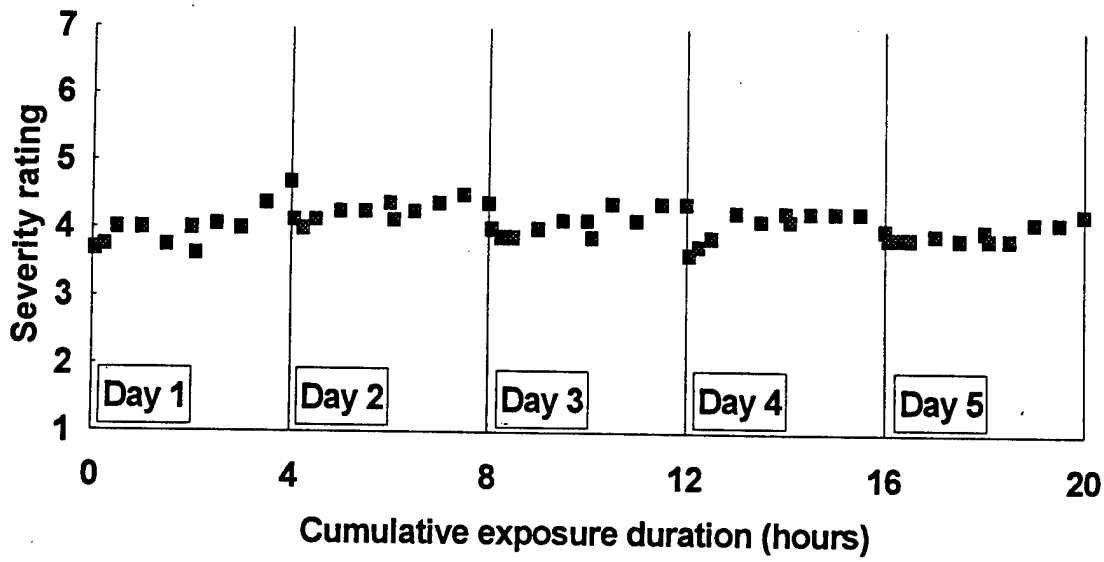

Figure F-131. Subjective severity ratings as a function of cumulative exposure duration for 4 hour repeated shock exposures in five consecutive days.

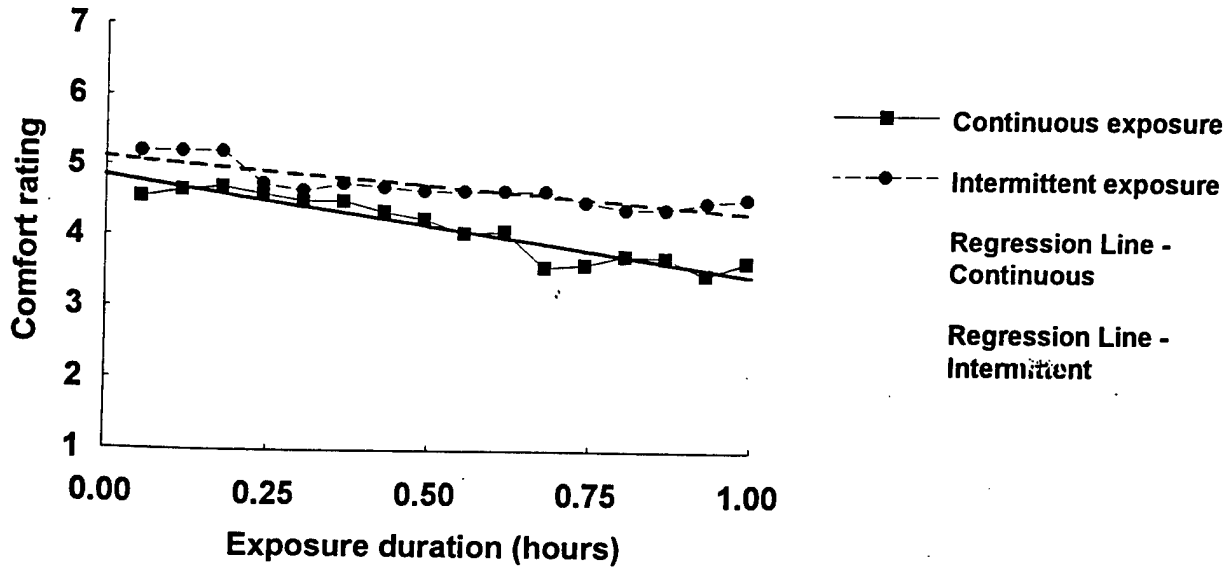

Figure F-132. Comparison between subjective comfort ratings to continuous and intermittent shock exposures.

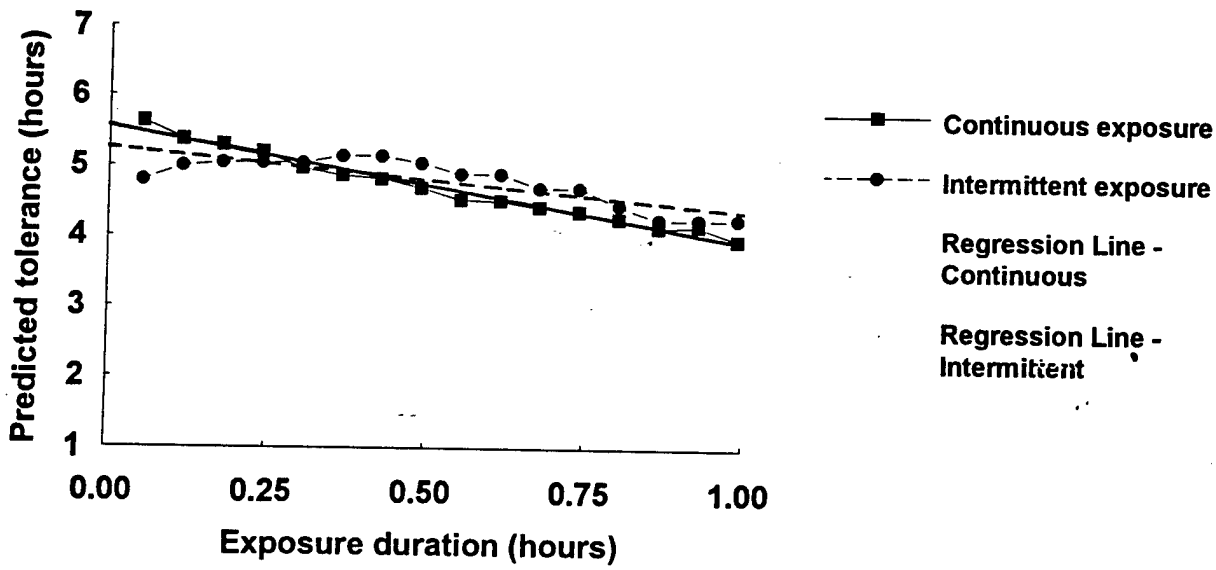

Figure F-133. Comparison between subjective predicted tolerance ratings to continuous and intermittent shock exposures.

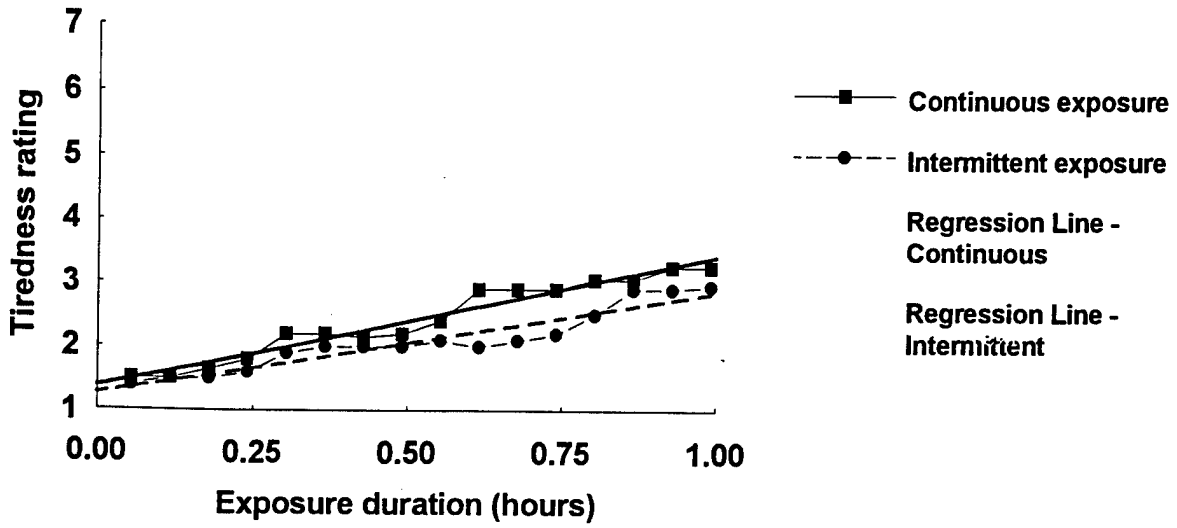

Figure F-134. Comparison between subjective tiredness ratings to continuous and intermittent shock exposures.

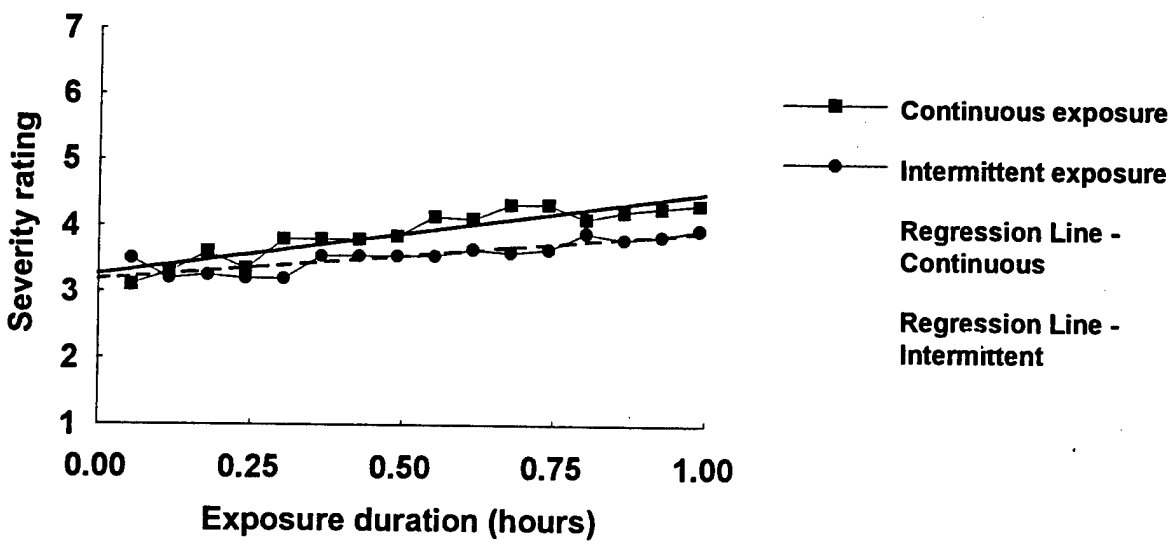

Figure F-135. Comparison between subjective severity ratings to continuous and intermittent shock exposures.

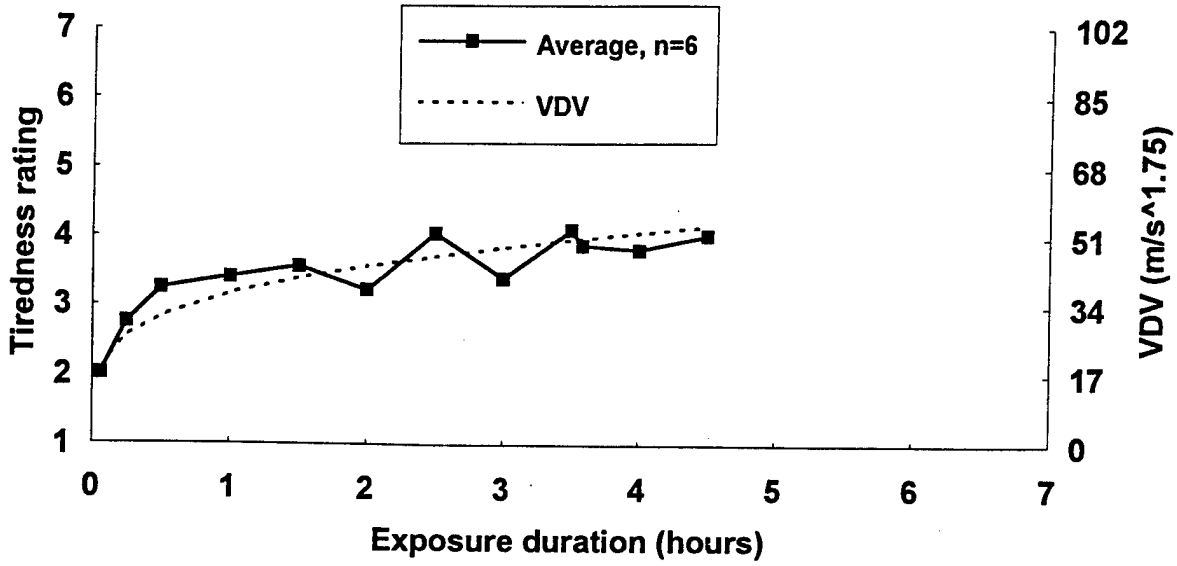

Figure F-136. Comparison of tiredness ratings and the VDV as a function of time for a prolonged exposure to repeated shocks.

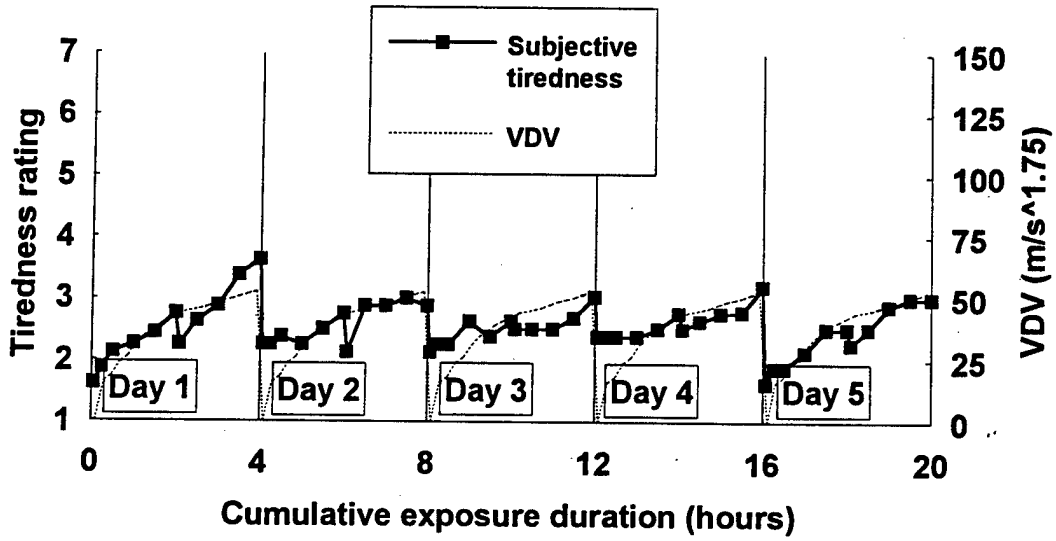

Figure F-137. Comparison between subjective tiredness ratings and the VDV as a function of cumulative exposure duration for 4 hour repeated shock exposures in five consecutive days.

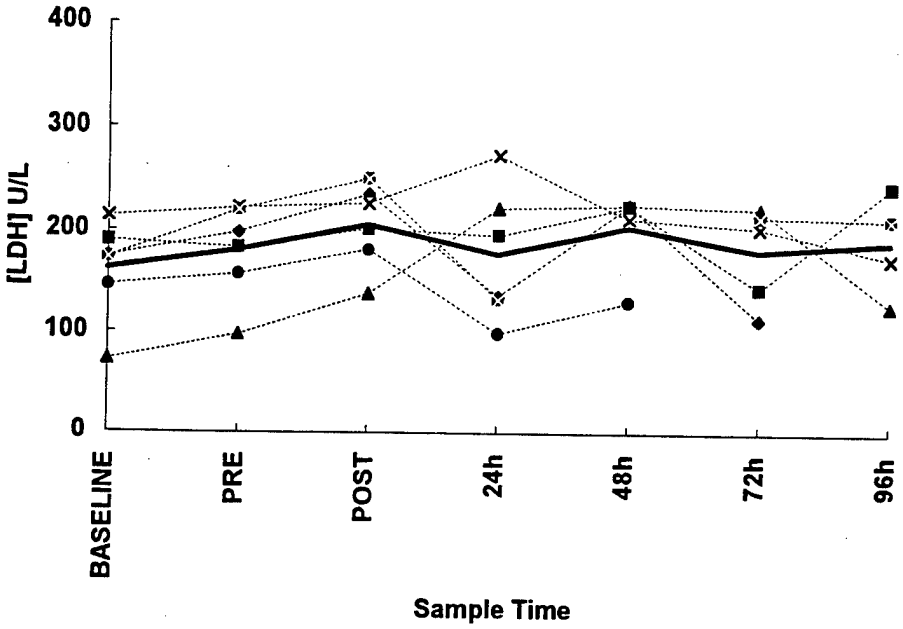

Figure F-138. The individual subject responses of blood lactate dehydrogenase (LDH) in Experiment LT2 with a motion exposure including 4 g shocks in the -x axis.

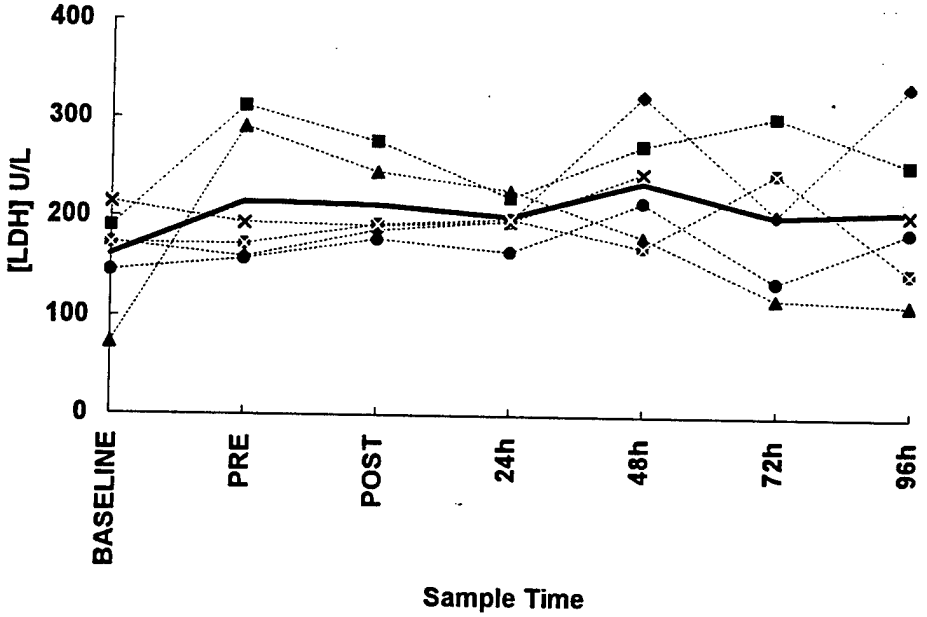

Figure F-139. The individual subject responses of blood lactate dehydrogenase (LDH) in Experiment LT2 with a motion exposure including 4 g shocks in the +z axis.

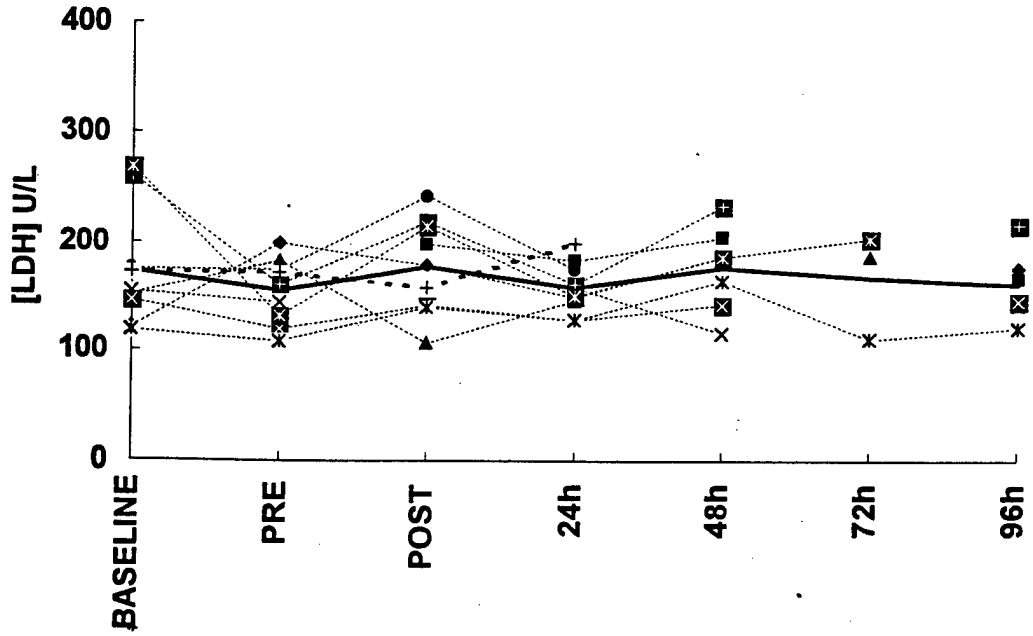

Figure F-140. The individual subject responses of blood lactate dehydrogenase (LDH) in Experiment LT3 with up to 7 hours of motion exposure including 2 and 4 g shocks in ± x, y and z axes.

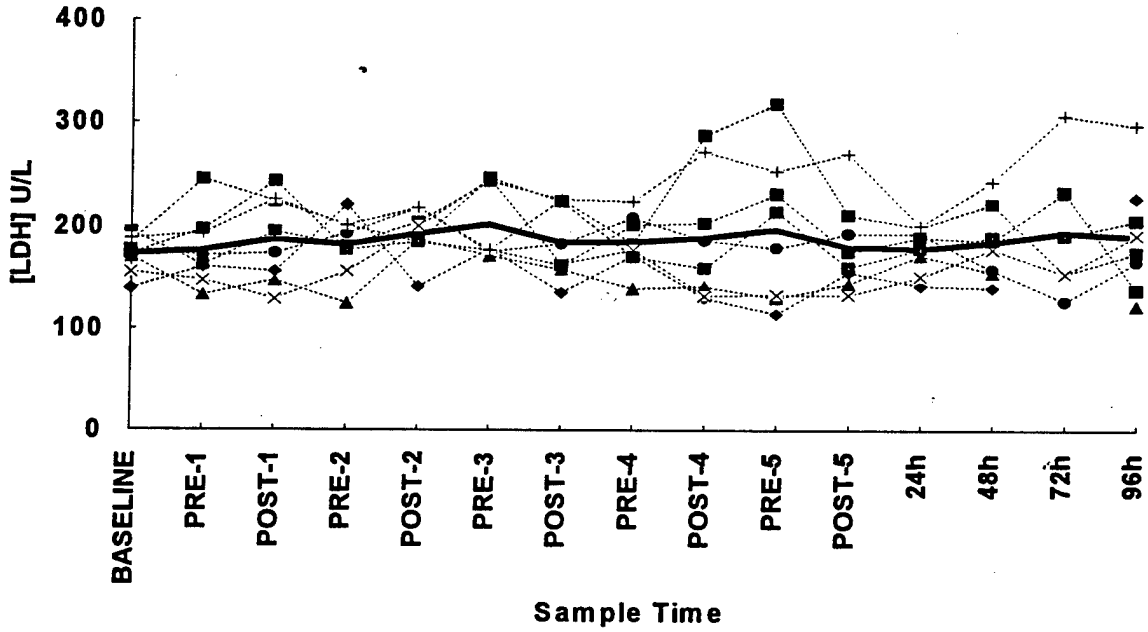

Figure F-141. The individual subject responses of blood lactate dehydrogenase (LDH) in Experiment LT4 with up to 5 days of 4 hours per day of motion exposure including 2 and 4 g shocks in ± x, y and z axes.

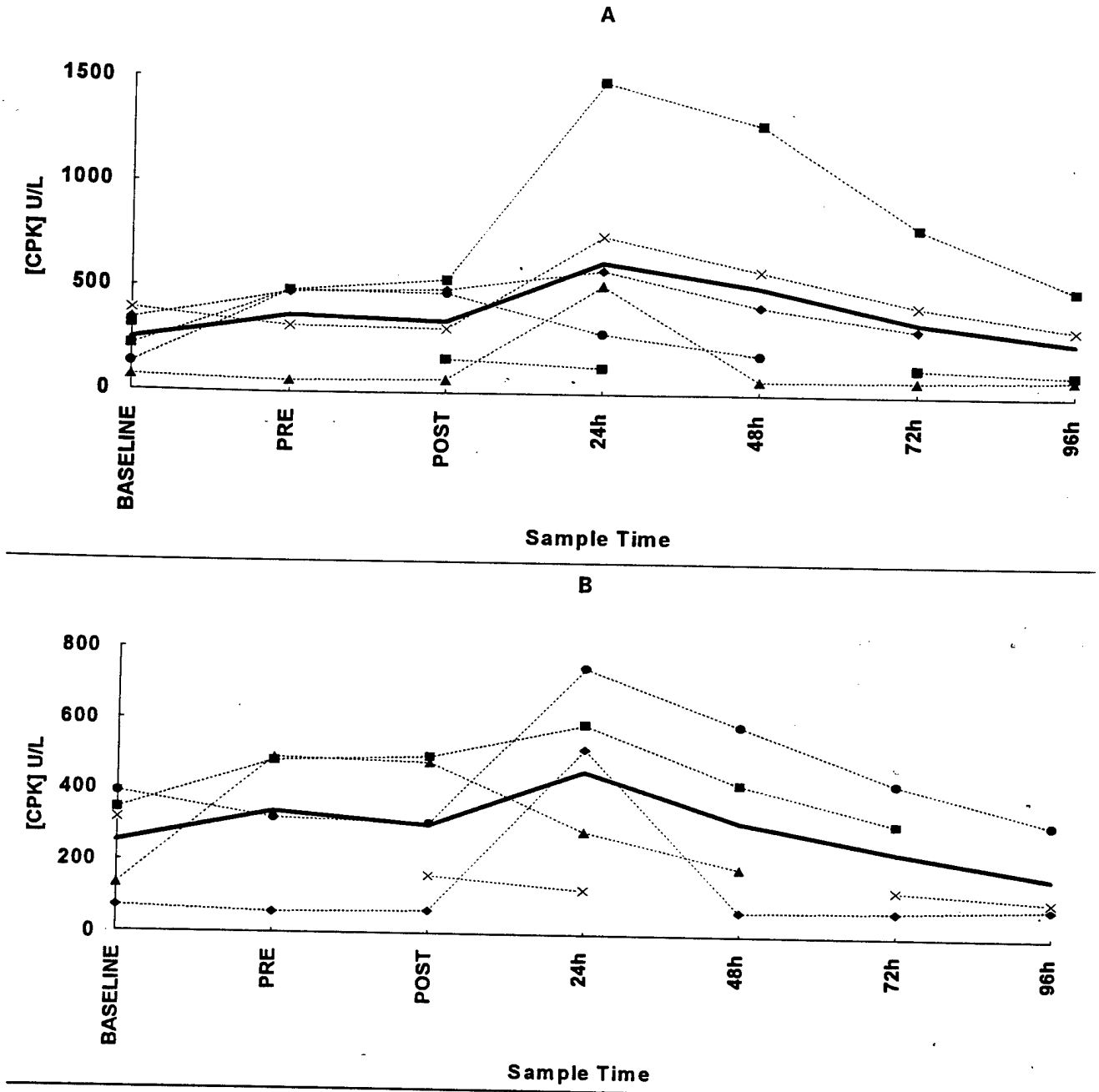

Figure F-142: The individual subject responses of blood creatine phosphokinase (CPK) in Experiment LT2 with a motion exposure including 4 g shocks in the -x axis. Graph A includes data from all subjects (n=10). In graph B, the data for one subject, who had consistent clinically elevated CPK, are eliminated (n=9).

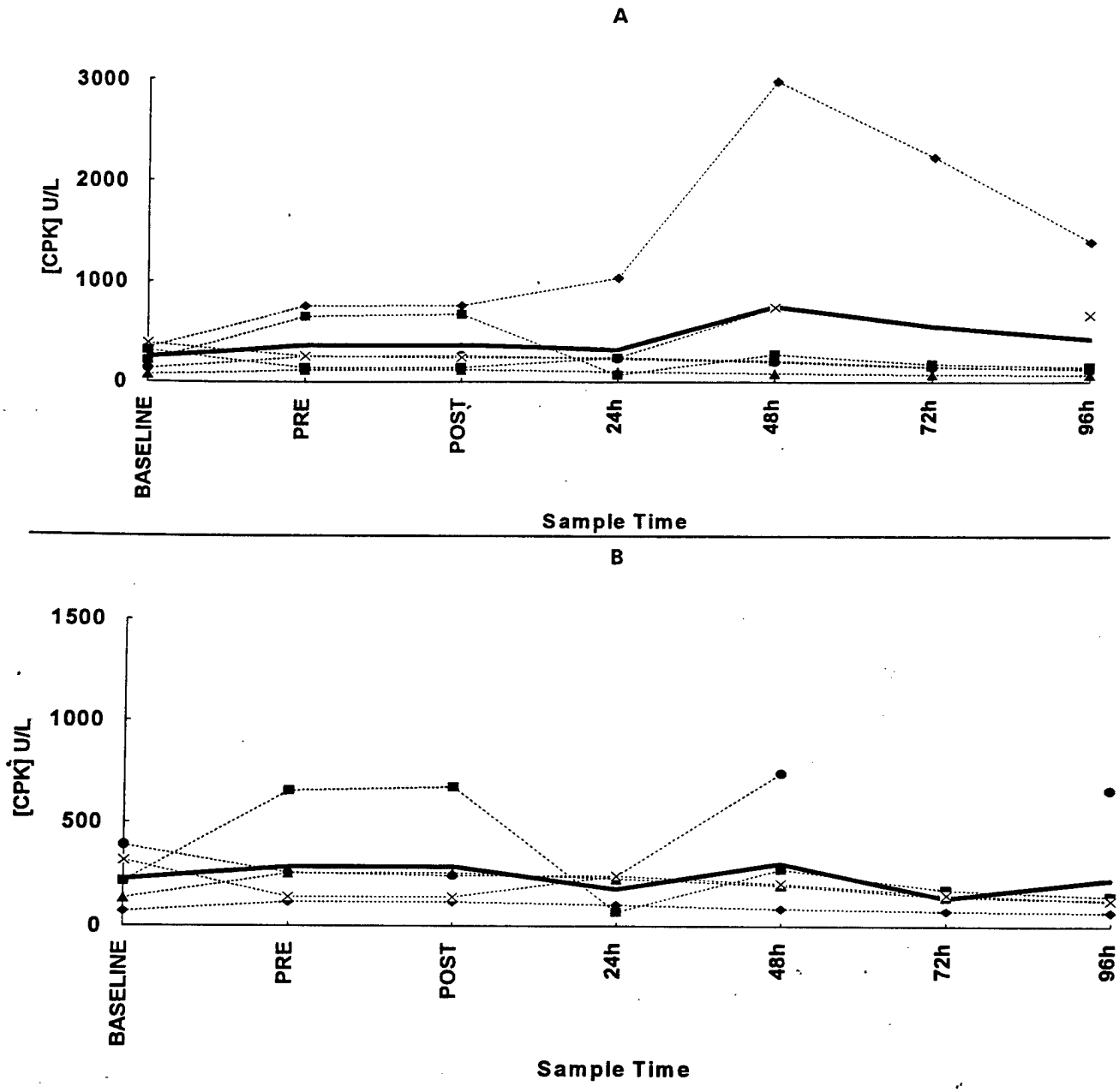

Figure F-143. The individual subject responses of blood creatine phosphokinase (CPK) in Experiment LT2 with a motion exposure including 4 g shocks in the +z axis. Graph A includes data from all subjects (n=10). In graph B, the data for one subject, who had consistent clinically elevated CPK, are eliminated (n=9).

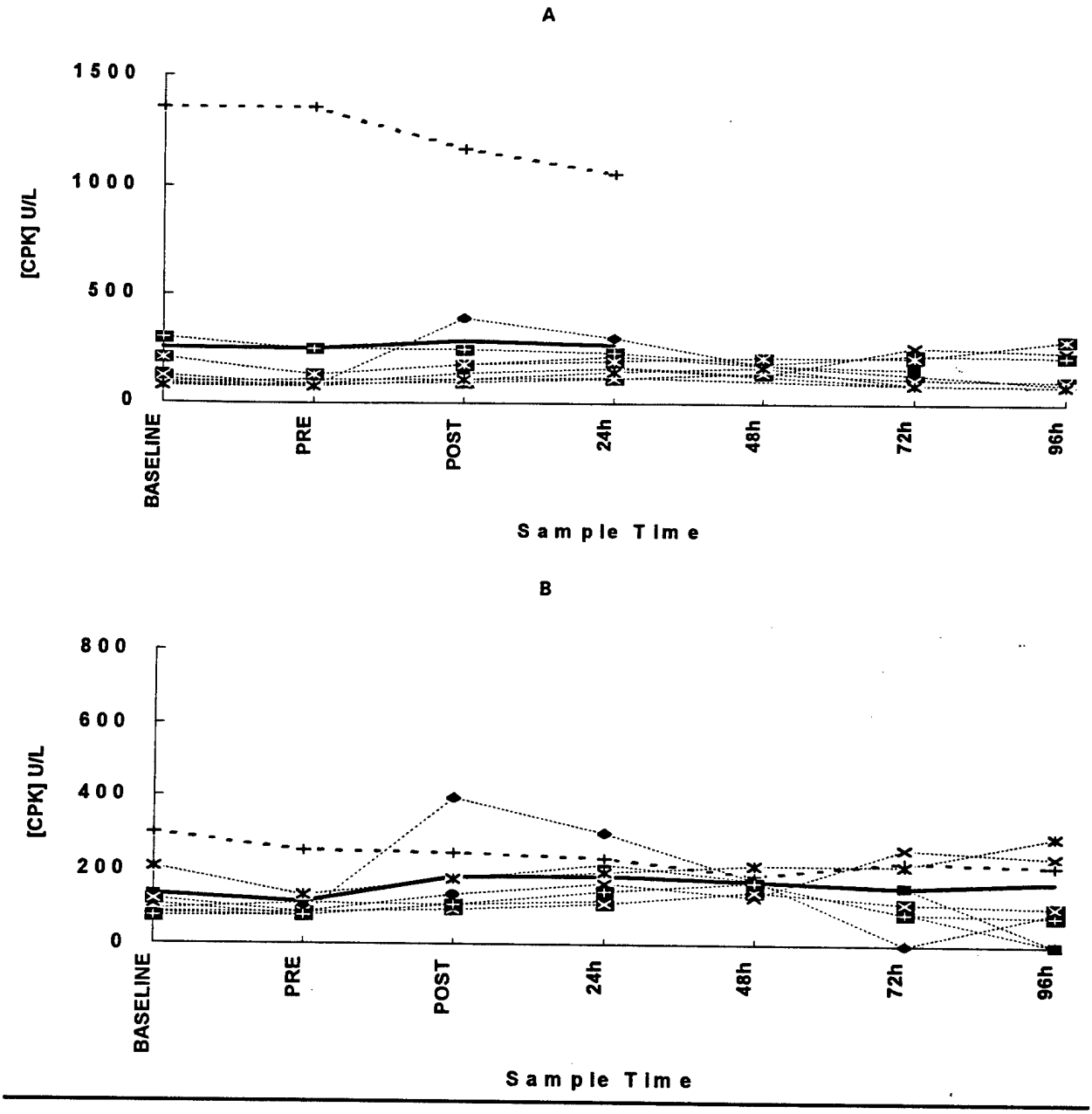

Figure F-144. The individual subject responses of blood creatinine phosphokinase (CPK) in Experiment LT3 with up to 7 hours of motion exposure including 2 and 4 g shocks in ± x, y and z axes. Graph A includes data from all subjects (n=10). In graph B, the data for one subject who had consistent clinically elevated CPK, are eliminated (n=9).

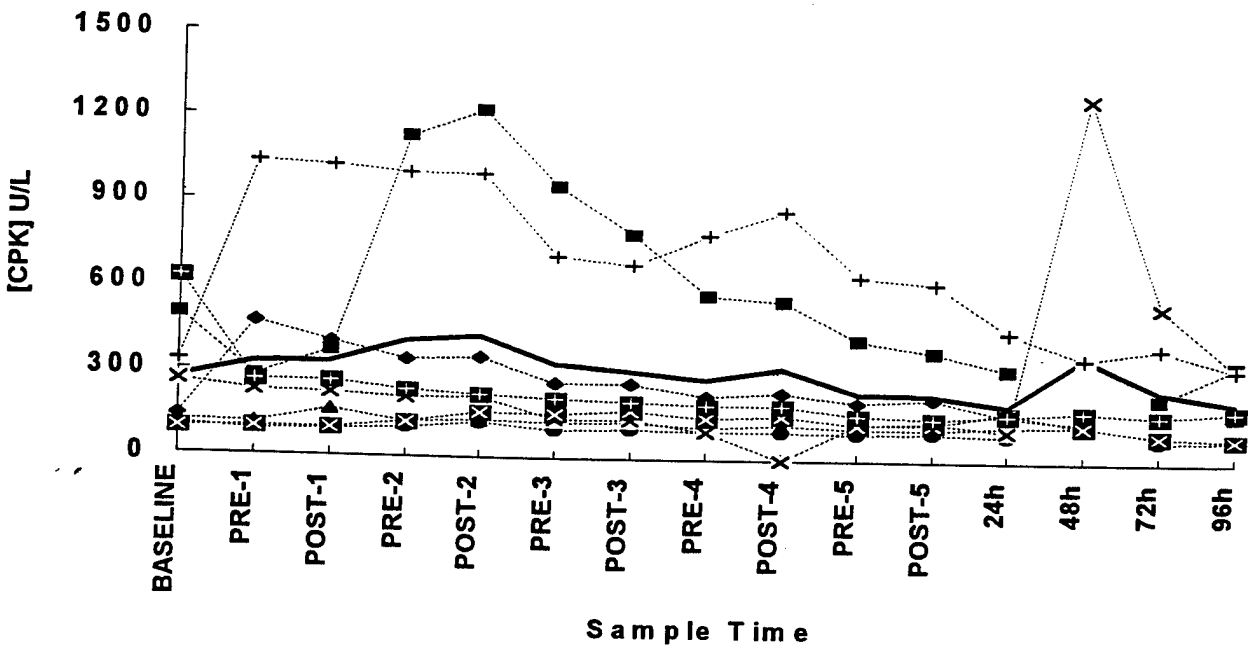

Figure F-145. The individual subject responses of blood creatine phosphokinase (CPK) in Experiment LT4 with up to 5 days of 4 hours per day of motion exposure including 2 and 4 g shocks in ± x, y and z axes.

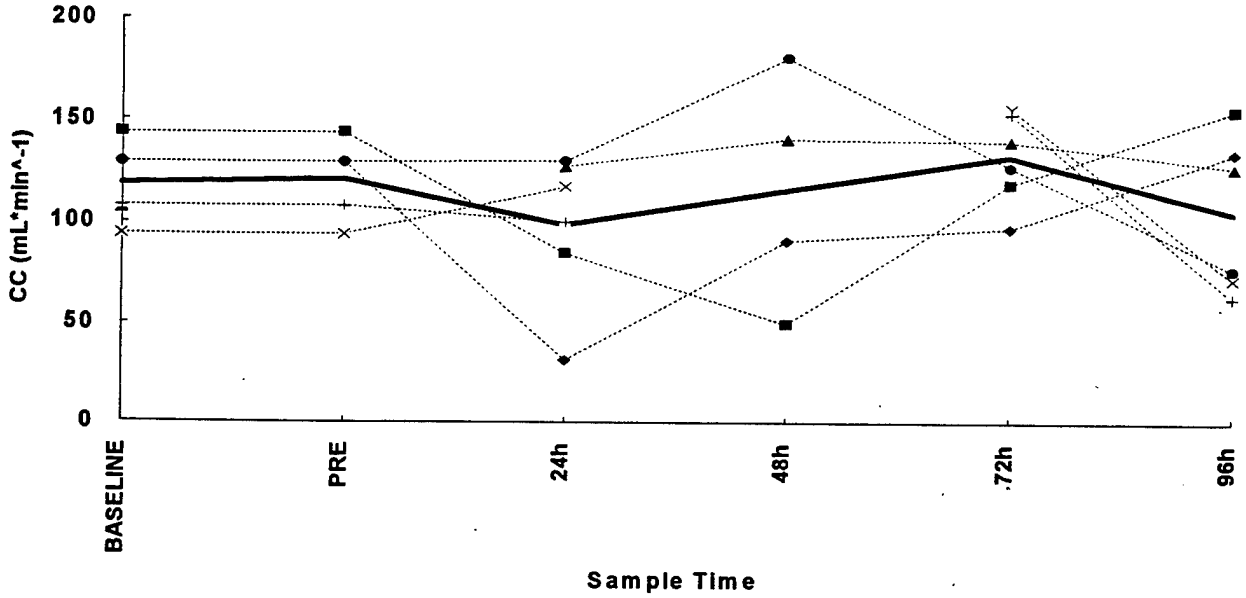

Figure F-146. The individual subject responses of Creatinine Clearance (CC) in Experiment LT2 with a motion exposure including 4 g shocks in the -x axis.

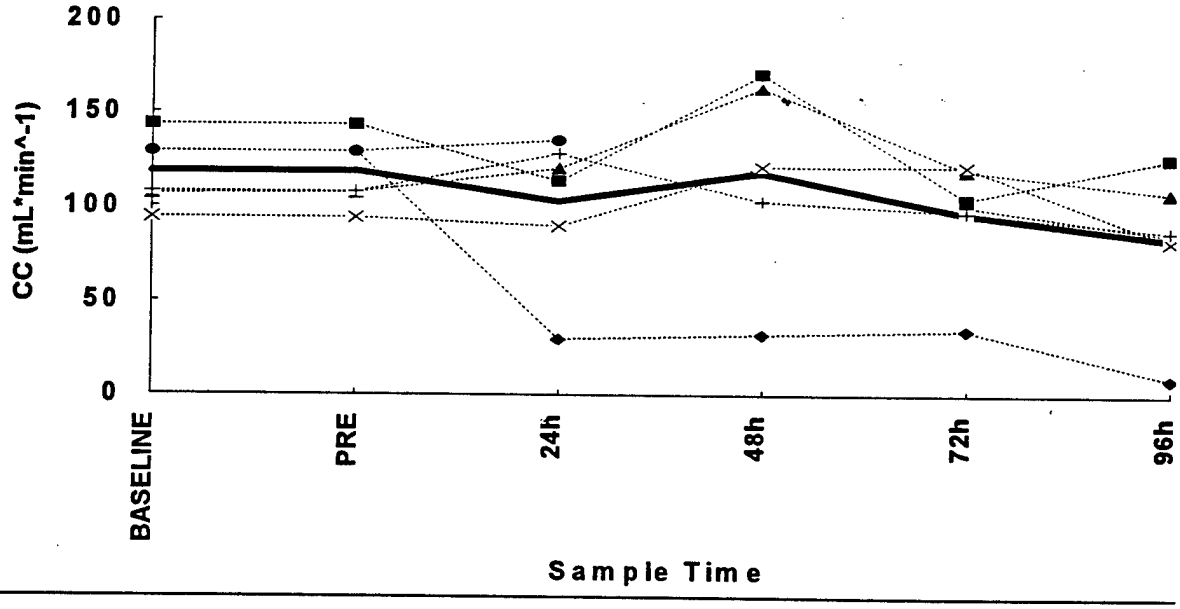

Figure F-147. The individual subject responses of Creatinine Clearance (CC) in Experiment LT2 with a motion exposure including 4 g shocks in the +z axis.

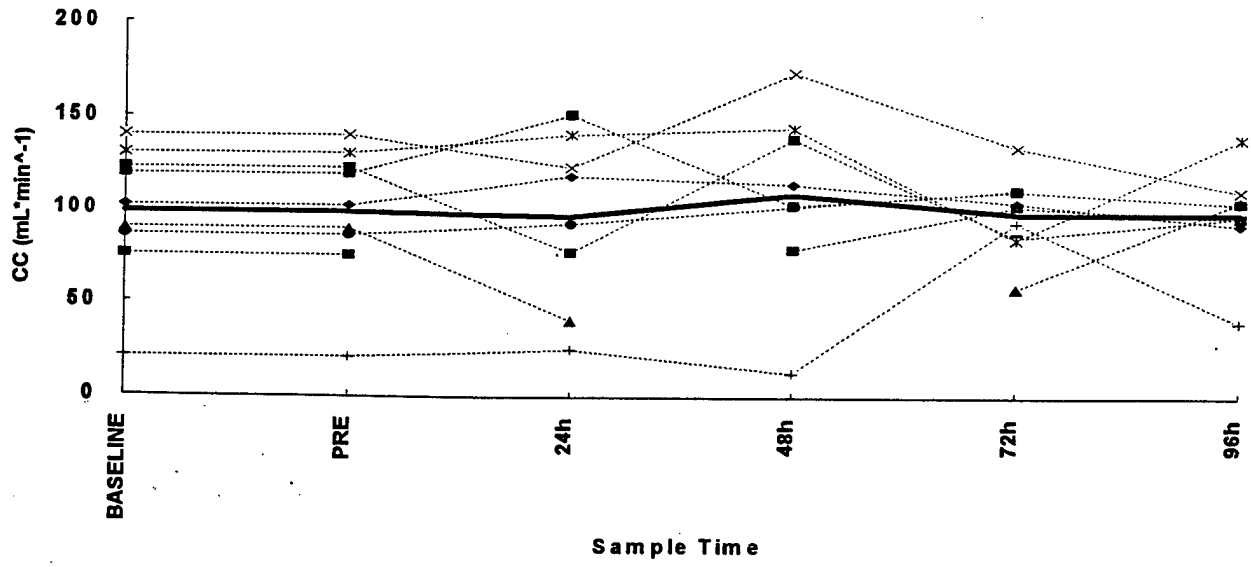

Figure F-148. The individual subject responses of Creatinine Clearance (CC) in Experiment LT3 with up to 7 hours of motion exposure including 2 and 4 g shocks in ± x, y and z axes.

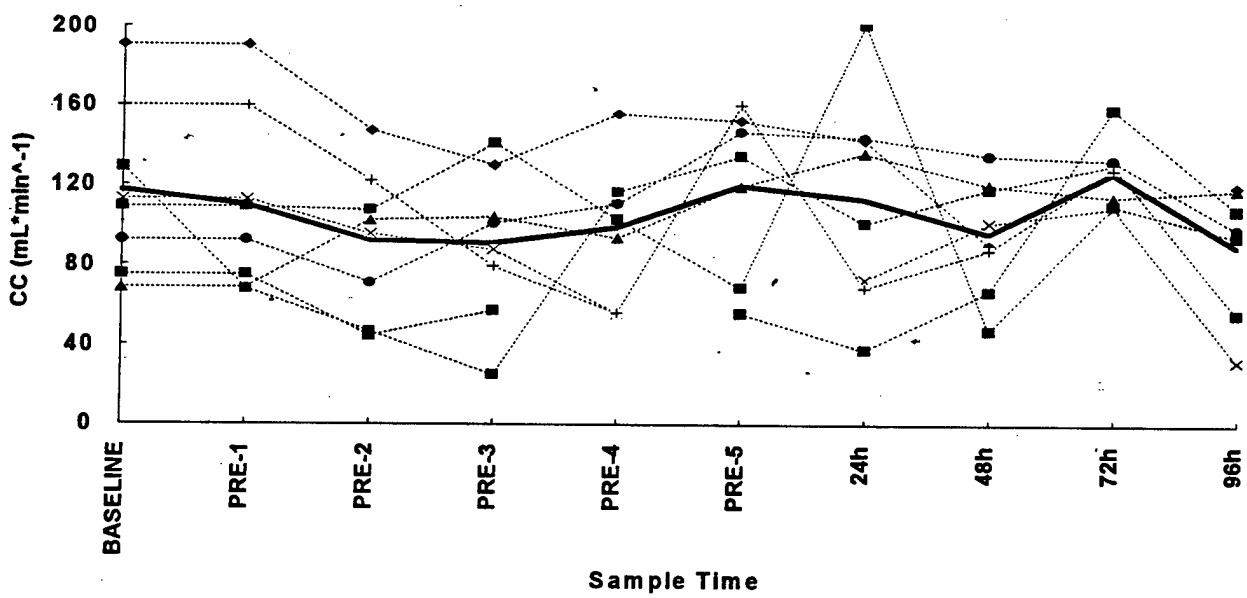

Figure F-149. The individual subject responses of Creatinine Clearance (CC) in Experiment LT4 with up to 5 days of 4 hours per day of motion exposure including 2 and 4 g shocks in ± x, y and z axes.

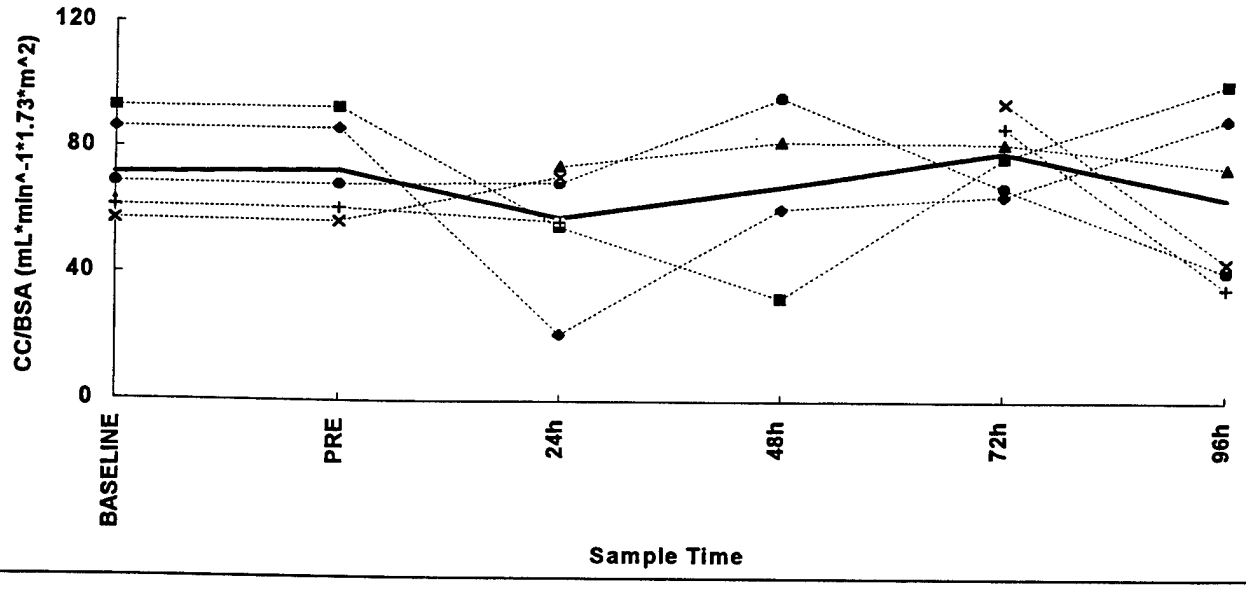

Figure F-150. The individual subject responses of Creatinine Clearance (CC) normalized to body surface area (BSA) in Experiment LT2 with a motion exposure including 4 g shocks in the -x axis.

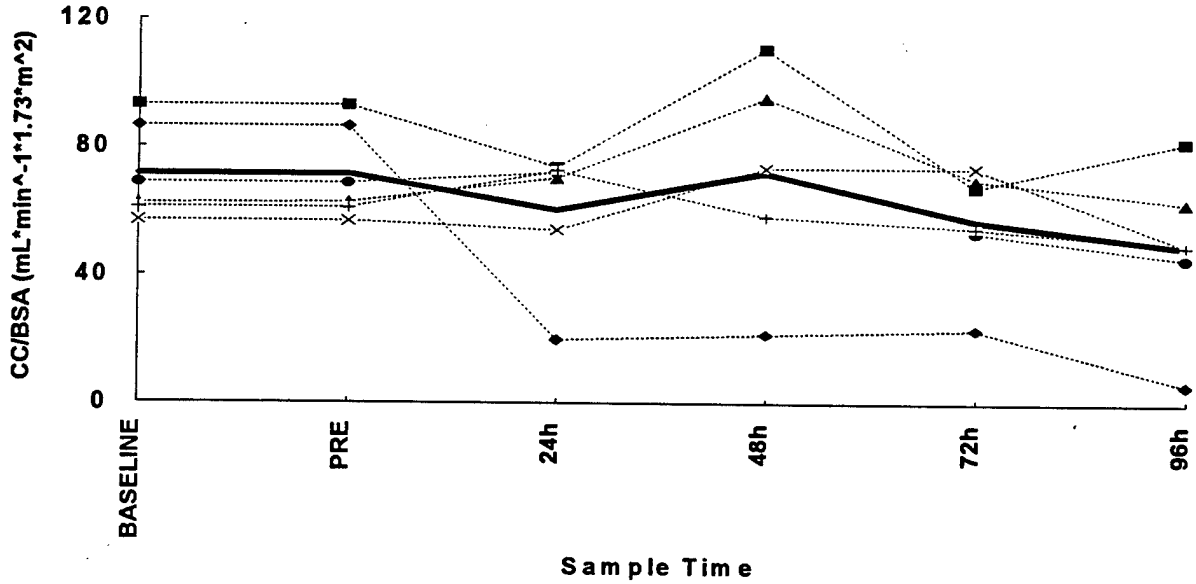

Figure F-151. The individual subject responses of Creatinine Clearance (CC) normalized to body surface area (BSA) in Experiment LT2 with a motion exposure including 4 g shocks in the +z axis.

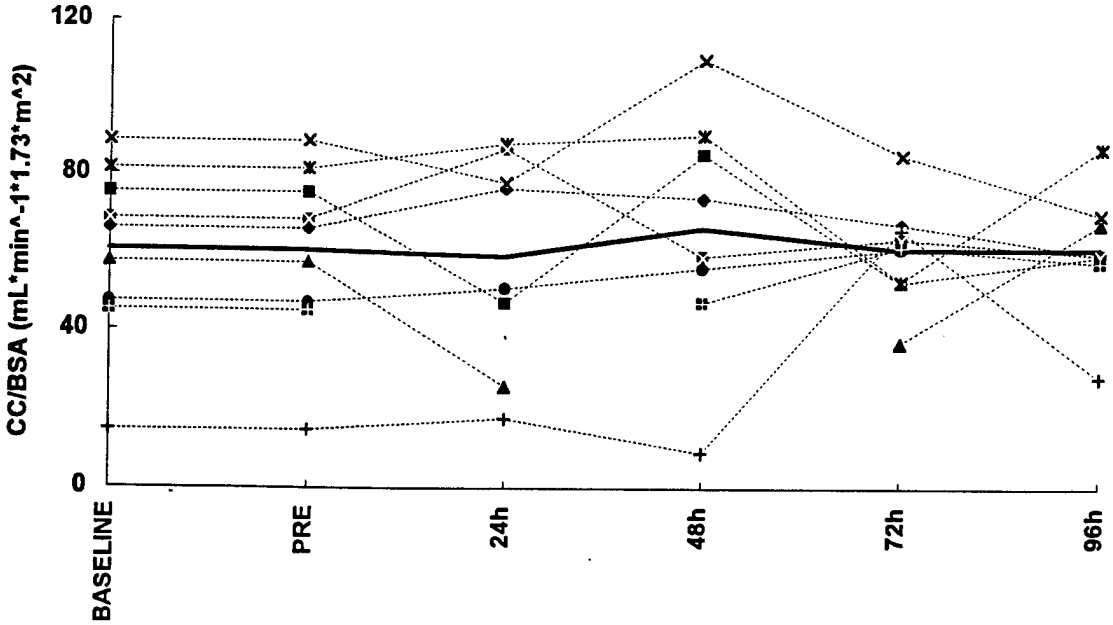

Figure F-152. The individual subject responses of Creatinine Clearance (CC) normalized to body surface area (BSA) in Experiment LT3 with up to 7 hours of motion exposure including 2 and 4 g shocks in ± x, y and z axes.

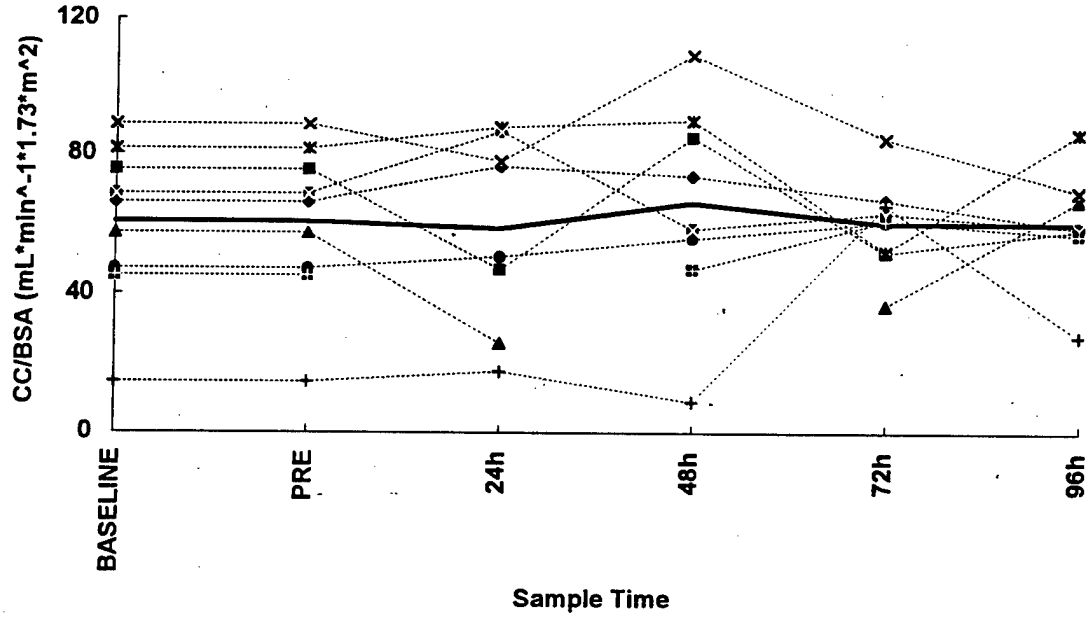

Figure F-153. The individual subject responses of Creatinine Clearance (CC) normalized to body surface area (BSA) in Experiment LT4 with up to 5 days of 4 hours per day of motion exposure including 2 and 4 g shocks in ± x, y and z axes.

Appendix G
Glossary

$\neq$	not equal to
ς	fraction of critical damping ratio
δ	amplitude
τ	period of the waveform
$^{\circ}$	degrees
ϖ_n	natural frequency
%	percent
$\pm$	plus or minus
+x	positive x-axis vibration or shock according to biodynamic convention: forward (ISO 2631,1982)
+y	positive y-axis vibration or shock according to biodynamic convention: to left (ISO 2631,1982)
+z	positive z-axis vibration or shock according to biodynamic convention: upward (ISO 2631,1982)
-x	negative x-axis vibration or shock according to biodynamic convention: backward (ISO 2631,1982)
-y	negative y-axis vibration or shock according to biodynamic convention: to right (ISO 2631,1982)
-z	negative z-axis vibration or shock according to biodynamic convention: downward (ISO 2631,1982)
<	less than
>	greater than
ANOVA	analysis of variance
ASCC	Air Standardization Coordinating Committee
a_w	frequency weighted acceleration
BCRI	BC Research Inc.
bpm	beats per minute (cardiac)
BS	British Standards
BSA	body surface area
BUN	blood urea nitrogen
C1	first cervical vertebra
Ca^{2+}	Calcium
CC	creatinine clearance
cm	centimeter
cm^2	centimeters squared
CPK	creatine phosphokinase
CV	coefficient of variation
DRI	Dose Response Index

ECG	electrocardiogram or electrocardiography
EMG	electromyogram or electromyography
f	frequency
FFT	Fast Fourier Transform
FG	Fairley-Griffin
f_i	filtering cut-off frequency
Freq.	frequency
g	gravitational acceleration: 9.8 m/s
g/dl	grams per deciliter
GEDAP	Generalized Data Acquisition/Analysis Programs
GFR	glomerular filtration rate
GI	gastro-intestinal
gm	grams
h	hours
$H(\varpi)$	transfer function
Hb	Hemoglobin
HHA	Health Hazard Assessment
HP	Hewlett Packard
Hz	Hertz (cycles/second)
IP	internal pressure
IRED	infra-red emitting diodes
ISO	International Standards Organization
IU/L	International units per liter
K^+	Potassium
kg	kilograms
$kg \cdot ms^{-2} \cdot volt^{-1}$	kilogram meters per second squared per volt (force per volt)
L/day	liters per day
L2	second lumbar vertebra
L2 x	acceleration at L2 in the X axis
L3	third lumbar vertebra
L3 y	acceleration at L3 in the Y axis
L4	fourth lumbar vertebra
L4 z	acceleration at L4 in the z axis
L5	fifth lumbar vertebra
lbs	pounds
LDH	lactate dehydrogenase
LL	left lumbar
LSE	least squares estimate
LT	left thoracic
LT1	Long-term experiment 1

LT2	Long-term experiment 2
LT3	Long-term experiment 3
LT4	Long-term experiment 4
LT5	Long-term experiment 5
m	meters
$ms^{-1.75}$	VDV dose units
ms^{-2}	meters per second squared
$ms^{-2} \cdot volt^{-1}$	meters per second per volt
m/s^1.75	VDV units
m/s^2	meters per second squared
m^2	meters squared
MARS	Multiaxis ride simulator
mEq/L	milli Equivalents per liter
MF	mean frequency
mg	milligrams
$mg \cdot dl^{-1}$	milligrams per deciliter
mg/kg/24 hrs	milligrams per kilogram per 24 hours
Mg^{2+}	Magnesium
min	minute
min^{-1}	per minute
ml	milliliter
$ml \cdot min^{-1}$	milliliter per minute`
$ml/min/1.73m^2$	milliliters per minute per 1.73 meters squared body surface area
mm	millimeters
mm^3	millimeters cubed
mmHg	millimeters of Mercury
$mmHg \cdot m^{-1} \cdot sec^2$	millimeters of Mercury per unit of acceleration
$mmHg \cdot volt^{-1}$	millimeters of Mercury per volt
mmol/L	millimoles per liter
mOsm	milliosmoles
ms	milliseconds
MUAP	motor unit action potential
MVC	Maximum Voluntary Contraction
$N \cdot volt^{-1}$	Newtons per volt (force per volt)
n=	subject sample number
No.	number
ODAU	Optotrak Data Acquisition Unit (timing pulse)
PC	personal computer
pH	acidity units
Ph.D.	Doctor of Philosophy

psi	pounds per square inch
$rads \cdot s^{-1}$	radians per second (angular acceleration)
RBC	red blood cells (erythrocytes)
RL	right lumbar
rms	root mean square
RT	right thoracic
s	seconds
SAE	Society of Automotive Engineers
sec	seconds
SR	severity rating
SST	serum separator tubes
ST1	Short-term experiment 1
Sx	seat acceleration in the x axis
Sy	seat acceleration in the y axis
Syn Work	Synthetic Work Environment performance battery task
Sz	seat acceleration in the z axis
T1	first thoracic vertebra
T1 x	acceleration at T1 in the x axis
T2	second thoracic vertebra
T2 y	acceleration at T2 in the y axis
T3	third thoracic vertebra
T3 z	acceleration at T3 in the z axis
T9	ninth thoracic vertebra
TGV	tactical ground vehicle
TP	Total protein
U/L	units per liter
$Units*liter^{-1}$	units per liter
USAARL	United States Army Aeromedical Research Laboratory
USAMRDALC	United States Army Aeromedical Medical Research, Development, Acquisition and Logistics Command
V	volts
VDV	vibration dose value
W_b	BS 6841 z axis frequency weighting filter
WBC	white blood cells (leukocytes)
WBV	whole-body vibration
W_d	BS 6841 x and y axis frequency weighting filter